Tuning Hydrogel Degradation for Cartilage Tissue Engineering

by

Stacey C. Skaalure

B.S., Rice University, 2009

A thesis submitted to the

Faculty of the Graduate School of the

University of Colorado in partial fulfillment

Of the requirement for the degree of

Doctor of Philosophy

Department of Chemical and Biological Engineering

2014

This thesis entitled:

Tuning Hydrogel Degradation for Cartilage Tissue Engineering

written by Stacey C. Skaalure

has been approved for the Department of Chemical and Biological Engineering

_____

Stephanie J. Bryant, Ph.D.

_____

Joel L. Kaar, Ph.D.

Date:_____

The final copy of this thesis has been examined by the signatories, and we find that both the content and the form meet acceptable presentation standards of scholarly work in the above mentioned discipline.

Abstract

Skaalure, Stacey C. (Ph.D., Chemical and Biological Engineering)

Tuning hydrogel degradation for cartilage tissue engineering

Thesis directed by Dr. Stephanie J. Bryant

Cartilage tissue engineering using biodegradable scaffolds as carriers for cartilage cells (chondrocytes) presents a promising strategy to regenerate cartilage damaged by age, injury, or disease. State-of-the-art clinical therapies implement chondrocytes harvested from the patient, however these treatments suffer from patient-to-patient variability and ineffectiveness due to aging. Photopolymerizable poly(ethylene glycol) (PEG) hydrogel scaffolds that can be modified to permit tunable degradation present an opportunity to tailor scaffolds to the patient's cells. Scaffold degradation is crucial to encourage cartilaginous matrix deposition by entrapped chondrocytes, however the rate of degradation must be matched to matrix deposition, which is a significant design challenge further complicated by the effects of age.

The goal of this thesis was to characterize degradable PEG hydrogels towards developing a suitable cartilage tissue engineering platform that can be applied to a wide range of patients regardless of age. Initial work focused on bulk hydrolytically degradable scaffolds with poly(lactic acid) in the PEG crosslinks. Chondrocytes were isolated from skeletally mature and immature (adult and juvenile) bovine cartilage, and encapsulated in hydrolytically degradable scaffolds, revealing lower anabolic and higher catabolic activity of adult cells, further motivating the need to tailor scaffolds to donor age. Bulk degrading scaffolds swelled with time, increasing the network mesh size and permitting diffusive matrix loss. To improve matrix

production and retention, degradable scaffolds were bioactively modified by entrapping a native matrix molecule involved in tissue assembly, and matching the culture medium to physiological osmolarity. Both strategies stimulated matrix deposition short-term but could not overcome long-term matrix loss due to bulk degradation. A new cartilage-specific enzymatically degradable hydrogel was created to encourage cell-localized degradation, by incorporating a peptide sequence into the PEG crosslinks that is degraded by chondrocyte-secreted enzymes. Enzymatically degradable scaffolds encouraged cartilaginous matrix deposition and interconnectivity. Experimental control over diffusion- and reaction dominated degradation (bulk vs. localized), both possible in enzymatically degradable hydrogels, was demonstrated using a model system where enzyme-laden microparticles simulated enzyme secretion from cells. This thesis demonstrated that enzymatically degradable hydrogels and bioactive modification are valuable tools to create a tunable degradable platform to promote tissue regeneration using cells from any patient.

Dedication

To my family and friends who always believed in me,

and told me that I can achieve anything I want in life.

Acknowledgements

I have always said that graduate school is a journey, and I personally found that the final destination couldn't be reached without considerable guidance, support, and encouragement from others along the way. The greatest source of support and guidance in my thesis work was from my research advisor, Dr. Stephanie Bryant. Your tough questions and high expectations kept me thinking and persevering, but your consistently supportive and positive approach was incredibly crucial to my ability to accomplish successful work in the lab. You always believed in my abilities and encouraged me to venture outside of my comfort zone and explore new directions in my thesis work, and for that I am extremely grateful and I know that I was lucky to have you as an advisor, mentor, and role model. I would also like to thank my committee members: Dr. Kristi Anseth, Dr. Natalie Ahn, Dr. Franck Vernerey, and Dr. Joel Kaar. Having the opportunity to work alongside some of your students and hear your feedback on my thesis work was extremely valuable to my development as a scientist. Additionally, my undergraduate research advisor, Dr. Kyriacos Athanasiou, initially sparked my interest in cartilage tissue engineering and helped me to develop early research lab skills. More importantly, his continued mentorship and encouragement to this day has meant so much to me as I begin to navigate a career in biotechnology.

I am very grateful to all of the various funding sources that have supported my research efforts throughout graduate school at CU. These include a Chancellor's Fellowship from the University of Colorado, a Pharmaceutical Biotechnology Training Grant from the National Institute of Health, a National Science Foundation Graduate Research Fellowship, a Bioscience Discovery and Evaluation grant from the State of Colorado, and grants from the National Institute of Health (#1R01AR065441 and #R21AR061011).

I truly believe I would not have been able to accomplish so much in the lab without the help of our very supportive and collaborative lab environment. The Bryant lab members have a reputation for being some of the nicest and most helpful people in the building, and I hope that legacy continues. I am particularly grateful to Drs. Justine Roberts and Nikki Farnsworth, two people who tolerated my incessant questions when I was new to the lab (and even not quite so new!) and taught me so many of the skills that I have continued to develop. I also thank previous members, Drs. Stephanie Hume, Garret Nicodemus, Aaron Lynn, Kathryn Penzkover, and Carsten Schnatwinkel for sharing some of their expertise with me before moving on to new endeavors. The current or recent lab members, including Luke Amer, Elizabeth Aisenbrey, Aaron Aziz, Stanley Chu, and Drs. Mark Swartzlander, Alexander Neumann and Sadhana Sharma, have been a lot of fun to work with and have truly helped to establish a lab culture of openness and collaboration. My lab work was also made more successful and fulfilling with the contributions of several undergraduate students that I had the privilege to mentor. These students include Shash Dimson, Saikripa Radhakrishnan, Ian Milligan, Jaimie Stewart, Ashley Pennington, Joe Quinn, and Joe Villanueva. Your positive attitudes, openness to learning, and variety of personalities were a pleasure to be around and work alongside!

Last but not least, my family and friends, near and far, deserve many thanks for their support, and for dealing with the many ups and downs that one inevitably experiences throughout graduate school. It was a difficult but rewarding journey that was at times hard on friends and family who did not live close to me, but I am grateful for their efforts to continuously provide support and encouragement. Although I try to be a fiercely independent person, I can't help but acknowledge that I couldn't have accomplished all of this on my own.

Table of Contents

List of Tables

List of Figures

Chapter 1

Introduction and Background

1.1 Cartilage Composition and the Effects of Aging

Articular cartilage covers the ends of bones within the joint, providing an elastic load-bearing surface that reduces friction during joint articulation (hence the name, articular cartilage) [1,2]. The function of articular cartilage is primarily mechanical, and its load bearing properties arise from a unique tissue composition, which is comprised of cartilage cells (chondrocytes), extracellular matrix (ECM) molecules, and interstitial fluid. The cells are responsible for regulating the extracellular environment, where in healthy tissue, there should be a balance between anabolic (matrix-producing) and catabolic (matrix-destructive) processes [2]. Injury, tissue degeneration due to age, and osteoarthritis can disrupt this balance. Aging in particular is a major contributor to musculoskeletal impairment, as aging further increases the risk of joint injuries and decreases the ability to heal [3]. Cartilage injury and disease are highly destructive, leading to pain, loss of mobility, and decreased quality of life [4]. The fact that cartilage has a very limited capacity for self-repair makes cartilage disorders a significant healthcare challenge. In order to repair or regenerate damaged cartilage in patients of any age, it is necessary to first understand the biological composition and metabolism of healthy cartilage, as well as age-related changes in cartilage biology.

1.1.1 Cartilage cells

Cartilage is composed of one main cell type, known as chondrocytes, that are sparsely populated within an avascular extracellular matrix, and make up less than 10% of the tissue volume [5]. Because the cells are sparse, chondrocytes primarily interact with their surrounding matrix, and not with other cells. The chondrocytes are responsible for regulating the surrounding

tissue homeostasis, where cartilage is not static but highly dynamic, as cells constantly process and turn over matrix molecules [2,6]. Cartilage is aneural and avascular, therefore the nutrient supply and waste removal are regulated by the synovial fluid (the viscous fluid contained within the joint capsule) and interstitial fluid within the tissue, where the water content in cartilage is 70-85% of the total tissue mass [1]. The synovial and interstitial fluids are highly pressurized under normal cyclic mechanical loading [5], inducing fluid flow throughout the highly hydrated cartilage tissue.

1.1.2 Extracellular matrix

Cartilage extracellular matrix is composed of collagens (10-30% of cartilage wet weight), proteoglycans (3-10% of wet weight), and lesser amounts of non-collagenous proteins, glycoproteins, lipids, and salts dissolved in the interstitial fluid [5]. Collagens are the main component, creating an elastic meshwork that entraps proteoglycans. The primary collagen in cartilage is collagen type II, which accounts for 90-98% of total articular cartilage tissue collagen [6] and provides cartilage with tensile strength. The other main ECM molecule in cartilage is aggrecan, the aggregating proteoglycan responsible for cartilage compressive strength, where smaller non-aggregating proteoglycans are more associated with matrix organization and maintaining chondrocyte function [2,7,8] (Fig. 1).

The main matrix molecule that is unique to articular cartilage is collagen type II. Collagen II is a triple helix of three identical polypeptide chains, which crosslink with other collagen II triple helices to form collagen fibrils, contributing to the tensile strength [6]. Other collagens play a role in cartilage. Collagen VI is found mostly immediately surrounding chondrocytes in the pericellular matrix and is thought to play a role in transducing mechanical signals to chondrocytes [9–11]. Collagens IX and XI are involved in stabilizing the collagen II network [11]. Collagens which are not found in healthy articular cartilage include collagen I and X. Collagen X is found in the calcified cartilage (close to underlying bone) and is a marker of hypertrophic cartilage cells that is also produced abundantly by osteoarthritic cells [6,12]. Collagen I is

characteristic of fibrocartilage and is a component of repair cartilage that has inferior tissue mechanics [13,14].

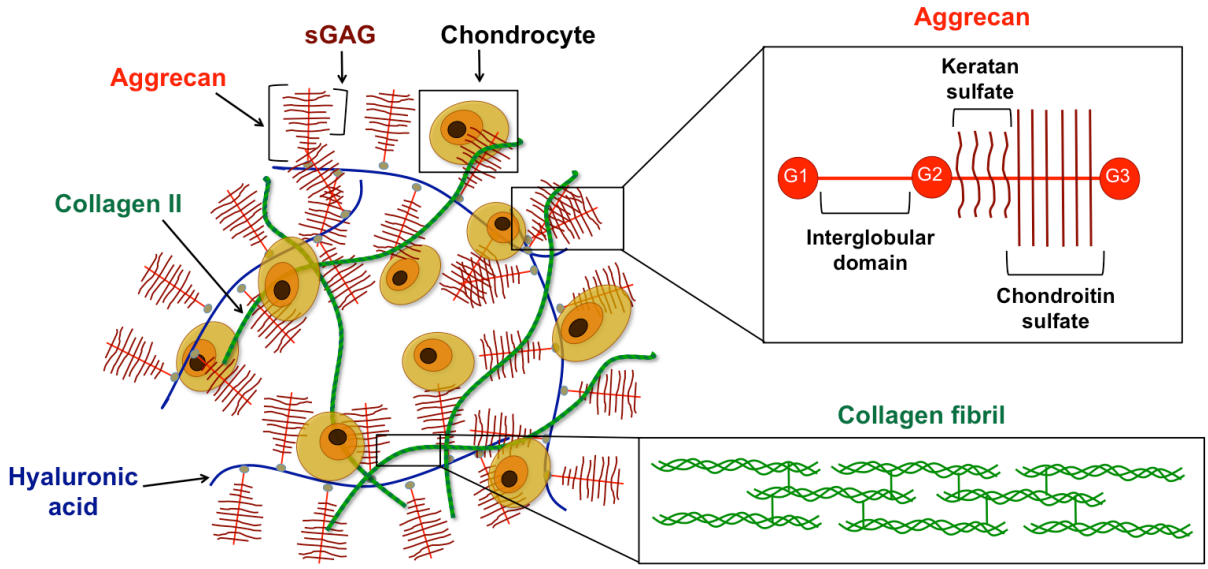

Figure 1.1 Schematic of articular cartilage extracellular matrix, consisting of chondrocytes surrounded by a collagen II network with entrapped aggrecan aggregates, bound to hyaluronic acid filaments.

Large aggregating proteoglycans, known as aggrecan, are entrapped within the collagen network. Aggrecans are composed of a linear core protein with three globular domains [15]. Between the second and third globular domains, the core protein binds approximately 300 negatively charged sulfated glycosaminoglycan (sGAG) chains [16,17], where chondroitin sulfate is the predominant sGAG, and keratan sulfate is less abundant [8,17]. The fixed negative charges associated with sGAGs on aggrecan molecules lead to elevated cation (Na^+, K^+, and H^+) concentration and lower anion (Cl^- and HCO_3^-) concentration in the interstitial fluid [18]. This results in an unusually high osmolarity (350-450 mOsm) compared to most tissues [19], and the osmotic swelling pressure induced by the fixed charge density is largely responsible for aggrecan's resistance to compression [1,20]. The presence of highly swollen aggrecans entrapped within an elastic collagen network contributes to the overall mechanical properties of

cartilage, where the Young's modulus of cartilage ranges from 450 to 800 kPa [1]. Aggrecans are known as 'aggregating' proteoglycans because they assemble along hyaluronic acid (HA), a linear non-sulfated glycosaminoglycan that can bind up to 100 aggrecans per molecule [16,17]. HA is also capable of binding the CD44 membrane receptor in chondrocytes [17,21], thereby contributing to the organization and retention of aggrecans within cartilage tissue.

1.1.3 Matrix metabolism

Tissue catabolism is necessary for matrix turnover during homeostasis and transport of ECM from the pericellular space to the extracellular space, yet an imbalance in anabolic and catabolic activity is symptomatic of both aging and osteoarthritis [22–24]. Within native cartilage, matrix turnover is relatively slow, as the half-lives of aggrecan and collagen molecules are on the order of 15-100 days and 100 years, respectively [17,25,26].

The main family of catabolic enzymes that degrade cartilage are the zinc-dependent matrix metalloproteinases (MMPs). Four MMPs (MMP-1, -8, -13, and -14) are known as the 'collagenases' due to their ability to cleave the triple helix of collagens I, II, and III [2,6,11,27], and MMP-13 is noted as the most active against collagen [2,11]. These collagenases however have limited activity against crosslinked collagen fibrils, which require initial processing by other enzymes, such as MMP-3, before collagenases can cleave the collagen monomers [11].

The aggrecan core protein can be degraded by several MMPs, but is most specifically degraded by a separate group of enzymes known as the 'aggrecanases.' The aggrecanases belong to the ADAMTS family (A Disintegrin And Metalloproteinase domain with ThromboSpondin motifs), where ADAMTS-4 and -5 are also known as aggrecanase-1 and -2, respectively, which are the main aggrecanases that degrade aggrecan [2,28,29]. The aggrecanases cleave at one main site between globular domains 1 and 2 (the 'interglobular domain, IGD) between amino acid residues 373-374, and four additional sites in the sGAG-bearing region between globular domains 2 and 3, where the latter sites are indicated as the more efficient sites of aggrecanase cleavage [30]. Several MMPs including MMP-3, -7, -8, -12

and -13 can degrade aggrecan in the IGD at an MMP-specific site between amino acid residues 341 and 342, which is considered to be indicative of normal tissue homeostasis [31,32], but this degradation typically occurs many days later than the more aggrecan-specific aggrecanases in response to catabolic cytokines and typically after the core protein has been deglycosylated [33–35]. Cleavage at the 341-342 site is most commonly associated with MMP-3 [36,37]. MMPs can degrade several additional sites between globular domains 2 and 3 (the sGAG-bearing region), but degradation of the aggrecan core protein by MMPs is overall much less efficient than the aggrecanases [35,38,39].

1.1.4 Effects of aging and osteoarthritis

Chondrocyte metabolism and cartilage tissue composition change with age, and these changes increase the risk of developing osteoarthritis. With aging, chondrocytes are less proliferative [40] and have lower viability due to increased oxidative stress [41], contributing to decreased tissue cellularity with age [42]. Besides cellularity, extracellular matrix composition and metabolism also change with age. Chondrocytes in older patients are less receptive to growth factor stimulation, decreasing their ability to repair damaged tissue and produce new matrix [3,43], and newly synthesized matrix is less likely to assemble properly [44]. As subjects age, cartilage contains smaller aggrecans that have fewer sGAG side chains [45] and lack the third globular domain [17], due to increased aggrecan catabolism [46–48]. With age, both MMP and aggrecanase-mediated cleavage of the aggrecan IGD are increased, resulting in destructive loss of functional sGAG-bearing fragments [30] which reduces the ability of tissue to resist compressive forces. Collagen fibrils are more crosslinked in older subjects, actually making them more resistant to proteolytic degradation [6], which is likely a protective mechanism against increased collagenase activity with age, which is even more elevated in osteoarthritis [27,49]. Additional changes that occur specifically in osteoarthritis are an increased abundance of collagen X, which is an indicator of hypertrophy [12], highly elevated

aggrecanase activity [30,50], and increased production of inflammatory cytokines that stimulate matrix degradation [51].

1.2 Damage to Cartilage by Injury and Osteoarthritis

Cartilage is an avascular and aneural tissue with limited ability to self-heal, therefore tissue damaged by injury or disease (e.g., osteoarthritis) will only worsen without treatment. Joint injuries in particular are a major risk factor for developing osteoarthritis [52,53], which is a disease characterized by loss of articular cartilage that causes pain and decreased mobility, and is one of the major causes of disability in the United States [4,52]. After age 40, the risk of developing osteoarthritis increases greatly with each decade [22]. Joint injuries such as focal lesions are noted risk factors for developing osteoarthritis by inducing loss of aggrecan fragments from cartilage tissue [29,50,54], mediated mostly by aggrecanases [29] but also by MMP-3 [52]. Other injuries including meniscal and ligament damage can alter the mechanical environment experienced by cartilage within the joint [6,43]. Altered mechanical forces can increase inflammatory cytokine production, which in turn increases cartilage catabolism [51], by elevating MMP and aggrecanase activity [38]. Osteoarthritis is associated with age because chondrocytes in older patients are more limited in their ability to regenerate damaged and degraded cartilage [43]. While there is no cure for osteoarthritis, there are various interventions in clinical use that are designed to treat symptoms, replace joint function, or treat injuries in order to prevent osteoarthritis, which are summarized in the following section.

1.3 Current Treatments for Cartilage Damage and Osteoarthritis

1.3.1 Treatment of symptoms

Osteoarthritis cannot be cured or reversed with current medical technology, therefore one of the most common treatments is simply symptom management, where pain is the most debilitating symptom. A variety of pain-relieving medications are used, however pain management does not address cartilage damage and simply masks symptoms [55]. Hyaluronic acid is clinically used to relieve pain associated with osteoarthritis through a process known as

viscosupplementation, where high MW HA is injected directly into the damaged joint [56]. This treatment can also improve joint lubrication but is only temporary, requiring repeated injections.

1.3.2 Common surgical interventions

Various surgical interventions exist in order to encourage or improve cartilage healing, because joint injuries, even for young athletes, greatly increase the risk for developing osteoarthritis [57]. Debridement is one of the simplest techniques, involving removal of damaged or torn cartilage and smoothing the remaining cartilage to promote healing. This technique resulted in improved outcomes for young athletes, however regenerated tissue contained mechanically inferior fibrocartilage [58]. Mosaicplasty is a technique where osteochondral plugs (containing both cartilage and underlying bone) are transplanted from a cadaver (allogeneic) or a non-load bearing region of the patient's cartilage (autologous). Limitations of this technique include donor site morbidity, potential disease transmission when cadaver tissue is used, and poor integration with existing tissue [55,59]. Microfracture is a technique where microfractures are surgically introduced into subchondral bone underlying a cartilage defect in order to stimulate infiltration of mesenchymal stem cells (MSCs) and growth factors to promote healing, but regenerated tissue is composed of predominantly fibrocartilage [55,59]. Small cartilage lesions (<2.5 cm^2) are best treated by microfracture, whereas more sophisticated cell-based techniques are required for larger lesions [60]. The most dramatic surgical intervention is full joint arthroplasty, which is more commonly implemented in older patients, whereas the previously described treatments are indicated for younger patients. In arthroplasty, severely damaged, aged or diseased joints are fully replaced by a prosthetic, which restores the joint function but does limit physical activity. This treatment is a last resort, as it is highly invasive, and implants are prone to wear out or loosen over time [23,55,59].

1.3.3 Cell-based therapies

Cell-based techniques are promising because they involve delivering the patient's own chondrocytes (autologous cells) to cartilage lesions to promote formation of new tissue that

should theoretically be identical to the existing tissue. Autologous chondrocyte implantation (ACI) involves harvesting the patient's cartilage from a non-load bearing site, isolating the chondrocytes, expanding the cells in 2-dimensional culture, and injecting those cells into the defect site, holding them in place with a periosteal patch or a collagen membrane [59,61–63]. ACI has been most successful in young active patients, specifically those less than 35 years old [60,64], and is not indicated for patients over 50 years of age [59,61,62]. A second-generation ACI technique was developed, called matrix-assisted ACI, or MACI, which is not yet FDA approved. This technique is similar to ACI, but chondrocytes are implanted into the cartilage defect embedded within a three-dimensional scaffold [65,66]. ACI and MACI are the most promising surgical techniques to treat cartilage lesions that result in the best clinical outcomes [67], and the advent of MACI [65,66] brings the opportunity to tailor scaffolds to patients from a wider age range by investigating the impact of using different scaffolds and bioactive factors.

1.4 The Cartilage Tissue Engineering Approach

Tissue engineering approaches designed to regenerate damaged or diseased tissues typically consist of some combination of scaffolds, a cell source, and bioactive factors. The cartilage tissue engineering approach mainly aims to prevent the development of osteoarthritis after cartilage injury by regenerating or replacing injured cartilage. Cartilage tissue engineering provides the opportunity to regenerate damaged cartilage in a minimally invasive manner that can salvage the existing joint, which is a great improvement over pain management or full joint arthroplasty [22,23]. An additional goal is to improve the quality of newly formed articular cartilage, as treatments such as debridement and microfracture result in fibrocartilage, which ultimately degenerates with time. Another goal is to expand treatments to older patients, because the likelihood of developing osteoarthritis after injury increases greatly with age [22], meaning that current tissue engineering techniques cannot address the needs of a large fraction of patients with joint disorders. Towards these goals, a wide variety of cell sources, scaffolds, and bioactive factors have been investigated.

1.4.1 Cell source

Any cells that have the capacity to produce cartilaginous matrix, particularly collagen II and aggrecan, can be used for cartilage tissue engineering applications. The most obvious cell type to use is chondrocytes, which are used in autologous chondrocyte implantation. A limitation of autologous chondrocytes is that the harvested cell number tends to be quite low, necessitating expansion in 2-dimensional culture, which can result in de-differentiation away from the chondrocyte phenotype [68]. Mesenchymal stem cells (MSCs) can be derived from adult tissue, typically from the bone marrow, which can be harvested fairly easily and non-invasively. These cells can be chemically stimulated to differentiate into a variety of cell types including chondrocytes, and can also be expanded in 2-dimensional culture [69]. A limitation of MSCs is that they tend to 'terminally' differentiate into hypertrophic chondrocytes that express large quantities of collagen X, resembling the process of endochondral ossification during bone development, when cartilage is first formed and then mineralized to form bone [70]. Adipose-derived adult stem cells harvested from subcutaneous adipose tissue show characteristics similar to MSCs in that they can be differentiated into chondrocytes, however hypertrophic differentiation is a similar limitation [71]. Human embryonic stem cells have been differentiated into chondrocytes [72], but these cells still present many challenges due to their potential immunogenicity and teratoma formation [73]. Induced pluripotent stem cells are a promising new cell source where somatic cells are reprogrammed to become similar to embryonic stem cells. A recent study demonstrated that chondrogenic differentiation was possible using induced pluripotent stem cells derived from osteoarthritic chondrocytes, which could enable tissue engineering using cells from osteoarthritic sources [74]. At present however, the best cell source for regenerating cartilage is primary cells isolated from the patient.

1.4.2 Biomaterial scaffolds

Biomaterial scaffolds are considered particularly crucial for culturing and implanting chondrocytes (or cells that will be differentiated into chondrocytes), because the rounded

chondrocyte phenotype is lost in 2-dimensional culture but can be maintained in materials that interact with cells in 3 dimensions [75]. The mechanical function of cartilage can be aided by biomaterial scaffolds, which can maintain mechanical integrity within the joint environment until the cells are able to produce their own cartilaginous matrix. The ideal scaffold will provide initial mechanical support to the cells and surrounding tissue, but ultimately degrade to permit entrapped cells to deposit matrix and integrate with the existing joint environment. A wide variety of natural and synthetic materials have been investigated as cartilage tissue engineering scaffolds, where some of the most interesting and promising scaffolds have characteristics of both natural and synthetic materials.

1.4.2.1 Natural materials

Natural materials are attractive cell carriers because they are biologically-derived, making them highly biocompatible materials that have been successful in *in vivo* systems. Protein-based natural materials used for cartilage engineering include collagen, fibrin, laminin, and gelatin [23]. Of these, collagen is advantageous because of its ability to mimic the native ECM, and it encouraged articular cartilage production by MSCs, but suffered from poor mechanical properties [76]. Additionally, the source material for these natural scaffolds can be expensive. Cell-mediated degradation can occur in some natural material scaffolds, but it is difficult to form reproducible or mechanically robust hydrogels with these materials [77]. Carbohydrate-based natural materials include hyaluronic acid, agarose, alginate, and chitosan [23]. Hyaluronic acid is an attractive material due to its involvement in cartilage matrix organization [17], but it typically must undergo some type of chemical functionalization to permit crosslinking into a more solid material [78–81], therefore will be reviewed in further detail below. Agarose has been thoroughly investigated for cartilage tissue engineering, particularly in studies involving mechanical loading, which tended to increase matrix deposition by chondrocytes and improve construct mechanical properties [82–85]. Agarose however cannot be degraded by chondrocytes, which is a major limitation.

1.4.2.2 Synthetic material scaffolds

Synthetic polymers are attractive due to their consistency, abundance, and simple processing into scaffolds. Poly(lactic acid) (PLA), poly(glycolic acid) (PGA) and polycaprolactone (PCL) are simple hydrolytically erodible polymers that can be cast into macroporous scaffolds for cartilage tissue engineering, but these materials are inelastic and the large pores resemble more of a 2-dimensional surface from the chondrocyte perspective [86–88]. Additionally, inflammation can be a problem due to long-term material presence inducing the foreign body response [87], or due to cytotoxic degradation products [23]. In recent years, the synthetic materials that have gained the most attention for cartilage tissue engineering applications are synthetic hydrogels, which are crosslinked polymers, and thus will be the focus of the rest of this section.

1.4.2.3 Hydrogels

Hydrogels are composed of hydrophilic macromolecules that are chemically crosslinked to form an insoluble, but water swellable, three-dimensional network. Examples of synthetic monomers include poly(ethylene glycol) (PEG), poly(vinyl alcohol) (PVA), and poly(2-hydroxyethyl methacrylate) (PHEMA) [89], which can be crosslinked with a variety of chemical modifications, of which vinyl groups such as acrylates and methacrylates have been widely studied because they are amenable to free-radical polymerization [90,91]. In particular, photopolymerization, which uses light to initiate free-radical polymerization, is promising due to the spatial and temporal control over polymerization, with fast reaction times and limited cellular damage during photo-encapsulation [90,92]. Hydrogels are highly attractive cell carriers [77,89] because their elasticity and highly swollen environment mimic that of cartilage tissue and permit extracellular matrix (ECM) and nutrient transport while physically entrapping cells into the crosslinked network [77,91,93,94]. PEG-based hydrogels in particular have been employed extensively in cartilage tissue engineering due to their ability to maintain the chondrocyte phenotype and permit cartilaginous tissue formation [95–97]. However, long-term presence of

the hydrogel can induce the foreign body reaction initiating an adverse inflammatory response [98], and inhibit ECM deposition [99], which are crucial for effective tissue regeneration. Therefore scaffold biodegradation is necessary. However degradation rates must be matched to the rate of matrix deposition in order to maintain overall mechanical integrity of the implant, and prevent encapsulated cells and new ECM from being released from the scaffold.

1.4.2.4 Hydrolytically degradable hydrogels

A wide variety of biodegradable hydrogels have been developed in recent years, and hydrolytically degradable hydrogels are promising due to their ability to fine tune the rate of degradation and the degradation behavior. Bulk hydrolytic degradation is made possible using materials that contain hydrolytically labile esters, such as poly(lactic acid) (PLA) [91]. For example, hydrolytically degradable hydrogels made from triblock co-polymers of PLA-*b*-PEG-*b*-PLA di(meth)acrylate (PEG-PLA hydrogels) with varying numbers of oligo-lactic acid repeat units to tune degradation have been well characterized for tissue engineering applications [95–97,100,101]. PEG-PLA hydrogels demonstrated improvements in macroscopic matrix elaboration by chondrocytes [96,102,103], and tuning the number of poly(lactic acid) repeats and the hydrogel formulation were shown to affect tissue engineering outcomes [95,97]. Although PEG-PLA scaffolds greatly improved cartilaginous matrix elaboration in one study with encapsulated chondrocytes, they also observed an 8-fold decrease in compressive modulus by 4 weeks [103]. In the absence of cells, degradation behavior of hydrolytically degradable hydrogels is characterized by an exponential drop in compressive modulus with time and an exponential increase in swelling [104,105]. Therefore, tuning the degradation exactly to matrix deposition and elaboration is important, but challenging.

1.4.2.5 Cell-mediated hydrogel degradation

Synthetic photopolymerizable scaffolds that degrade by cell-mediated mechanisms are promising for tissue regeneration by encapsulated cells due to their ability to permit cell-specified spatial and temporal control over degradation. Some naturally derived materials such

as collagen are innately able to degrade by cell-mediated mechanisms, but synthetic modification to permit crosslinking provides more control over degradation and the ability to create scaffolds of higher modulus than the natural materials alone. For example, chondroitin sulfate, which is degradable by chondroitinase, was methacrylated to permit crosslinking and was used to encapsulate chondrocytes [106,107]. Hyaluronic acid, which is degradable by hyaluronidase, has been similarly modified with methacrylates, thiols, or hydrazides to permit crosslinking [79–81,108], and hydrogels made by photo-polymerization of methacrylated hyaluronic acid have been investigated as cell carriers for cartilage tissue engineering [79,80,109,110]. Although HA can be degraded by hyaluronidases, these enzymes are restricted to the cell membrane and intracellularly to chondrocytes [111], meaning that HA-based degradable materials may require additional modification to facilitate degradation to be suitable for cartilage tissue engineering.

Synthetic materials such as PEG are appealing as a 'blank slate' that can be further functionalized with bioactive moieties [112], such as short enzymatically-sensitive peptide sequences incorporated into the crosslinks. These hydrogels were first introduced by West and Hubbell [113] who incorporated collagenase-sensitive and plasmin-sensitive peptide substrates to encourage cell migration, which led to the development of a variety of hydrogels incorporating MMP-degradable peptides to encourage cell migration and improve tissue engineering outcomes using encapsulated cells [114–123]. However, research towards designing these types of hydrogels for cartilage regeneration has been limited. Bahney *et al.* [118] incorporated an MMP-7 specific peptide into PEG-diacrylate hydrogels to encourage chondrogenesis of human mesenchymal stem cells, which increased collagen II but decreased proteoglycan deposition and cellularity compared to non-degradable hydrogels. Park *et al*. [122] crosslinked PEG scaffolds via a step-growth method with an MMP-sensitive peptide that increased collagen II and aggrecan gene expression for adult chondrocytes, but matrix deposition was pericellularly restricted.

A new PEG-based platform for cell-mediated degradation was introduced, based on a specific type of thiol-ene polymerization, using thiols and norbornenes, which enable photopolymerization [120]. This type of step growth polymerized hydrogels forms a homogeneous network structure made by reacting multi-arm PEG-norbornene and dithiol crosslinkers in the presence of a photoinitiator and light. This system has been investigated as cell carriers for tissue engineering that can be degraded through cell-mediated mechanisms [101,120,121]. By crosslinking multi-arm PEG-norbornene hydrogels with bis-cysteine (dithiol) peptides, cell-mediated degradation can be targeted to a variety of enzymes and cell types, and degradation kinetics can be controlled by using peptides optimized for specific enzymes [119]. Additionally, Roberts and Bryant recently observed [124] that radical damage to cartilage cells during photopolymerization was decreased in PEG hydrogels formed from thiol-norbornene monomers compared to diacrylate monomers, making this system attractive for a broad range of tissue engineering applications.

1.4.3 Incorporating bioactive factors

Synthetic hydrogels in particular are amenable to various types of bioactive modification in order to encourage matrix production by encapsulated cells. The goal of incorporating bioactive factors is typically to better mimic the native tissue environment in an effort to improve chondrogenic differentiation or stimulate production of more cartilaginous matrix. Bioactivity can be introduced into scaffolds by manipulating the culture environment, adding exogenous factors, or incorporating molecules into the hydrogel network. The traditional cell culture environment, even within 3-dimensional scaffolds, does not replicate several characteristics that are present in the native joint environment. For example, osmolarity in cartilage is typically elevated compared to standard chondrocyte culture medium, and studies which intended to replicate physiological osmolarity with elevated culture medium osmolarity (400-480 mOsm) showed improved chondrocyte survival and matrix production in short-term experiments [19,125,126]. Cartilage is also hypoxic, where oxygen concentration ranges from 1-7% [127], and

chondrocytes cultured in a 5% oxygen environment exhibited increased cartilaginous matrix production compared to standard 21% oxygen [128]. Because cartilage exists *in vivo* in a highly dynamic mechanical environment, many groups have attempted to replicate these environments for stem cells or chondrocytes in three-dimensional culture, which can improve chondrogenic differentiation and cartilaginous matrix production [82,129,130]. However, the effect on catabolic activity is complex, as different mechanical regimes can either increase or decrease catabolism [131–134].

Growth factors and extracellular matrix molecules have been incorporated into scaffolds in a variety of ways in order to mimic native cartilage and increase cartilaginous matrix production. The main growth factors that have been investigated for inducing chondrogenic differentiation and/or increasing matrix production are TGF-β1-3, BMP-2, -4, -6, -7, -13, and -14, bFGF, and IGF-1 [23,127]. These can be introduced into the culture medium requiring diffusion into scaffolds, presented to encapsulated cells by covalently tethering [135–137], or tethering by binding growth factors to adhesive peptides [138]. The strategy of controllably presenting growth factors is particularly attractive because it can greatly decrease the quantity of growth factors used, decreasing cost of materials. Cartilaginous matrix molecules such as chondroitin sulfate and hyaluronic acid can be similarly introduced by exogenous supplementation [139], physical entrapment [140], covalent incorporation [141], or adhesion using matrix-binding peptides [142]. With the wide variety of cell sources, scaffolds, and bioactive factors available, the possible combinations are almost limitless, which helps to explain the broad scope of cartilage tissue engineering research.

1.5 Challenges in Cartilage Tissue Engineering

While many advances have been made in the field of cartilage tissue engineering, there are still a number of challenges and hurdles to overcome before these techniques can be successfully implemented. One major challenge is developing hydrogels for cartilage tissue engineering that have a high enough compressive modulus to withstand the forces experienced

in the joint. The Young's modulus of cartilage ranges from 450 to 800 kPa [1], but when scaffolds with different compressive moduli have been compared, the best cartilaginous matrix deposition has typically occurred in relatively soft hydrogels. In two studies investigating the effect of hydrogel crosslink density on matrix production by chondrocytes, the lowest crosslink density hydrogels (35-50 kPa) best supported matrix deposition [143,144]. Additionally, a study comparing methacrylated hyaluronic acid hydrogels with different modulus found that the scaffolds which best supported cartilaginous neotissue formation by encapsulated mesenchymal stem cells had the lowest initial modulus (<10 kPa) [145]. Nutrient transport and extracellular matrix diffusion are improved in low crosslink density hydrogels, which may help explain the improvements in tissue production in softer hydrogels. A potential solution to this problem is to encapsulate cells in degradable hydrogels that initially have a high modulus to withstand mechanical forces, but would degrade over time to permit matrix deposition and improve diffusion [97].

Degradable hydrogels provide an opportunity to encourage macroscopic matrix deposition and elaboration by entrapped chondrocytes, however degradation rates must be matched to matrix deposition rates in order to maintain overall scaffold mechanical integrity. Bulk hydrolytically degradable scaffolds tend to degrade either too quickly or too slow [95,105,146], making attempts to match scaffold degradation to matrix production difficult [97,144]. Cell-mediated degradable hydrogels are more promising in their potential to match degradation to matrix production, but the complex degradation that can occur in these systems is both difficult to control and characterize [119,122].

A major challenge in cartilage tissue engineering is regenerating tissue with cells derived from older patients. Juvenile chondrocytes from skeletally immature donors are typically used for cartilage tissue engineering research because they produce large quantities of matrix, but these cells may not be the best model system to develop clinically relevant tissue engineering therapies that must ultimately be implemented in adult or aging patients. Adult chondrocytes

from skeletally mature donors have also been investigated in a variety of scaffolds, but there has typically been little distinction between these cells sources, even though they can behave quite differently in tissue engineering environments. Only a few studies have actually compared tissue regeneration potential of chondrocytes from different aged donors. One study observed decreased matrix synthesis for bovine chondrocytes from skeletally mature donors (adult) compared to those from skeletally immature donors (juvenile) when dynamically loaded in PEG hydrogels [134]. Another study investigated chondrocytes from 3 different aged bovine donors (fetal, adult, and aged) entrapped in agarose hydrogels, and found that both matrix production and cellular proliferation decreased with age [148]. The effect of donor age is therefore crucial to investigate when the intended application of a scaffold system is autologous cell-based tissue engineering therapies, which are currently used in a clinical setting.

1.6 Thesis Approach

The advent of MACI [66] brings the opportunity to tailor scaffolds to autologous chondrocytes isolated from patients from a wider age range than is currently possible. The ultimate goal is to develop degradable hydrogel scaffolds with tunable degradation that can support cartilage regeneration using cells from patients of any age. In this thesis, PEG-based degradable materials are used, because they are photopolymerizable and injectable, support cartilaginous matrix production [95–97,102,103], and because the chemistry can be easily tailored to introduce different degradable functionalities [112,149]. Photoinitiated chain-growth polymerization of PEG-poly(lactic acid)-dimethacrylate (PEG-PLA) monomers (mixed with a small amount of PEG-dimethacrylate monomers to slow degradation), which form relatively heterogeneous networks that degrade by bulk hydrolytic degradation [104,105], were used for objectives 1 and 2 (Fig. 2A). Photoinitiated step-growth polymerization of PEG-based thiol-norbornene monomers, which form more homogeneous network structures where crosslinks can be any dithiol molecule such as a *bis*-cysteine peptide [120], were used for objective 3 (Fig. 2B).

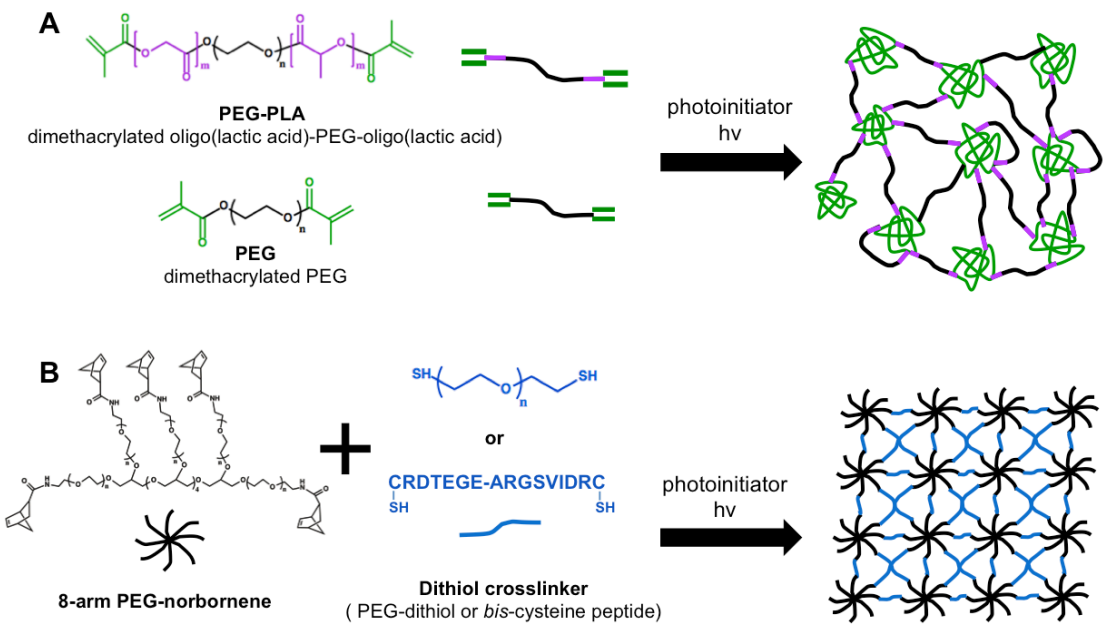

Figure 1.2 Schematic of PEG-PLA and PEG thiol-norbornene hydrogels. (A) PEG–PLA and PEG dimethacrylate were copolymerized to form degradable chain growth networks. (B) 8-arm PEG-norbornene was reacted with PEG-dithiol or *bis*-cysteine peptide to form step growth networks.

Chapter 2 outlines the specific objectives that will be addressed in this thesis. Briefly, the first objective, which is presented in chapter 3, explores the tissue engineering potential of chondrocytes isolated from skeletally mature and immature (adult and juvenile) bovine cartilage when encapsulated in hydrolytically degradable PEG-PLA hydrogels. Because of the decreased matrix synthesis and increased catabolism exhibited by adult bovine chondrocytes, two relevant bioactive factors are investigated in the second objective. Specifically, in chapter 4 hyaluronic acid is incorporated into degradable PEG-PLA hydrogels in an attempt to increase matrix production and retention by adult chondrocytes, and in chapter 5 the effects of chondrocyte culture medium osmolarity is investigated to probe the long-term effects of physiological osmolarites similar to the native environment. The third objective explores cell-mediated degradable hydrogels and characterizes their use for cartilage tissue engineering. In chapter 6, a novel aggrecanase-degradable hydrogel is introduced and matrix production and metabolism are compared for encapsulated juvenile and adult chondrocytes, and in chapter 7, an

experimental modeling approach is used to determine how to control the type of degradation that can occur in complex cell-mediated degradable systems. Chapter 8 summarizes the overall conclusions from the work presented in this thesis, and provides future recommendations that may further aid in developing tailorable degradable hydrogels for cartilage tissue engineering that can ultimately be adapted for the clinic.

1.7 References

[1] Mansour JM. Biomechanics of Cartilage. In: Oatis CA, editor. Kinesiol. Mech. pathomechanics Hum. Mov., Baltimore, MD: Lippincott Williams & Wilkins; 2003, p. 66–75.

[2] Manicourt DH, Devogelaer JP, Thonar EJMA. Products of Cartilage Metabolism. In: Seibel MJ, Robins SP, Bilezikian JP, editors. Dyn. Bone Cartil. Metab., vol. 1, Burlington: Elsevier; 2006, p. 421–49.

[3] Buckwalter JA, Woo SL, Goldberg VM, Hadley EC, Booth F, Oegema TR, et al. Soft-tissue aging and musculoskeletal function. J Bone Jt Surg Am 1993;75:1533–48.

[4] Hootman JM, Helmick CG. Projections of US prevalence of arthritis and associated activity limitations. Arthritis Rheum 2006;54:226–9.

[5] Ateshian GA, Hung CT. Functional Properties of Native Articular Cartilage. In: Guilak F, Butler DL, Goldstein SA, Mooney DJ, editors. Funct. Tissue Eng., New York: Springer-Verlag; 2003, p. 46–68.

[6] Martel-Pelletier J, Boileau C, Pelletier J-P, Roughley PJ. Cartilage in normal and osteoarthritis conditions. Best Pract Res Clin Rheumatol 2008;22:351–84.

[7] Hardingham TE, Fosang AJ. Proteoglycans - Many Forms and Many Functions. Faseb J 1992;6:861–70.

[8] Hardingham TE. Proteoglycans and Glycosaminoglycans. In: Seibel MJ, Robins SP, Bilezikian JP, editors. Dyn. bone Cartil. Metab., Burlington: Elsevier Science; 2006, p. 85–98.

[9] Guilak F, Alexopoulos LG, Upton ML, Youn I, Choi JB, Cao L, et al. The pericellular matrix as a transducer of biomechanical and biochemical signals in articular cartilage. Ann New York Acad Sci Skelet Dev Remodel Heal Dis Aging 2006;1068:498–512.

[10] Engel J, Furthmayr H, Odermatt E, von der Mark H, Aumailley M, Fleischmajer R, et al. Structure and macromolecular organization of type VI collagen. Ann N Y Acad Sci 1985;460:25–37.

[11] Eyre D. Collagen of articular cartilage. Arthritis Res 2002;4:30–5.

[12] Vondermark K, Kirsch T, Nerlich A, Kuss A, Weseloh G, Gluckert K, et al. Type-X Collagen-Synthesis in Human Osteoarthritic Cartilage - Indication of Chondrocyte Hypertrophy. Arthritis Rheum 1992;35:806–11.

[13] Eyre DR, Wu JJ. Collagen of fibrocartilage: a distinctive molecular phenotype in bovine meniscus. FEBS Lett 1983;158:265–70.

[14] Mandelbaum BR, Browne JE, Fu F, Micheli L, Mosely JBJ, Erggelet C, et al. Articular Cartilage Lesions of the Knee. Am J Sport Med 1998;26:853–61.

[15] Paulsson M, Morgelin M, Wiedemann H, Beardmore-Gray M, Dunham D, Hardingham T, et al. Extended and globular protein domains in cartilage proteoglycans. Biochem J 1987;245:763–72.

[16] Buckwalter JA, Rosenberg LC. Electron-Microscopic Studies of Cartilage Proteoglycans - Direct Evidence for the Variable Length of the Chondroitin Sulfate-Rich Region of Proteoglycan Subunit Core Protein. J Biol Chem 1982;257:9830–9.

[17] Knudson CB, Knudson W. Cartilage proteoglycans. Semin Cell Dev Biol 2001;12:69–78.

[18] Hall AC, Horwitz ER, Wilkins RJ. The cellular physiology of articular cartilage. Exp Physiol 1996;81:535–45.

[19] Urban JPG, Hall AC, Gehl KA. Regulation of Matrix Synthesis Rates by the Ionic and Osmotic Environment of Articular Chondrocytes. J Cell Physiol 1993;154:262–70.

[20] Roughley PJ. The structure and function of cartilage proteoglycans. Eur Cell Mater 2006;12:92–101.

[21] Knudson CB. Hyaluronan Receptor-Directed Assembly of Chondrocyte Pericellular Matrix. J Cell Biol 1993;120:825–34.

[22] Martin JA, Buckwalter JA. Aging, articular cartilage chondrocyte senescence and osteoarthritis. Biogerontology 2002;3:257–64.

[23] Nesic D, Whiteside R, Brittberg M, Wendt D, Martin I, Mainil-Varlet P. Cartilage tissue engineering for degenerative joint disease. Adv Drug Deliv Rev 2006;58:300–22.

[24] Forsyth CB, Cole A, Murphy G, Bienias JL, Im HJ, Loeser RF. Increased matrix metalloproteinase-13 production with aging by human articular chondrocytes in response to catabolic stimuli. Journals Gerontol Ser a-Biological Sci Med Sci 2005;60:1118–24.

[25] Mok SS, Masuda K, Hauselmann HJ, Aydelotte MB, Thonar EJMA. Aggrecan Synthesized by Mature Bovine Chondrocytes Suspended in Alginate - Identification of 2 Distinct Metabolic Matrix Pools. J Biol Chem 1994;269:33021–7.

[26] Hauselmann HJ, Masuda K, Hunziker EB, Neidhart M, Mok SS, Michel BA, et al. Adult human chondrocytes cultured in alginate form a matrix similar to native human articular cartilage. Am J Physiol Physiol 1996;271:C742–C752.

[27] Wu W, Billinghurst RC, Pidoux I, Antoniou J, Zukor D, Tanzer M, et al. Sites of collagenase cleavage and denaturation of type II collagen in aging and osteoarthritic articular cartilage and their relationship to the distribution of matrix metalloproteinase 1 and matrix metalloproteinase 13. Arthritis Rheum 2002;46:2087–94.

[28] Edwards DR, Porter S, Clark IM, Kevorkian L. The ADAMTS metalloproteinases. Biochem J 2005;386:15–27.

[29] Caterson B, Flannery CR, Hughes GE, Little CB. Mechanisms involved in cartilage proteoglycan catabolism. Matrix Biol 2000;19:333–44.

[30] Nagase H, Kashiwagi M. Aggrecanases and cartilage matrix degradation. Arthritis Res Ther 2003;5:94–103.

[31] Fosang AJ, Last K, Stanton H, Weeks DB, Campbell IK, Hardingham TE, et al. Generation and novel distribution of matrix metalloproteinase-derived aggrecan fragments in porcine cartilage explants. J Biol Chem 2000;275:33027–37.

[32] Sandy JD. A contentious issue finds some clarity: on the independent and complementary roles of aggrecanase activity and MMP activity in human joint aggrecanolysis. Osteoarthritis Cartilage 2006;14:95–100.

[33] Fosang AJ, Last K, Maciewicz RA. Aggrecan is degraded by matrix metalloproteinases in human arthritis - Evidence that matrix metalloproteinase and aggrecanase activities can be independent. J Clin Invest 1996;98:2292–9.

[34] Fosang AJ, Last K, Knauper V, Murphy G, Neame PJ. Degradation of cartilage aggrecan by collagenase-3 (MMP-13). Febs Lett 1996;380:17–20.

[35] Durigova M, Nagase H, Mort JS, Roughley PJ. MMPs are less efficient than ADAMTS5 in cleaving aggrecan core protein. Matrix Biol 2011;30:145–53.

[36] Fosang AJ, Neame PJ, Hardingham TE, Murphy G, Hamilton JA. Cleavage of cartilage proteoglycan between G1 and G2 domains by stromelysins. J Biol Chem 1991;266:15579–82.

[37] Flannery CR, Lark MW, Sandy JD. Identification of a stromelysin cleavage site within the interglobular domain of human aggrecan. Evidence for proteolysis at this site in vivo in human articular cartilage. J Biol Chem 1992;267:1008–14.

[38] Lark MW, Gordy JT, Weidner JR, Ayala J, Kimura JH, Williams HR, et al. Cell-mediated Catabolism of Aggrecan. J Biol Chem 1995;270:2550–6.

[39] Ilic MZ, Handley CJ, Robinson HC, Mok MT. Mechanism of Catabolism of Aggrecan by Articular Cartilage. Arch Biochem Biophys 1992;294:115–22.

[40] McCormick A, Campisi J. Cellular aging and senescence. Curr Opin Cell Biol 1991;3:230–4.

[41] Carlo Jr. MD, Loeser RF. Increased oxidative stress with aging reduces chondrocyte survival: correlation with intracellular glutathione levels. Arthritis Rheum 2003;48:3419–30.

[42] Stockwell RA. The Cell Density of Human Articular and Costal Cartilage. J Anat 1967;101:753–63.

[43] Loeser RF. Molecular Mechanisms of Cartilage Destruction: Mechanics, Inflammatory Mediators, and Aging Collide. Arthritis Rheum 2006;54:1357–60.

[44] Bayliss MT, Howat S, Davidson C, Dudhia J. The organization of aggrecan in human articular cartilage - Evidence for age-related changes in the rate of aggregation of newly synthesized molecules. J Biol Chem 2000;275:6321–7.

[45] Verbruggen G, Cornelissen M, Almqvist KF, Wang L, Elewaut D, Broddelez C, et al. Influence of aging on the synthesis and morphology of the aggrecans synthesized by differentiated human articular chondrocytes. Osteoarthr Cartil 2000;8:170–9.

[46] Sztrolovics R, Alini M, Roughley PJ, Mort JS. Aggrecan degradation in human intervertebral disc and articular cartilage. Biochem J 1997;326:235–41.

[47] Sandy JD, Plaas AHK. Age-Related-Changes in the Kinetics of Release of Proteoglycans from Normal Rabbit Cartilage Explants. J Orthop Res 1986;4:263–72.

[48] Pratta MA, Tortorella MD, Arner EC. Age-related changes in aggrecan glycosylation affect cleavage by aggrecanase. J Biol Chem 2000;275:39096–102.

[49] Billinghurst RC, Dahlberg L, Ionescu M, Reiner A, Bourne R, Rorabeck C, et al. Enhanced cleavage of type II collagen by collagenases in osteoarthritic articular cartilage. J Clin Invest 1997;99:1534–45.

[50] Struglics A, Larsson S, Hansson M, Lohmander LS. Western blot quantification of aggrecan fragments in human synovial fluid indicates differences in fragment patterns between joint diseases. Osteoarthr Cartil 2009;17:497–506.

[51] Middleton J, Manthey A, Tyler J. Insulin-like growth factor (IGF) receptor, IGF-I, interleukin-1 beta (IL-1 beta), and IL-6 mRNA expression in osteoarthritic and normal human cartilage. J Histochem Cytochem 1996;44:133–41.

[52] Buckwalter JA, Mankin HJ, Grodzinsky AJ. Articular Cartilage and Osteoarthritis. AAOS Instr Course Lect 2005;54:465–80.

[53] Gelber AC. Joint Injury in Young Adults and Risk for Subsequent Knee and Hip Osteoarthritis. Ann Intern Med 2000;133:321.

[54] Lohmander LS, Ionescu M, Jugessur H, Poole AR. Changes in joint cartilage aggrecan after knee injury and in osteoarthritis. Arthritis Rheum 1999;42:534–44.

[55] Mollon B, Kandel R, Chahal J, Theodoropoulos J. The clinical status of cartilage tissue regeneration in humans. Osteoarthritis Cartilage 2013;21:1824–33.

[56] Goldberg VM, Buckwalter JA. Hyaluronans in the treatment of osteoarthritis of the knee: evidence for disease-modifying activity. Osteoarthr Cartil 2005;13:216–24.

[57] Maffulli N, Longo UG, Gougoulias N, Loppini M, Denaro V. Long-term health outcomes of youth sports injuries. Br J Sports Med 2010;44:21–5.

[58] Levy AS, Lohnes J, Sculley S, LeCroy M, Garrett W. Chondral Delamination of the Knee in Soccer Players. Am J Sports Med 1996;24:634–9.

[59] Vanlauwe J, Almqvist F, Bellemans J, Huskin JP, Verdonk R, Victor J. Repair of symptomatic cartilage lesions of the knee The place of autologous chondrocyte implantation. Acta Orthop Belg 2007;73:145–58.

[60] Bekkers JEJ, Inklaar M, Saris DBF. Treatment selection in articular cartilage lesions of the knee: a systematic review. Am J Sports Med 2009;37 Suppl 1:148S–55S.

[61] Richardson JB, Caterson B, Evans EH, Ashton BA, Roberts S. Repair of human articular cartilage after implantation of autologous chondrocytes. J Bone Jt Surgery-British Vol 1999;81B:1064–8.

[62] Gillogly SD, Myers TH. Treatment of full-thickness chondral defects with autologous chondrocyte implantation. Orthop Clin North Am 2005;36:433–46.

[63] Samuelson EM, Brown DE. Cost-effectiveness analysis of autologous chondrocyte implantation: a comparison of periosteal patch versus type I/III collagen membrane. Am J Sports Med 2012;40:1252–8.

[64] Bartlett W, Skinner JA, Gooding CR, Carrington RWJ, Flanagan AM, Briggs TWR, et al. Autologous chondrocyte implantation versus matrix-induced autologous chondrocyte implantation for osteochondral defects of the knee: a prospective, randomised study. J Bone Joint Surg Br 2005;87:640–5.

[65] Brittberg M. Cell carriers as the next generation of cell therapy for cartilage repair: a review of the matrix-induced autologous chondrocyte implantation procedure. Am J Sports Med 2010;38:1259–71.

[66] Kon E, Verdonk P, Condello V, Delcogliano M, Dhollander A, Filardo G, et al. Matrix-Assisted Autologous Chondrocyte Transplantation for the Repair of Cartilage Defects of the Knee Systematic Clinical Data Review and Study Quality Analysis. Am J Sports Med 2009;37:156S–166S.

[67] Perera JR, Gikas PD, Bentley G. The present state of treatments for articular cartilage defects in the knee. Ann R Coll Surg Engl 2012;94:381–7.

[68] Schnabel M, Marlovits S, Eckhoff G, Fichtel I, Gotzen L, Vécsei V, et al. Dedifferentiation-associated changes in morphology and gene expression in primary human articular chondrocytes in cell culture. Osteoarthritis Cartilage 2002;10:62–70.

[69] Tuan RS. Stemming cartilage degeneration: adult mesenchymal stem cells as a cell source for articular cartilage tissue engineering. Arthritis Rheum 2006;54:3075–8.

[70] Ichinose S, Yamagata K, Sekiya I, Muneta T, Tagami M. Detailed examination of cartilage formation and endochondral ossification using human mesenchymal stem cells. Clin Exp Pharmacol Physiol 2005;32:561–70.

[71] Guilak F, Awad HA, Fermor B, Leddy HA, Gimble JA. Adipose-derived adult stem cells for cartilage tissue engineering. Biorheology 2004;41:389–99.

[72] Koay EJ, Hoben GMB, Athanasiou KA. Tissue engineering with chondrogenically differentiated human embryonic stem cells. Stem Cells 2007;25:2183–90.

[73] Drukker M, Benvenisty N. The immunogenicity of human embryonic stem-derived cells. Trends Biotechnol 2004;22:136–41.

[74] Wei Y, Zeng W, Wan R, Wang J, Zhou Q, Qiu S, et al. Chondrogenic Differentiation of Induced Pluripotent Stem Cells from Osteoarthritc Chondrocytes in Alginate Matrix. Eur Cell Mater 2012;23:1–12.

[75] Darling EM, Athanasiou KA. Retaining zonal chondrocyte phenotype by means of novel growth environments. Tissue Eng 2005;11:395–403.

[76] Wakitani S, Goto T, Pineda S, Young R, Mansour J, Caplan A, et al. Mesenchymal cell-based repair of large, full-thickness defects of articular cartilage. J Bone Jt Surg 1994;76:579–92.

[77] Nicodemus GD, Bryant SJ. Cell encapsulation in biodegradable hydrogels for tissue engineering applications. Tissue Eng Part B-Reviews 2008;14:149–65.

[78] Kim IL, Mauck RL, Burdick JA. Hydrogel design for cartilage tissue engineering: A case study with hyaluronic acid. Biomaterials 2011;32:8771–82.

[79] Burdick JA, Chung C, Jia XQ, Randolph MA, Langer R. Controlled degradation and mechanical behavior of photopolymerized hyaluronic acid networks. Biomacromolecules 2005;6:386–91.

[80] Burdick JA, Prestwich GD. Hyaluronic Acid Hydrogels for Biomedical Applications. Adv Mater 2011;23:H41–H56.

[81] Shu XZ, Liu Y, Luo Y, Roberts MC, Prestwich GD. Disulfide Cross-Linked Hyaluronan Hydrogels. Biomacromolecules 2002;3:1304–11.

[82] Mauck RL, Seyhan SL, Ateshian GA, Hung CT. Influence of seeding density and dynamic deformational loading on the developing structure/function relationships of chondrocyte-seeded agarose hydrogels. Ann Biomed Eng 2002;30:1046–56.

[83] Mauck RL, Soltz MA, Wang CCB, Wong DD, Chao PHG, Valhmu WB, et al. Functional tissue engineering of articular cartilage through dynamic loading of chondrocyte-seeded agarose gels. J Biomech Eng Asme 2000;122:252–60.

[84] Kelly TAN, Ng KW, Wang CCB, Ateshian GA, Hung CT. Spatial and temporal development of chondrocyte-seeded agarose constructs in free-swelling and dynamically loaded cultures. J Biomech 2006;39:1489–97.

[85] Byers BA, Mauck RL, Chiang IE, Tuan RS. Transient exposure to transforming growth factor beta 3 under serum-free conditions enhances the biomechanical and biochemical maturation of tissue-engineered cartilage. Tissue Eng Part A 2008;14:1821–34.

[86] Athanasiou K, Agrawal C, Barber F, Burkhart S. Orthopaedic applications for PLA-PGA biodegradable polymers. Arthrosc J Arthrosc Relat Surg 1998;14:726–37.

[87] Athanasiou K. Sterilization, toxicity, biocompatibility and clinical applications of polylactic acid/ polyglycolic acid copolymers. Biomaterials 1996;17:93–102.

[88] Eyrich D, Wiese H, Maier G, Skodacek D, Appel B, Sarhan H, et al. In vitro and in vivo cartilage engineering using a combination of chondrocyte-seeded long-term stable fibrin gels and polycaprolactone-based polyurethane scaffolds. Tissue Eng 2007;13:2207–18.

[89] Slaughter BV, Khurshid SS, Fisher OZ, Khademhosseini A, Peppas NA. Hydrogels in regenerative medicine. Adv Mater 2009;21:3307–29.

[90] Nuttelman CR, Rice MA, Rydholm AE, Salinas CN, Shah DN, Anseth KS. Macromolecular monomers for the synthesis of hydrogel niches and their application in cell encapsulation and tissue engineering. Prog Polym Sci 2008;33:167–79.

[91] Ifkovits JL, Burdick JA. Review: photopolymerizable and degradable biomaterials for tissue engineering applications. Tissue Eng 2007;13:2369–85.

[92] West JL, Nguyen KT. Photopolymerizable hydrogels for tissue engineering applications. Biomaterials 2002;23:4307–14.

[93] Bryant SJ, Anseth KS. Photopolymerization of Hydrogel Scaffolds. In: Ma PX, Elisseeff JH, editors. Scaffolding Tissue Eng., Boca Raton, FL: CRC Press, Inc.; 2006, p. 71–90.

[94] Anseth KS, Kloxin AM, Kloxin CJ, Bowman CN. Mechanical Properties of Cellularly Responsive Hydrogels and Their Experimental Determination. Adv Mater 2010;22:3484–94.

[95] Bryant SJ, Durand KL, Anseth KS. Manipulations in hydrogel chemistry control photoencapsulated chondrocyte behavior and their extracellular matrix production. J Biomed Mater Res Part A 2003;67A:1430–6.

[96] Bryant SJ, Anseth KS. Hydrogel properties influence ECM production by chondrocytes photoencapsulated in poly(ethylene glycol) hydrogels. J Biomed Mater Res 2002;59:63–72.

[97] Bryant SJ, Bender RJ, Durand KL, Anseth KS. Encapsulating Chondrocytes in degrading PEG hydrogels with high modulus: Engineering gel structural changes to facilitate cartilaginous tissue production. Biotechnol Bioeng 2004;86:747–55.

[98] Lynn AD, Blakney AK, Kyriakides TR, Bryant SJ. Temporal progression of the host response to implanted poly(ethylene glycol)-based hydrogels. J Biomed Mater Res Part A 2011;96A:621–31.

[99] Nicodemus GD, Skaalure SC, Bryant SJ. Gel structure has an impact on pericellular and extracellular matrix deposition, which subsequently alters metabolic activities in chondrocyte-laden PEG hydrogels. Acta Biomater 2011;7:492–504.

[100] Mason MN, Metters AT, Bowman CN, Anseth KS. Predicting controlled-release behavior of degradable PLA-b-PEG-b-PLA hydrogels. Macromolecules 2001;34:4630–5.

[101] Gould ST, Darling NJ, Anseth KS. Small peptide functionalized thiol-ene hydrogels as culture substrates for understanding valvular interstitial cell activation and de novo tissue deposition. Acta Biomater 2012;8:3201–9.

[102] Anseth KS, Bryant SJ. Controlling the spatial distribution of ECM components in degradable PEG hydrogels for tissue engineering cartilage. J Biomed Mater Res Part A 2003;64A:70–9.

[103] Roberts JJ, Nicodemus GD, Greenwald EC, Bryant SJ. Degradation Improves Tissue Formation in (Un)Loaded Chondrocyte-laden Hydrogels. Clin Orthop Relat Res 2011.

[104] Metters AT, Anseth KS, Bowman CN. Fundamental studies of a novel, biodegradable PEG-b-PLA hydrogel. Polymer (Guildf) 2000;41:3993–4004.

[105] Anseth KS, Metters AT, Bryant SJ, Martens PJ, Elisseeff JH, Bowman CN. In situ forming degradable networks and their application in tissue engineering and drug delivery. J Control Release 2002;78:199–209.

[106] Bryant SJ, Davis-Arehart KA, Luo N, Shoemaker RK, Arthur JA, Anseth KS. Synthesis and Characterization of Photopolymerized Multifunctional Hydrogels: Water-Soluble Poly(Vinyl Alcohol) and Chondroitin Sulfate Macromers for Chondrocyte Encapsulation. Macromolecules 2004;37:6726–33.

[107] Li Q, Williams CG, Sun DDN, Wang J, Leong K, Elisseeff JH. Photocrosslinkable polysaccharides based on chondroitin sulfate. J Biomed Mater Res Part A 2004;68A:28–33.

[108] Prestwich GD, Marecak DM, Marecek JF, Vercruysse KP, Ziebell MR. Controlled chemical modification of hyaluronic acid: synthesis, applications, and biodegradation of hydrazide derivatives. J Control Release 1998;53:93–103.

[109] Chung C, Erickson IE, Mauck RL, Burdick JA. Differential behavior of auricular and articular chondrocytes in hyaluronic acid hydrogels. Tissue Eng Part A 2008;14:1121–31.

[110] Chung C, Burdick JA. Influence of Three-Dimensional Hyaluronic Acid Microenvironments on Mesenchymal Stem Cell Chondrogenesis. Tissue Eng Part A 2009;15:243–54.

[111] Stern R, Asari AA, Sugahara KN. Hyaluronan fragments: An information-rich system. Eur J Cell Biol 2006;85:699–715.

[112] Zhu JM. Bioactive modification of poly(ethylene glycol) hydrogels for tissue engineering. Biomaterials 2010;31:4639–56.

[113] West JL, Hubbell JA. Polymeric Biomaterials with Degradation Sites for Proteases Involved in Cell Migration. Macromolecules 1999;32:241–4.

[114] Park Y, Lutolf MP, Hubbell JA, Hunziker EB, Wong M, et al. Bovine Primary Chondrocyte Culture in Synthetic Matrix Hydrogels as a Scaffold for Cartilage Repair 2004;10.

[115] Lutolf MP, Lauer-Fields JL, Schmoekel HG, Metters AT, Weber FE, Fields GB, et al. Synthetic matrix metalloproteinase-sensitive hydrogels for the conduction of tissue regeneration: engineering cell-invasion characteristics. Proc Natl Acad Sci U S A 2003;100:5413–8.

[116] Lutolf MP, Raeber GP, Zisch AH, Tirelli N, Hubbell JA. Cell-Responsive Synthetic Hydrogels. Adv Mater 2003;15:888–92.

[117] West JL, Lee SH, Miller JS, Moon JJ. Proteolytically degradable hydrogels with a fluorogenic substrate for studies of cellular proteolytic activity and migration. Biotechnol Prog 2005;21:1736–41.

[118] Bahney CS, Hsu C-W, Yoo JU, West JL, Johnstone B. A bioresponsive hydrogel tuned to chondrogenesis of human mesenchymal stem cells. FASEB J 2011;25:1486–96.

[119] Patterson J, Hubbell JA. Enhanced proteolytic degradation of molecularly engineered PEG hydrogels in response to MMP-1 and MMP-2. Biomaterials 2010;31:7836–45.

[120] Fairbanks BD, Schwartz MP, Halevi AE, Nuttelman CR, Bowman CN, Anseth KS. A Versatile Synthetic Extracellular Matrix Mimic via Thiol-Norbornene Photopolymerization. Adv Mater 2009;21:5005–10.

[121] Aimetti AA, Machen AJ, Anseth KS. Poly(ethylene glycol) hydrogels formed by thiol-ene photopolymerization for enzyme-responsive protein delivery. Biomaterials 2009;30:6048–54.

[122] Park Y, Lutolf MP, Hubbell JA, Hunziker EB, Wong M. Bovine primary chondrocyte culture in synthetic matrix metalloproteinase-sensitive poly(ethylene glycol)-based hydrogels as a scaffold for cartilage repair. Tissue Eng 2004;10:515–22.

[123] Johnstone B, Bahney CS, Hsu CW, Yoo JU, West JL. A bioresponsive hydrogel tuned to chondrogenesis of human mesenchymal stem cells. Faseb J 2011;25:1486–96.

[124] Roberts JJ, Bryant SJ. Comparison of photopolymerizable thiol-ene PEG and acrylate-based PEG hydrogels for cartilage development. Biomaterials 2013.

[125] Villanueva I, Bishop NL, Bryant SJ. Medium Osmolarity and Pericellular Matrix Development Improves Chondrocyte Survival When Photoencapsulated in Poly(Ethylene Glycol) Hydrogels at Low Densities. Tissue Eng Part A 2009;15:3037–48.

[126] Amin AK, Huntley JS, Bush PG, Simpson AHRW, Hall AC. Osmolarity influences chondrocyte death in wounded articular cartilage. J Bone Jt Surgery-American Vol 2008;90A:1531–42.

[127] Vinatier C, Mrugala D, Jorgensen C, Guicheux J, Noel D. Cartilage engineering: a crucial combination of cells, biomaterials and biofactors. Trends Biotechnol 2009;27:307–14.

[128] Domm C, Schünke M, Christesen K, Kurz B. Redifferentiation of dedifferentiated bovine articular chondrocytes in alginate culture under low oxygen tension. Osteoarthritis Cartilage 2002;10:13–22.

[129] Waldman SD, Couto DC, Grynpas MD, Pilliar RM, Kandel RA. A single application of cyclic loading can accelerate matrix deposition and enhance the properties of tissue-engineered cartilage. Osteoarthr Cartil 2006;14:323–30.

[130] Bian L, Zhai DY, Zhang EC, Mauck RL, Burdick JA. Dynamic Compressive Loading Enhances Cartilage Matrix Synthesis and Distribution and Suppresses Hypertrophy in hMSC-Laden Hyaluronic Acid Hydrogels. Tissue Eng Part A 2012;18:715–24.

[131] Bryant SJ, Nicodemus GD. Mechanical loading regimes affect the anabolic and catabolic activities by chondrocytes encapsulated in PEG hydrogels. Osteoarthr Cartil 2010;18:126–37.

[132] De Croos JNA, Dhaliwal SS, Grynpas MD, Pilliar RM, Kandel RA. Cyclic compressive mechanical stimulation induces sequential catabolic and anabolic gene changes in chondrocytes resulting in increased extracellular matrix accumulation. Matrix Biol 2006;25:323–31.

[133] Kisiday JD, Lee JH, Siparsky PN, Frisbie DD, Flannery CR, Sandy JD, et al. Catabolic Responses of Chondrocyte-Seeded Peptide Hydrogel to Dynamic Compression. Ann Biomed Eng 2009;37:1368–75.

[134] Farnsworth NL, Antunez LR, Bryant SJ. Dynamic compressive loading differentially regulates chondrocyte anabolic and catabolic activity with age. Biotechnol Bioeng 2013;110:2046–57.

[135] DeLong SA, Moon JJ, West JL. Covalently immobilized gradients of bFGF on hydrogel scaffolds for directed cell migration. Biomaterials 2005;26:3227–34.

[136] McCall JD, Anseth KS. Thiol-ene photopolymerizations provide a facile method to encapsulate proteins and maintain their bioactivity. Biomacromolecules 2012;13:2410–7.

[137] McCall JD, Luoma JE, Anseth KS. Covalently tethered transforming growth factor beta in PEG hydrogels promotes chondrogenic differentiation of encapsulated human mesenchymal stem cells. Drug Deliv Transl Res 2012;2:305–12.

[138] Mann BK, Schmedlen RH, West JL. Tethered-TGF-β increases extracellular matrix production of vascular smooth muscle cells. Biomaterials 2001;22:439–44.

[139] Kawasaki K, Ochi M, Uchio Y, Adachi N, Matsusaki M. Hyaluronic acid enhances proliferation and chondroitin sulfate synthesis in cultured chondrocytes embedded in collagen gels. J Cell Physiol 1999;179:142–8.

[140] Lindenhayn K, Perka C, Spitzer R, Heilmann H, Pommerening K, Mennicke J, et al. Retention of hyaluronic acid in alginate beads: aspects for in vitro cartilage engineering. J Biomed Mater Res 1999;44:149–55.

[141] Bryant SJ, Villanueva I, Gladem SK, Kessler J. Dynamic loading stimulates chondrocyte biosynthesis when encapsulated in charged hydrogels prepared from poly(ethylene glycol) and chondroitin sulfate. Matrix Biol 2010;29:51–62.

[142] Roberts JJ, Nicodemus GD, Giunta S, Bryant SJ. Incorporation of biomimetic matrix molecules in PEG hydrogels enhances matrix deposition and reduces load-induced loss of chondrocyte-secreted matrix. J Biomed Mater Res Part A 2011;97A:281–91.

[143] Bryant SJ, Anseth KS. Hydrogel properties influence ECM production by chondrocytes photoencapsulated in poly(ethylene glycol) hydrogels. J Biomed Mater Res 2002;59:63–72.

[144] Nicodemus GD, Skaalure SC, Bryant SJ. Gel structure has an impact on pericellular and extracellular matrix deposition, which subsequently alters metabolic activities in chondrocyte-laden PEG hydrogels. Acta Biomater 2011;7:492–504.

[145] Chung C, Beecham M, Mauck RL, Burdick JA. The influence of degradation characteristics of hyaluronic acid hydrogels on in vitro neocartilage formation by mesenchymal stem cells. Biomaterials 2009;30:4287–96.

[146] Roberts JJ, Nicodemus GD, Greenwald EC, Bryant SJ. Degradation Improves Tissue Formation in (Un)Loaded Chondrocyte-laden Hydrogels. Clin Orthop Relat Res 2011.

[147] Skaalure SC, Milligan IL, Bryant SJ. Age impacts extracellular matrix metabolism in chondrocytes encapsulated in degradable hydrogels. Biomed Mater 2012;7.

[148] Tran-Khanh N, Hoemann CD, McKee MD, Henderson JE, Buschmann MD. Aged bovine chondrocytes display a diminished capacity to produce a collagen-rich, mechanically functional cartilage extracellular matrix. J Orthop Res 2005;23:1354–62.

[149] Kloxin AM, Kloxin CJ, Bowman CN, Anseth KS. Mechanical Properties of Cellularly Responsive Hydrogels and Their Experimental Determination. Adv Mater 2010;22:3484–94.

Chapter 2

Objectives

Autologous cell-based tissue engineering therapies are extremely promising for regenerating damaged cartilage in order to prevent osteoarthritis, however current clinically applied therapies are only indicated for younger patients [1]. Because cartilage degeneration and the progression to osteoarthritis are most associated with patient aging, cell-based cartilage tissue engineering must be expanded to a wider age range in order to address the clinical need. New research into matrix-assisted autologous cell therapies provides an opportunity to design scaffolds tailored to the patient's cells [2], and PEG-based degradable hydrogel scaffolds are promising cell carriers because they are photopolymerizable, injectable, and support cartilaginous matrix production [3–7], and they can be easily tailored to introduce different degradable functionalities [8,9]. Degradation is an essential scaffold characteristic in order to promote new cartilaginous matrix formation by encapsulated cartilage cells (chondrocytes), effectively regenerating a cartilaginous tissue that is identical to the patient's native cartilage.

This research tests the overall hypothesis that PEG hydrogels incorporating tunable degradation and bioactive modifications to mimic the native tissue environment enhance cartilaginous matrix production and elaboration by chondrocytes isolated from different aged donors. The long-term project aim is to create a highly tunable degradable hydrogel platform that supports cartilaginous matrix production by chondrocytes isolated from donors of any age, in order to expand current autologous cell-based tissue engineering therapies. The following research objectives were proposed in order to test this hypothesis:

2.1 Objective 1

The first objective of this thesis was to determine the effect of donor age on cartilaginous neotissue production and metabolism in hydrolytically degradable PEG hydrogels, which represent a simple, bulk-degrading platform. Juvenile chondrocytes (isolated from skeletally immature donors) and adult chondrocytes (isolated from skeletally mature donors) exhibited different metabolic behavior in mechanically loaded non-degradable PEG hydrogels and in agarose hydrogels [10,11], therefore it was hypothesized that adult chondrocytes would exhibit decreased anabolic and increased catabolic activity compared to juvenile chondrocytes within hydrolytically degradable PEG hydrogels. To evaluate the effects of cell donor age on matrix metabolism, both juvenile and adult chondrocytes were encapsulated in hydrolytically degradable PEG hydrogels, and matrix production and elaboration were assessed quantitatively and qualitatively, while matrix catabolism was assessed by Western blots to probe for degraded extracellular matrix fragments.

2.2 Objective 2

The second objective of this thesis was to enhance cellularity (viability and proliferation) and matrix production by adult chondrocytes in hydrolytically degradable PEG hydrogels by mimicking the native environment through: (a) entrapping hyaluronic acid, and (b) manipulating osmolarity of the culture medium. The results from objective 1 indicated that adult chondrocytes were more limited in their ability to produce and retain extracellular matrix, and that matrix catabolism was elevated, therefore the degradable PEG platform was bioactively modified in an attempt to overcome these limitations. It was hypothesized that adding bioactive modifications intended to mimic the native environment to degradable PEG hydrogels would improve cellularity (viability and proliferation) and matrix production by encapsulated adult chondrocytes.

2.2.1 Objective 2a

The first sub-objective was to investigate the effects of incorporating the native extracellular matrix molecule hyaluronic acid (HA) into degradable PEG hydrogels to create a cartilage mimetic environment. HA plays a role in matrix assembly and has also been shown to

improve matrix production and proliferation [12,13], but the effects of HA are highly dependent on its molecular weight [14]. It was hypothesized that entrapping the native matrix molecule hyaluronic acid into degradable PEG hydrogels would improve cellularity and matrix production by encapsulated adult chondrocytes, and that higher concentrations of high MW HA would lead to the largest improvements. A semi-interpenetrating network was formed to introduce hyaluronic acid (of varying molecular weight and concentration) into hydrolytically degradable PEG hydrogels to create a cartilage mimetic hydrogel, and cell-laden hydrogels were assessed for cellularity, matrix production, and catabolic activity.

2.2.2 Objective 2b

The second sub-objective was to investigate the effects of increasing the culture medium osmolarity to physiologically relevant levels to better mimic native cartilage. Cartilage osmolarity is elevated compared to most tissues and compared to standard chondrocyte culture medium [15], and previous studies demonstrated improved chondrocyte survival and matrix production by elevated culture medium osmolarity in short-term experiments [15–17]. It was hypothesized that elevating the culture medium osmolarity to match physiological levels would increase long-term matrix production by adult chondrocytes. Cell-laden hydrolytically degradable PEG hydrogels were cultured in a physiologically relevant osmotic environment (achieved by adding either salts or sucrose to the culture medium) and cellularity, matrix production, and catabolic activity were assessed.

2.3 Objective 3

The third objective of this thesis was to develop and characterize a cartilage-specific enzymatically degradable PEG hydrogel. Because degradation in this system is cell-specified, it provides an opportunity to better tune hydrogel degradation to match the cell source, compared to bulk degrading systems. It was hypothesized that cell-mediated degradable hydrogels would encourage matrix production and elaboration by chondrocytes from different aged donors, and that the localization of cell-mediated degradation could be experimentally controlled.

2.3.1 Objective 3a

The first sub-objective was to assess matrix production and metabolism by cells that exhibit different metabolic behavior within a novel cartilage-specific enzymatically degradable hydrogel. An enzymatically degradable peptide was synthesized based on a specific site of extracellular matrix degradation identified in objective 1, which was used as a crosslinker in a PEG-based thiol-norbornene hydrogel [18]. It was hypothesized that the enzymatically degradable hydrogel would encourage both matrix production and elaboration by chondrocytes from different aged donors that exhibit different metabolic activity, compared to non-degrading hydrogels.

2.3.2 Objective 3b

The second sub-objective was to characterize the degradation behavior within enzymatically degradable hydrogels. Computational models that simulate enzymatically degradable hydrogels predicted that degradation in these systems could be either reaction- or diffusion-dominated, where the former results in localized degradation surrounding cells, and the latter results in bulk degradation [19,20]. To probe how hydrogel structure affects degradation characteristics, but in the absence of matrix-producing cells, an experimental model system was developed implementing enzyme-laden microspheres to mimic enzyme release from cells. It was hypothesized that reaction- or diffusion-dominated degradation could be experimentally controlled by varying the initial hydrogel crosslink density, when degradation kinetics are constant.

2.4 References

[1] Gillogly SD, Myers TH. Treatment of full-thickness chondral defects with autologous chondrocyte implantation. Orthop Clin North Am 2005;36:433–46.

[2] Kon E, Verdonk P, Condello V, Delcogliano M, Dhollander A, Filardo G, et al. Matrix-assisted autologous chondrocyte transplantation for the repair of cartilage defects of the

knee: systematic clinical data review and study quality analysis. Am J Sports Med 2009;37 Suppl 1:156S–66S.

[3] Bryant SJ, Anseth KS. Hydrogel properties influence ECM production by chondrocytes photoencapsulated in poly(ethylene glycol) hydrogels. J Biomed Mater Res 2002;59:63–72.

[4] Anseth KS, Bryant SJ. Controlling the spatial distribution of ECM components in degradable PEG hydrogels for tissue engineering cartilage. J Biomed Mater Res Part A 2003;64A:70–9.

[5] Roberts JJ, Nicodemus GD, Greenwald EC, Bryant SJ. Degradation Improves Tissue Formation in (Un)Loaded Chondrocyte-laden Hydrogels. Clin Orthop Relat Res 2011.

[6] Bryant SJ, Durand KL, Anseth KS. Manipulations in hydrogel chemistry control photoencapsulated chondrocyte behavior and their extracellular matrix production. J Biomed Mater Res Part A 2003;67A:1430–6.

[7] Bryant SJ, Bender RJ, Durand KL, Anseth KS. Encapsulating Chondrocytes in degrading PEG hydrogels with high modulus: Engineering gel structural changes to facilitate cartilaginous tissue production. Biotechnol Bioeng 2004;86:747–55.

[8] Zhu JM. Bioactive modification of poly(ethylene glycol) hydrogels for tissue engineering. Biomaterials 2010;31:4639–56.

[9] Kloxin AM, Kloxin CJ, Bowman CN, Anseth KS. Mechanical Properties of Cellularly Responsive Hydrogels and Their Experimental Determination. Adv Mater 2010;22:3484–94.

[10] Farnsworth NL, Antunez LR, Bryant SJ. Dynamic compressive loading differentially regulates chondrocyte anabolic and catabolic activity with age. Biotechnol Bioeng 2013;110:2046–57.

[11] Tran-Khanh N, Hoemann CD, McKee MD, Henderson JE, Buschmann MD. Aged bovine chondrocytes display a diminished capacity to produce a collagen-rich, mechanically functional cartilage extracellular matrix. J Orthop Res 2005;23:1354–62.

[12] Knudson CB, Knudson W. Cartilage proteoglycans. Semin Cell Dev Biol 2001;12:69–78.

[13] Kawasaki K, Ochi M, Uchio Y, Adachi N, Matsusaki M. Hyaluronic acid enhances proliferation and chondroitin sulfate synthesis in cultured chondrocytes embedded in collagen gels. J Cell Physiol 1999;179:142–8.

[14] Stern R, Asari AA, Sugahara KN. Hyaluronan fragments: An information-rich system. Eur J Cell Biol 2006;85:699–715.

[15] Urban JPG, Hall AC, Gehl KA. Regulation of Matrix Synthesis Rates by the Ionic and Osmotic Environment of Articular Chondrocytes. J Cell Physiol 1993;154:262–70.

[16] Villanueva I, Bishop NL, Bryant SJ. Medium Osmolarity and Pericellular Matrix Development Improves Chondrocyte Survival When Photoencapsulated in Poly(Ethylene Glycol) Hydrogels at Low Densities. Tissue Eng Part A 2009;15:3037–48.

[17] Xu X, Urban JPG, Tirlapur UK, Cui Z. Osmolarity effects on bovine articular chondrocytes during three-dimensional culture in alginate beads. Osteoarthr Cartil 2010;18:433–9.

[18] Fairbanks BD, Schwartz MP, Halevi AE, Nuttelman CR, Bowman CN, Anseth KS. A Versatile Synthetic Extracellular Matrix Mimic via Thiol-Norbornene Photopolymerization. Adv Mater 2009;21:5005–10.

[19] Vernerey FJ, Greenwald EC, Bryant SJ. Triphasic mixture model of cell-mediated enzymatic degradation of hydrogels. Comput Methods Biomech Biomed Engin 2012;15:1197–210.

[20] Dhote V, Vernerey FJ. Mathematical model of the role of degradation on matrix development in hydrogel scaffold. Biomech Model Mechanobiol 2014;13:167–83.

Chapter 3

Age Impacts Extracellular Matrix Metabolism in Chondrocytes Encapsulated in Degradable Hydrogels

As appearing in *Biomedical Materials* 2012

3.1 Abstract

Encapsulation of autologous adult cartilage cells (chondrocytes) in hydrolytically degradable hydrogels may provide a clinically viable tissue engineering therapy for replacement of damaged or osteoarthritic cartilage. When designing a tissue engineering scaffold, it is crucial to evaluate adult chondrocytes due to their limited growth potential. The objective for this study was to compare extracellular matrix anabolic and catabolic metabolism by juvenile and adult chondrocytes in hydrolytically degradable hydrogels. Cells were photo-encapsulated in bimodal degradable hydrogels composed of slow-degrading poly(ethylene glycol) (PEG) and the fast-degrading copolymer oligo(lactic acid)-*b*-PEG-*b*-oligo(lactic acid) crosslinks, and cultured through 4 weeks. Cell density was significantly higher in constructs containing adult cells, contributing to higher glycosaminoglycan (GAG) content per wet weight. However, juvenile cells exhibited higher collagen content per cell. Immunohistochemical visualization revealed cartilage-specific aggrecan and collagen II deposition by both adult and juvenile cells. Immunohistochemically-stained catabolically degraded collagen fragments and Western blot-detected degraded aggrecan fragments, especially those associated with an osteoarthritic state, were more abundant in constructs with adult cells. Overall, bimodal degradable hydrogel environments were supportive of viable adult cells. However, major challenges with adult cells include their reduced collagen productivity and high catabolic activity, which may impact the quality of the engineered tissues.

3.2 Introduction

Osteoarthritis is a degenerative disease characterized by a loss of cartilage in articular joints; causing severe pain, loss of mobility, and an overall diminished quality of life. Estimates of disease prevalence predict that by the year 2030, at least 25% of the adult population in the United States will suffer from osteoarthritis [1], indicative of a burgeoning burden on the health care system. The avascular nature of cartilage tissue means that there is limited potential for cartilage to self-repair, whereby any damage gone untreated will only worsen with time. Advanced clinical therapies such as Autologous Chondrocyte Implantation (ACI), which involves injecting autologous cartilage cells (chondrocytes) harvested from non-load-bearing areas of adult articular cartilage into the damaged portion of the tissue, has shown some success in young patients [2,3]. However, the effectiveness of this therapy diminishes as the patient age increases, representing a significant obstacle as the majority of patients are from a more mature demographic. We can hypothesize that injecting cells laden in a polymer scaffold carrier designed to promote tissue growth will improve tissue regeneration in older patients. However, as most cartilage tissue engineering research employs juvenile chondrocytes, there is little current understanding of the particular needs of adult chondrocytes in tissue engineering scaffolds. Due to the known changes that occur with age in native tissue, it can be hypothesized that synthesis of new extracellular matrix may be limited, and catabolic degradation of tissue may be elevated with age [4]. Towards developing a clinically viable therapy, it is imperative that we gain a better understanding of the tissue engineering potential of adult chondrocytes.

One promising tissue engineering system for replacement of cartilage damaged due to injury and the effects of osteoarthritis is cell-laden photopolymerizable and biodegradable hydrogels, which can be injected and polymerized *in situ*. Advantages of photopolymerization include the ability to perform minimally invasive surgeries, and use of materials that can flow to easily fill a tissue defect. Photopolymerization provides temporal control in the gelation process [5], and can be performed arthroscopically [6] or transdermally [7]. Biodegradation is a pre-

requisite in any tissue engineering system and is necessary to provide space for cells to deposit new extracellular matrix and form a macroscopic tissue. Indeed, it was previously demonstrated that chondrocytes encapsulated in non-or slow degrading photopolymerized hydrogels were restricted with increased gel crosslinking in their ability to deposit new matrix [8,9], while fast degrading photopolymerized hydrogels support macroscopic tissue evolution [10,11].

The use of PEG-based photopolymerizable hydrogels is advantageous due to the ease of functionalization, manipulation of the formulation to alter hydrogel properties [12] and their ability to maintain the chondrocyte phenotype [13–15]. Hydrolytically degradable PEG-based hydrogels that include oligo-lactic acid in the PEG crosslink have been well characterized for cartilage tissue engineering applications, showing improved tissue deposition by juvenile chondrocytes [11,13–15]. This hydrogel platform is particularly promising for designing photopolymerizable and biodegradable hydrogels for adult chondrocytes because it provides tunable hydrogel degradation through changes in the number of lactic acid units and overall crosslinking density, and copolymerization of macromolecular monomers (macromers) with different degradation rates [14,16].

Neotissue formed by chondrocytes encapsulated in hydrogels must be comprised of the main components of cartilage extracellular matrix (ECM), aggrecan and collagen II. Collagen II fibrils form a dense elastic mesh throughout the tissue, providing tensile strength and a structural meshwork to entrap aggrecan molecules [17]. Aggrecans are composed of a core protein associated with many (up to 300) negatively charged sulfated glycosaminoglycan (GAG) sidechains. Aggrecans assemble along hyaluronan filaments to form larger functional aggregates [18]. Cartilage ECM is extremely dynamic and constantly undergoes reorganization by catabolic enzymes known as matrix metalloproteinases (MMPs) and aggrecanases (ADAMTS). While catabolic activity is necessary for tissue reorganization, an imbalance of catabolic and anabolic activity is more likely to occur with age and is characteristic of an osteoarthritic disease state [19].

Juvenile cells are typically utilized in cartilage tissue engineering models due to their robustness, yet clinically applied therapies utilize autologous cells from adult patients [2,3]. Adult cells may be more difficult to employ in tissue engineered systems due to their diminished proliferation [20], lower viability [21] and cell density [22], decreased anabolic activity [4] and increased catabolic activity [23] in native tissue. The tissue composition itself is also different in adult cartilage, characterized by a more tightly crosslinked collagen network [24], altered aggrecan glycosylation patterns [25], and smaller, less glycosylated aggrecans and aggregates [4,26]. Despite these factors, little research has been conducted to investigate the tissue engineering potential of adult chondrocytes. A study comparing fetal, young, and adult bovine chondrocytes in agarose gels observed significant decreases in cell density, collagen, and GAG content with age [27]. This preliminary work suggests that encapsulating adult chondrocytes in any hydrogel system will present significant challenges.

In this study, the tissue engineering potential of adult chondrocytes in hydrolytically degradable PEG-based hydrogels was examined *in vitro* by comparing to juvenile chondrocytes. We employed bimodal degradable hydrogels formed by copolymerization of slow degrading PEG macromers with fast degrading PEG macromers as a means to provide more structural integrity to the hydrogels while maintaining the ability to degrade fully over the long term. Of particular interest were any differences in extracellular matrix production and organization, and catabolic activity. Our findings indicate that age of the cells, i.e. the age of the donor from which the cells were isolated, did affect extracellular matrix production and catabolic activity, both of which were elevated in gels containing adult cells. This study represents a step towards designing appropriate scaffolds to support adult chondrocytes that could be applied in a clinical setting, but identifies that high levels of catabolic activity may present challenges and should be investigated further.

3.3 Materials and Methods

3.3.1 Materials

D,L Lactides and Hoechst 33258 were from Polysciences, Inc. (Warrington, PA). Collagenase type II and papain were from Worthington Biochemical (Lakewood, NJ). Ethyl ether, ethylene diamine tetraacetic acid (EDTA), Triton X-100 and calcium chloride were from Fisher Scientific (Fair Lawn, NJ). Irgacure 2959 was from Ciba Specialty Chemicals (Tarrytown, NY). Fetal bovine serum (FBS) was from Atlanta Biologicals (Lawrenceville, GA). The LIVE/DEAD® assay, phosphate-buffered saline (PBS), penicillin-streptomycin (P/S), fungizone, gentamicin, HEPES buffer, minimal essential medium non-essential amino acids (MEM-NEAA), trypan blue, DAPI, AlexaFluor 488-conjugated goat anti-rabbit IgG, and AlexaFluor 546-conjugated goat anti-mouse IgG were from Invitrogen (Carlsbad, CA). Poly(ethylene glycol) MW 4600, methacrylic anhydride, L-proline, L-ascorbic acid, sodium chloride, potassium chloride, bovine serum albumin (BSA), dimethyl methylene blue (DMMB), chondroitinase ABC, hyaluronidase, lipopolysaccharides (LPS) from *S. enterica*, Tris-HCl and sodium azide were from Sigma-Aldrich (St. Louis, MO).

Aggrecan antibody (A1059-53E) and collagen II antibody (C5710-20F) for immunohistochemistry were from US Biologicals (Swampscott, MA). C1,2C antibody was from IBEX Pharmaceuticals (Quebec, Canada). For Western blot analysis, primary mouse monoclonal antibodies to aggrecan (1042005), N-terminal neoepitope ARG (1042001), and N-terminal neoepitope FFGV (1042004) were from MD Biosciences (St. Paul, MN). BCA protein assay kit was from Thermo Scientific Pierce (Rockford, IL). Western blot gels, membranes, buffers, Tween-20 and blot equipment were from BioRad Laboratories (Hercules, CA).

3.3.2 Macromer synthesis

The triblock copolymer oligo(lactic acid)-*b*-PEG-*b*-oligo(lactic acid) (LA-PEG-LA) was synthesized by reacting poly(ethylene glycol) (PEG, MW 4600) with lactides in a molar ratio of 1:3 as described by Sawhney *et al.* [28]. PEG (MW 4600) and LA-PEG-LA were endcapped with methacrylate groups by microwave methacrylation [29] to produce slow degrading, or essentially non-degrading on the time scale of the experiments, PEG-dimethacrylate (PEGDM),

and the fast degrading macromer PEG-LA-dimethacrylate (PEG-LA-DM). Briefly, methacrylic anhydride and PEG or LA-PEG-LA were reacted at a 10:1 molar ratio at 400W for 15 minutes total. Macromers were purified by repeated precipitation in ethyl ether. Number of lactic acid units incorporated and degree of methacrylate substitution were determined by ^{1}H-NMR. On average, 2 lactic acid repeat units were added to each side of the PEG. Methacrylate endcapping substitution for PEGDM was 93% and for PEG-LA-DM was 91%.

3.3.3 Chondrocyte isolation

Bovine chondrocytes were isolated from articular cartilage harvested from the femoral-patellar groove of a 1-3-week-old calf (Research 87, Marlborough, MA), referred to as juvenile chondrocytes. Bovine chondrocytes were also isolated from the metacarpal-phalangeal joints of two 1-2 year old steers (Arapahoe Meat Co., Lafayette, CO), referred to as adult chondrocytes. In brief, cartilage slices were washed in phosphate-buffered saline (PBS) supplemented with 1% penicillin streptomycin (P/S), 0.5 μg ml^{-1} fungizone and 20 μg ml^{-1} gentamicin (PBS-antis), and digested in 0.2% collagenase type II in DMEM with 5% FBS for 16-17 hours at 37 °C. Isolated chondrocytes were washed in PBS-antis + 0.02% EDTA, pelleted and rinsed 3 times and then passed through a 100 μm cell strainer. Cells were suspended in chondrocyte medium (DMEM supplemented with 10% FBS, 1% P/S, 10 mM HEPES, 0.1 M MEM-NEAA, 0.4 μM L-proline, 50 μg ml^{-1} L-ascorbic acid, 0.5 μg ml^{-1} fungizone and 20 μg ml^{-1} gentamicin) and counted using the trypan blue exclusion assay, yielding an adult cell initial viability of 77% and a juvenile cell initial viability of 83%. KCl and NaCl were added to the medium (molar ratio 1:22) to increase the osmolarity to 400 mOsm, confirmed by osmometer measurement (5002 Osmette A, Precision Systems, Inc., Natick, MA).

3.3.4 Hydrogel formation

A 15% w/w macromer solution was prepared in chondrocyte medium, where 5% of the macromer mass was PEGDM and 95% of the mass was degradable PEG-LA-DM, with 0.05% w/w Irgacure 2959 as the photoinitiator. This formulation was chosen because it retained an

intact hydrogel once PEG-LA crosslinks were cleaved as determined by accelerated degradation tests in a basic aqueous solution. Chondrocytes were mixed with macromer solution at 20 million cells ml^{-1} and photopolymerized into 40 µl cylindrical constructs (5 mm diameter x 2 mm height) for 10 min with 365 nm light (6 mW/cm^2). Constructs were cultured in chondrocyte medium for up to 29 days at 37 °C in 5% CO_2, and medium was changed every 2-3 days. At the beginning and end of the study, cell viability in constructs (n = 2) was assessed using a LIVE/DEAD® membrane integrity assay. Images were acquired using a confocal laser scanning microscope (CLSM, Zeiss LSM 510, Thornwood, NY) at 10x magnification.

3.3.5 Biochemical analysis

On days 1, 8, 15, 22, and 29, hydrogel constructs were removed from culture (n = 3), weighed, snap frozen in liquid nitrogen and stored at -80 °C. Hydrogel constructs were homogenized and digested by papain for 16 hours at 60 °C. Gel constructs were assessed for DNA content (and cell density) using Hoechst 33258, assuming 7.7 pg of DNA per chondrocyte [30]. Collagen content in the gels was measured using the hydroxyproline assay, where hydroxyproline is assumed to make up 10% of collagen [31]. Constructs were assayed for GAG content using the dimethyl methylene blue (DMMB) dye assay [32]. GAG and collagen content in the hydrogels were normalized to both gel wet weight and number of cells for each construct.

3.3.6 Immunohistochemical analysis

On day 29, constructs (n = 2) were fixed in 4% paraformaldehyde, dehydrated, paraffin embedded and sectioned to 10 µm-thick slices. Sections were analyzed by anti-aggrecan (1:5), anti-collagen type II (1:50), and anti-C1,2C collagen fragments (1:100). Sections were treated with appropriate enzymes for 1 h at 37 °C: hyaluronidase (200 U) for collagen II and C1,2C stains, and chondroitinase ABC (10 mU) and keratanase I (4 mU) for aggrecan. Sections were probed with AlexaFluor 488 or 546-conjugated secondary antibodies and counterstained with DAPI for cell nuclei. All samples were processed at the same time to minimize sample-to-sample variation resulting from the staining procedure. A laser scanning confocal microscope

was used to acquire images with a 40x oil objective using the same settings and post-processing for all images. Negative controls were performed on cell-laden hydrogel sections that received no primary antibody treatment, showing no positive staining. Positive controls were performed on sections of juvenile hyaline cartilage. For C1,2C staining, sections of juvenile and adult cartilage, and adult cartilage treated with lipopolysaccharide (LPS), were examined as controls. Adult cartilage explants were treated immediately with LPS at 1 μg ml^{-1} for 18 hours to activate matrix catabolism [33].

3.3.7 Western blot analysis

Constructs at days 1, 15, and 29 (n = 2) were snap-frozen in liquid nitrogen and stored at -80 °C until analysis. The constructs were later thawed and homogenized in lysis buffer (0.05 M Tris-HCl (pH 7.5), 0.2 M NaCl, 0.01 M $CaCl_2$, 0.02% NaN_3 and 0.05% Triton X-100). Samples were run through homogenizer columns to separate PEG from lysate. Construct lysate (n = 2) was assayed for aggrecan and its degradation products by Western blot analysis. All samples were first measured for total protein content using the BCA protein assay kit, and deglycosylated overnight with chondroitinase-ABC and keratanase I at 37 °C. The same amount of total protein per sample was loaded into the wells (5 mg/well) of 10% Tris-HCl gels. Proteins were separated by size using gel electrophoresis for 40 min at 200V and then transferred to PVDF membranes for 1 h at 100 V (Criterion Blotter system, BioRad). Membranes were probed with mouse primary antibodies for the IGD domain of aggrecan (EPEEPFTFAPEI, 6B4) and epitopes FFGV (BC-14) and ARG (BC-3). Secondary detection was performed using an AlexaFluor 546 anti-mouse 2° antibody, and imaging was performed using the BioRad VersaDoc 4000MP system (3.5 AP, 100-200 second exposure). Semi-quantitative analysis was performed using Bio-Rad Quantity One 4.6.6 software with individual lane background corrections, and relative quantity of proteins of interest was calculated by integrating the lane density profiles in the regions of the bands of interest.

3.3.8 Statistical analysis

Data are shown as mean ± standard deviation. GAG and collagen content and cell density as a function of culture time and age were analyzed by two-way analysis of variance (ANOVA), and significant differences due to age at each time point were analyzed by Tukey's HSD with $\alpha = 0.05$. Integrals of western blotting density spectrum as a function of culture time and age were analyzed by two-way ANOVA with Fisher's LSD post-hoc analysis, $\alpha = 0.05$.

3.4 Results

3.*4.1 Cell density as a function of cellular age and culture time*

Juvenile and adult chondrocytes were encapsulated in hydrolytically degradable hydrogels made from copolymerized PEGDM and PEG-LA-DM macromers. Cell density per construct was calculated from measured DNA content, where day 1 indicates 24 hours post-encapsulation (Fig. 3.1A). Cell density per construct was significantly affected by both culture time and age of cells ($p < 0.0001$ for each). There was a higher cell density in gels containing adult cells from days 8-29 ($p < 0.05$). Cell density initially increased through day 8, then decreased through day 29. Gel wet weights (Fig. 3.1B) increased significantly with time ($p < 0.0001$) but were not affected by age ($p = 0.78$), or therefore any differences in cell density due to age. Cell viability images from LIVE/DEAD® staining qualitatively showed cell density and cell clustering patterns (Fig. 3.1C). Images from early time points in the study (days 2-4) revealed that cells were dispersed throughout the gels for both juvenile and adult cells and that cell density was higher for adult cells, which corresponds with the results in Fig. 3.1A. At late points (days 27-29), cells formed clusters of various sizes throughout the degrading hydrogels, whereby larger clusters were more prevalent in gels containing adult cells.

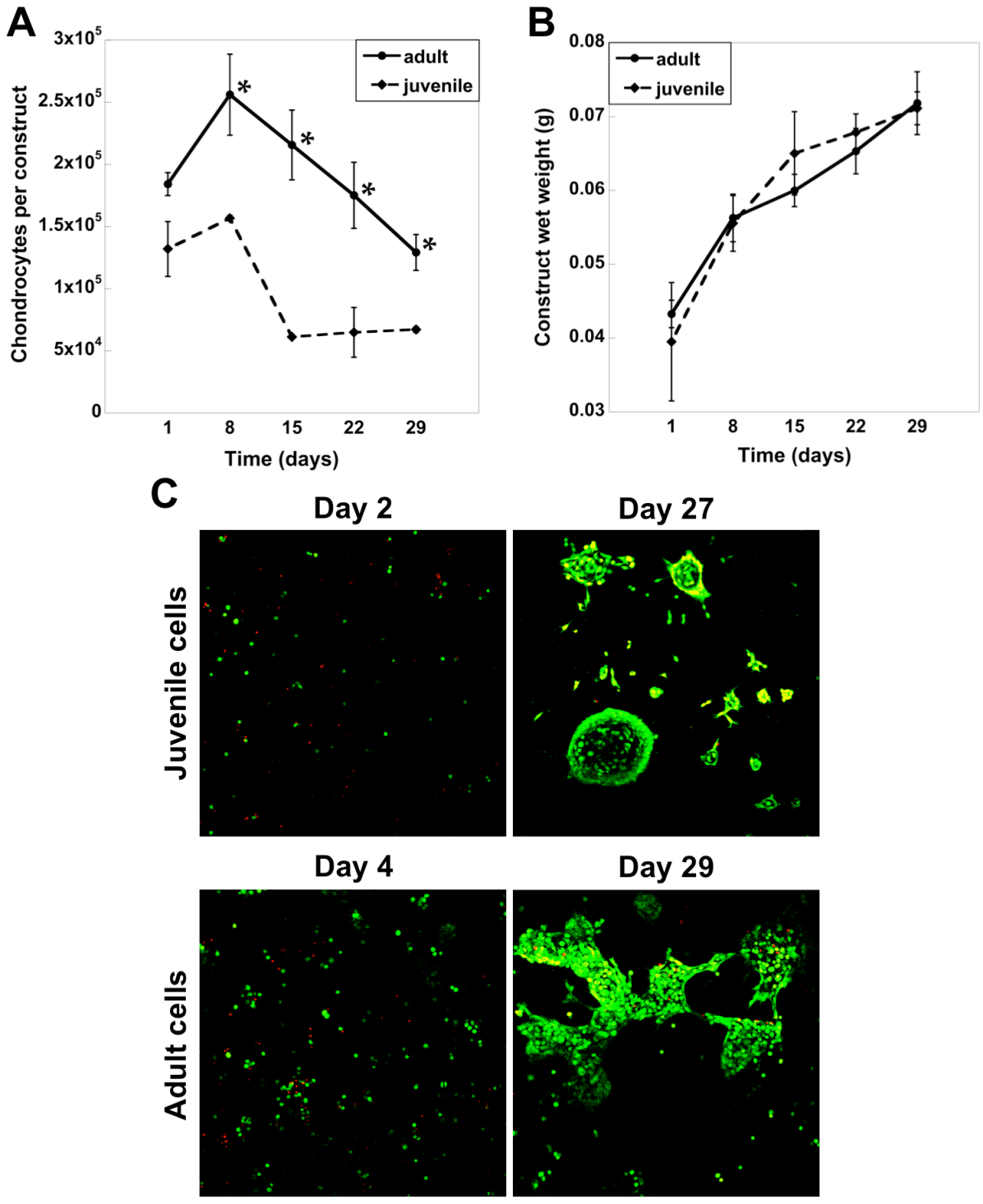

Figure 3.1 (A) Cell density measured as chondrocytes per construct as a function of encapsulated cell age and culture time. Day 1 indicates 24 hours post-encapsulation. * indicates significant difference from juvenile cells at a specified time point ($p < 0.05$). (B) Wet weight of cell-laden hydrogels over culture time. (C) Viability and cell clustering morphology of juvenile and adult cells at early (days 2 and 4) and late (days 27 and 29) time points in the study. Live cells fluoresce green, dead cells fluoresce red. Scale bars indicate 200 μm.

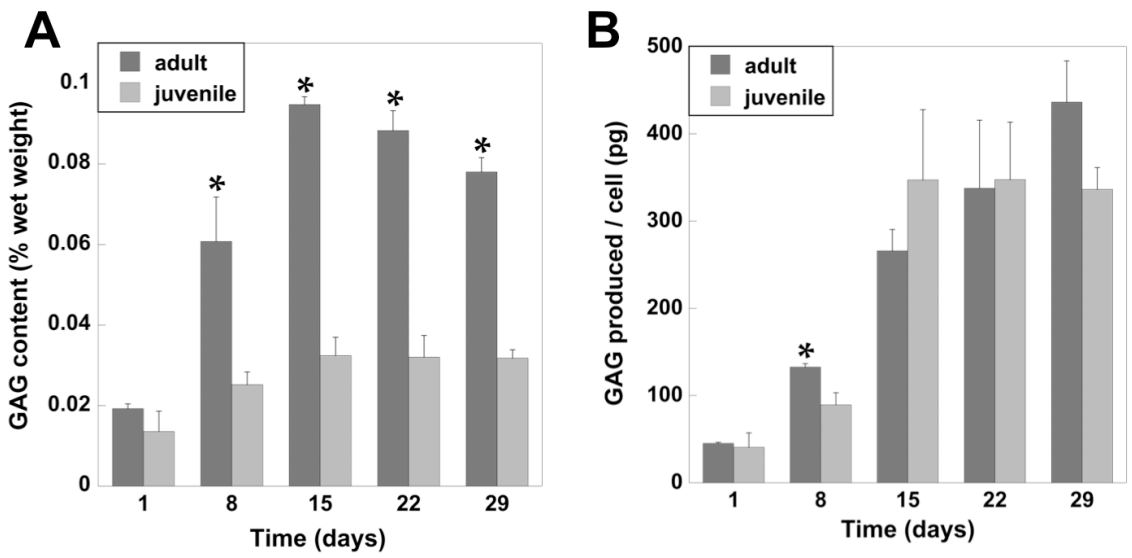

Figure 3.2 (A) Amount of GAGs accumulated in the constructs as a function of cell age and culture time, normalized to hydrogel wet weights. * indicates significantly different from juvenile at specified time point ($p < 0.05$). (B) Total GAG produced in constructs normalized to cell number.

3.4.2 Matrix deposition as a function of cellular age and culture time

GAG content in the constructs normalized to gel wet weight (Fig. 3.2A) was significantly affected by both culture time and age of cells ($p < 0.0001$ for both). Although GAG per wet weight was similar on day 1, by days 8 through 29, GAG content in the constructs containing adult cells was significantly higher than juvenile cells ($p < 0.05$). GAG content also increased up to day 15 and then decreased significantly by day 29 ($p = 0.03$). GAG produced per cell (Fig. 3.2B) was significantly affected by time ($p < 0.0001$) where it increased with time through day 15 and then leveled off. GAG per cell was similar for juvenile and adult cells at all time points except day 8, where adult cells produced more GAG/cell ($p = 0.03$).

The relative size and quantity of aggrecans retained in the constructs was probed by Western blot analysis after deglycosylation (Fig. 3.3). As differences in total protein content were found with age and culture time, the same amount of total protein was loaded into each well for gel electrophoresis, which gives an indication of the fraction of aggrecan secreted by

cells relative to total protein. Total protein measured in the constructs with adult cells on days 1, 15, and 29 was 127±4, 201±31, and 233±16 mg, respectively. Total protein measured in the constructs with juvenile cells on days 1, 15, and 29 was 82 ± 5, 130 ± 26, and 157 ± 40 mg, respectively. The main aggrecans found in the constructs (Fig. 3.3A) from both age groups were ~75 and 275 kD, with the larger aggrecan only detected after day 1. A greater quantity of both sizes of aggrecan was present in constructs with adult cells. The smaller aggrecan was only detected at day 1 in the juvenile samples, but was detected throughout the culture period in the adult samples.

Collagen content in the constructs was normalized to both gel wet weight and cells per construct (Fig. 3.4). Collagen per wet weight (Fig. 3.4A) significantly increased with time (p = 0.0005) but was not significantly affected by age of the cells. Only on day 15 was collagen per wet weight significantly higher in gels containing adult cells (p = 0.004). Collagen normalized to cell density (Fig. 3.4B) was significantly affected by both time (p <0.0001) and age (p = 0.0003). Collagen per cell increased with time, and the juvenile cells produced significantly more collagen per cell than adult cells on days 8, 15 and 22 (p < 0.05).

3.4.3 Matrix organization

The distribution and deposition of extracellular matrix molecules was examined by immunofluorescence techniques. Aggrecan (Fig. 3.3B) and collagen II (Fig. 3.4C), two of the main components of cartilage extracellular matrix, showed staining primarily in the pericellular region. While aggrecan staining appeared to be similar among both adult and juvenile individual cells, the pericellular staining for collagen II was qualitatively more intense yet also more spatially limited in sections containing adult cells. It should be noted that these images show that there is a lower cell density of juvenile cells compared to adult cells, which correlates with the measured chondrocytes per construct shown in Fig. 3.1A. Representative images of cell clusters indicate differences in cluster organization and ECM content. Much larger clusters were visible in constructs with adult cells. Collagen II content in the clusters was similar between

juvenile and adult cells, yet clusters with juvenile cells contained noticeably higher aggrecan content.

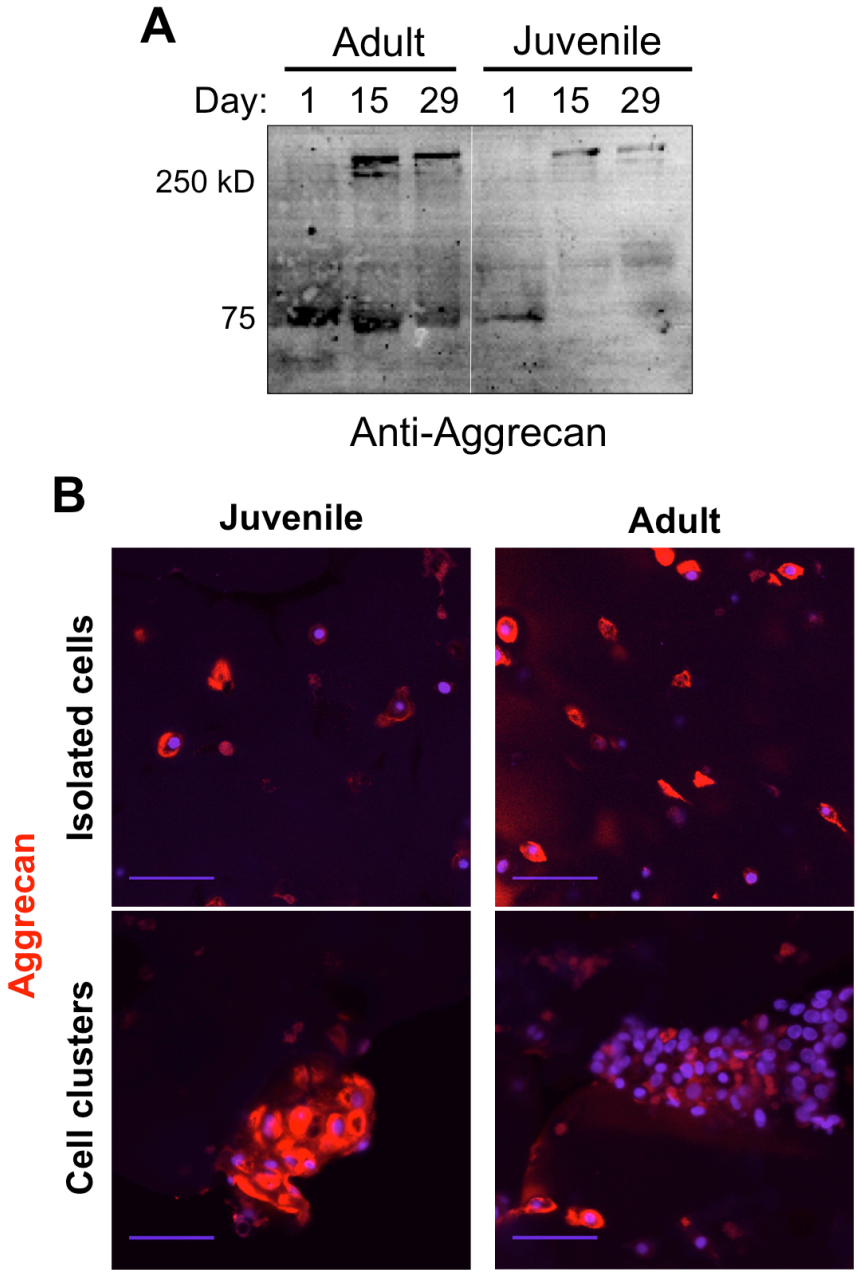

Figure 3.3 Western blot detection of aggrecan in the constructs (A) as a function of cell age on days 1, 15, and 29 of culture. An anti-IGD probe was used to detect the interglobular domain of aggrecan between the G1 and G2 domains. (B) Immunohistochemical analysis of aggrecan deposition in constructs containing either juvenile or adult cells, cultured to 29 days. Both individual cells and cell clusters were analyzed, as indicated. Sections were stained red with an anti-aggrecan antibody, and counterstained with DAPI (blue) for cell nuclei. Scale bars represent 50 μm.

3.4.4 Catabolic degradation of matrix as a function of cellular age and culture time

The catabolic activity of collagenases (MMP-1, -8, -13 and -14) was examined by immunofluorescent analysis of C1,2C, a collagenase-catabolized fragment of collagen (Fig. 3.5). This fragment was localized pericellularly, and was only visible in the adult cells condition. For comparison, C1,2C was also examined in sections of juvenile and adult cartilage, and adult cartilage catabolically activated by LPS. C1,2C was not detected in juvenile cartilage, and was faintly visible pericellularly in a few cells in the adult cartilage. Intense staining for C1,2C was visible pericellularly in adult cartilage treated with LPS.

The catabolic activity of aggrecanases (ADAMTS-4 and -5) and matrix metalloproteinases (MMPs) was assessed by Western blot analysis for their respective aggrecan degradation products (Fig. 3.6 and supplementary figures). Same total protein of juvenile and adult samples was loaded into each well, facilitating comparison of the relative abundance of degradation products present among all samples. In the constructs, the N-terminal FFGV fragment of MMP-cleaved aggrecan was only detected at ~75 kD (Fig. 3.6A). This fragment was most abundant at day 1 for both adult and juvenile cells, and was least abundant at day 29. Semi-quantitative analysis of the relative band intensities was performed (Fig. 3.6B). The quantity of MMP-cleaved aggrecan was significantly affected by age (p = 0.03), yet there were no statistically significant differences between juvenile and adult conditions at any time point. In general, there was a greater quantity of this fragment in the constructs containing adult cells. The N-terminal ARG fragments of ADAMTS-cleaved aggrecan were detected in the constructs at ~10, 15, and 75 kD (Fig. 3.6C). The most prominent band was at ~75 kD and was visually more abundant in the adult cells condition. The lower MW fragments were also more visually abundant in gels containing adult cells. Quantitative analysis was performed on the ~75 kD fragment only (Fig. 3.6D), revealing that quantity of ADAMTS-cleaved aggrecan was significantly affected by time (p = 0.03), but was only significantly different due to

age on day 29 (p = 0.0001). Generally, there was more of this fragment in gels containing adult cells, and this quantity was highest on day 1 and lowest at day 29.

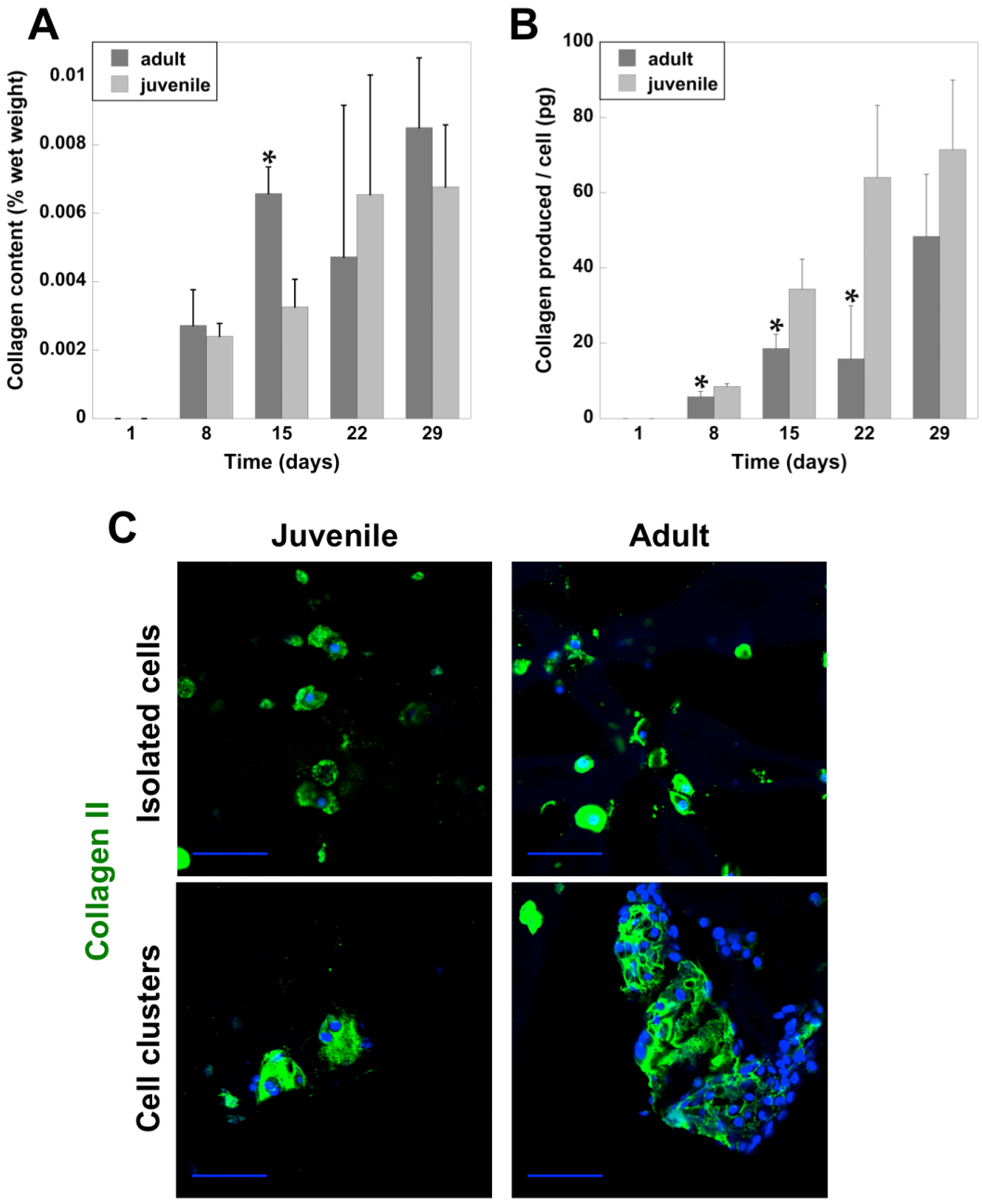

Figure 3.4 (A) Amount of collagen accumulated in the constructs as a function of cell age and culture time, normalized to hydrogel wet weights. (B) Total collagen produced in constructs normalized to cell count. * indicates significantly different from juvenile at specified time point (p < 0.05). (C) Immunohistochemical analysis of collagen II deposition in constructs containing either juvenile or adult cells, cultured to 29 days. Both individual cells and cell clusters were analyzed, as indicated. Sections were stained green with an anti-collagen II antibody, and counterstained with DAPI (blue) for cell nuclei. Scale bars represent 50 μm.

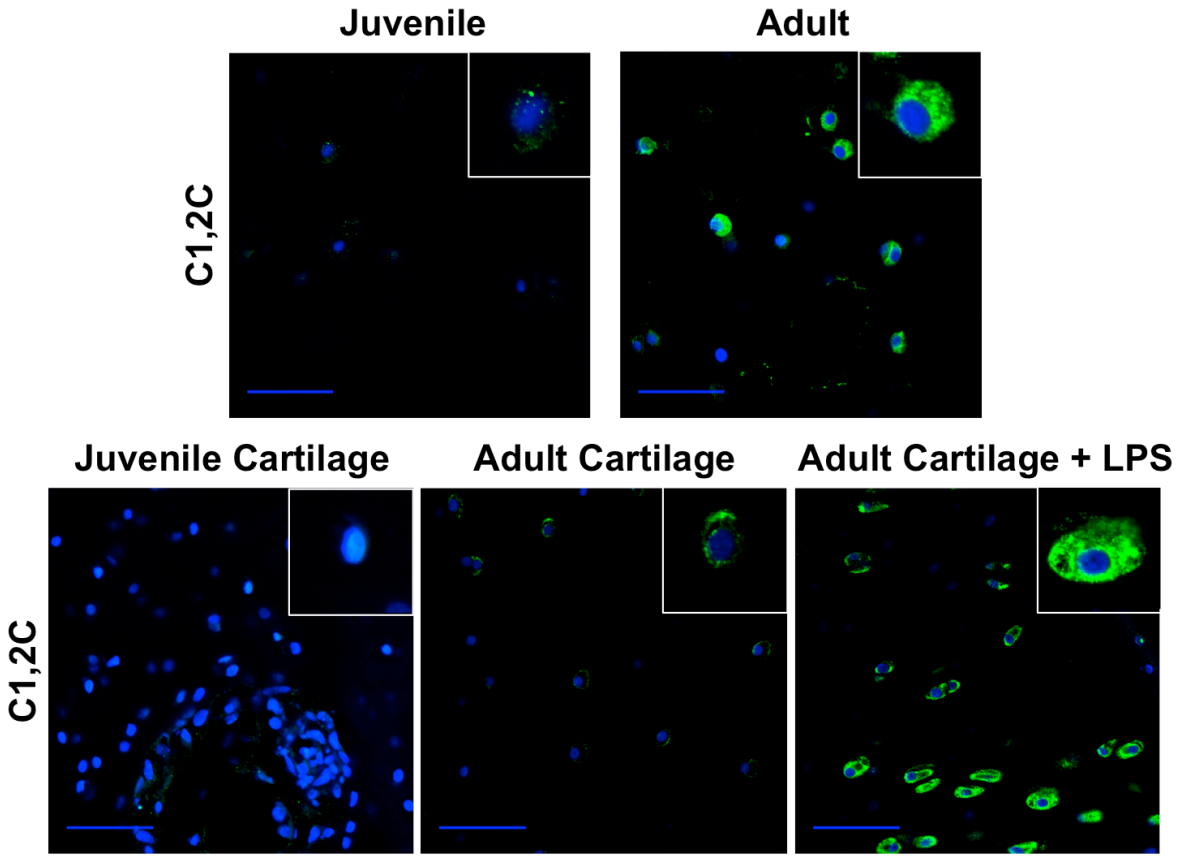

Figure 3.5 Immunohistochemical analysis of presence of C1,2C catabolized collagen fragments in constructs containing either juvenile or adult cells, cultured to 29 days. Control samples of juvenile and adult cartilage, and adult cartilage treated with LPS were similarly analyzed. Sections were stained green with an anti-C1,2C antibody, and counterstained with DAPI (blue) for cell nuclei. Scale bars represent 50 μm.

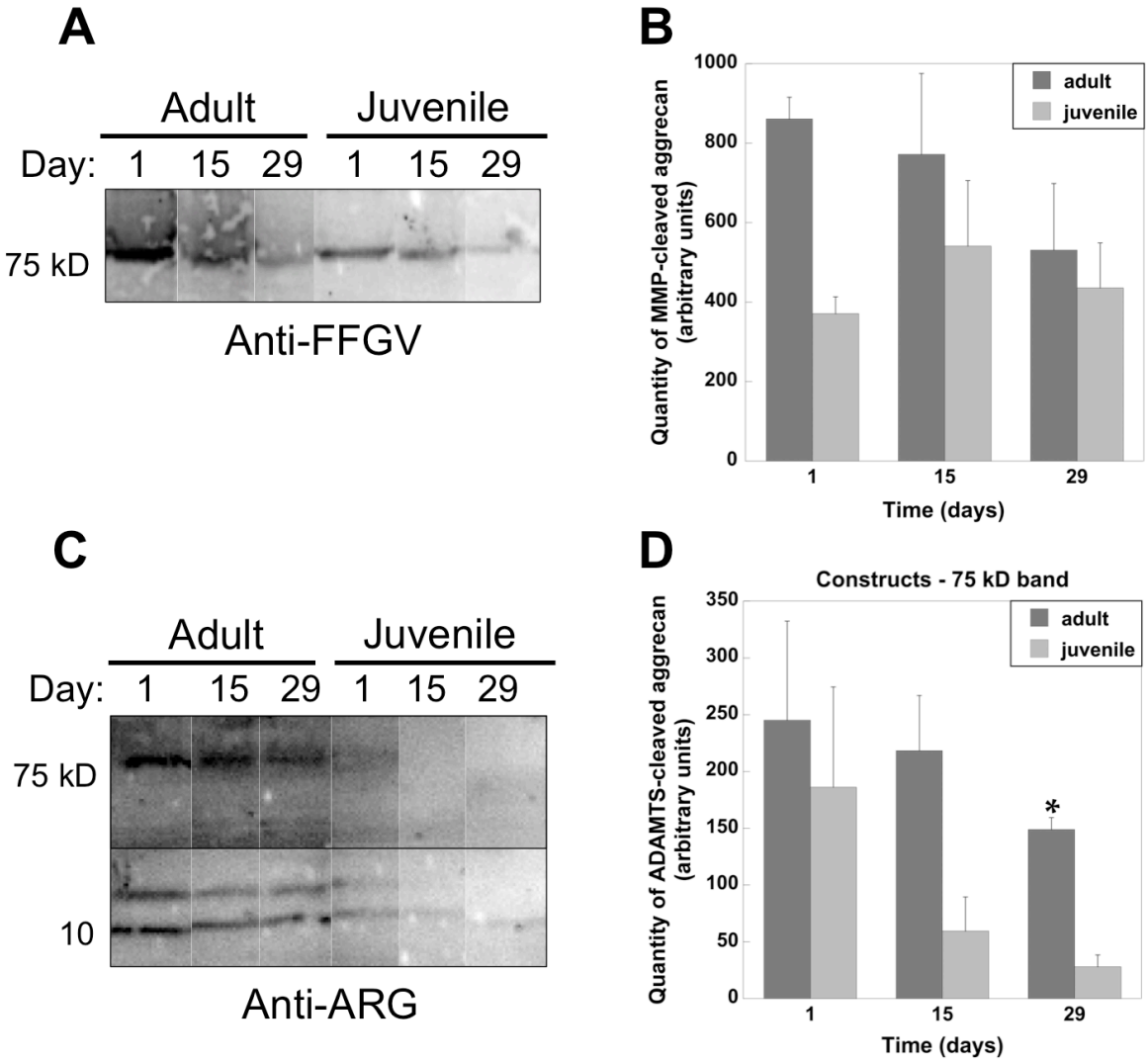

Figure 3.6 Western blot detection of MMP-cleaved FFGV aggrecan fragments (A) and aggrecanase-cleaved ARG aggrecan fragments (C) in the constructs as a function of cell age on days 1, 15, and 29 of culture. Estimate of relative quantity of FFGV fragments (B) and ARG fragments (D) by semi-quantitative analysis of Western blot bands in the constructs. * indicates significantly different from juvenile at specified time point ($p < 0.05$).

3.5 Discussion

To move towards developing a functional cartilage tissue engineering strategy employing adult cells, juvenile and adult chondrocytes were encapsulated in hydrolytically degradable hydrogels, which partially degraded on the time scale of the experiments. Because adult chondrocytes will be employed in clinically viable therapies utilizing injectable hydrogels, it

was of interest to investigate their tissue production and catabolism in degradable hydrogels compared to more commonly studied juvenile cell sources. Hydrolytically degradable functionalities were included in the PEG hydrogels to promote neotissue deposition and organization throughout the culture period. Overall, encapsulation of adult chondrocytes in hydrolytically degradable gels supported growth of cartilaginous extracellular matrix comprised of aggrecan and collagen II with higher cell densities and GAG contents per wet weight. However, collagen content was lower and extracellular matrix catabolism was higher when compared to juvenile chondrocytes.

Hydrolytically degradable chemistry was incorporated to encourage infiltration of aggrecans and collagen II into the extracellular space, yet degradation that is not uniform or occurs too rapidly may result in loss of cells and matrix to the culture medium. The increase of gel wet weights over time can be attributed mainly to the increased swelling associated with degradation as lactic acid crosslinks are cleaved, which is not observed in non-degrading PEG hydrogels [34]. A decrease in crosslinking density corresponds with an increase in mesh size, meaning that newly formed matrix molecules or clusters of cells and neo-matrix may diffuse through and eventually out of the hydrogels. The effects of this phenomenon were apparent in Fig. 3.1, where cell density in both age conditions initially increased and then decreased. The decrease in cell density occurring after day 8 is largely attributed to a loss of individual and clustered cells to the culture medium due to gel degradation, which has been observed in other studies using the same hydrogel system (unpublished observations). However, cell death and subsequent degradation of the DNA may have also contributed to the decreased cell density. The LIVE/DEAD® images shows that a large number of cells that survived to week 4 were part of larger interconnected clusters, which may have formed by cells coalescing during gel degradation and/or cell proliferation. The use of bimodal degradable hydrogels appears to have caused heterogeneous degradation patterns, characterized by areas of individual cells and areas of tight clustering of cells in some portions of the hydrogels.

Aggrecans are proteoglycans consisting of a core protein with multiple functional domains, including a long glycosaminoglycan (GAG) attachment region. Sulfated GAGs are the functional component of aggrecan, yet are also found in perlecan, and to a lesser extent small leucine-rich proteoglycans like decorin and biglycan [35]. Due to catabolic degradation at several sites along the aggrecan core protein, GAGs can be lost to the culture medium *in vitro* and the synovial fluid *in vivo* [18]. *In vivo*, the glycosylated aggrecan monomers (1-4 MDa [36]) and larger aggregan aggregates that form along hyaluronan filaments are large enough to be retained by the collagen framework, but in a hydrolytically degradable system with heterogeneous structure, it is likely that some of the aggrecans and large perlecans (and therefore GAGs) will be lost from the constructs. The decrease in GAG per wet weight in the adult constructs after day 15 could be attributed to the increased hydrogel mesh size throughout degradation, or increased aggrecan catabolism, or a combination. The Western blots of aggrecan detected in the constructs showed that aggrecans of ~75 and 250 kD (deglycosylated) were retained in the gels, and that the larger aggrecans were only present after day 1. Most of the aggrecan found in the constructs was likely retained pericellularly, bound by hyaluronan to the cell surface [37], as suggested by immunohistochemical staining. Immunohistochemistry indicated that pericellular deposition of aggrecan was not affected by age, yet aggrecan was less present in adult cell cluster formation.

Tissue production and organization by encapsulated chondrocytes was affected by the age of the cells. GAG produced per wet weight was significantly greater in gels containing adult cells, yet normalization to cell density revealed that this increase was largely due to the higher cell number of the adult cells. As GAG per wet weight indicates the overall tissue engineering potential of this system, the observed increases in total GAG content in hydrogels is a positive result for using adult cells. The cell density of adult cells was significantly greater than young cells at nearly every time point throughout the culture period, despite that all gels were seeded at the same initial seeding density. Because gel wet weights increased similarly throughout the

study, we can surmise that the difference in cell density was not due to discrepancies in gel degradation or swelling behavior and therefore is likely due to differences in survivability. For this study, all cells were encapsulated and cultured in chondrocyte medium adjusted from 330 to 400 mOsm by the addition of salts, which was previously found to improve adult cell survival during photoencapsulation [38]. While this osmotic condition is more physiologically relevant, its beneficial effects may not be as pronounced in juvenile cell cultures. In addition, cell seeding density may affect survivability, where we have observed higher percent viability of juvenile cells when encapsulated at the higher cell density (50 vs. 20 million cells ml^{-1}) (unpublished observations), which according to DNA measurements of native tissue explants is more physiological for juvenile cells. It is also possible that juvenile cells may be more susceptible to cell death during the photopolymerization process. Further investigations are merited, but are beyond the focus of this study.

Collagen content normalized to wet weight was mostly similar between the age conditions, however collagen per cell was greater in juvenile cells on days 8, 15, and 29. The immunohistochemical images of collagen production support that overall collagen content was similar, both pericellularly and in the formation of macroscopic tissue clusters. Our findings mirror those found by Tran-Khanh *et al.* [27], who cultured fetal, young, and adult chondrocytes in agarose gels. They similarly observed that collagen per cell and proline incorporation rates decreased significantly with the age of the cell. They also found that GAG per cell and sulfate incorporation rates were not greatly affected by age, and GAG per cell was only significantly decreased in adult cells compared to fetal cells at day 26. However, they observed significantly lower adult cell densities compared to the younger cells, which further suggests that the viability of the adult cells in our system may have been improved either by the increased osmolarity or their enhanced survival during photopolymerization.

Assessment of catabolic activity via western blots and immunohistochemistry revealed stark differences due to the age of the cells. Immunohistochemical staining of the C1,2C

collagenase-degraded fragment of collagen showed positive staining for this fragment only in the pericellular region of adult cells. Faint positive staining was also visible in adult cartilage samples, and intense staining was visible in samples of adult cartilage treated with LPS. A study comparing C1,2C localization in healthy human adult and osteoarthritic cartilage showed that this fragment is indeed located primarily pericellularly, and staining intensity increased with age and in osteoarthritis [39]. Because of the intensity of C1,2C staining both in the hydrogels with adult cells and the adult cartilage controls catabolically activated by pro-inflammatory LPS, our results suggest that adult cells in the hydrogels may be exhibiting a state of remodeling similar to that induced by inflammation [40]. LPS induces activity of several collagenases including MMP-1 (Collagenase-1) [17] and MMP-13 [41], and it was observed in osteoarthritic cartilage explants that newly synthesized collagens were rapidly degraded by collagenases [42]. The C1,2C fragment is generated by cleavage of the a chain and the partial unwinding of the collagen triple helix to expose neoepitopes [17] by any of four collagenases (MMP-1, -8, -13, and -14), which are involved in homeostasis and disease. In human osteoarthritic cartilage explants, C1,2C release was inhibited by treating with inhibitors for MMP-8 and MMP-13 [42], demonstrating the important role these specific catabolic enzymes play in an osteoarthritic disease state. As collagenase activity is critical to growth, development, and homeostasis and there is evidence for the role of MMPs in functional cartilage tissue engineering, it is possible that elevated C1,2C fragments may be a sign of constructive tissue remodeling. However, the observed minimal staining of C1,2C in the juvenile cells, which have higher collagen deposition, supports the idea that this remodeling response in the adult cells may be indicative of a disease state.

Catabolic degradation of the aggrecan core protein was assessed by probing for two N-terminal neoepitopes at the ARG and FFGV cleavage sites. The ARG fragment is generated mainly by aggrecanase activity (predominantly ADAMTS -4 and -5), and the FFGV fragment is generated mainly by matrix metalloproteinases (e.g., MMP-1, -3, -8, -13), all of which are found

in cartilage [17]. Both cleavage sites are found in the interglobular domain of aggrecan, therefore their cleaved fragments are similar in size. Further processing by ADAMTS-1 and -4 along the core protein results in varying fragment sizes [17]. Generation of the FFGV fragment by MMPs is associated with normal matrix turnover, and is necessary to transport newly formed aggrecans from the pericellular space into the less metabolically active extracellular space [43]. This fragment was detected in constructs containing both juvenile and adult cells, and was most abundant at day 1. FFGV presence is representative of enzymatic activity intended to transport functional GAG-laden aggrecan fragments to the extracellular space where they could then assemble along hyaluronan filaments into larger aggregates. As the hydrogel mesh size increased with degradation, unassembled aggrecans could be released. On the other hand, ARG fragments are typically associated with cartilage catabolism. In fact, the majority of aggrecan fragments found in synovial fluid of osteoarthritic patients have the ARG N-terminal sequence, meaning that the activity of aggrecanases is more associated with a disease state [44,45]. While ARG fragments were detected from cells of both ages, these fragments were most abundant in the adult cells condition. Therefore the adult cells show osteoarthritic-like degradation activity, which could be detrimental to the formation of a functional neotissue.

The role that catabolic activity plays in tissue development in a tissue engineering system is somewhat ambiguous. It is understood that some level of proteolytic tissue remodeling is important for neotissue development [43,46], yet elevated amounts can lead to an osteoarthritic disease state. Presence of catabolic degradation products can also act as a positive-feedback mechanism, whereby presence of degraded fragments of collagen have been shown to induce production of pro-inflammatory cytokines like interleukin-1 and tumor necrosis factor-α, that can lead to further increases in catabolic activity creating a vicious cycle and escalating tissue degradation [47]. The major enzymes that act on aggrecans can have very different impacts on neotissue development. Aggrecanase inhibitors increased the dynamic compressive modulus, while MMP inhibitors decreased the modulus and decreased GAG

accumulation when applied during tissue development in agarose scaffolds [48]. These findings further suggest that aggrecanase activity may be more detrimental in general to tissue development, while MMPs are essential for reorganization that leads to increased tissue deposition. Therefore efforts to alleviate catabolic activity should focus on decreasing activity of matrix degrading enzymes that shift the balance to catabolism, in particular the aggrecanases.

There are several limitations with regard to the present study, which are worth noting. Hydrogels were designed with a small fraction of slow-degrading PEG crosslinks to retain a crosslinked network throughout the experiment. However, it is possible that this small amount of slow-degrading chemistry was enough to limit deposition of large ECM molecules to the pericellular space, as we have seen in previous studies using slow-degrading PEG macromers only [8]. Moving towards a fully degradable hydrogel will be necessary for macroscopic tissue elaboration, as has been shown for juvenile chondrocytes in PEG-LA hydrogels [10], and is a future focus of our research. It is also worth noting that the use of lower cell densities in our study, compared to previous studies with PEG-LA hydrogels may have also played into the limited permeation of ECM. Another limitation in this study is the fact that juvenile and adult chondrocytes were isolated from different joints due to the practicality of obtaining joints from different age groups. While chondrocytes of both ages were isolated from articular hyaline cartilage and therefore should be physiologically similar, slight differences in the anatomy of the load-bearing regions and thickness of the tissue could potentially cause functional differences in cell behavior. We were also limited by the age of the adult cells, as the adult chondrocytes were isolated from 1-2 year old steers. This donor provided us a mature adult cell source, yet they may not represent an elderly population. Nonetheless, we demonstrated that adult cells, even in this age group, exhibit increased catabolic activity over juvenile chondrocytes. This finding is likely to be even more pronounced in a much older cell source.

While the adult cells were able to maintain high cell densities and secrete cartilage-specific ECM molecules, notably aggrecan and collagen II, in bimodal degradable hydrogels, a

significant loss of cells throughout the culture period was observed. Several strategies may be investigated to overcome these limitations. The loss of cells and GAGs reported in this study may have been in part attributed to the observed heterogeneity in the degradation behavior of the partially degradable gel as a result of differences in the hydrophilicity of the PEG macromer chemistries. This observation suggests that employing PEG macromers of similar chemistries and/or a different type of degradable chemistry such as enzyme-sensitive hydrogels [49–51], in conjunction with complete degradation, may offer advantages over the current hydrogel chemistry. Additionally, we recently reported on the incorporation of matrix-retaining analogs into the hydrogel to minimize the loss of newly synthesized matrix molecules [52,53]. Other applicable interventions could include treatment with growth factors to promote ECM production [54] or inhibit selective catabolic activity [55], compressive mechanical loading [56,57] to stimulate chondrocytes to produce new matrix, or some combination of interventions.

3.6 Conclusions

Adult chondrocytes were encapsulated in hydrolytically degradable hydrogels, and tissue production and catabolic activity was compared to juvenile cells. The long-term goal is to develop a clinically relevant injectable hydrogel scaffold system that will encourage encapsulated adult chondrocytes to produce a functional cartilaginous tissue. In this system, cell density and GAG and aggrecan contents were increased in hydrogels containing adult cells, while collagen produced per cell was greater in constructs with juvenile cells. However, catabolic activity that degrades collagens and aggrecans was elevated in constructs containing adult cells, representing a major challenge in developing a functional tissue engineering strategy. Overall, this study provides support for the use of autologous adult chondrocytes for functional cartilage tissue engineering, which represent a feasible cell source for tissue engineering therapies. However, additional strategies will be required to fully realize the tissue engineering potential of adult chondrocytes and minimize negative effects due to catabolism. Our findings could be extended to the use of stem cell-based therapies, where differentiated

embryonic stem cells will likely behave similarly to juvenile chondrocytes, and induced pluripotent stem cells may behave more similarly to adult chondrocytes.

3.7 Acknowledgements

This research was supported by a Bioscience Discovery and Evaluation grant from the State of Colorado and the University of Colorado, a fellowship from the National Science Foundation Graduate Research Fellowship Program (NSF GRFP), a National Institute of Health (NIH) Pharmaceutical Biotechnology Training Grant, and a Chancellor's Fellowship from the University of Colorado. The authors would like to thank Shash Dimson for assisting with immunohistochemical staining, and Ian L Milligan for co-authoring the manuscript.

3.8 Supplementary Figures

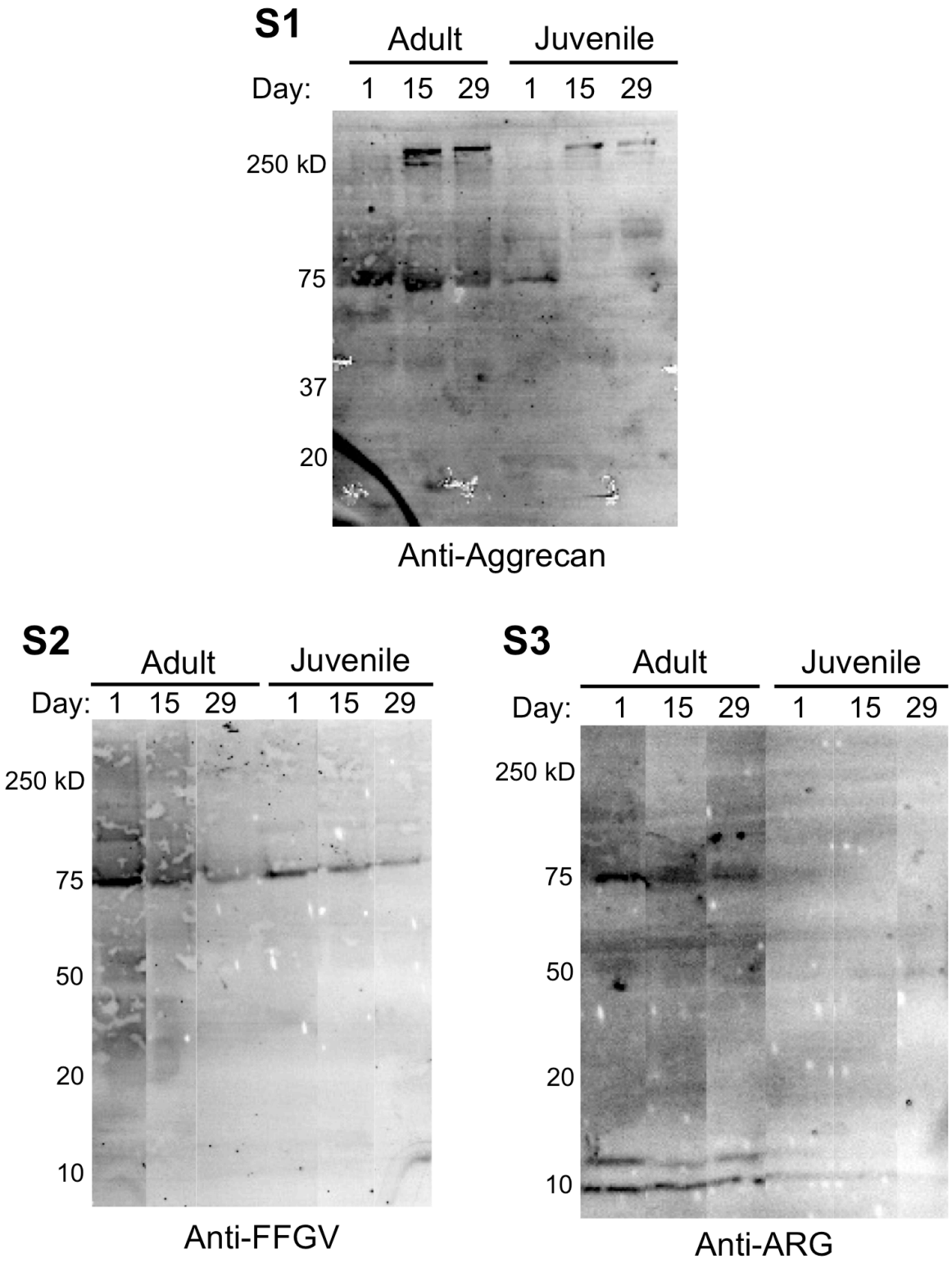

Figure 3.S1 Full-length Western blots, where partial blots are shown in Figures 3.3 and 3.6.

3.9 References

[1] Hootman JM, Helmick CG. Projections of US prevalence of arthritis and associated activity limitations. Arthritis Rheum 2006;54:226–9.

[2] Richardson JB, Caterson B, Evans EH, Ashton BA, Roberts S. Repair of human articular cartilage after implantation of autologous chondrocytes. J Bone Jt Surgery-British Vol 1999;81B:1064–8.

[3] Gillogly SD, Myers TH. Treatment of full-thickness chondral defects with autologous chondrocyte implantation. Orthop Clin North Am 2005;36:433–46.

[4] Martin JA, Buckwalter JA. Aging, articular cartilage chondrocyte senescence and osteoarthritis. Biogerontology 2002;3:257–64.

[5] West JL, Nguyen KT. Photopolymerizable hydrogels for tissue engineering applications. Biomaterials 2002;23:4307–14.

[6] Anseth KS, Metters AT, Bryant SJ, Martens PJ, Elisseeff JH, Bowman CN. In situ forming degradable networks and their application in tissue engineering and drug delivery. J Control Release 2002;78:199–209.

[7] Elisseeff J, Anseth K, Sims D, McIntosh W, Randolph M, Yaremchuk M, et al. Transdermal photopolymerization of poly(ethylene oxide)-based injectable hydrogels for tissue-engineered cartilage. Plast Reconstr Surg 1999;104:1014–22.

[8] Nicodemus GD, Skaalure SC, Bryant SJ. Gel structure has an impact on pericellular and extracellular matrix deposition, which subsequently alters metabolic activities in chondrocyte-laden PEG hydrogels. Acta Biomater 2011;7:492–504.

[9] Sontjens SHM, Nettles DL, Carnahan MA, Setton LA, Grinstaff MW. Biodendrimer-based hydrogel scaffolds for cartilage tissue repair. Biomacromolecules 2006;7:310–6.

[10] Roberts JJ, Nicodemus GD, Greenwald EC, Bryant SJ. Degradation Improves Tissue Formation in (Un)Loaded Chondrocyte-laden Hydrogels. Clin Orthop Relat Res 2011.

[11] Anseth KS, Bryant SJ. Controlling the spatial distribution of ECM components in degradable PEG hydrogels for tissue engineering cartilage. J Biomed Mater Res Part A 2003;64A:70–9.

[12] Kloxin AM, Kloxin CJ, Bowman CN, Anseth KS. Mechanical Properties of Cellularly Responsive Hydrogels and Their Experimental Determination. Adv Mater 2010;22:3484–94.

[13] Bryant SJ, Durand KL, Anseth KS. Manipulations in hydrogel chemistry control photoencapsulated chondrocyte behavior and their extracellular matrix production. J Biomed Mater Res Part A 2003;67A:1430–6.

[14] Bryant SJ, Bender RJ, Durand KL, Anseth KS. Encapsulating Chondrocytes in degrading PEG hydrogels with high modulus: Engineering gel structural changes to facilitate cartilaginous tissue production. Biotechnol Bioeng 2004;86:747–55.

[15] Bryant SJ, Anseth KS. Hydrogel properties influence ECM production by chondrocytes photoencapsulated in poly(ethylene glycol) hydrogels. J Biomed Mater Res 2002;59:63–72.

[16] Mason MN, Metters AT, Bowman CN, Anseth KS. Predicting controlled-release behavior of degradable PLA-b-PEG-b-PLA hydrogels. Macromolecules 2001;34:4630–5.

[17] Manicourt DH, Devogelaer JP, Thonar EJMA. Products of Cartilage Metabolism. In: Seibel MJ, Robins SP, Bilezikian JP, editors. Dyn. Bone Cartil. Metab., vol. 1, Burlington: Elsevier; 2006, p. 421–49.

[18] Roughley PJ. The structure and function of cartilage proteoglycans. Eur Cell Mater 2006;12:92–101.

[19] Nesic D, Whiteside R, Brittberg M, Wendt D, Martin I, Mainil-Varlet P. Cartilage tissue engineering for degenerative joint disease. Adv Drug Deliv Rev 2006;58:300–22.

[20] McCormick A, Campisi J. Cellular aging and senescence. Curr Opin Cell Biol 1991;3:230–4.

[21] Carlo Jr. MD, Loeser RF. Increased oxidative stress with aging reduces chondrocyte survival: correlation with intracellular glutathione levels. Arthritis Rheum 2003;48:3419–30.

[22] Stockwell RA. The Cell Density of Human Articular and Costal Cartilage. J Anat 1967;101:753–63.

[23] Forsyth CB, Cole A, Murphy G, Bienias JL, Im HJ, Loeser RF. Increased matrix metalloproteinase-13 production with aging by human articular chondrocytes in response to catabolic stimuli. Journals Gerontol Ser a-Biological Sci Med Sci 2005;60:1118–24.

[24] Buckwalter JA, Woo SL, Goldberg VM, Hadley EC, Booth F, Oegema TR, et al. Soft-tissue aging and musculoskeletal function. J Bone Jt Surg Am 1993;75:1533–48.

[25] Pratta MA, Tortorella MD, Arner EC. Age-related changes in aggrecan glycosylation affect cleavage by aggrecanase. J Biol Chem 2000;275:39096–102.

[26] Verbruggen G, Cornelissen M, Almqvist KF, Wang L, Elewaut D, Broddelez C, et al. Influence of aging on the synthesis and morphology of the aggrecans synthesized by differentiated human articular chondrocytes. Osteoarthr Cartil 2000;8:170–9.

[27] Tran-Khanh N, Hoemann CD, McKee MD, Henderson JE, Buschmann MD. Aged bovine chondrocytes display a diminished capacity to produce a collagen-rich, mechanically functional cartilage extracellular matrix. J Orthop Res 2005;23:1354–62.

[28] Sawhney AS, Pathak CP, Hubbell JA. Bioerodible Hydrogels Based on Photopolymerized Poly(ethylene glycol)-co-poly(alpha-hydroxy acid) Diacrylate Macromers. Macromolecules 1993;26:581–7.

[29] Lin-Gibson S, Bencherif S, Cooper JA, Wetzel SJ, Antonucci JM, Vogel BM, et al. Synthesis and characterization of PEG dimethacrylates and their hydrogels. Biomacromolecules 2004;5:1280–7.

[30] Kim YJ, Sah RLY, Doong JYH, Grodzinsky AJ. Fluorometric Assay of DNA in Cartilage Explants Using Hoechst-33258. Anal Biochem 1988;174:168–76.

[31] Woessner JF. Determination of Hydroxyproline in Tissue and Protein Samples Containing Small Proportions of This Imino Acid. Arch Biochem Biophys 1961;93:440–7.

[32] Templeton DM. The basis and applicability of the dimethylmethylene blue binding assay for sulfated glycosaminoglycans. Connect Tissue Res 1988;17:23–32.

[33] Lee MS, Ikenoue T, Trindade MCD, Wong N, Goodman SB, Schurman DJ, et al. Protective effects of intermittent hydrostatic pressure on osteoarthritic chondrocytes activated by bacterial endotoxin in vitro. J Orthop Res 2003;21:117–22.

[34] Metters A, Anseth KS, Bowman CN. Fundamental studies of a novel, biodegradable PEG-b-PLA hydrogel. Polymer (Guildf) 2000;41:3993–4004.

[35] Hardingham T. Proteoglycans and Glycosaminoglycans. In: Seibel MJ, Robins SP, Bilezikian JP, editors. Dyn. Bone Cartil. Metab., vol. 1, Burlington: Elsevier; 2006, p. 85.

[36] Hardingham TE, Fosang AJ. Proteoglycans - Many Forms and Many Functions. Faseb J 1992;6:861–70.

[37] Knudson CB, Knudson W. Cartilage proteoglycans. Semin Cell Dev Biol 2001;12:69–78.

[38] Villanueva I, Bishop NL, Bryant SJ. Medium Osmolarity and Pericellular Matrix Development Improves Chondrocyte Survival When Photoencapsulated in Poly(Ethylene Glycol) Hydrogels at Low Densities. Tissue Eng Part A 2009;15:3037–48.

[39] Poole AR, Wu W, Billinghurst RC, Pidoux I, Antoniou J, Zukor D, et al. Sites of collagenase cleavage and denaturation of type II collagen in aging and osteoarthritic articular cartilage and their relationship to the distribution of matrix metalloproteinase 1 and matrix metalloproteinase 13. Arthritis Rheum 2002;46:2087–94.

[40] Welgus HG, Campbell EJ, Bar-Shavit Z, Senior RM, Teitelbaum SL. Human alveolar macrophages produce a fibroblast-like collagenase and collagenase inhibitor. J Clin Invest 1985;76:219–24.

[41] Rossa C, Liu M, Bronson P, Kirkwood KL. Transcriptional activation of MMP-13 by periodontal pathogenic LPS requires p38 MAP kinase. J Endotoxin Res 2007;13:85–93.

[42] Dahlberg L, Billinghurst RC, Manner P, Nelson F, Webb G, Ionescu M, et al. Selective enhancement of collagenase-mediated cleavage of resident type II collagen in cultured osteoarthritic cartilage and arrest with a synthetic inhibitor that spares collagenase 1 (matrix metalloproteinase 1). Arthritis Rheum 2000;43:673–82.

[43] Mok SS, Masuda K, Hauselmann HJ, Aydelotte MB, Thonar EJMA. Aggrecan Synthesized by Mature Bovine Chondrocytes Suspended in Alginate - Identification of 2 Distinct Metabolic Matrix Pools. J Biol Chem 1994;269:33021–7.

[44] Sandy JD, Flannery CR, Neame PJ, Lohmander LS. The Structure of Aggrecan Fragments in Human Synovial-Fluid - Evidence for the Involvement in Osteoarthritis of a Novel Proteinase Which Cleaves the Glu-373-Ala-374 Bond of the Interglobular Domain. J Clin Invest 1992;89:1512–6.

[45] Lohmander LS, Neame PJ, Sandy JD. The Structure of Aggrecan Fragments in Human Synovial-Fluid - Evidence That Aggrecanase Mediates Cartilage Degradation in Inflammatory Joint Disease, Joint Injury, and Osteoarthritis. Arthritis Rheum 1993;36:1214–22.

[46] De Croos JNA, Dhaliwal SS, Grynpas MD, Pilliar RM, Kandel RA. Cyclic compressive mechanical stimulation induces sequential catabolic and anabolic gene changes in chondrocytes resulting in increased extracellular matrix accumulation. Matrix Biol 2006;25:323–31.

[47] Poole AR, Nelson F, Dahlberg L, Tchetina E, Kobayashi M, Yasuda T, et al. Proteolysis of the collagen fibril in osteoarthritis. Proteases Regul Biol Process 2003;70:115–23.

[48] Connelly JT, Wilson CG, Levenston ME. Characterization of proteoglycan production and processing by chondrocytes and BMSCs in tissue engineered constructs. Osteoarthr Cartil 2008;16:1092–100.

[49] Wong M, Park Y, Lutolf MP, Hubbell JA, Hunziker EB. Bovine primary chondrocyte culture in synthetic matrix metalloproteinase-sensitive poly(ethylene glycol)-based hydrogels as a scaffold for cartilage repair. Tissue Eng 2004;10:515–22.

[50] West JL, Lee SH, Miller JS, Moon JJ. Proteolytically degradable hydrogels with a fluorogenic substrate for studies of cellular proteolytic activity and migration. Biotechnol Prog 2005;21:1736–41.

[51] Fairbanks BD, Schwartz MP, Halevi AE, Nuttelman CR, Bowman CN, Anseth KS. A Versatile Synthetic Extracellular Matrix Mimic via Thiol-Norbornene Photopolymerization. Adv Mater 2009;21:5005–10.

[52] Yoo HS, Lee EA, Yoon JJ, Park TG. Hyaluronic acid modified biodegradable scaffolds for cartilage tissue engineering. Biomaterials 2005;26:1925–33.

[53] Bryant SJ, Villanueva I, Gladem SK, Kessler J. Dynamic loading stimulates chondrocyte biosynthesis when encapsulated in charged hydrogels prepared from poly(ethylene glycol) and chondroitin sulfate. Matrix Biol 2010;29:51–62.

[54] Yaeger PC, Masi TL, de Ortiz JL, Binette F, Tubo R, McPherson JM. Synergistic action of transforming growth factor-beta and insulin-like growth factor-I induces expression of type II collagen and aggrecan genes in adult human articular chondrocytes. Exp Cell Res 1997;237:318–25.

[55] Sandy JD, Gamett D, Thompson V, Verscharen C. Chondrocyte-mediated catabolism of aggrecan: aggrecanase-dependent cleavage induced by interleukin-1 or retinoic acid can be inhibited by glucosamine. Biochem J 1998;335:59–66.

[56] Nicodemus GD, Bryant SJ. The role of hydrogel structure and dynamic loading on chondrocyte gene expression and matrix formation. J Biomech 2008;41:1528–36.

[57] Kelly TAN, Ng KW, Wang CCB, Ateshian GA, Hung CT. Spatial and temporal development of chondrocyte-seeded agarose constructs in free-swelling and dynamically loaded cultures. J Biomech 2006;39:1489–97.

Chapter 4

Semi-interpenetrating Networks of Hyaluronic Acid in Degradable PEG Hydrogels for Cartilage Tissue Engineering

As appearing in *Acta Biomaterialia* 2014

4.1 Abstract

Hydrolytically biodegradable poly(ethylene glycol) (PEG) hydrogels offer a promising platform for chondrocyte encapsulation and tuning degradation for cartilage tissue engineering, but offer no bioactive cues to encapsulated cells. This study tests the hypothesis that a semi-interpenetrating network of entrapped hyaluronic acid (HA), a bioactive molecule that binds cell surface receptors on chondrocytes, and crosslinked degradable PEG improves matrix synthesis by encapsulated chondrocytes. Degradation was achieved by incorporating oligo (lactic acid) segments into the crosslinks. The effects of HA molecular weight (MW) (2.9×10^4 and 2×10^6 Da) and concentration (0.5 and 5 mg g^{-1}) were investigated. Bovine chondrocytes were encapsulated in semi-interpenetrating networks and cultured to 4 weeks. A steady release of HA was observed over the course of the study with 90% released by 4 weeks. Incorporation of HA led to significantly higher cell numbers throughout the culture period. After eight days, HA increased collagen content per cell, increased aggrecan-positive cells, while decreasing deposition of hypertrophic collagen X, but these effects were not sustained long term. Measuring total sGAG and collagen content within the constructs and released to the culture medium after 4 weeks revealed that total matrix synthesis was elevated by high concentrations of HA, indicating that HA stimulated matrix production although this matrix was not retained within the hydrogels. Matrix degrading enzymes were elevated in the low, but not high MW HA. Overall, incorporating high MW HA into degrading hydrogels increased chondrocyte number

and sGAG and collagen production, warranting further investigations to improve retention of newly synthesized matrix molecules.

4.2 Introduction

Encapsulating autologous chondrocytes (cartilage cells) from adult patients in a bioactive semi-interpenetrating network (sIPN) composed of degradable crosslinked poly(ethylene glycol) (PEG) and linear hyaluronic acid (HA) offers a promising strategy for cartilage regeneration. Hydrophilic PEG hydrogels maintain the chondrocyte phenotype and support cartilage-specific matrix production [1–3], but non-degrading hydrogels inhibit matrix deposition and evolution [4], motivating the need for degradation. Degradable PEG hydrogels incorporating oligomers of lactic acid into the crosslinks (PEG-PLA hydrogels) have been investigated for cartilage tissue engineering and shown to promote macroscopic tissue deposition [1,2,5–7]. Because PEG-PLA hydrogels are bioinert, introducing bioactivity into the hydrogel by entrapping extracellular matrix molecules such as HA can facilitate initial cell-matrix interactions and provide a framework for newly secreted matrix, primarily consisting of aggrecan and collagen II molecules, to assemble. We hypothesize that enhancing early matrix deposition may improve long-term tissue engineering outcomes in degradable hydrogels.

HA is clinically used to relieve pain associated with osteoarthritis, namely through direct injection of HA (5-7 x 10^6 Da) into osteoarthritic joints; a process known as viscosupplementation [8]. HA is a linear non-sulfated glycosaminoglycan, typically ranging between 1 x 10^5 and 2 x 10^6 Da [9], which binds many aggrecan monomers (up to 100 per molecule) each of which is composed of a core protein and ~300 negatively charged sulfated glycosaminoglycan (sGAG) sidechains [10,11]. Assembly of aggrecans along HA occurs pericellularly where HA remains attached to the CD44 receptor in chondrocytes [11]. The aggrecan aggregates are then released into the extracellular matrix giving rise to the high osmolarity in cartilage and contributing to its high compressive strength [12]. HA has also been implicated in tissue repair and wound healing processes, because of its antioxidant properties

(e.g. ability to scavenge free radicals) [13]. Due to the many benefits of HA, numerous studies have investigated varying techniques to incorporate HA into scaffolds for cartilage tissue engineering, including entrapment in collagen or alginate scaffolds [14,15], adhesion to scaffold surfaces [16], incorporation into fibers [17], or chemical functionalization to permit crosslinking [18–21].

The HA backbone includes side groups that are amenable to functionalization, where adding thiol or methacrylate groups permits crosslinking via a Michael type click reaction or radical polymerization, respectively, into 3D networks. Thiol-modified HA can form 3D scaffolds through formation of disulfide bonds or by reacting with PEG diacrylate monomers, although these reactions are typically slow and yield scaffolds with low elastic modulus (<10 kPa) [21–24], whereas the Young's modulus of cartilage ranges from 450 to 800 kPa [25]. Nonetheless, a synthetic ECM scaffold composed of thiol-modified HA and gelatin reacted with PEG diacrylate showed promise as a cell carrier for mesenchymal stem cells that regenerated hyaline-like cartilage in a rabbit osteochondral defect model [26]. Hydrogels made by photo-polymerization of methacrylated HA have been investigated as cell carriers for cartilage tissue engineering [19,20] and shown to enhance chondrogenesis compared to photo-polymerized bioinert PEG hydrogels [27]. Although HA can be degraded by hyaluronidases, these enzymes are restricted to the cell membrane and intracellularly to chondrocytes [28], requiring the introduction of degradable sequences in HA hydrogels [29]. Additionally, the methacrylated HA hydrogels that best supported cartilaginous neotissue formation by encapsulated mesenchymal stem cells had low initial modulus (<10 kPa) [30]. This further motivates a need to design high moduli hydrogels with properties approaching that of native cartilage [4,18] that can be polymerized *in situ* and withstand *in vivo* forces.

An alternative approach to chemical modification of hyaluronan is to design hydrogels that offer independent control over the hydrogel structure and the introduction of bioactivity, where the former is controlled through a synthetic hydrogel to achieve high initial modulus (200

kPa for this study) concomitant with hydrogel degradation to facilitate macroscopic tissue development. This study therefore tests the hypothesis that a sIPN composed of soluble HA and a hydrolytically degradable PEG network promotes tissue deposition and retention by encapsulated adult chondrocytes. A clear distinction has been made between 'low' molecular weight (MW) HA (< 3.5 x 10^4 Da) and 'high' MW HA (> 2 x 10^5 Da) [31], where low MW HA contributes to an inflammatory response which is attributed to HA fragments playing a role in signaling tissue damage [28,32], and high MW HA delivered to chondrocytes in 3D scaffolds increased cell number and sGAG synthesis [14,33]. These observations suggest that HA size may affect neotissue production. Physiological concentrations of HA in the synovial fluid can reach up to 3 mg ml^{-1} (10^6 Da) [34], and in human articular cartilage ranges from 0.5 to 2.5 mg g^{-1} [35]. For this study, HA of low MW (2.9 x 10^4), which is near the catabolic range [36,37], and high MW (2 x 10^6 Da), which is in the anabolic range [14,31,38,39], and low and high concentration (0.5 and 5 mg g^{-1} hydrogel) was entrapped in a hydrolytically degradable crosslinked PEG to produce a sIPN. Initially studies were performed to characterize the retention of HA in degradable hydrogels in the absence and presence of encapsulated cells. Skeletally mature adult bovine chondrocytes were encapsulated in the sIPN to investigate the effects of HA size and/or dose on tissue production, elaboration and destruction. Adult chondrocytes were chosen because they exhibit decreased metabolic activity and tissue synthesis capabilities, but increased catabolic activity compared to skeletally immature juvenile chondrocytes when encapsulated in PEG hydrogels [40,41], making adult chondrocytes a more clinically relevant model [42,43].

4.3 Materials and Methods

4.3.1 Materials

D,L Lactides and Hoechst 33258 were from Polysciences, Inc. (Warrington, PA). Collagenase type II, pepsin A, and papain were from Worthington Biochemical (Lakewood, NJ). Ethyl ether, ethylene diamine tetraacetic acid (EDTA), Triton X-100 and calcium chloride were

from Fisher Scientific (Fair Lawn, NJ). Irgacure 2959 was from Ciba Specialty Chemicals (Tarrytown, NY). Fetal bovine serum (FBS) was from Atlanta Biologicals (Lawrenceville, GA). The LIVE/DEAD® assay, phosphate-buffered saline (PBS), penicillin-streptomycin (P/S), fungizone, gentamicin, HEPES buffer, minimal essential medium non-essential amino acids (MEM-NEAA), trypsin-EDTA, trypan blue, CellTracker™ Red CMTPX, DAPI, AlexaFluor 488-conjugated goat anti-rabbit IgG, and AlexaFluor 546-conjugated goat anti-mouse IgG were from Invitrogen (Carlsbad, CA). Poly(ethylene glycol) MW 4600, methacrylic anhydride, L-proline, L-ascorbic acid, sodium chloride, potassium chloride, bovine serum albumin (BSA), dimethyl methylene blue (DMMB), chondroitinase ABC, hyaluronidase, protease from *Streptomyces griseus*, 5-aminofluorescein, 1-ethyl-3-(3-dimethylaminopropyl)carbodiimide (EDC), tris-HCl and sodium azide were from Sigma-Aldrich (St. Louis, MO). Keratanase I was from MP Biomedical (Solon, OH). Sodium hyaluronate was from Lifecore Biomedical (Chaska, MN). Mouse anti-aggrecan antibody (A1059-53E) and rabbit anti-collagen II antibody (C5710-20F) for immunohistochemistry were from US Biologicals (Swampscott, MA). Rabbit anti-collagen X antibody (ab58632) and rabbit anti-collagen I antibody (ab34710) were from Abcam (Cambridge, MA). Rabbit anti-C1,2C (collagenase-generated collagen neoepitope) antibody (50-1035) was from IBEX Pharmaceuticals (Quebec, Canada). Generic MMP and aggrecanase-1 SensoLyte™ assay kits were from Anaspec (Fremont, CA). Human ADAMTS-4 was from Millipore (Billerica, MA). Retrievagen A antigen retrieval solution was from BD Biosciences (San Jose, CA).

4.3.2 Macromer synthesis

The triblock copolymer oligo(lactic acid)-*b*-PEG-*b*-oligo(lactic acid) (LA-PEG-LA) was synthesized by reacting poly(ethylene glycol) (PEG, MW 4600) with lactides at a 1:3 molar ratio as previously described [44]. Briefly, PEG was melted at 90 °C in a temperature controlled oil bath followed by the addition of lactides and the catalyst stannous octoate. The temperature was increased to 140 °C and the reaction proceeded for 6 hours, after which the product was

recovered and purified by repeated precipitation in ethyl ether. PEG (MW 4600) and LA-PEG-LA were endcapped with methacrylates following microwave addition [45] to create the stable macromer PEG-dimethacrylate (PEGDM), and the hydrolytically degradable macromer PEG-LA-dimethacrylate (PEG-LA-DM), respectively. Briefly, methacrylic anhydride and PEG or LA-PEG-LA were reacted at a 10:1 molar ratio. Macromers were purified by precipitation in ethyl ether. ^{1}H-NMR spectroscopy was used to determine number of lactic acids (δ = 5.2 ppm) incorporated and degree of methacrylate substitution (δ = 5.6 and 6.2 ppm) per PEG molecule (δ = 3.4 – 3.9 ppm). On average, two lactic acid repeat units were added to each side of PEG. Methacrylate endcapping substitution for PEGDM was 93% and for PEG-LA-DM was 91%.

4.3.3 Chondrocyte isolation

Skeletally mature (referred to as adult) bovine articular chondrocytes were isolated from the metacarpal-phalangeal joints of three 1-2 year old steers (Arapahoe Meat Co., Lafayette, CO). Briefly, cartilage slices were washed in phosphate-buffered saline (PBS) supplemented with 1% penicillin streptomycin (P/S), 0.5 μg ml^{-1} fungizone and 20 μg ml^{-1} gentamicin (PBS-antis), and digested 16 hours at 37 °C in 0.2% collagenase type II in DMEM with 5% FBS. Isolated chondrocytes were washed in PBS-antis + 0.02% EDTA, pelleted and washed in PBS-antis and then passed through a 100 μm cell strainer. Cells were maintained in chondrocyte medium (DMEM supplemented with 10% FBS, 1% P/S, 10 mM HEPES, 0.1 M MEM-NEAA, 0.4 μM L-proline, 50 μg ml^{-1} L-ascorbic acid, 0.5 μg ml^{-1} fungizone and 20 μg ml^{-1} gentamicin). Medium was supplemented with KCl and NaCl (molar ratio 1:22) to adjust to 400 mOsm, confirmed by osmometer measurement (5002 Osmette A, Precision Systems, Inc., Natick, MA). 400 mOsm culture medium was previously shown to improve adult cell survival during encapsulation [46]. Cell viability was determined by trypan blue exclusion assay, yielding a viability of 96%.

4.3.4 Fluorescent hyaluronan synthesis, interaction with cells, and release

HA (2.9 x 10^4 and 2 x 10^6 Da) was fluorescently labeled with 5-aminofluorescein (491/515 nm excitation/emission) according to Ogamo *et al.* [47]. Briefly, 5-aminofluorescein was added to hyaluronan in pH 4.75 hydrochloric acid-pyridine solution at 1.6 molar equivalents per disaccharide. EDC was added and reacted overnight. Solution was dialyzed, precipitated repeatedly in ethanol with 1.25% w/w sodium acetate, dialyzed again and recovered by lyophilization. Interaction of fluorescent HA with cells was confirmed by incubating freshly isolated chondrocytes with 0.5 μM CellTracker Red for 45 minutes, then with 0.25 mg ml^{-1} fluorescent HA in chondrocyte medium overnight (20 hours) in suspension culture. Cells were recovered by centrifugation, washed in PBS-antis, fixed in 10% formalin for 15 minutes, and imaged by confocal laser scanning microscopy (CLSM, Zeiss LSM 510, Thornwood, NY) at 630x magnification. Selected samples were treated with 0.25% trypsin for 30 minutes at 37 °C prior to formalin fixation. For release studies, acellular hydrogels (n = 4) with 0.5 or 5 mg g^{-1} of fluorescent HA were incubated in PBS-antis, and cell-laden hydrogels (n = 3) encapsulated with 20 million cells ml^{-1} and fluorescent HA were cultured in chondrocyte medium. Fluorescent HA content in the conditioned medium, which was replaced every 2-3 days, was quantified at 491 nm on a NanoDrop 1000 spectrophotometer by comparing to standard curves of fluorescent HA dissolved in either PBS-antis or chondrocyte medium (Thermo Fisher Scientific, Fair Lawn, NJ). After 4 weeks the hydrogels were fully degraded in 2.5 M NaOH to quantify total fluorescent HA content per hydrogel. In all experiments, samples were protected from light.

4.3.5 Hydrogel formation

A 15% w/w macromer solution of 95:5 weight ratio PEG-LA-DM: PEGDM was prepared in chondrocyte medium. This formulation was identified to have a minimum number of the non-degradable crosslinks to prevent reverse gelation [48]. Low or high (2.9 x 10^4 or 2 x 10^6) MW HA was added to the macromer solutions at low or high (0.5 or 5 mg g^{-1} macromer solution) concentrations, and macromer solutions were sterile-filtered (0.2 μm). Chondrocytes were mixed with macromer solution at 20 million cells ml^{-1} and photopolymerized with 0.05% w/w

Irgacure 2959 into cylindrical constructs (5 mm diameter x 2 mm height) for 10 min with 365 nm light (6 mW cm^{-2}). Constructs were cultured in chondrocyte medium for up to 29 days at 37 °C in 5% CO_2 with fresh medium exchanges every 2-3 days. Cell viability in constructs (n = 2) was assessed using a LIVE/DEAD® membrane integrity assay at days 1, 15, and 29. Images were acquired using a confocal laser scanning microscope at 100x magnification.

4.3.6 Hydrogel characterization

Acellular hydrogels were assessed for wet weight and initial compressive modulus after swelling 24 hours in chondrocyte medium (n = 4). Hydrogels were compressed to 15% strain at a strain rate of 0.5 mm min^{-1}, to obtain stress-strain curves (MTS Synergie 100, 10N). The modulus was estimated as the slope of the linear region of stress-strain curves. For each construct, wet weight and its corresponding dry weight (after lyophilization) were measured to calculate mass swelling ratio q, using $q = M_s / M_d$, where M_s and M_d are swollen mass and dry mass. Acellular hydrogels with no entrapped HA (n = 2) were formed in chondrocyte medium and initial hydrogel mass was measured immediately following formation. Hydrogels were maintained in chondrocyte medium for 4 weeks and samples were taken periodically to lyophilize and measure dry mass. Percent polymer mass loss due to hydrolytic degradation was calculated as $\% \, mass \, loss = \frac{0.15M_i - M_d}{0.15M_i} \times 100$, where M_i is initial hydrogel mass.

4.3.7 Biochemical analysis

On select days, hydrogel constructs were removed (n = 3), weighed, snap frozen in liquid nitrogen and stored at -80 °C. Hydrogels were homogenized and digested with papain for 16 hours at 60°C. DNA content was measured using Hoechst 33258, and cell content was determined by assuming 7.7 pg of DNA per chondrocyte [49]. Collagen was measured in the gels and conditioned media using the hydroxyproline assay, where hydroxyproline is assumed to make up 10% of collagen [50]. Constructs and conditioned media were assayed for GAG

content using the dimethyl methylene blue (DMMB) dye assay [51]. GAG and collagen content in the hydrogels were normalized to cell number.

4.3.8 Immunohistochemical analysis

On day 29, constructs (n = 2) were fixed in 4% paraformaldehyde, dehydrated, paraffin embedded and sectioned to 10 μm. Sections were treated with primary antibodies against aggrecan (1:5), collagen type II (1:50), collagen type X (1:50), collagen type I (1:50), and C1,2C (1:100). Before primary antibody treatment, sections underwent antigen retrieval, then were treated with appropriate enzymes for 1 h at 37 °C: hyaluronidase (200 U) for aggrecan, collagen II, and C1,2C; chondroitinase ABC (10 mU) and keratanase I (4 mU) for aggrecan; pepsin A (280 kU) for collagens I and X; and protease (400 U) and 0.25% trypsin for collagen X. Sections were probed with AlexaFluor 488 or 546-conjugated secondary antibodies and counterstained with DAPI. A laser scanning confocal microscope was used to acquire images with a 40x oil objective using the same settings and post-processing for all images. Cell-laden hydrogel sections that received no primary antibody treatment were used as negative controls, showing no positive staining. Sections of hyaline cartilage were used as positive controls.

4.3.9 Enzyme activity assays

Constructs at select days (n = 2) were snap-frozen in liquid nitrogen and stored at -80 °C. The constructs were homogenized in Sensolyte kit assay buffer with 0.1% Triton-X 100. Construct lysate was assayed for activity of MMPs and ADAMTS-4 with Sensolyte 520 assay kits containing substrates specific for ADAMTS-4 (aggrecanase-1) and generic MMPs (probes for MMP-1, 2, 3, 7, 8, 9, 10, 12, 13, and 14 simultaneously). Activity was measured as amount of cleaved substrate generated after incubating 1 h at 37 °C with cell lysate samples. Human ADAMTS-4 and collagenase II were used as positive controls for active enzymes. Conditioned medium samples were analyzed but active enzymes were not detected.

4.3.10 Statistical analysis

Data are presented as mean (standard deviation). Measures of HA release, hydrogel properties, biochemical content, enzyme activity, and immunohistochemical quantitation were analyzed by two-way ANOVA where the factors were culture time and hydrogel formulation, followed by one-way ANOVA with Fisher's LSD post-hoc test, $\alpha = 0.05$, to determine significant difference between conditions at specific time points. Normal probability plots of the residuals were generated and were found to support the normal distribution assumption (plots not shown).

4.4 Results

4.4.1 Characterization of acellular sIPN hydrogels

Semi-interpenetrating networks of crosslinked degradable PEG-LA and HA were characterized by compressive modulus and mass swelling ratio 24 h after swelling and by release of fluorescently labeled HA over the course of 31 days (Fig. 4.1). Hydrogel formulation as an overall factor did not significantly affect compressive modulus ($p = 0.12$), but did affect mass swelling ratio q ($p = 0.001$) (Fig. 4.1 A, B). There was an initial burst release of ~10% of the entrapped HA, followed by a steady release of HA over the course of approximately one month, and HA release was significantly affected by hydrogel formulation and time ($p < 0.03$ for all comparisons), as determined by 2-way ANOVA (Fig. 4.1C). Mass loss due to hydrolytic degradation in acellular hydrogels with no entrapped HA was assessed (Fig. 4.1D) revealing rapid polymer mass loss up to 15 days followed by little to no additional mass loss.

4.4.2 HA interaction with chondrocytes

The ability of the fluorescently labeled HA to interact with chondrocytes was confirmed by incubating fluorescent HA in the presence of chondrocytes in a suspension culture (Fig. 4.2A, and supplemental figure 4.S1). The fluorescent HA remained co-localized with chondrocytes after several wash steps. Following trypsin treatment to remove any pericellular bound HA, the majority of the fluorescent HA was lost, but a small amount remained and was visible intracellularly. When chondrocytes were co-encapsulated with fluorescent HA, the hydrogel formulation and time affected HA release ($p < 0.004$ for all comparisons) as

determined by 2-way ANOVA (Fig. 4.2B), where early release was slower with low initial concentrations of HA. In all conditions by four weeks, ~90% of the initially encapsulated HA was released.

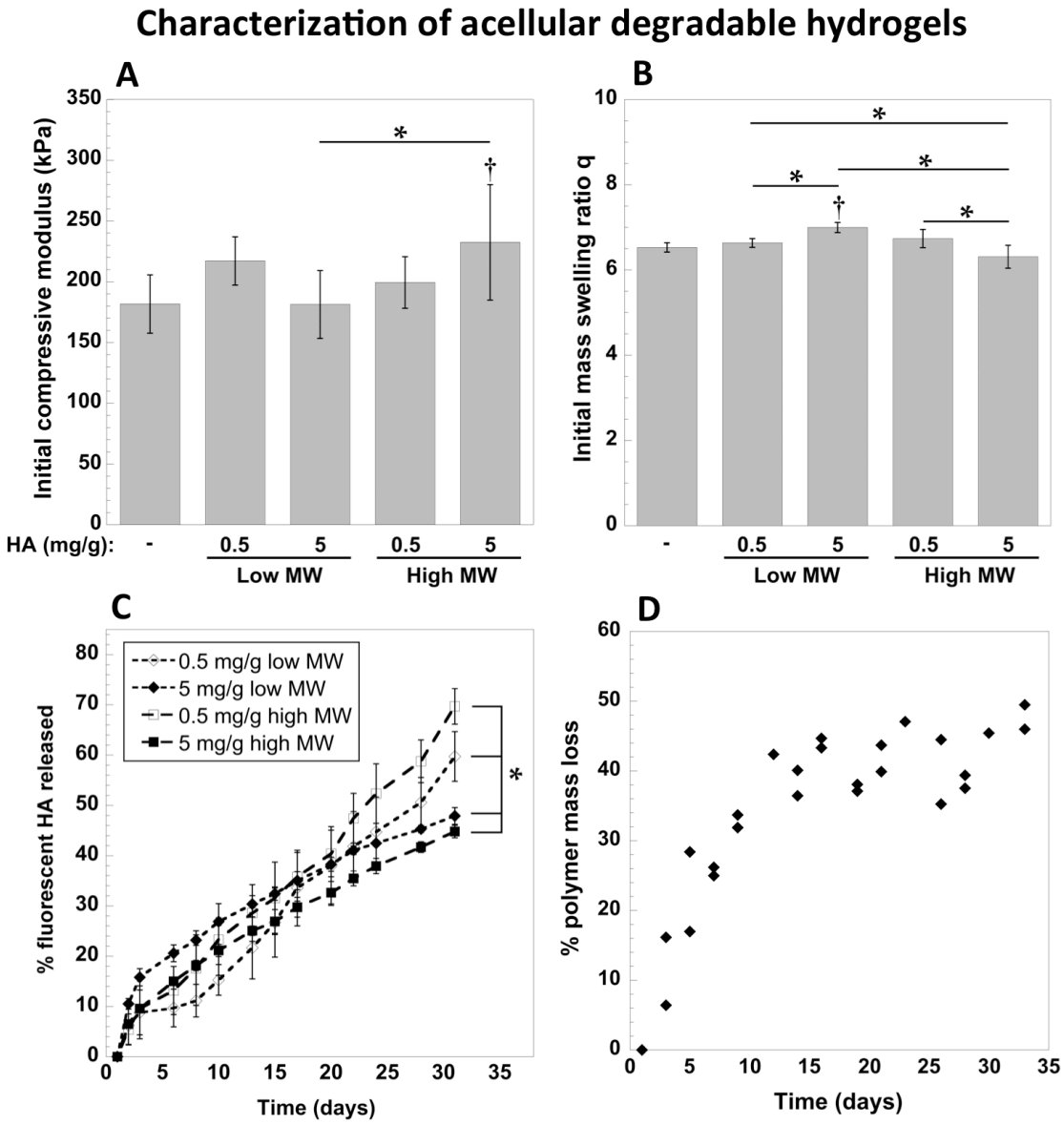

Figure 4.1 (A) Equilibrium compressive modulus and (B) mass swelling ratio *q* of acellular hydrogels containing hyaluronic acid (HA) of low or high MW (2.9×10^4 or 2×10^6 Da) measured 1 day after hydrogel formation. † indicates significantly different from no HA, * indicates significant difference between treatment conditions ($p < 0.05$). (C) Percent release of fluorescently labeled HA from acellular degradable hydrogels in PBS as a function of time. * indicates significant difference between release profiles with varied HA MW and concentration ($p < 0.05$). (D) Percent polymer mass loss from acellular hydrolytically degrading hydrogels (with no entrapped HA) incubated in chondrocyte medium.

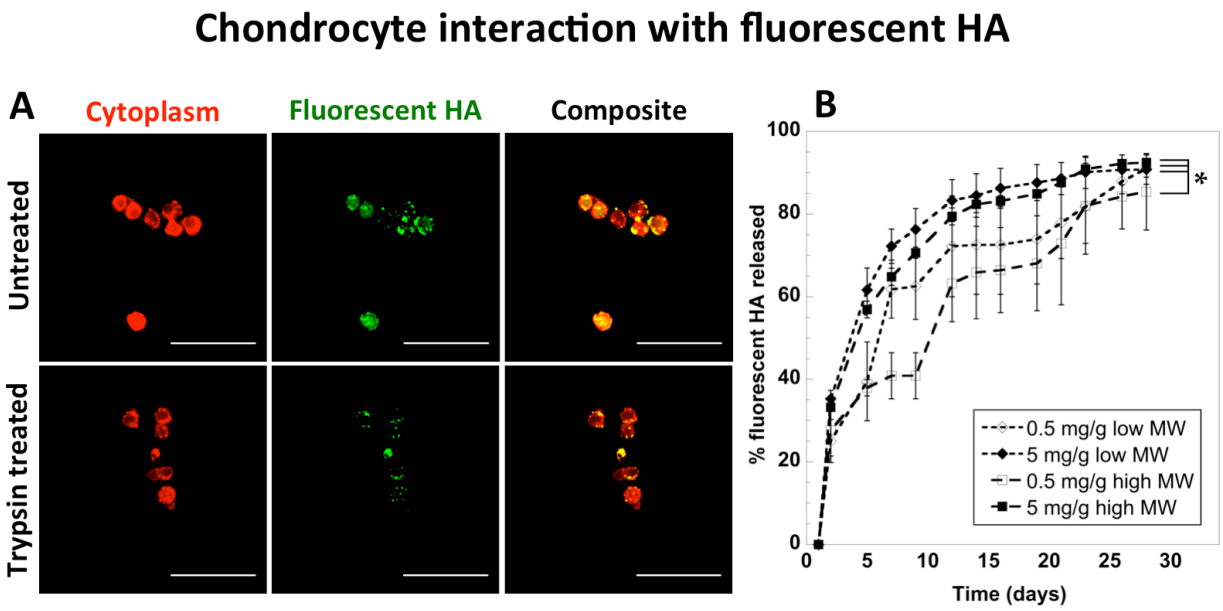

Figure 4.2 (A) Adult chondrocytes (CellTracker Red) in suspension interacting with fluorescently labeled HA (5-aminofluorescein, green) of low MW (2.9 x 10^4 Da) for 20 hours, with or without subsequent 30 minute trypsin treatment. Scale bars indicate 50 μm. (B) Percent release of fluorescently labeled HA from cell-laden degradable hydrogels in culture medium as a function of time. * indicates significant difference between release profiles with varied HA MW and concentration ($p < 0.05$).

4.4.3 Cell viability and cell number

Representative cell viability images from LIVE/DEAD® staining qualitatively showed cell density and formation of cell clusters over four weeks of culture (Fig. 4.3A). One day post-encapsulation, cell viability was similarly high for all conditions with cells fairly evenly dispersed throughout the hydrogels. Cell clustering was apparent at day 15, and large interconnected clusters were observed at 29 days. Individual cells were also prevalent in all conditions throughout the study, appearing similar to day 1 (images not shown). DNA content was used to measure cell number per initial hydrogel dry weight (i.e., one day after encapsulation) (Fig. 4.3B) and over the four week culture period (Fig 4.3C). Initially, cell number per dry weight was lowest for the low MW HA regardless of concentration ($p < 0.01$), and for the high concentration

of high MW HA (p = 0.02), compared to no HA. Over the entire culture period, cell number normalized to day 1 was affected by culture time (p = 0.0012), where cell number in the no HA

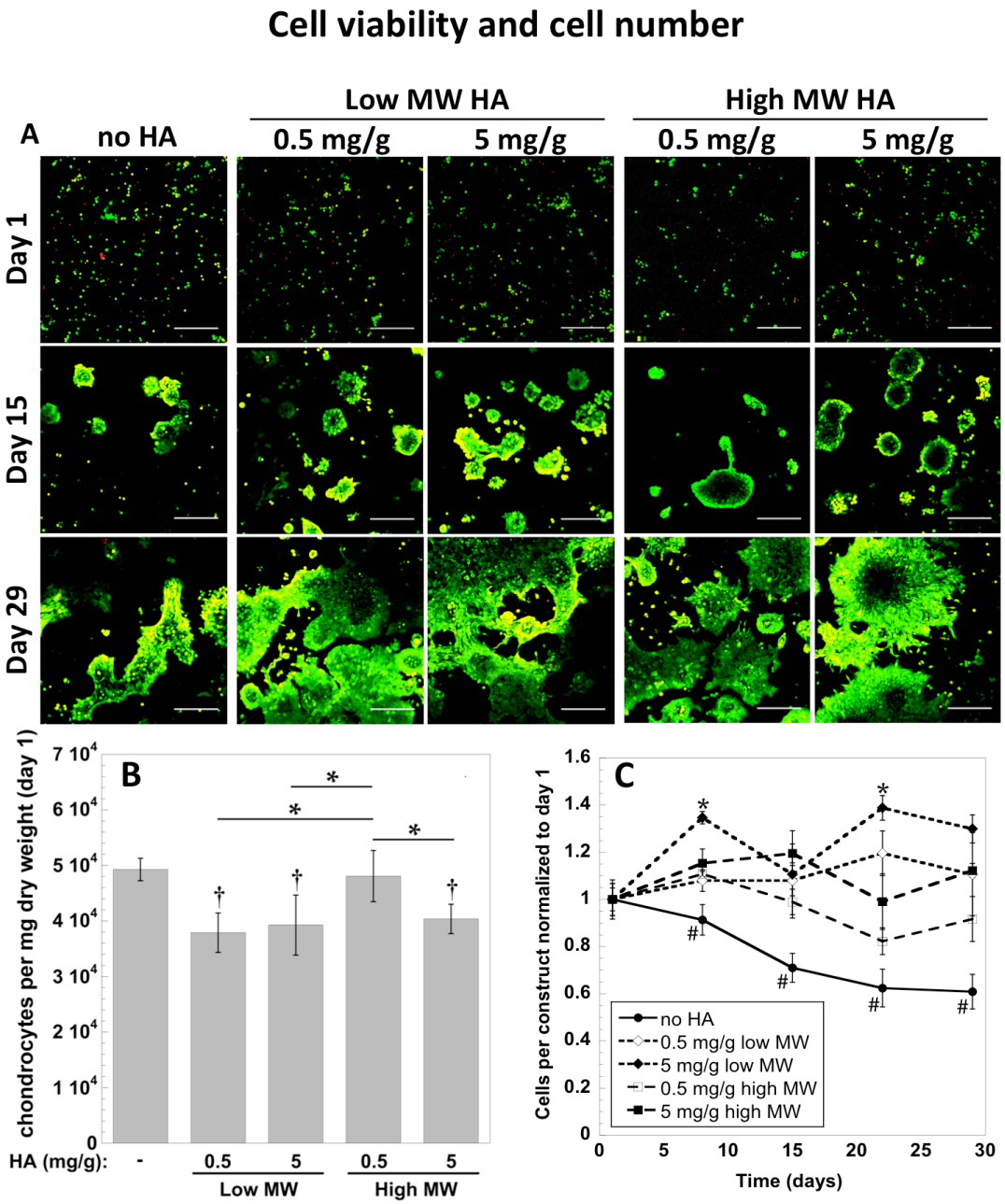

Figure 4.3 (A) Viability and cell clustering morphology of encapsulated cells at days 1, 15, and 29 with low or high MW HA (2.9 x 10^4 or 2 x 10^6 Da). Live cells are green, dead cells are red. Scale bars indicate 200 μm. (B) Chondrocytes per construct measured 1 day after encapsulation. † indicates significantly different from no HA, * indicates significant difference between treatment conditions (p < 0.05). (C) Cells per construct normalized to day 1. # indicates significant difference from all HA conditions, * indicates different from all conditions (p < 0.05).

group decreased with time (Fig. 4.3C). HA incorporation significantly improved cell content compared to the no HA group ($p < 0.015$), where the mean highest cell numbers by four weeks were measured in the hydrogels with high concentrations of low MW HA (240,000 ± 10,000 cells per construct) and high MW HA (280,000 ± 8,000 cells per construct). Gel formulation did not affect hydrogel degradation, as cell-laden gel wet weights increased significantly with time ($p < 0.0001$) from about 40 to 55 mg per gel and was similar regardless of gel formulation (data not shown).

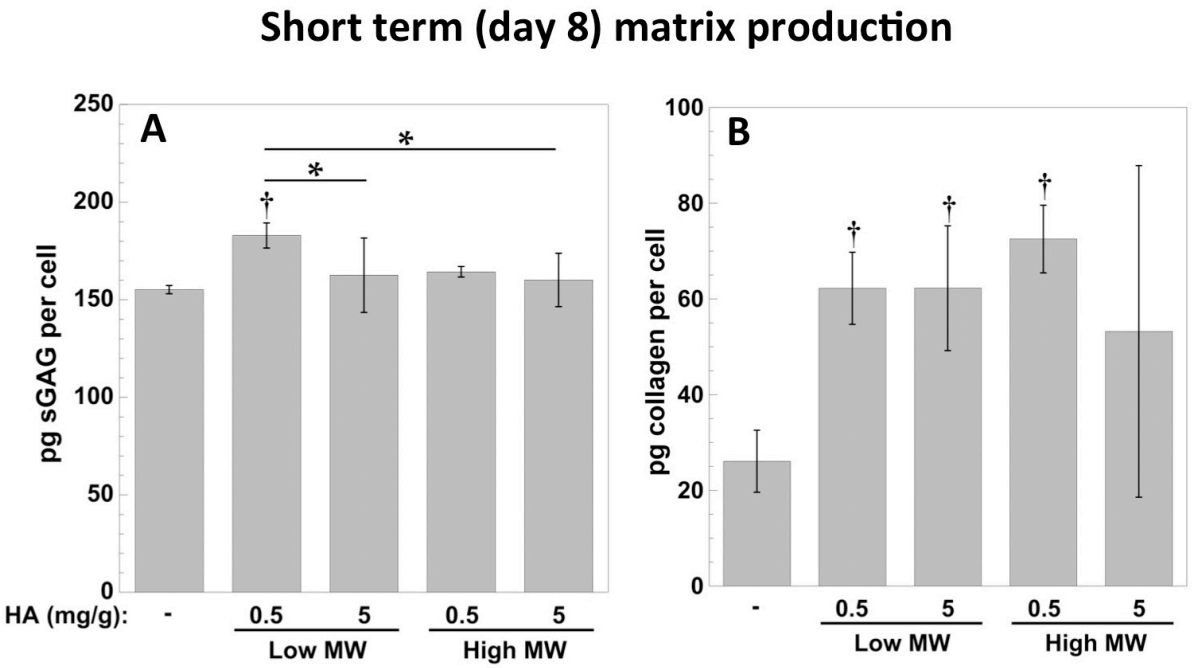

Figure 4.4 Quantity of sGAG (A) or collagen (B) measured after 8 days of culture in constructs with low or high MW HA (2.9 x 10^4 or 2 x 10^6 Da), normalized to cell number. **†** indicates significantly different from no HA, * indicates significant difference between treatment conditions ($p < 0.05$).

4.4.4 Biochemical and immunohistochemical content in the short-term (8 days)

To analyze the effect of HA at early time points, biochemical content after 8 days of culture was quantitatively assessed for sGAG and collagens, and immunohistochemically stained for collagen II, aggrecan, and collagen X (Fig. 4.4, 4.5). Collagen I and collagenase-generated neoepitope C1,2C were assessed immunohistochemically and staining was minimal

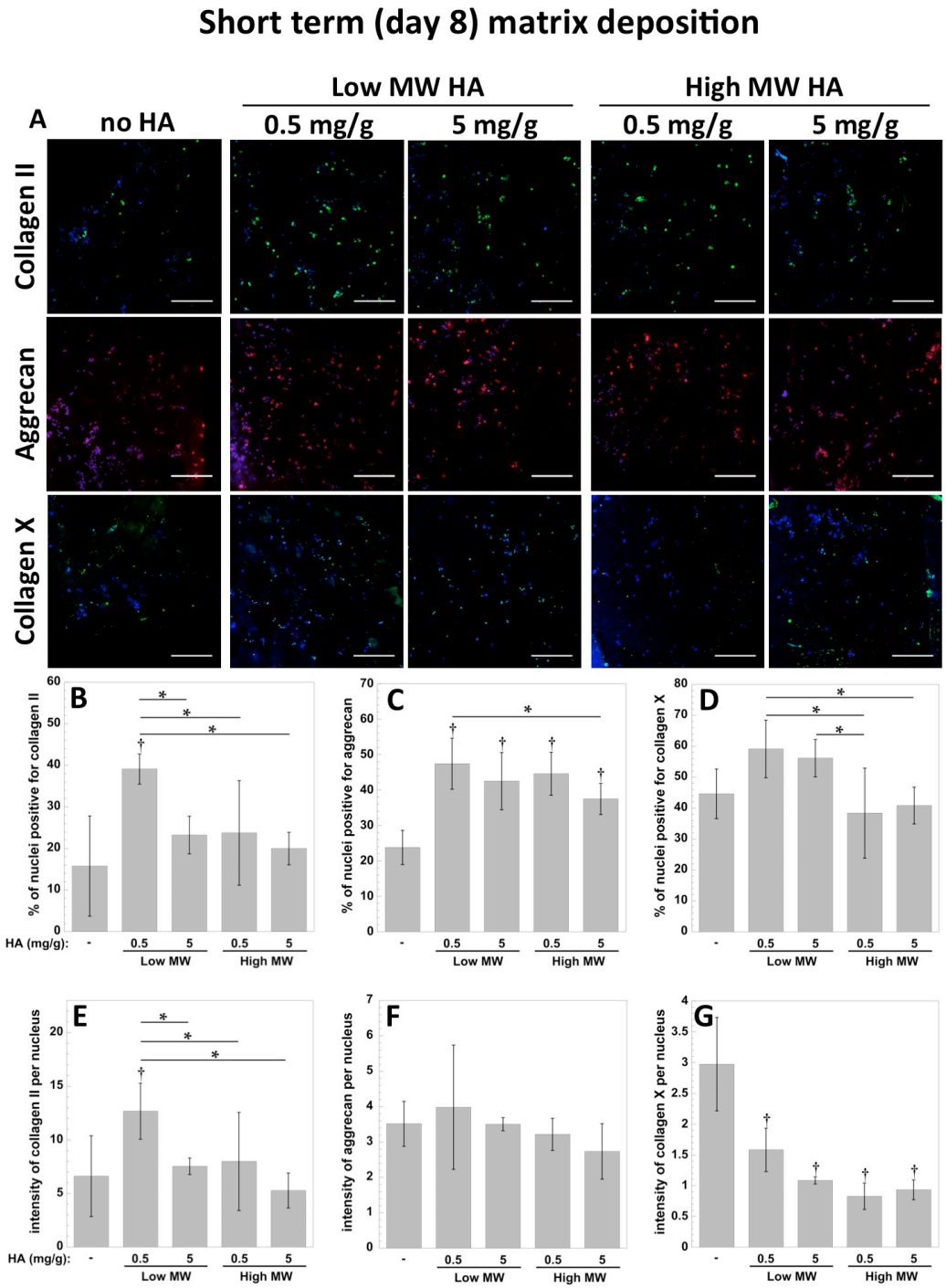

Figure 4.5 (A) Immunohistochemical visualization of collagen II (green), aggrecan (red), and collagen X (green) deposition in constructs after 8 days of culture with low or high MW HA (2.9 x 10^4 or 2 x 10^6 Da). Nuclei are blue, scale bars indicate 200 μm. (B - G) Semi-quantitative analysis of day 8 immunohistochemical images (n = 3-4 images) to estimate percentage of cells staining positive (B – D) or intensity per nucleus (E-G) for collagen II (B, E), aggrecan (C, F), and collagen X (D, G). † indicates significantly different from no HA, * indicates significant difference between treatment conditions ($p < 0.05$).

with no observable differences due to HA (data not shown). From Fig. 4.2B, approximately 40% to 70% of initially entrapped HA was released after 8 days. At this time point, mean sGAG content was elevated in the low MW, low concentration HA formulation (Fig. 4.4A). Improvement in collagen content with HA incorporation was more pronounced, where all conditions except for high MW, high concentration HA were elevated over the no HA group ($p < 0.015$) (Fig. 4.4B). Qualitative and semi-quantitative analysis of specific extracellular matrix molecules further corroborated early improvements in matrix deposition by HA (Fig. 4.5). Collagen II and X and aggrecan were all observed pericellularly (Fig. 4.5A). Semi-quantitative analysis of images revealed that both the percentage of nuclei staining positive for collagen II and intensity per nucleus were elevated by low MW, low concentration HA ($p < 0.009$) (Fig. 4.5B, E), and that nuclei staining positive for aggrecan was significantly increased by all HA conditions ($p < 0.015$) (Fig. 4.5C), although intensity of aggrecan per nucleus was unaffected (Fig. 4.5F). Percentage of nuclei staining positive for collagen X was not different from the no HA condition, although low MW HA yielded more nuclei staining positive for collagen X compared to high MW HA ($p < 0.05$), but staining intensity per nucleus was significantly decreased by all HA conditions ($p < 0.003$) (Fig. 4.5D, G).

4.4.5 Biochemical and immunohistochemical content in the long term (29 days)

To investigate the long-term impact of the HA sIPN, biochemical and immunohistochemical analyses were performed after 29 days of culture (Fig. 4.6, 4.7). Samples were collected on days 15, 22, and 29 but only day 29 is presented, which represents the cumulative matrix elaboration in the long-term. Fig. 4.2B it was estimated that after 4 weeks, approximately 90% of initially entrapped HA was released from the hydrogels. After 4 weeks of culture, HA led to a significantly lower quantity of sGAG per cell in the hydrogels ($p < 0.015$) (Fig. 4.6A). However, the cumulative amount of sGAGs produced by the chondrocytes over the course of the study, including that which was retained in the constructs and that which was released to the culture medium, was highest in the conditions with high concentration HA

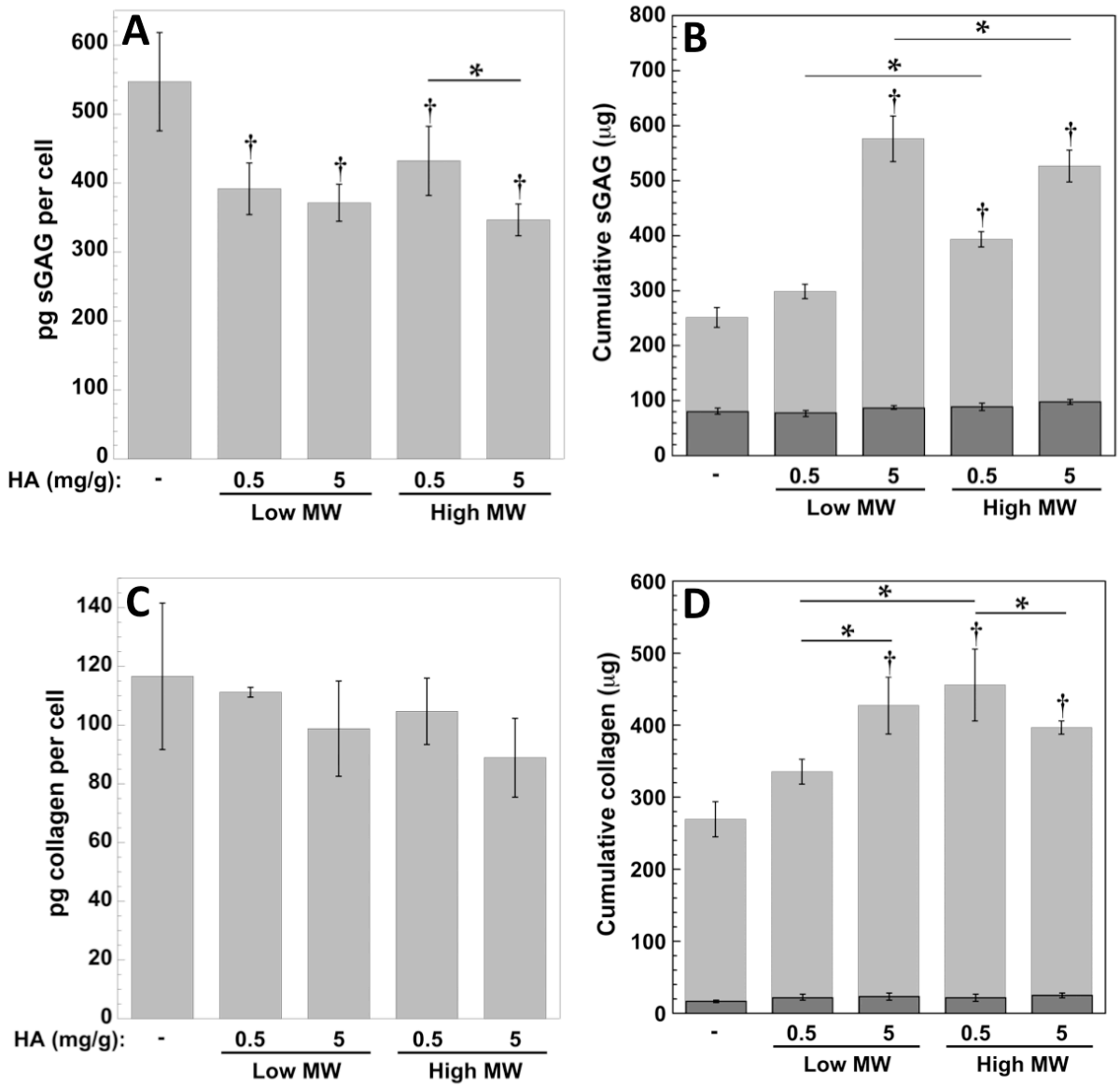

Figure 4.6 Quantity of sGAG (A) or collagen (C) measured after 29 days of culture in constructs with low or high MW HA (2.9 x 10^4 or 2 x 10^6 Da), normalized to cell number. Cumulative sGAG (B) or collagen (D) released to the culture medium through day 29 (▒), or present in the constructs at day 29 (■). † indicates significantly different from no HA, * indicates significant difference between treatment conditions ($p < 0.05$).

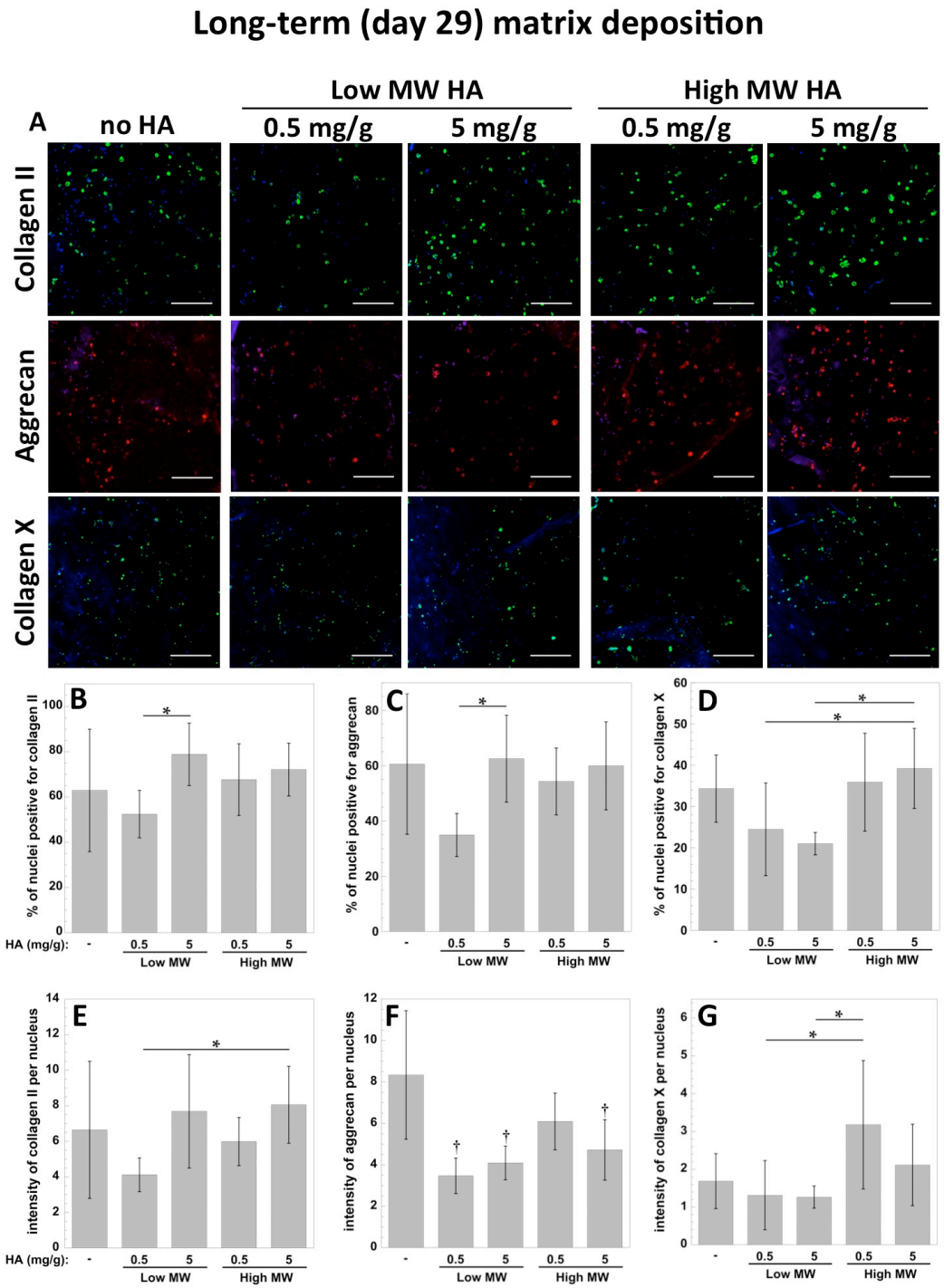

Figure 4.7 (A) Immunohistochemical visualization of collagen II (green), aggrecan (red), and collagen X (green) deposition in constructs after 29 days of culture with low or high MW HA (2.9 x 10^4 or 2 x 10^6 Da). Nuclei are blue, scale bars indicate 200 μm. (B-G) Semi-quantitative analysis of day 29 immunohistochemical images (n = 3-4 images) to estimate percentage of cells staining positive (B-D) or intensity per nucleus (E-G) for collagen II (B, E), aggrecan (C, F), and collagen X (D, G). † indicates significantly different from no HA, * indicates significant difference between treatment conditions ($p < 0.05$).

regardless of MW (Fig. 4.6B). No difference was observed among conditions for total collagen content in the hydrogel on a per cell basis or per construct. However, when total amount of collagen produced by the cells over the course of the study was determined, the high MW HA at both concentrations, and low MW HA at high concentration led to similarly high total collagen production (Fig. 6D). Qualitative and semi-quantitative analysis for specific extracellular matrix molecules present at 29 days was performed on regions with single cells (Fig. 4.7). Regions containing clusters of cells were analyzed qualitatively (Fig. 4.8). In single cells, collagen II and X as well as aggrecan were localized pericellularly. Overall, there were no significant improvements due to HA incorporation, and aggrecan staining intensity per cell was decreased by HA (Fig. 4.7F). Collagen II and X deposition was noticeably more intense when compared to day 8, and at day 29 a greater percentage of cells stained positive for collagen II compared to collagen X, where the inverse was true at day 8. Interestingly the clusters, which were not observed after 8 days, were prominent by 29 days (Fig. 4.8), appeared to have greater collagen X staining and reduced staining for collagen II and aggrecan. Staining for collagen I and collagenase-generated neoepitope C1,2C remained minimal at day 29.

4.4.6 Catabolic enzyme activity

Active matrix degrading enzymes were detected in the constructs for all conditions but not in the culture medium (Fig. 4.9). Generic MMP activity measured per cell increased significantly with time ($p = 0.002$). No significant differences were observable at early (day 1) or late (day 29) time points, however at day 15, MMP activity was significantly elevated by low MW HA compared to the no HA condition ($p < 0.04$). Aggrecanase-1 activity increased significantly with time ($p = 0.003$) but was not statistically different among the different conditions ($p = 0.14$); although mean levels were slightly elevated by low MW HA at day 15 and slightly decreased by high MW HA at day 29, compared to no HA.

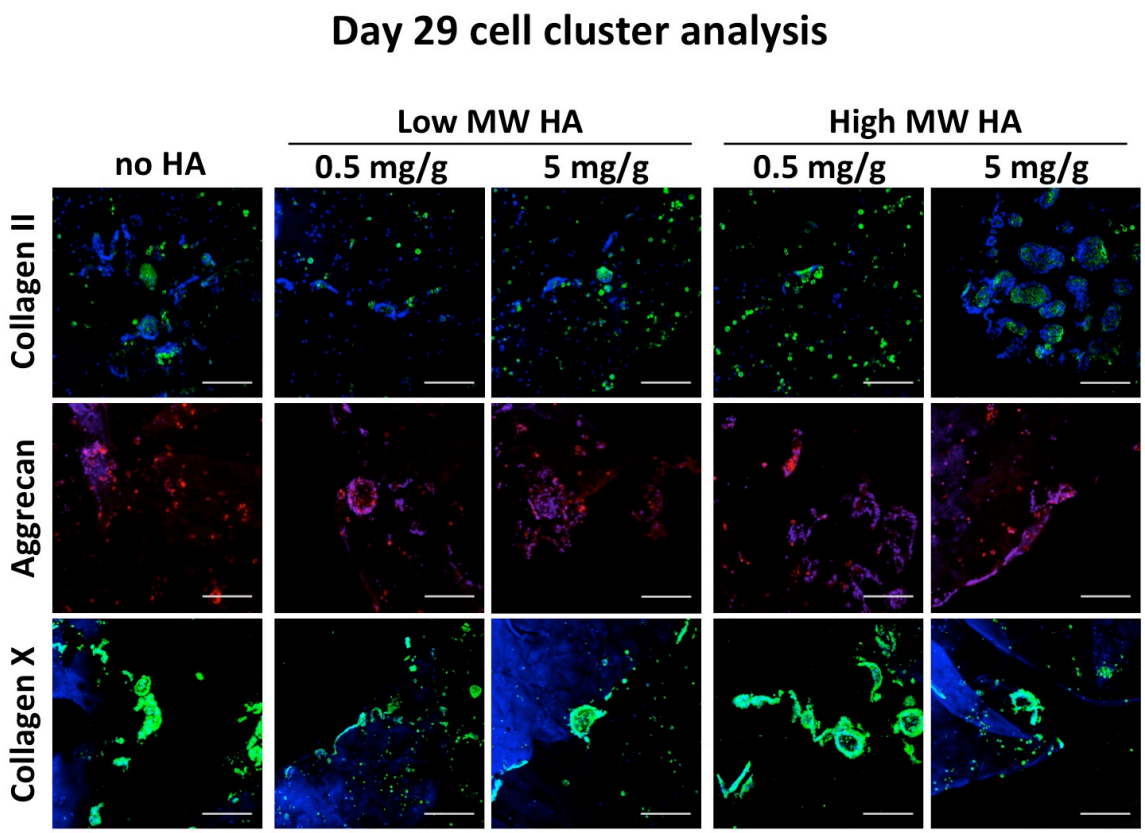

Figure 4.8 Immunohistochemical visualization of collagen II (green), aggrecan (red), and collagen X (green) content within cell clusters formed after 29 days of culture with low or high MW HA (2.9 x 10^4 or 2 x 10^6 Da). Nuclei are blue, scale bars indicate 200 μm.

4.5 Discussion

Towards developing a cartilage tissue engineering strategy employing adult cells, chondrocytes isolated from skeletally mature donors were encapsulated in a sIPN composed of crosslinked hydrolytically degradable PEG to control for degradation and linear HA to introduce bioactivity. The results from this study suggest that HA when simply entrapped in degrading hydrogels is able to bind directly to chondrocytes leading to improved cartilage-like ECM synthesis and quality. Long-term, the total amount of ECM synthesized was elevated in the HA sIPN hydrogels, but a majority of the ECM was released. The latter is attributed to a combination of bulk hydrogel degradation and the continued release of HA throughout the study.

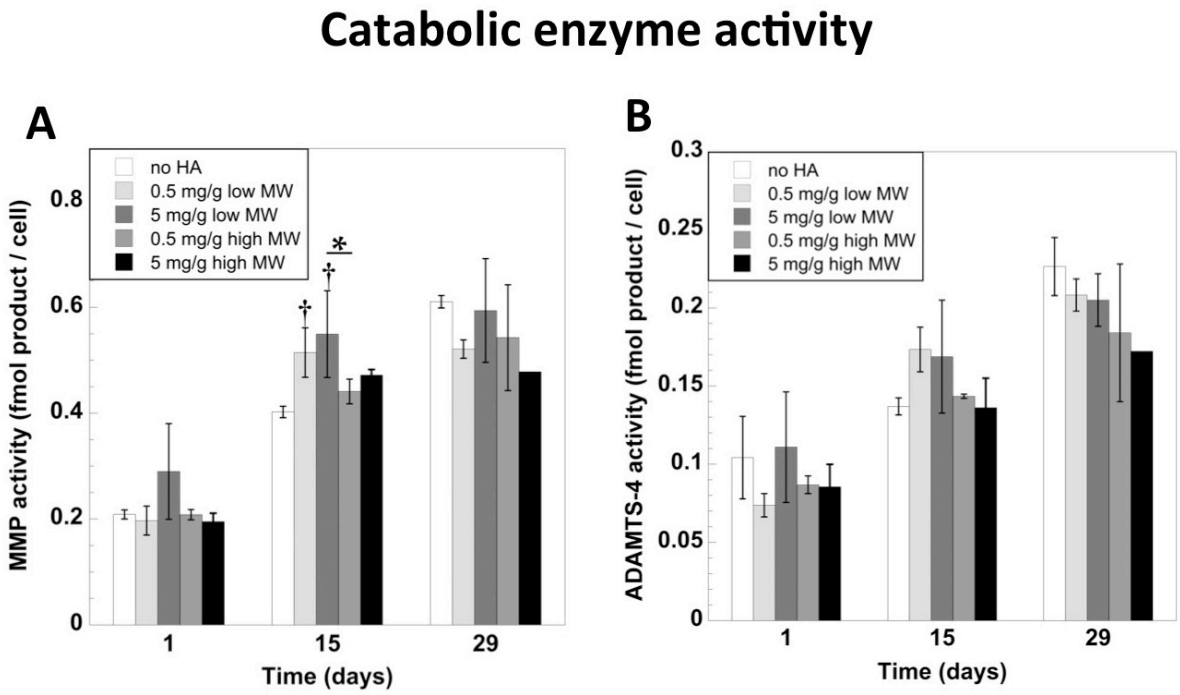

Figure 4.9 Activity of MMPs (A) or ADAMTS-4 (B) per cell in constructs with low or high MW HA (2.9 x 10^4 or 2 x 10^6 Da), compared to the no HA condition. **†** indicates significantly different from no HA, * indicates significant difference between treatment conditions ($p < 0.05$).

Nonetheless, these findings show that simple entrapment of a bioactive molecule can lead to significant improvements in tissue synthesis.

Incorporating HA into hydrolytically degradable hydrogels maintained cell number over the course of the study independent of HA molecular weight and concentration. In the absence of HA, cell number dropped significantly by ~40% by the end of the study and was 1.6-2.2-fold lower than the HA sIPNs. The former is consistent with previous work by our group [40] and is in part attributed to the degradation and mass loss of the hydrogel which can cause release of cells. The latter is consistent with previous observations, which showed for example that either delivering HA exogenously to chondrocytes in collagen hydrogels or entrapping HA in alginate hydrogels with encapsulated chondrocytes led to overall improved cell number [14,15]. This improvement in cell number by HA can be attributed to stimulated proliferation, as suggested by others [13,52,53], or possibly increased cell retention via cell surface receptors (e.g., CD44),

which bind HA [52]. In support of the latter, we confirmed that chondrocytes indeed bind HA pericellularly.

Overall, HA sIPNs improved cartilage-like tissue deposition and quality at early culture times. Most notably, HA significantly improved total collagen content while significantly reducing collagen X staining intensity per cell within one week of culture regardless of HA MW or concentration. The percentage of cells staining positive for aggrecan was significantly increased by HA, however staining intensity per cell was not elevated, which may explain why sGAG quantity in the hydrogels was unaffected by HA. While total collagen content encompasses most types of collagen, our data suggests an improved quality of neocartilage deposition because collagen X is substantially reduced, while collagen II is largely maintained, and collagen I is minimal. Collagen X is an indicator of hypertrophy and is produced abundantly by osteoarthritic cells [54]. Our data suggest that HA especially at early time points maintains a healthy chondrocyte phenotype.

Long-term the beneficial effects of HA diminished, which in part is attributed to its continued release over time. In general, the tissue formed in the hydrogels was similar among the PEG and HA sIPN hydrogels with the exception of sGAG content and aggrecan staining intensity per cell, which was significantly reduced in HA sIPN hydrogels. Because aggrecan assembles extracellularly along HA [39], and there was sustained HA release throughout 4 weeks in the presence of cells, it is possible that sIPN gels containing entrapped HA contributed to diffusive loss of aggrecans from the constructs. Interestingly though, the total amount of sGAG and collagen content synthesized over the course of 4 weeks was significantly higher in the HA sIPN hydrogels with the exception of the low MW HA at low concentration. The majority of the ECM synthesized, however, was released to the culture medium and was especially pronounced at high concentrations. To determine if the release of ECM molecules was a result of matrix catabolism, MMP and aggrecanase activity were measured, and degraded collagen (the C1,2C neoepitope) was observed, where C1,2C staining was minimal and was unaffected

by HA. Aggrecanase activity was similar among all hydrogels. MMP activity, however, was elevated at day 15 in the low MW HA sIPN, but not in high MW HA sIPN. These findings suggest that for high MW HA sIPN, the elevated loss of ECM was likely not due to catabolism, but simply diffusive loss in degrading hydrogels and/or a lack of proper matrix assembly, the latter which is prevalent in adult chondrocytes [55]. Only the high concentration of low MW HA sIPN showed elevated levels of sGAG and collagen, but this was concomitant with elevated MMP activity. This finding is consistent with observations that HA oligosaccharides lead to increased expression of MMP-3 [36] and MMP-13 [37] in chondrocytes. These findings suggest that high MW HA sIPNs enhance neocartilage synthesis, but that degradation of the hydrogel and release of HA leads to reduced matrix retention.

Because the entrapped HA is not covalently bound to the PEG network, it can either interact with cells and participate in matrix assembly or diffuse out of the degrading hydrogels. The fluorescent HA release studies revealed that ~90% of the initially entrapped HA was released from the hydrogels after 4 weeks (Fig. 4.2B), which is attributed to degradation of the hydrogel as previous studies in non-degrading PEG hydrogels measured much lower HA release [56]. The amount remaining in the gels equates to ~4 pg HA per cell (for the low concentration) or ~15 pg HA per cell (for the high concentration), where 1 pg of low MW HA equals ~20 million molecules, and 1 pg of high MW HA equals ~300,000 molecules, meaning that a considerable amount of HA should be retained after 4 weeks. The ability of chondrocytes to interact with fluorescently labeled HA was confirmed, and treating with trypsin to remove extracellularly associated fluorescent HA revealed that only a portion of the HA was intracellularized regardless of MW. This is consistent with other reports, which showed that bovine chondrocytes are able to endocytose fluorescein-labeled HA through a CD44-associated receptor-mediated process into discrete intracellular vesicles [57], and interestingly fibroblast uptake of extracellular fluorescein-HA was increased during cell proliferation [53]. Cell-mediated catabolism of HA can only occur intracellularly or on the cell membrane [28], whereas

extracellular degradation of HA mostly occurs via free radicals [58]. It is possible that some fraction of HA not released from the hydrogels after 4 weeks was internalized where it may have affected cellular processes but could not participate in matrix assembly. Long-term benefits in matrix production but not retention were observed most prominently at high concentrations of HA regardless of MW, suggesting that cellular interaction with HA may not be dependent on the molecular weight of HA in the range of 10^4-10^6 Da.

Hydrolytic degradation of PEG-LA hydrogels was highly heterogeneous, as evidenced by the prevalence of both cell clusters and individual chondrocytes. Interestingly the extracellular matrix composition of the clusters appears to be characteristic of hypertrophic cartilage neotissue as seen by the intense collagen X staining, and minimal collagen II and aggrecan staining. However the individual cells remained more hyaline cartilage-like with many more cells staining positive for collagen II and aggrecan than for collagen X. A limitation of this study was the fast degradation rate of the hydrogels, which led to hydrogel swelling and loss of newly synthesized matrix regardless of HA incorporation. An ongoing focus of our research is improving hydrogel degradation to match matrix production. Another limitation of this study was the lack of mechanical stimulation, which is well known to be critical for maintaining cartilage homeostasis [5,59,60] and has also been shown to decrease collagen X expression [61]. In addition, the hydrogels were designed with a small fraction of non-degradable crosslinks, which likely contributed to the localized pericellular matrix surrounding individual cells.

4.6 Conclusions

Mature chondrocytes encapsulated in a hydrolytically degradable semi-interpenetrating network with bioactive HA produced a cartilaginous neotissue characterized by collagen II and aggrecan. We investigated the long-term culture effects of entrapped HA on chondrocytes, revealing improved cell content and initial boosts in tissue deposition and decreased hypertrophy, yet these effects were diminished as the HA and neotissue diffused out of the degrading hydrogel network. However, overall sGAG and collagen production were greatly

increased by high concentrations of high MW HA supporting the idea that HA improves bioactivity, specifically chondrocyte anabolism long-term, which is consistent with our hypothesis that facilitating early matrix deposition with HA improves matrix production long-term. Low MW HA was less promising showing higher catabolism suggesting that high molecular weights around 10^6 Da are more favorable. However, efforts are needed to retain HA and neotissue within degrading hydrogels. To overcome this shortcoming, our group is developing hydrogels with HA-retaining peptides that minimize loss of entrapped HA and newly synthesized tissue [56,62]. Overall, incorporating HA into synthetic scaffolds remains a promising strategy to improve cartilage tissue regeneration utilizing clinically relevant mature autologous cells and degradable scaffolds.

4.7 Acknowledgements

This research was supported by NIH grant # R21AR061011, a Bioengineering Discovery and Evaluation Grant from the State of Colorado, a fellowship from the National Science Foundation Graduate Research Fellowship Program (NSF GRFP), a National Institute of Health (NIH) Pharmaceutical Biotechnology Training Grant, and a Chancellor's Fellowship from the University of Colorado. The authors would like to thank Shash O Dimson and Ashley M Pennington, who co-authored the manuscript.

4.8 Supplementary Figures

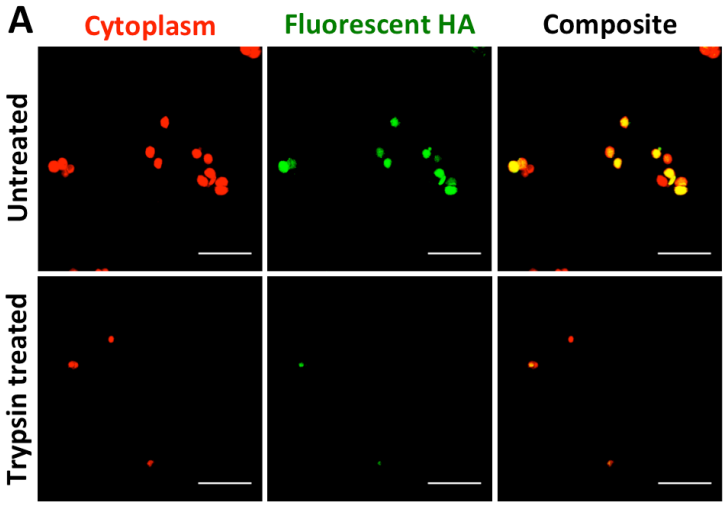

Figure 4.S1 Adult chondrocytes (CellTracker Red) in suspension interacting with fluorescently labeled HA (5-aminofluorescein, green) of high MW (2 x 10^6 Da) for 20 hours, with or without subsequent 30 minute trypsin treatment. Scale bars indicate 50 μm.

4.9 References

[1] Bryant SJ, Durand KL, Anseth KS. Manipulations in hydrogel chemistry control photoencapsulated chondrocyte behavior and their extracellular matrix production. J Biomed Mater Res Part A 2003;67A:1430–6.

[2] Bryant SJ, Anseth KS. Hydrogel properties influence ECM production by chondrocytes photoencapsulated in poly(ethylene glycol) hydrogels. J Biomed Mater Res 2002;59:63–72.

[3] Bryant SJ, Chowdhury TT, Lee DA, Bader DL, Anseth KS. Crosslinking density influences chondrocyte metabolism in dynamically loaded photocrosslinked poly(ethylene glycol) hydrogels. Ann Biomed Eng 2004;32:407–17.

[4] Nicodemus GD, Skaalure SC, Bryant SJ. Gel structure has an impact on pericellular and extracellular matrix deposition, which subsequently alters metabolic activities in chondrocyte-laden PEG hydrogels. Acta Biomater 2011;7:492–504.

[5] Roberts JJ, Nicodemus GD, Greenwald EC, Bryant SJ. Degradation Improves Tissue Formation in (Un)Loaded Chondrocyte-laden Hydrogels. Clin Orthop Relat Res 2011.

[6] Bryant SJ, Bender RJ, Durand KL, Anseth KS. Encapsulating Chondrocytes in degrading PEG hydrogels with high modulus: Engineering gel structural changes to facilitate cartilaginous tissue production. Biotechnol Bioeng 2004;86:747–55.

[7] Anseth KS, Bryant SJ. Controlling the spatial distribution of ECM components in degradable PEG hydrogels for tissue engineering cartilage. J Biomed Mater Res Part A 2003;64A:70–9.

[8] Goldberg VM, Buckwalter JA. Hyaluronans in the treatment of osteoarthritis of the knee: evidence for disease-modifying activity. Osteoarthr Cartil 2005;13:216–24.

[9] Itano N, Sawai T, Yoshida M, Lenas P, Yamada Y, Imagawa M, et al. Three isoforms of mammalian hyaluronan synthases have distinct enzymatic properties. J Biol Chem 1999;274:25085–92.

[10] Buckwalter JA, Rosenberg LC. Electron-Microscopic Studies of Cartilage Proteoglycans - Direct Evidence for the Variable Length of the Chondroitin Sulfate-Rich Region of Proteoglycan Subunit Core Protein. J Biol Chem 1982;257:9830–9.

[11] Knudson CB, Knudson W. Cartilage proteoglycans. Semin Cell Dev Biol 2001;12:69–78.

[12] Roughley PJ. The structure and function of cartilage proteoglycans. Eur Cell Mater 2006;12:92–101.

[13] Chen WYJ, Abatangelo G. Functions of hyaluronan in wound repair. Wound Repair Regen 1999;7:79–89.

[14] Kawasaki K, Ochi M, Uchio Y, Adachi N, Matsusaki M. Hyaluronic acid enhances proliferation and chondroitin sulfate synthesis in cultured chondrocytes embedded in collagen gels. J Cell Physiol 1999;179:142–8.

[15] Lindenhayn K, Perka C, Spitzer RS, Heilmann HH, Pommerening K, Mennicke J, et al. Retention of hyaluronic acid in alginate beads: Aspects for in vitro cartilage engineering. J Biomed Mater Res 1999;44:149–55.

[16] Park TG, Yoo HS, Lee EA, Yoon JJ. Hyaluronic acid modified biodegradable scaffolds for cartilage tissue engineering. Biomaterials 2005;26:1925–33.

[17] Yamane S, Iwasaki N, Majima T, Funakoshi T, Masuko T, Harada K, et al. Feasibility of chitosan-based hyaluronic acid hybrid biomaterial for a novel scaffold in cartilage tissue engineering. Biomaterials 2005;26:611–9.

[18] Kim IL, Mauck RL, Burdick JA. Hydrogel design for cartilage tissue engineering: A case study with hyaluronic acid. Biomaterials 2011;32:8771–82.

[19] Burdick JA, Chung C, Jia XQ, Randolph MA, Langer R. Controlled degradation and mechanical behavior of photopolymerized hyaluronic acid networks. Biomacromolecules 2005;6:386–91.

[20] Burdick JA, Prestwich GD. Hyaluronic Acid Hydrogels for Biomedical Applications. Adv Mater 2011;23:H41–H56.

[21] Shu XZ, Liu Y, Luo Y, Roberts MC, Prestwich GD. Disulfide Cross-Linked Hyaluronan Hydrogels. Biomacromolecules 2002;3:1304–11.

[22] Shu XZ, Liu Y, Palumbo FS, Luo Y, Prestwich GD. In situ crosslinkable hyaluronan hydrogels for tissue engineering. Biomaterials 2004;25:1339–48.

[23] Prestwich GD. Hyaluronic acid-based clinical biomaterials derived for cell and molecule delivery in regenerative medicine. J Control Release 2011;155:193–9.

[24] Ghosh K, Shu XZ, Mou R, Lombardi J, Prestwich GD, Rafailovich MH, et al. Rheological characterization of in situ cross-linkable hyaluronan hydrogels. Biomacromolecules 2005;6:2857–65.

[25] Mansour JM. Biomechanics of Cartilage. In: Oatis CA, editor. Kinesiol. Mech. pathomechanics Hum. Mov., Baltimore, MD: Lippincott Williams & Wilkins; 2003, p. 66–75.

[26] Liu Y, Shu XZ, Prestwich GD. Osteochondral Defect Repair with Autologous Bone Marrow-Derived Mesenchymal Stem Cells in an Injectable, In Situ, Cross-Linked Synthetic Extracellular Matrix. Tissue Eng 2006;12:3405–16.

[27] Chung C, Burdick JA. Influence of Three-Dimensional Hyaluronic Acid Microenvironments on Mesenchymal Stem Cell Chondrogenesis. Tissue Eng Part A 2009;15:243–54.

[28] Stern R, Asari AA, Sugahara KN. Hyaluronan fragments: An information-rich system. Eur J Cell Biol 2006;85:699–715.

[29] Sahoo S, Chung C, Khetan S, Burdick J a. Hydrolytically degradable hyaluronic acid hydrogels with controlled temporal structures. Biomacromolecules 2008;9:1088–92.

[30] Chung C, Beecham M, Mauck RL, Burdick JA. The influence of degradation characteristics of hyaluronic acid hydrogels on in vitro neocartilage formation by mesenchymal stem cells. Biomaterials 2009;30:4287–96.

[31] Allison DD, Grande-Allen KJ. Review. Hyaluronan: A powerful tissue engineering tool. Tissue Eng 2006;12:2131–40.

[32] Noble PW. Hyaluronan and its catabolic products in tissue injury and repair. Matrix Biol 2002;21:25–9.

[33] Lindenhayn K, Perka C, Spitzer R, Heilmann H, Pommerening K, Mennicke J, et al. Retention of hyaluronic acid in alginate beads: aspects for in vitro cartilage engineering. J Biomed Mater Res 1999;44:149–55.

[34] Praest BM, Greiling H, Kock R. Assay of synovial fluid parameters: hyaluronan concentration as a potential marker for joint diseases. Clin Chim Acta 1997;266:117–28.

[35] Holmes MWA, Bayliss MT, Muir H. Hyaluronic-Acid in Human Articular-Cartilage - Age-Related-Changes in Content and Size. Biochem J 1988;250:435–41.

[36] Ohno S, Ohno-Nakahara M, Knudson CB, Knudson W. Induction of MMP-3 by Hyaluronan Oligosaccharides in Temporomandibular Joint Chondrocytes. J Dent Res 2005;84:1005–9.

[37] Ohno S, Im H-J, Knudson CB, Knudson W. Hyaluronan oligosaccharides induce matrix metalloproteinase 13 via transcriptional activation of NFkappaB and p38 MAP kinase in articular chondrocytes. J Biol Chem 2006;281:17952–60.

[38] Yoo HS, Lee EA, Yoon JJ, Park TG. Hyaluronic acid modified biodegradable scaffolds for cartilage tissue engineering. Biomaterials 2005;26:1925–33.

[39] Knudson CB. Hyaluronan Receptor-Directed Assembly of Chondrocyte Pericellular Matrix. J Cell Biol 1993;120:825–34.

[40] Skaalure SC, Milligan IL, Bryant SJ. Age impacts extracellular matrix metabolism in chondrocytes encapsulated in degradable hydrogels. Biomed Mater 2012;7.

[41] Farnsworth NL, Antunez LR, Bryant SJ. Dynamic compressive loading differentially regulates chondrocyte anabolic and catabolic activity with age. Biotechnol Bioeng 2013;110:2046–57.

[42] Richardson JB, Caterson B, Evans EH, Ashton BA, Roberts S. Repair of human articular cartilage after implantation of autologous chondrocytes. J Bone Jt Surgery-British Vol 1999;81B:1064–8.

[43] Gillogly SD, Myers TH. Treatment of full-thickness chondral defects with autologous chondrocyte implantation. Orthop Clin North Am 2005;36:433–46.

[44] Sawhney AS, Pathak CP, Hubbell JA. Bioerodible Hydrogels Based on Photopolymerized Poly(Ethylene Glycol)-Co-Poly(Alpha-Hydroxy Acid) Diacrylate Macromers. Macromolecules 1993;26:581–7.

[45] Lin-Gibson S, Bencherif S, Cooper JA, Wetzel SJ, Antonucci JM, Vogel BM, et al. Synthesis and characterization of PEG dimethacrylates and their hydrogels. Biomacromolecules 2004;5:1280–7.

[46] Villanueva I, Bishop NL, Bryant SJ. Medium Osmolarity and Pericellular Matrix Development Improves Chondrocyte Survival When Photoencapsulated in Poly(Ethylene Glycol) Hydrogels at Low Densities. Tissue Eng Part A 2009;15:3037–48.

[47] Ogamo A, Matsuzaki K, Uchiyama H, Nagasawa K. Preparation and Properties of Fluorescent Glycosaminoglycuronans Labeled with 5-Aminofluorescein. Carbohydr Res 1982;105:69–85.

[48] Metters AT, Anseth KS, Bowman CN. A statistical kinetic model for the bulk degradation of PLA-b-PEG-b-PLA hydrogel networks: Incorporating network non-idealities. J Phys Chem B 2001;105:8069–76.

[49] Kim YJ, Sah RLY, Doong JYH, Grodzinsky AJ. Fluorometric Assay of DNA in Cartilage Explants Using Hoechst-33258. Anal Biochem 1988;174:168–76.

[50] Woessner JF. Determination of Hydroxyproline in Tissue and Protein Samples Containing Small Proportions of This Imino Acid. Arch Biochem Biophys 1961;93:440–7.

[51] Templeton DM. The Basis and Applicability of the Dimethylmethylene Blue Binding Assay for Sulfated Glycosaminoglycans. Connect Tissue Res 1988;17:23–32.

[52] Ishida O, Tanaka Y, Morimoto I, Takigawa M, Eto S. Chondrocytes are regulated by cellular adhesion through CD44 and hyaluronic acid pathway. J Bone Miner Res 1997;12:1657–63.

[53] Evanko SP, Wight TN. Intracellular Localization of Hyaluronan in Proliferating Cells. J Histochem Cytochem 1999;47:1331–41.

[54] Von der Mark K, Kirsch T, Nerlich A, Kuss A, Weseloh G, Gluckert K, et al. Type-X Collagen-Synthesis in Human Osteoarthritic Cartilage - Indication of Chondrocyte Hypertrophy. Arthritis Rheum 1992;35:806–11.

[55] Bayliss MT, Howat S, Davidson C, Dudhia J. The organization of aggrecan in human articular cartilage - Evidence for age-related changes in the rate of aggregation of newly synthesized molecules. J Biol Chem 2000;275:6321–7.

[56] Roberts JJ, Nicodemus GD, Giunta S, Bryant SJ. Incorporation of biomimetic matrix molecules in PEG hydrogels enhances matrix deposition and reduces load-induced loss of chondrocyte-secreted matrix. J Biomed Mater Res Part A 2011;97A:281–91.

[57] Hua Q, Knudson CB, Knudson W. Internalization of Hyaluronan by Chondrocytes Occurs Via Receptor-Mediated Endocytosis. J Cell Sci 1993;106:365–75.

[58] Kvam BJ, Fragonas E, Degrassi A, Kvam C, Matulova M, Pollesello P, et al. Oxygen-Derived Free-Radical (Odfr) Action on Hyaluronan (Ha), on 2 Ha Ester Derivatives, and on the Metabolism of Articular Chondrocytes. Exp Cell Res 1995;218:79–86.

[59] Guilak F, Butler DL, Goldstein SA. Functional tissue engineering - The role of biomechanics in articular cartilage repair. Clin Orthop Relat Res 2001:S295–S305.

[60] Darling EM, Athanasiou KA. Biomechanical strategies for articular cartilage regeneration. Ann Biomed Eng 2003;31:1114–24.

[61] Bian L, Zhai DY, Zhang EC, Mauck RL, Burdick JA. Dynamic Compressive Loading Enhances Cartilage Matrix Synthesis and Distribution and Suppresses Hypertrophy in hMSC-Laden Hyaluronic Acid Hydrogels. Tissue Eng Part A 2012;18:715–24.

[62] Roberts JJ, Elder RM, Neumann AJ, Jayaraman A, Bryant SJ. Interaction of Hyaluronan Binding Peptides with Glycosaminoglycans in Poly(ethylene glycol) Hydrogels. Biomacromolecules 2014.

Chapter 5

Physiological Osmolarities do not Enhance Long-term Tissue Synthesis in Chondrocyte-laden Degradable PEG Hydrogels

Submitted to *Journal of Biomedical Materials Research: Part A* 2014

5.1 Abstract

Encapsulating chondrocytes in synthetic and degradable hydrogels for cartilage tissue engineering enables tuning of scaffold degradation, but provides no biological cues. Culture medium that recapitulates the physiological osmolarity of the interstitial fluid in cartilage can enhance matrix synthesis in the short term, but long-term benefits remain to be determined. This study investigates the long-term effect of culture medium osmolarity on tissue synthesis using chondrocytes isolated from three skeletally mature bovine donors encapsulated in degradable poly(ethylene glycol) hydrogels. The cell-laden hydrogels were cultured up to 4 weeks in standard chondrocyte-specific medium (330 mOsm) or medium adjusted by sucrose or salts (NaCl and KCl) to reach a physiological osmolarity (400 mOsm). Neo-cartilaginous matrix synthesis and matrix catabolism were evaluated by quantitative and immunofluorescence methods. Hydrogel degradation kinetics of acellular constructs were not affected by medium osmolarity or osmolyte. Matrix composition was predominantly aggrecan and collagen type II for all conditions. One day after encapsulation, total collagen accumulated in the constructs was elevated in 400 mOsm medium, regardless of osmolyte. However, this effect did not persist and at 4 weeks, total collagen synthesized and released to the medium was highest in 330 mOsm medium. Medium osmolarity had minimal effects of sulfated glycosaminoglycan content and did not affect catabolic activity. These findings suggest that culture medium at physiological osmolarities may not be beneficial for long-term chondrocyte culture in degradable hydrogels,

but that initially culturing chondrocytes at a higher osmolarity may enhance early tissue deposition.

5.2 Introduction

Photopolymerizable and biodegradable poly(ethylene glycol) (PEG) hydrogels are a promising cell encapsulation platform for cartilage regeneration [1,2]. Incorporating oligo(lactic acid) into the crosslinks of PEG hydrogels (PEG-LA hydrogels) offers a robust method to introduce hydrolytic degradation and support macroscopic neo-tissue deposition [3,4]. However, this platform lacks biological cues, which may be important for tissue engineering strategies that employ chondrocytes isolated from older donors where tissue production is limited [5].

Within cartilage, the fixed negative charges associated with sulfated glycosaminoglycans (sGAGs) on aggrecan molecules lead to elevated cation (Na^+, K^+, and H^+) concentration and lower anion (Cl^- and HCO_3^-) concentration in the interstitial fluid [6]. This results in an unusually high osmolarity (350-450 mOsm) compared to most tissues [7] and standard culture medium (330 mOsm). Several studies have demonstrated that introducing osmolytes in the form of salts or sucrose into the culture medium can significantly improve extracellular matrix synthesis by chondrocytes. For example, an osmotic challenge of 400 mOsm applied for four hours to isolated chondrocytes or cartilage explants enhanced proteoglycan and collagen synthesis rates over higher or lower osmolarities [7]. Furthermore, encapsulating chondrocytes in PEG hydrogels in 400-450 mOsm medium significantly improved cell viability post-encapsulation [8]. Longer-term cultures of chondrocytes in alginate beads have also been shown to enhance sGAG production after 6 days with 370 mOsm medium [9] and after 12 days with 380 mOsm medium, although collagen content was unaffected in the latter [10].

The aim of this study was therefore to investigate whether culture conditions that better mimic the extracellular osmotic environment of the interstitial fluid in cartilage could improve longer-term tissue production by chondrocytes encapsulated in degradable hydrogels. Specifically, bovine articular chondrocytes isolated from skeletally mature donors, and

encapsulated in PEG-LA hydrogels were cultured in 330 (standard culture medium) or 400 (cartilage) mOsm medium up to 4 weeks. Osmolarity was adjusted using either non-ionic (sucrose) or ionic (salts) osmolytes, where the latter affects ionic strength and osmolarity. Cartilaginous matrix production and catabolism were assessed.

5.3 Materials and Methods

5.3.1 Materials

Collagenase II, pepsin A, and papain (Worthington Biochemical, Lakewood, NJ), Irgacure 2959 (Ciba Specialty Chemicals, Tarrytown, NY), fetal bovine serum (FBS) (Atlanta Biologicals, Lawrenceville, GA), Retrievagen A (BD Biosciences, San Jose, CA), and keratanase I (MP Biomedical, Solon, OH) were used. Antibodies for aggrecan (A1059-53E) and collagen II (C5710-20F) (US Biologicals, Swampscott, MA), C1,2C (50-1035) (IBEX Pharmaceuticals, Quebec, Canada), collagen I (ab34710) and X (ab58632) (Abcam, Cambridge, MA) were used. Generic MMP and aggrecanase-1 SensoLyte™ kits were from Anaspec (Fremont, CA). Cell culture medium supplements and secondary antibodies (AlexaFluor 488, 546) were from Invitrogen (Carlsbad, CA). Remaining chemicals and enzymes were from Sigma-Aldrich (St. Louis, MO).

5.3.2 Macromer synthesis

Oligo(lactic acid)-*b*-PEG-*b*-oligo(lactic acid) (LA-PEG-LA) was synthesized by reacting poly(ethylene glycol) (PEG, MW 4600) with lactides. PEG and LA-PEG-LA were reacted with methacrylic anhydride to produce PEG-dimethacrylate (PEGDM) and PEG-LA-dimethacrylate (PEG-LA-DM), respectively [11,12]. ^{1}H-NMR determined that on average, 2.2 lactic acid repeats were added to each side of PEG, and methacrylate substitution was 93% (PEGDM) and 91% (PEG-LA-DM).

5.3.3 Chondrocyte isolation

Bovine chondrocytes were isolated as previously described [12] from the metacarpal-phalangeal joints of three 1-2 year old steers (Arapahoe Meat Co., Lafayette, CO). Cartilage

was processed separately by donor and isolated in three solutions: 330 mOsm (standard), 400 mOsm (standard with 1:22 molar ratio of KCl to NaCl (to maintain ratio in DMEM [7])), and 400 mOsm (standard with sucrose), confirmed by osmometry (5002 Osmette A, Precision Systems, Inc., Natick, MA). Standard chondrocyte medium (330 mOsm) consisted of DMEM with 10% FBS, 1% penicillin-streptomycin, 10 mM HEPES, 0.1 M MEM-NEAA, 0.4 μM L-proline, 50 μg/ml L-ascorbic acid, 0.5 μg/ml fungizone and 20 μg/ml gentamicin. Initial viability was assessed with trypan blue, yielding initial cell viabilities of: 88 ± 3% (donor 1), 87 ± 2% (donor 2), and 91 ± 1% (donor 3), which for 400 mOsm (salts) medium was consistently lower by ~3%.

5.3.4 Hydrogel formation

A 15% w/w macromer solution was prepared in culture medium (330, 400 (salts), or 400 (sucrose) mOsm), where 5% of the macromer mass was PEGDM and 95% was PEG-LA-DM, with 0.05% w/w Irgacure 2959 photoinitiator, which produces a hydrogel with an initial compressive modulus of ~180 kPa [13]. Chondrocytes were suspended at 20 million cells ml^{-1} and photopolymerized into cylindrical constructs (5 mm diameter, 2 mm height) for 10 min with 365 nm light (6 mW cm^{-2}). Constructs were cultured in respective culture medium up to 4 weeks at 37 °C in 5% CO_2, changing medium every 2-3 days. Cell viability (LIVE/DEAD® membrane integrity assay) was assessed after 1 day. Images were acquired at 100x magnification using a confocal laser-scanning microscope (CLSM, Zeiss LSM 510, Thornwood, NY).

5.3.5 Hydrogel characterization

Acellular hydrogels (*n* = 2 per time point) were formed and incubated in respective culture medium conditions for 33 days. Degradation was characterized by percent polymer mass loss at time *t* due to hydrolytic degradation by:

$$\%\, mass\ loss = \frac{0.15M_i - M_d}{0.15M_i} \times 100 \quad (1)$$

where M_i is the initial hydrogel mass immediately after polymerization and M_d is the dry polymer mass at time *t*. *Q* is the instantaneous volumetric swelling ratio, which was estimated from the

swollen hydrogel and dry polymer masses, M_s and M_d, respectively, using the polymer density ρ_p (1.07 g ml^{-1}) and solvent density ρ_s (1 g ml^{-1}):

$$Q = 1 + \frac{\rho_p}{\rho_s}\left(\frac{M_s}{M_d} - 1\right) \quad (2)$$

The rate of ester bond cleavage of the PEG-LA gels is assumed to follow first order reaction kinetics [14] characterized by a pseudo-first order hydrolysis rate constant *k'*. For highly swollen networks (*Q* > 10), *Q* with respect to time *t* depends on *k'* and the number of ester repeats per block *j* (for this system, *j* = 2.2) [15]:

$$Q \sim e^{\frac{6}{5}jk't} \quad (3)$$

By fitting experimental data for *Q* versus time to equation 3, *k'* was estimated for each medium condition. The instantaneous *Q* is assumed to be reasonably equivalent to the equilibrium *Q*, especially for these highly hydrophilic materials [15].

5.3.6 Biochemical analysis

On select days, hydrogel constructs (3 technical replicates per donor; *n* = 3 donors) were weighed, snap frozen in liquid nitrogen and stored at -80 °C. Hydrogels were homogenized, digested (papain for 16 h at 60 °C), and assayed for cell number by DNA (Hoechst 33258) assuming 7.7 pg DNA/cell [16], sGAG (dimethyl methylene blue), and total collagen (hydroxyproline) assuming 10% hydroxyproline in collagen [17]. Collagen and sGAG were also measured in the culture medium.

5.3.7 Immunohistochemical analysis

On day 29, constructs (2 technical replicates per donor; *n* = 3 donors) were fixed in 4% paraformaldehyde, dehydrated, paraffin embedded and sectioned. Sections (10 μm) underwent antigen retrieval, then were treated with enzymes for 1 h at 37 °C: hyaluronidase (200 U) for aggrecan, C1,2C, and collagen II; chondroitinase ABC (10 mU) and keratanase I (4 mU) for aggrecan; pepsin A (280 kU) for collagens I and X; and protease (400 U) and 0.25% trypsin for collagen X. Sections were treated with primary antibodies against aggrecan (1:5), C1,2C

(1:100), and collagens type I (1:50), type II (1:50), and type X (1:50). Secondary antibodies were applied followed by DAPI. Sections were imaged at 100x and 400x magnification with confocal microscopy.

5.3.8 Enzyme activity

Constructs at select days (2 technical replicates per donor; n = 3 donors) were snap-frozen in liquid nitrogen and stored at -80 °C. Constructs were homogenized in Sensolyte™ assay buffer with 0.1% Triton X-100. Lysate (with no chemical activation) was assayed for MMP and aggrecanase-1 activity with Sensolyte™ 520 assay kits containing substrates specific for aggrecanase-1 and generic MMPs (including MMP-1-3, 7-10, and 12-14). Enzyme activity is expressed as moles of substrate cleaved per cell during 1 h incubation at 37 °C. Active enzymes were detected in the constructs but not in conditioned culture medium.

5.3.9 Statistical analysis

Each data point represents the mean of biological replicates (n = 3 donors), where there are n = 2-3 technical replicates averaged for each individual donor. The pseudo first order kinetic constant associated with hydrogel degradation was determined from nonlinear regression and a corresponding 95% confidence interval for k' was determined. Biological replicates were analyzed by 1- or 2-way ANOVA with medium osmolarity and time as factors and post-hoc analysis performed using Fisher's LSD (n = 3) with $\alpha = 0.05$ (Kaleidagraph 4.1.3). Normal Gaussian distribution of data was confirmed by generating normal probability plots of the residuals (Minitab 16).

5.4 Results

5.4.1 Hydrogel degradation

Degradable hydrogels were formed by photopolymerizing PEG-LA-DM with PEGDM (Fig. 5.1A-D). Polymer mass loss increased rapidly and then stabilized after 16 days. Medium condition did not affect mass loss behavior (Fig. 5.1E). The change in Q over the first 16 days

(Fig. 5.1F) was used to estimate the pseudo-first order hydrolysis rate constant, *k'*, which was statistically similar for all medium conditions.

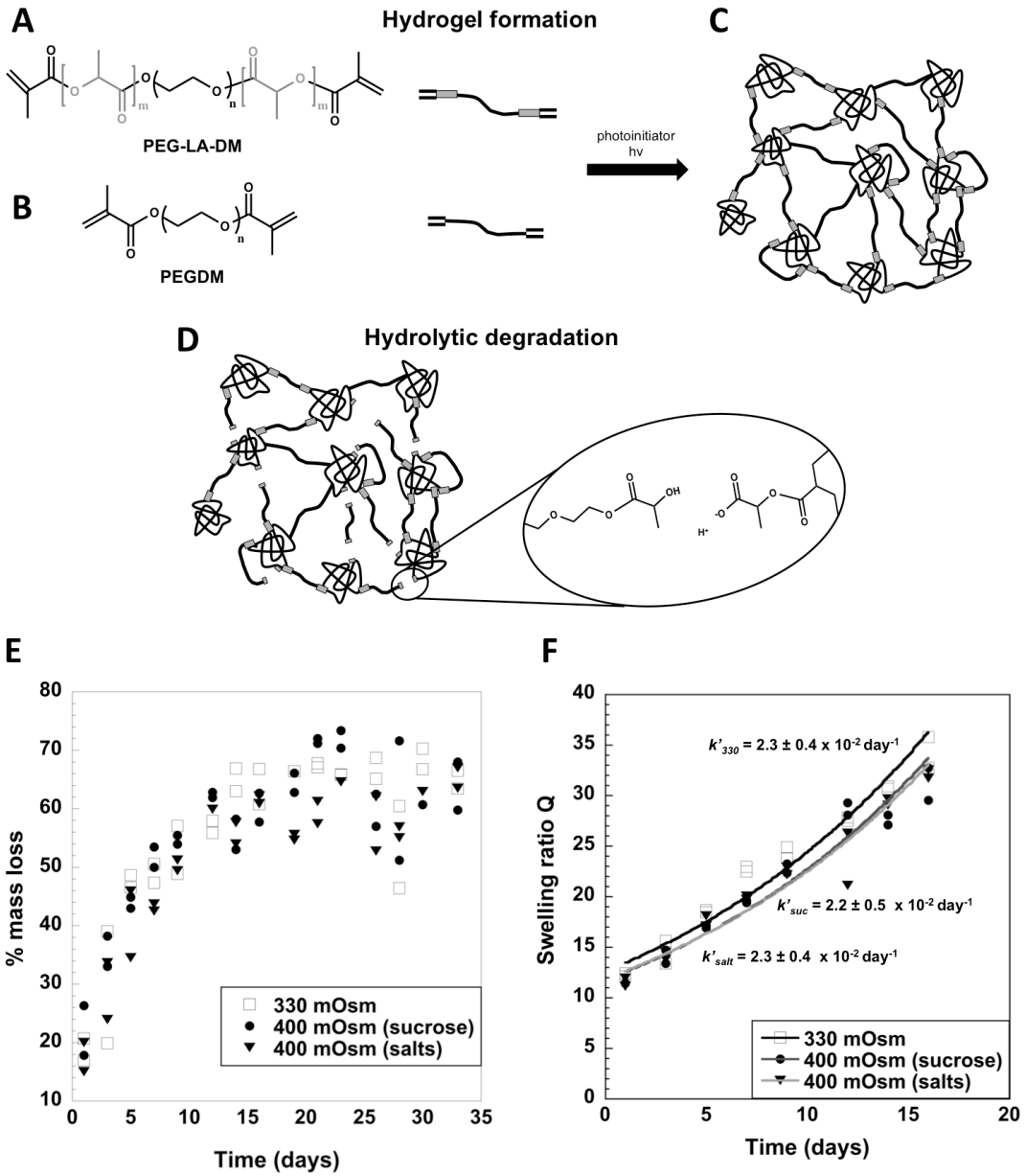

Figure 5.1 (A) Fast degrading PEG-LA-DM and (B) slow degrading PEGDM macromers are co-polymerized to (C) form a hydrogel. (D) Over time, crosslinks containing oligo(lactic acid) (LA) are cleaved, generating a localized negative charge. (E) Polymer mass loss of acellular hydrogels incubated in the different medium conditions (n = 2 per time point). (F) Volumetric swelling ratio Q measured over time for acellular hydrogels in different medium conditions through 16 days. Fitted pseudo-first order ester hydrolysis rate constants (k') are shown as mean values within 95% confidence intervals.

5.4.2 Cell viability and DNA content

Cell viability was qualitatively similar for all conditions immediately after encapsulation (Fig. 5.2A). DNA per wet weight was affected by time and osmolarity ($p < 0.0001$). DNA per wet weight was lower in 400 mOsm (salts) medium compared to 400 mOsm (sucrose) ($p = 0.007$) and 330 mOsm ($p = 0.023$) (Fig. 5.2B) at day 1 and day 15 ($p = 0.004$ compared to sucrose, and $p = 0.006$ compared to 330 mOsm), but was similar for all conditions by days 22 and 29.

5.4.3 Matrix organization and deposition

Immunohistochemistry images at 4 weeks (Fig. 5.2C) confirm pericellular deposition of aggrecan and collagen II for all medium osmolarity conditions. Collagen I staining was minimal, while collagen X was present in all conditions. Staining for the collagenase-generated C1,2C collagen neoepitope was minimal. Total collagen and sGAG contents were quantified in the hydrogels and in the culture medium after 1 day (Fig. 5.3A, B, E, F) and 4 weeks (Fig. 5.3C, D, G, H) of culture. Intermediate time points were assessed for sGAG and collagen content, and showed similar trends to 4 weeks, therefore only beginning and cumulative (4 weeks) measurements are presented for simplicity. One day after encapsulation, sGAG in the hydrogels was unaffected by osmolarity, but collagen in the hydrogels was elevated by 400 mOsm conditions ($p < 0.04$). After 4 weeks, cumulative sGAG released to the culture medium was unaffected by medium osmolarity, but cumulative collagen in the medium was greatest in 330 mOsm ($p < 0.05$). sGAG and collagen content in the hydrogels at 4 weeks was unaffected by medium osmolarity.

5.4.4 Catabolic enzyme activity

Aggrecanase-1 activity per cell increased with time ($p = 0.043$) and on day 15 was highest in 400 mOsm (sucrose) medium (compared to salts: $p = 0.015$, compared to 330 mOsm: $p = 0.033$) (Fig 5.4A). Generic MMP activity per cell increased with time ($p = 0.004$) and on day 15 was highest in 400 mOsm (sucrose) medium (compared to salts: $p = 0.009$) (Fig. 5.4B). By day 29, catabolic enzyme activity was similar for all conditions.

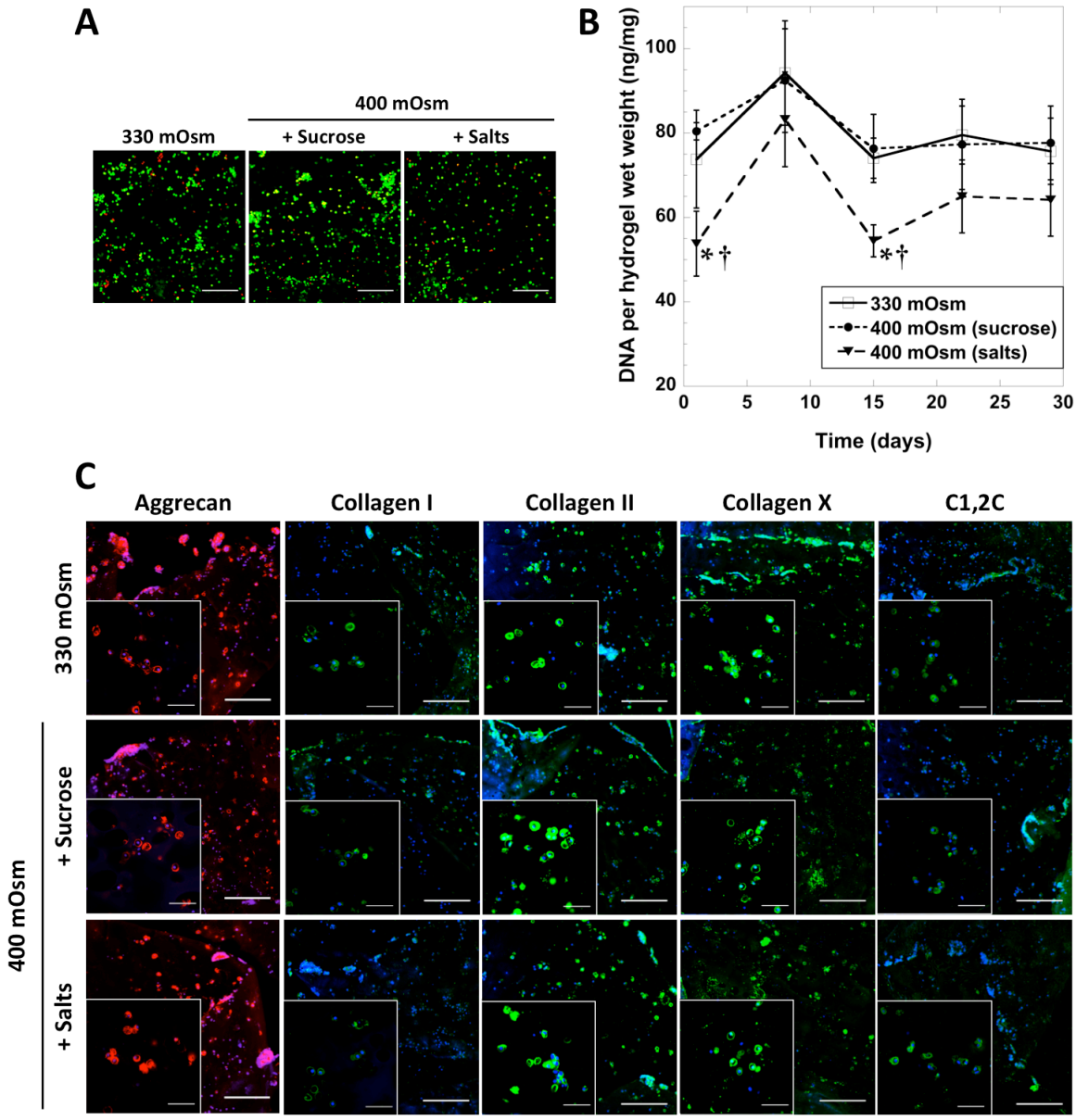

Figure 5.2 (A) Viability of encapsulated chondrocytes one day after encapsulation in degrading hydrogels cultured in the presence of different medium osmolarities and osmolytes. Live cells fluoresce green, dead cells fluoresce red. Scale bars indicate 200 μm. Representative images shown are from one donor (images were similar for the other two donors). (B) DNA per wet weight as a function of medium osmolarity and osmolyte and culture time. Day 1 indicates 24 hours post-encapsulation. Data represent the mean and standard deviation of n = 3 donors. * indicates significant difference from 330 mOsm, and † indicates significant difference from 400 mOsm (sucrose) at specified time point ($p < 0.05$). (C) Representative immunohistochemical images of constructs containing chondrocytes isolated from one donor (images were similar for the other two donors), stained for aggrecan (red), collagen I, II, and X (green), and C1,2C collagen fragments (green). Sections were counterstained with DAPI (blue) for cell nuclei. Scale bars represent 200 μm, inset image scale bars are 50 μm.

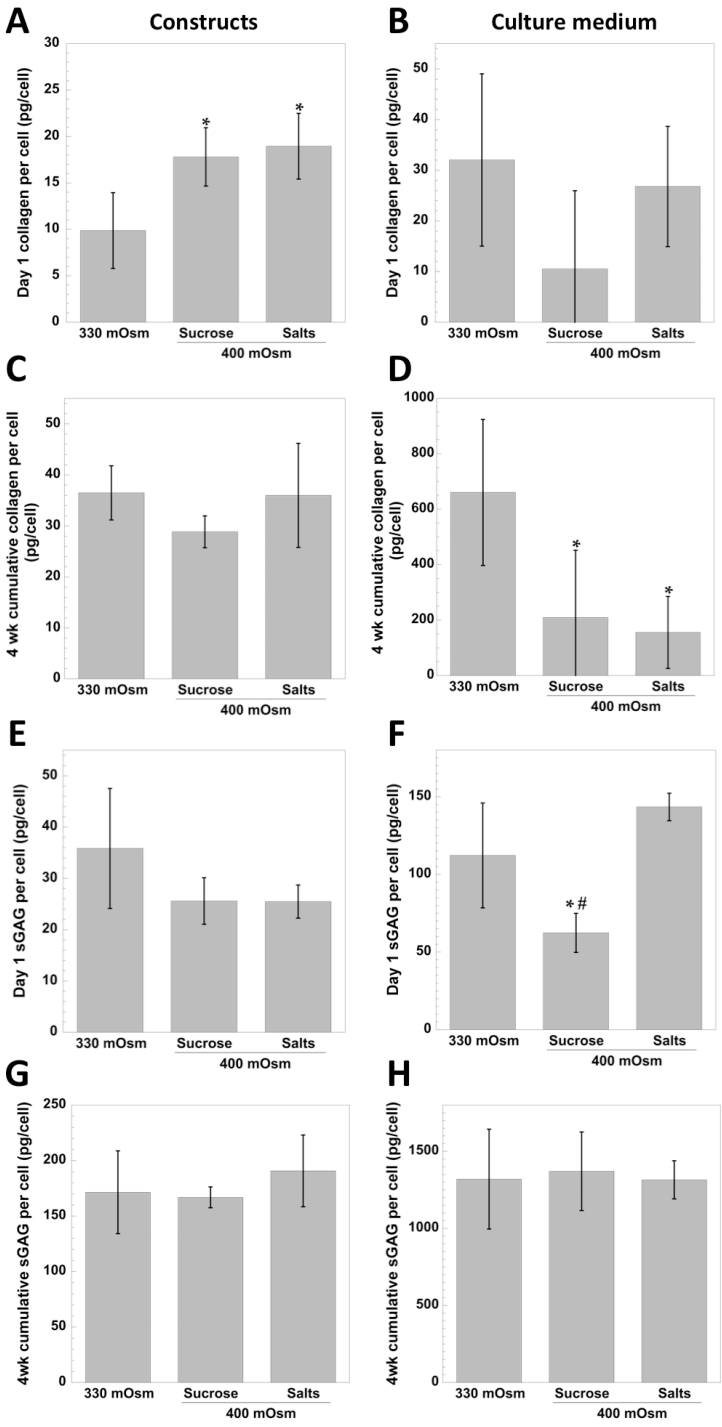

Figure 5.3 Total collagen (A-D) or sGAG (E-H) produced per cell that accumulated in the constructs (A, C, E, G) or was released to the culture medium (B, D, F, H) after 1 day or 4 weeks of culture. * indicates significant difference from 330 mOsm, and **#** indicates significant difference from 400 mOsm (salts) at specified time point ($p < 0.05$). Data represent the mean and standard deviation of $n = 3$ donors.

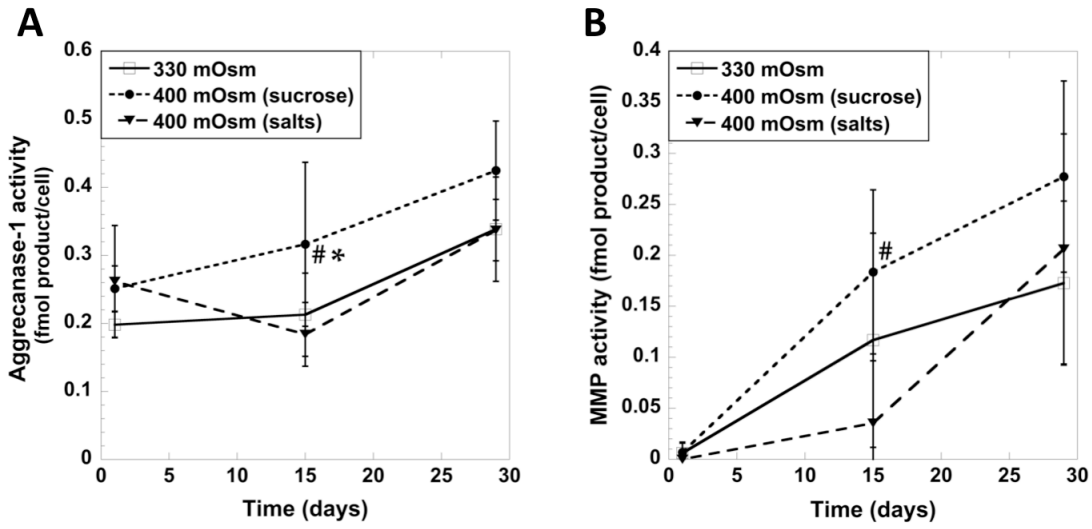

Figure 5.4 Activity of aggrecanase-1 (A) or MMPs (B) per cell in the constructs as a function of medium osmolarity and osmolyte and culture time. * indicates significant difference from 330 mOsm, and **#** indicates significant difference from 400 mOsm (salts) at specified time point ($p < 0.05$). Data represent the mean and standard deviation of $n = 3$ donors.

5.5 Discussion

This study demonstrates that for chondrocytes isolated from skeletally mature donors and encapsulated in degradable PEG-LA hydrogels, chondrocyte phenotype was maintained regardless of medium osmolarity, indicated by the prevalence of aggrecan and collagen II and minimal collagen I. While collagen deposition in the constructs was high after one day in 400 mOsm medium, longer-term overall synthesis was highest in 330 mOsm medium. These results suggest that in a degradable hydrogel system, the beneficial effects on tissue synthesis of a culture medium that mimics the osmolarity in native cartilage diminish over time.

PEG hydrogels were formed from fast degrading PEG-LA crosslinks and a small amount slow degrading PEG crosslinks to provide space for cellular proliferation and ECM evolution, while maintaining a hydrogel structure throughout tissue development. As the PEG-LA crosslinks are cleaved, carboxylate ions are generated leading to an overall negatively charged hydrogel. Increasing medium osmolarity and/or the type of osmolyte (ions versus sucrose) did not influence mass loss or swelling behavior during degradation. This observation is not

surprising given that standard culture medium has ions, which can shield the negative charges, such that any additional ions in the salt condition may have no further effect.

Cellularity measured by DNA content increased at day 8 for all conditions, but long-term returned to levels similar to day 1. This result is attributed to cell proliferation resulting from the initial and rapid hydrogel degradation during the first week, but eventually leading to loss of cells and associated matrix as the hydrogel further degrades. These findings are similar to those observed previously [12]. By day 16, hydrogel degradation is stabilized by the presence of slow degrading PEG crosslinks, which also appears to stabilize cellularity in the hydrogels. It is interesting to note that for each donor, DNA content was consistently lower in the 400 mOsm (salts) medium immediately following cell isolation and throughout hydrogel culture. This observation is attributed to the combined presence of the additional ions in the culture medium and negatively charged proteoglycans (present during tissue digestion and as cells begin depositing matrix), which attract ions and lead to an even higher osmolarity (> 400 mOsm) in the vicinity of the cell. Elevated extracellular ion concentration is known to activate ion channels on the cell membrane, affecting cellular metabolism [6,7,18,19].

In the short-term when hydrogel degradation was minimal, total collagen in the hydrogels one day post-encapsulation was 1.8-fold greater in the 400 mOsm conditions regardless of the osmolyte, which is consistent with previous reports [7], although collagen released to the culture medium after 1 day was statistically similar for all conditions. It is possible that the presence of sucrose, which stabilizes proteins by excluded volume effects [20], or elevated ions, which shield inhibitory electrostatic interactions with collagen [21], may aid in extracellular collagen fibril formation [21,22], thus enhancing short-term retention of collagen within the scaffolds. However, sGAG content in the constructs was similar, and quantity of matrix detected in the culture medium was unaffected by osmolarity after 1 day.

In the longer-term after hydrogel degradation, the amount of sGAGs and total collagens accumulated in the constructs was unaffected by osmolarity after 4 weeks. With hydrogel

degradation, cells and associated matrix may readily be lost to the culture medium. For cumulative matrix released to the culture medium over the course of 4 weeks, sGAGs were not affected by medium osmolarity, but total collagen released to the medium was greatest in 330 mOsm. The increased matrix release with 330 mOsm is not attributed to increased matrix catabolism as MMP activity was similar for all conditions, and cannot be attributed to hydrogel degradation because all hydrogels degraded similarly regardless of culture medium. These findings suggest that although in the short-term higher osmolarity may enhance tissue deposition, the benefits are not sustained. Previous studies have shown that pericellular proteoglycans bearing negatively charged sGAGs attract cations and elevate the extracellular osmolarity surrounding cells.[6] Studies have confirmed that within cartilage, osmolarity is ~30-50 mOsm higher than the immersion medium [7]. Therefore as cells lay down a pericellular matrix in the PEG-LA hydrogels, the local osmolarity sensed by the cells is likely higher and therefore more physiological in the 330 mOsm medium and comparable to previous reports of osmolarities (380 mOsm) that best promote matrix synthesis [9,10].

Overall, 400 mOsm culture medium regardless of osmolyte promoted collagen deposition after 1 day when total matrix production was low. However, 330 mOsm medium led to a higher amount of total collagen production over the course of 4 weeks. This observation may be attributed to the development of a pericellular matrix that effectively increases the extracellular osmolarity. These findings suggest that higher medium osmolarity may be beneficial in the short-term to enhance tissue production, but is not beneficial in long-term culture.

5.6 Acknowledgements

The authors would like to thank Saikripa Radhakrishnan for co-authoring the paper, Shash O. Dimson for assisting with immunohistochemical staining, and Ian L. Milligan for conducting hydrogel degradation experiments. This research was supported by NIH grant #1R01AR065441 and #R21AR061011, a Bioscience Discovery and Evaluation grant from the

State of Colorado, a fellowship from the National Science Foundation Graduate Research Fellowship Program (NSF GRFP), a National Institute of Health (NIH) Pharmaceutical Biotechnology Training Grant, and a Chancellor's Fellowship from the University of Colorado.

5.7 References

[1] Bryant SJ, Durand KL, Anseth KS. Manipulations in hydrogel chemistry control photoencapsulated chondrocyte behavior and their extracellular matrix production. J Biomed Mater Res Part A 2003;67A:1430–6.

[2] Bryant SJ, Anseth KS. Hydrogel properties influence ECM production by chondrocytes photoencapsulated in poly(ethylene glycol) hydrogels. J Biomed Mater Res 2002;59:63–72.

[3] Roberts JJ, Nicodemus GD, Greenwald EC, Bryant SJ. Degradation Improves Tissue Formation in (Un)Loaded Chondrocyte-laden Hydrogels. Clin Orthop Relat Res 2011.

[4] Anseth KS, Bryant SJ. Controlling the spatial distribution of ECM components in degradable PEG hydrogels for tissue engineering cartilage. J Biomed Mater Res Part A 2003;64A:70–9.

[5] Tran-Khanh N, Hoemann CD, McKee MD, Henderson JE, Buschmann MD. Aged bovine chondrocytes display a diminished capacity to produce a collagen-rich, mechanically functional cartilage extracellular matrix. J Orthop Res 2005;23:1354–62.

[6] Hall AC, Horwitz ER, Wilkins RJ. The cellular physiology of articular cartilage. Exp Physiol 1996;81:535–45.

[7] Urban JPG, Hall AC, Gehl KA. Regulation of Matrix Synthesis Rates by the Ionic and Osmotic Environment of Articular Chondrocytes. J Cell Physiol 1993;154:262–70.

[8] Villanueva I, Bishop NL, Bryant SJ. Medium Osmolarity and Pericellular Matrix Development Improves Chondrocyte Survival When Photoencapsulated in Poly(Ethylene Glycol) Hydrogels at Low Densities. Tissue Eng Part A 2009;15:3037–48.

[9] Negoro K, Kobayashi S, Takeno K, Uchida K, Baba H. Effect of osmolarity on glycosaminoglycan production and cell metabolism of articular chondrocyte under three-dimensional culture system. Clin Exp Rheumatol 2008;26:534–41.

[10] Xu X, Urban JPG, Tirlapur UK, Cui Z. Osmolarity effects on bovine articular chondrocytes during three-dimensional culture in alginate beads. Osteoarthr Cartil 2010;18:433–9.

[11] Lin-Gibson S, Bencherif S, Cooper JA, Wetzel SJ, Antonucci JM, Vogel BM, et al. Synthesis and characterization of PEG dimethacrylates and their hydrogels. Biomacromolecules 2004;5:1280–7.

[12] Skaalure SC, Milligan IL, Bryant SJ. Age impacts extracellular matrix metabolism in chondrocytes encapsulated in degradable hydrogels. Biomed Mater 2012;7.

[13] Skaalure SC, Dimson SO, Pennington AM, Bryant SJ. Semi-interpenetrating networks of hyaluronic acid in degradable PEG hydrogels for cartilage tissue engineering. Acta Biomater 2014.

[14] Metters AT, Anseth KS, Bowman CN. A statistical kinetic model for the bulk degradation of PLA-b-PEG-b-PLA hydrogel networks: Incorporating network non-idealities. J Phys Chem B 2001;105:8069–76.

[15] Mason MN, Metters AT, Bowman CN, Anseth KS. Predicting controlled-release behavior of degradable PLA-b-PEG-b-PLA hydrogels. Macromolecules 2001;34:4630–5.

[16] Kim YJ, Sah RLY, Doong JYH, Grodzinsky AJ. Fluorometric Assay of DNA in Cartilage Explants Using Hoechst-33258. Anal Biochem 1988;174:168–76.

[17] Woessner JF. Determination of Hydroxyproline in Tissue and Protein Samples Containing Small Proportions of This Imino Acid. Arch Biochem Biophys 1961;93:440–7.

[18] Mobasheri A. Regulation of Na+, K+-ATPase density by the extracellular ionic and osmotic environment in bovine articular chondrocytes. Physiol Res 1999;48:509–12.

[19] Hoffmann EK, Dunham PB. Membrane Mechanisms and Intracellular Signalling in Cell Volume Regulation. Int Rev Cytol 1995;161:173–262.

[20] Lee JC, Timasheff SN. The stabilization of proteins by sucrose. J Biol Chem 1981;256:7193–201.

[21] Scott JE. Proteoglycan-fibrillar collagen interactions. Biochem J 1988;252:313–23.

[22] Jimenez SA, Ala-Kokko L, Prockop DJ, Merryman CF, Shepard N, Dodge GR. Characterization of human type II procollagen and collagen-specific antibodies and their application to the study of human type II collagen processing and ultrastructure. Matrix Biol 1997;16:29–39.

Chapter 6

An Enzyme-sensitive PEG Hydrogel Based on Aggrecan Catabolism for Cartilage Tissue Engineering

Submitted to *Advanced Healthcare Materials* 2014

6.1 Abstract

Enzymatically degradable and photopolymerizable poly(ethylene glycol) (PEG) hydrogels present a promising platform for cartilage regeneration by encapsulated chondrocytes that dictate degradation behavior, which could improve autologous cell-based therapies that suffer from cell source variability. We demonstrate a novel cartilage-specific thiol-norbornene PEG hydrogel with CRDTEGE-ARGSVIDRC peptide crosslinks based on the site of aggrecan cleavage by aggrecanases. Bovine chondrocytes isolated from skeletally mature and immature (adult and juvenile) donors were encapsulated in PEG hydrogels with the aggrecanase-degradable crosslinker or non-degradable PEG-dithiol crosslinker and cultured to 12 weeks. Scaffold degradation was characterized by a two-fold decrease in compressive modulus without significant swelling, which is an improvement over bulk hydrolytic degradation. Enzymatically degradable hydrogels promoted matrix connectivity for juvenile cells, decreased fibrocartilage and hypertrophy, and did not stimulate catabolism or inflammation. Matrix deposition was observed in a highly catabolic environment with exogenous lipopolysaccharide, suggesting that tissue engineering with aggrecanase-sensitive scaffolds may be feasible in an osteoarthritic joint environment. Overall, we demonstrate a new enzymatically degradable hydrogel for cartilage tissue engineering based on aggrecan catabolism that can be degraded by cell donors of varying age and promotes the chondrocyte phenotype without inducing catabolism or inflammation.

6.2 Introduction

Encapsulating autologous chondrocytes (cartilage cells) in enzymatically biodegradable crosslinked poly(ethylene glycol) (PEG) hydrogels provides a platform where scaffold degradation is specified by the encapsulated cells. Here a novel cartilage-specific enzymatically degradable hydrogel with peptide crosslinks that mimic the aggrecanase cleavage site on aggrecan is presented. Autologous chondrocyte implantation (ACI) [1–3] has shown some success mainly in younger (<35 years) patients [4], and the advent of matrix-assisted ACI (MACI) [5] brings the opportunity to tailor scaffolds to patients from a wider age range. Decreased matrix synthesis and increased catabolism were observed for bovine chondrocytes from skeletally mature donors (adult) compared to those from skeletally immature donors (juvenile) when encapsulated in PEG hydrogels [6,7], therefore both adult and juvenile chondrocytes were used in this study in an effort to investigate the ability of cells from different age donors to degrade enzymatically sensitive hydrogels and deposit new cartilaginous matrix.

Scaffold degradation is crucial for matrix elaboration by chondrocytes, but in order to regenerate a macroscopic tissue while maintaining overall mechanical integrity, the rate and localization of scaffold degradation must be matched to the rate and localization of new matrix deposition, presenting a significant design challenge. Hydrophilic PEG hydrogels maintain the chondrocyte phenotype and support cartilage-specific matrix production [8–10], but non-degrading hydrogels inhibit matrix deposition and evolution [11]. Hydrolytically degradable PEG hydrogels that incorporate oligo(lactic acid) into the crosslinks promote macroscopic tissue deposition by juvenile chondrocytes [8,9,12–14], but this mode of uniform bulk degradation is characterized by hydrogel swelling, which decreases scaffold mechanics and contributes to significant loss of synthesized matrix from the constructs ([6] and Skaalure *et al.,* submitted). More recently, a cell-mediated degradation mode by incorporating enzyme-sensitive peptides into hydrogel crosslinks was introduced [15–20], where computational models predict that localized cell-mediated degradation will improve new matrix elaboration by entrapped

chondrocytes compared to bulk degradation [21,22]. However, research towards designing these types of hydrogels for cartilage regeneration has been limited. Bahney *et al.* [23] incorporated an MMP-7 specific peptide into PEG-diacrylate hydrogels to encourage chondrogenesis of human mesenchymal stem cells, which increased collagen II but decreased proteoglycan deposition and cellularity compared to non-degradable hydrogels. Park *et al*. [24] crosslinked PEG scaffolds via a step-growth method with an MMP-sensitive peptide that increased collagen II and aggrecan gene expression for adult chondrocytes, but matrix deposition was pericellularly restricted. In the presented work we employed 8-arm PEG molecules crosslinked with enzymatically degradable peptides via thiol-norbornene chemistry [16], which forms a homogeneous step-growth network that can be radically photopolymerized *in situ,* providing temporal and spatial control. This system is beneficial compared to acrylate-based PEG hydrogels due to improved network homogeneity and promotion of the chondrocyte phenotype, and decreased oxidative damage to cells during photopolymerization [25].

A novel cartilage-specific enzymatically sensitive peptide was designed based on chondrocyte metabolic activity observed *in vivo* and *in vitro*. Cartilage is composed mainly of elastic collagen II fibrils and proteoglycans (primarily aggrecan), and is sparsely populated with chondrocytes that interact with and process the extracellular matrix [26]. *In vivo*, aggrecan is turned over much more rapidly than collagen II [27], therefore we chose to target aggrecan catabolism for the design of a novel enzymatically degradable peptide. The aggrecan proteoglycan is composed of a linear core protein with three globular domains, where negatively charged sulfated glycosaminoglycan (sGAG) sidechains are bound to the core protein between globular domains 2 and 3 (G2 and G3) [27,28]. The region between G1 and G2 is termed the ‘interglobular domain’ (IGD), and contains the two main sites of aggrecan proteolysis by either matrix metalloproteinases (MMPs) or aggrecanases (A Disintegrin And Metalloproteinase domain with ThromboSpondin motifs, ADAMTS-4 and -5, also known as aggrecanase-1 and -2, respectively) [29], where aggrecanases cleave the IGD more efficiently than MMPs [30–32].

Therefore, we designed an aggrecanase-sensitive peptide based on its specific cleavage site within the IGD. The amino acid sequence TEGE-ARGSVI surrounding the E_{373}-A_{374} cleavage site is conserved between human and bovine aggrecan [33], and we flanked this sequence with 'RD' moieties to improve solubility [34] and thiol-containing cysteines to permit crosslinking, resulting in the final sequence CRDTEGE-ARGSVIDRC. This new aggrecanse-sensitive hydrogel was compared to non-degradable hydrogels crosslinked with PEG-dithiol and tested by encapsulating bovine chondrocytes exhibiting different anabolic and catabolic characteristics and evaluating scaffold modulus and matrix production, elaboration and catabolism over the course of twelve weeks.

6.3 Materials and Methods

6.3.1 Materials

8-arm PEG amine (MW 20,000) was from JenKem Technology USA (Allen, TX). 0-(7-azabenzotriazol-1-yl)-N,N,N',N'-tetramethyluronium hexafluorophosphate (HATU) and N,N'-diisopropylethylamine (DIEA) were from Chem-Impex International, Inc. (Wood Dale, IL). Hoechst 33258 was from Polysciences, Inc. (Warrington, PA). Collagenase type II, pepsin A, and papain were from Worthington Biochemical (Lakewood, NJ). Ethyl ether, N,N-dimethylformamide (DMF), bovine IL-6 ELISA kit, and Triton X-100 were from Fisher Scientific (Fair Lawn, NJ). SpectraPor 7 1000 MWCO dialysis tubing was from Spectrum Labs (Rancho Dominguez, CA). Aggrecanase-degradable peptide (CRDTEGE-ARGSVIDRC) was from GenScript (Piscataway, NJ). Irgacure 2959 was from Ciba Specialty Chemicals (Tarrytown, NY). Fetal bovine serum (FBS) was from Atlanta Biologicals (Lawrenceville, GA). The LIVE/DEAD® assay, phosphate-buffered saline (PBS), DMEM, penicillin-streptomycin (P/S), fungizone, gentamicin, HEPES buffer, GlutaGro (L-glutamine), minimal essential medium non-essential amino acids (MEM-NEAA), trypsin-EDTA, trypan blue, DAPI, AlexaFluor 488-conjugated goat anti-rabbit IgG, and AlexaFluor 546-conjugated goat anti-mouse IgG were from Invitrogen (Carlsbad, CA). 5-norbornene-2-carboxylic acid, PEG-dithiol, L-proline, L-ascorbic acid, bovine

serum albumin (BSA), dimethyl methylene blue (DMMB), lipopolysaccharides (LPS) from *S. enterica*, chondroitinase ABC, hyaluronidase, and protease from *Streptomyces griseus* were from Sigma-Aldrich (St. Louis, MO). Keratanase I was from MP Biomedical (Solon, OH). Mouse anti-aggrecan antibody (A1059-53E) and rabbit anti-collagen II antibody (C5710-20F) were from US Biologicals (Swampscott, MA). Rabbit anti-collagen I (ab34710), and X (ab58632) antibodies were from Abcam (Cambridge, MA). Rabbit anti-C1,2C (collagenase-generated collagen neoepitope) antibody (50-1035) was from IBEX Pharmaceuticals (Quebec, Canada). Generic MMP and aggrecanase-1 SensoLyte™ assay kits were from Anaspec (Fremont, CA). Human ADAMTS-4 was from Millipore (Billerica, MA). Retrievagen A antigen retrieval solution was from BD Biosciences (San Jose, CA).

6.3.2 Macromer synthesis

8-arm PEG amine (MW 20,000) was reacted with norbornene acid to synthesize 8-arm PEG-amide-norbornene (8armPEG-NB) [16,25,35]. Briefly, norbornene acid (8x molar excess compared to amine-terminated PEG arms) in DMF was pre-reacted for 5 minutes under argon with HATU (4x excess) and DIEA (4x excess) at room temperature. The pre-reacted mixture was combined with 8-arm PEG amine in DMF, and the reaction proceeded overnight under argon at room temperature. 8armPEG-NB was recovered by precipitation in ethyl ether, and purified by dialyzing against DI H_20 for 2-3 days. Dialyzed 8armPEG-NB was filtered (0.2 μm) and lyophilized. Using ^{1}H-NMR spectroscopy, norbornene conjugation (δ = 5.9 - 6.3 ppm) per 8-arm PEG molecule (δ = 3.4 – 3.9 ppm) was determined to be on average 100%.

6.3.3 Chondrocyte isolation from two distinct cell sources

Bovine articular chondrocytes were isolated from the metacarpal-phalangeal joints of four skeletally mature (1-2 year old) steers (Arapahoe Meat Co., Lafayette, CO), which are referred to as adult chondrocytes. Bovine chondrocytes were isolated from the femoral-patellar groove and articular condyles of a skeletally immature (1-3 week old) calf (Research 87, Marlborough, MA), which are referred to as juvenile chondrocytes. Briefly, cartilage slices were

washed in phosphate-buffered saline (PBS) supplemented with 1% penicillin-streptomycin (P/S), 0.5 μg ml^{-1} fungizone and 20 μg ml^{-1} gentamicin (PBS-antis), and digested 16 h at 37°C in 0.2% collagenase type II in DMEM with 5% FBS. Isolated chondrocytes were washed in PBS-antis + 0.02% EDTA, pelleted and washed in PBS-antis and then passed through a 100 μm cell strainer. Cells were maintained in chondrocyte medium (DMEM supplemented with 10% FBS, 1% P/S, 10 mM HEPES, 0.1 M MEM-NEAA, 0.4 μM L-proline, 50 μg ml^{-1} L-ascorbic acid, 4 mM L-glutamine, 0.5 m μg ml^{-1} fungizone and 20 μg ml^{-1} gentamicin). Cell viability was determined by trypan blue exclusion assay, yielding initial viabilities of 92% for adult chondrocytes, and 87% for juvenile chondrocytes.

6.3.4 Hydrogel formation

A 10% w/w macromer solution of 8armPEG-NB was prepared in chondrocyte medium, and non-degradable PEG-dithiol (PEGdSH, MW 1000) or degradable (CRDTEGE-ARGSVIDRC peptide) crosslinker were added at 0.45:1 and 0.65:1 thiol:norbornene molar ratios, respectively. These thiol:norbornene ratios yielded hydrogels after swelling overnight with similar initial compressive moduli for both degradable and non-degradable acellular formulations. Chondrocytes were mixed with macromer solution at 50 million cells ml^{-1} and photopolymerized with 0.05% w/w Irgacure 2959 into cylindrical constructs (5 mm diameter x 2 mm height) for 7 min with 365 nm light (6 mW cm^{-2}). Constructs were cultured in 4 ml chondrocyte medium (replaced twice per week) for up to 12 weeks at 37°C in 5% CO_2. Conditioned medium was snap frozen in liquid nitrogen, stored at -80 °C, and pooled together in three week increments. For the lipopolysaccharides (LPS) condition, culture medium was supplemented with 10 ng ml^{-1} LPS starting one day after encapsulation. Cell viability in constructs (n = 2) was assessed using a LIVE/DEAD® membrane integrity assay at 3 weeks. Images were acquired using a confocal laser-scanning microscope (CLSM, Zeiss LSM 510, Thornwood, NY) at 100x magnification. To assess hydrogel degradability, acellular hydrogels were formed in fresh chondrocyte medium and swelled overnight to equilibrium. The hydrogels were placed in cell-conditioned medium and

wet weight monitored for 7 hours. Cell-conditioned medium was prepared from chondrocytes that were placed in suspension culture at 1.5 million cells ml^{-1} and activated with 1 μg ml^{-1} LPS overnight. After activation, cells suspension was centrifuged and the supernatant collected as the cell-conditioned medium.

6.3.5 Hydrogel characterization

Hydrogels were assessed for wet weight and compressive modulus after 1 day, and week 3, 6, 9, and 12 (n = 3). Hydrogels were compressed to 15% strain at a strain rate of 0.5 mm/min, to obtain stress-strain curves (MTS Synergie 100, 10N). The modulus was estimated as the slope of the linear region of stress-strain curves. Hydrogels were lyophilized to measure dry weight. Hydrogel volume was determined from height and diameter measurements.

6.3.6 Biochemical analysis

On day 1 and weeks 3, 6, 9, and 12, hydrogel constructs were removed (n = 3), weighed, snap frozen in liquid nitrogen and stored at -80 °C. Hydrogels were lyophilized, then homogenized and digested with papain for 16 hours at 60 °C. DNA content was measured using Hoechst 33258, assuming 7.7 pg of DNA per chondrocyte [36]. The constructs and conditioned medium were assayed for collagen using the hydroxyproline assay, where hydroxyproline is assumed to make up 10% of collagen [37], and for sulfated GAGs using the dimethyl methylene blue (DMMB) dye assay [38]. GAG and collagen content were normalized to cell number.

6.3.7 Histological and immunohistochemical analysis

At weeks 6 and 12, constructs (n = 2) were fixed in 4% paraformaldehyde, dehydrated, paraffin embedded and sectioned to 10 μm. Sections were stained with Safranin-O/Fast Green to visualize sulfated glycosaminoglycans (sGAG) and visualized at 200x magnification with a bright field microscope (Axiovert 40 C, Zeiss, Thornwood, NY). Sections were treated with primary antibodies against aggrecan (1:5), collagen type II (1:50), collagen type X (1:50), collagen type I (1:50), and C1,2C (1:100). Before primary antibody treatment, sections underwent antigen retrieval, then were treated with appropriate enzymes for 1 h at 37 °C:

hyaluronidase (200 U) for aggrecan, collagen II, and C1,2C; chondroitinase ABC (10 mU) and keratanase I (4 mU) for aggrecan; pepsin A (280 kU) for collagens I and X; and protease (400 U) and 0.25% trypsin for collagen X. Sections were probed with AlexaFluor 488 or 546-conjugated secondary antibodies and counterstained with DAPI. A laser scanning confocal microscope was used to acquire images at 400x magnification using the same settings and post-processing for all images. Cell-laden hydrogel sections that received no primary antibody treatment were used as negative controls, showing no positive staining. Sections of juvenile and adult hyaline cartilage were used as positive controls.

6.3.8 Enzyme activity assays and IL-6 ELISA

On day 1 and at weeks 3, 6, 9, and 12, constructs (n = 3) were snap-frozen in liquid nitrogen and stored at -80 °C. The constructs were homogenized in Sensolyte kit assay buffer with 0.1% Triton X-100. Construct lysate and conditioned medium samples were assayed for activity of MMPs and ADAMTS-4 with Sensolyte 520 assay kits containing substrates specific for ADAMTS-4 (aggrecanase-1) and generic MMPs (probes for MMP-1- 3, 7-10, and 12-14 simultaneously). Activity was measured as amount of cleaved substrate generated after incubating 1 h at 37 °C with samples. Human ADAMTS-4 and collagenase II were used as positive controls for active enzymes. Conditioned culture medium (n = 3) from all time points was assayed for bovine interleukin-6 (IL-6) using a sandwich ELISA kit.

6.3.9 Statistical analysis

Data are presented as mean (standard deviation). Measures of wet weight, modulus, biochemical content, enzyme activity and IL-6 were analyzed by two-way ANOVA where the factors were culture time and hydrogel condition, followed by one-way ANOVA with Fisher's LSD post-hoc test, $\alpha = 0.05$, to determine significant difference between conditions at specific time points. Normal probability plots of the residuals were generated and were found to support the normal distribution assumption (plots not shown).

6.4 Results

6.4.1 Cell-mediated degradation of acellular hydrogels

The 8armPEG-NB macromer (Fig. 6.1A) was crosslinked with either non-degrading PEGdSH or the aggrecanase sensitive peptide (Fig. 6.1B, C) to form a three-dimensional network (Fig. 6.1D). Degradability of the aggrecanase sensitive crosslinker in a PEG hydrogel by chondrocytes was investigated by incubating acellular hydrogels in medium conditioned by adult chondrocytes stimulated with LPS (Fig. 6.1E). Hydrogel wet weight was measured as an indicator of hydrogel degradation. Compared to fresh chondrocyte medium, cell-conditioned medium led to an increase in hydrogel wet weight after 7 hours (p = 0.02).

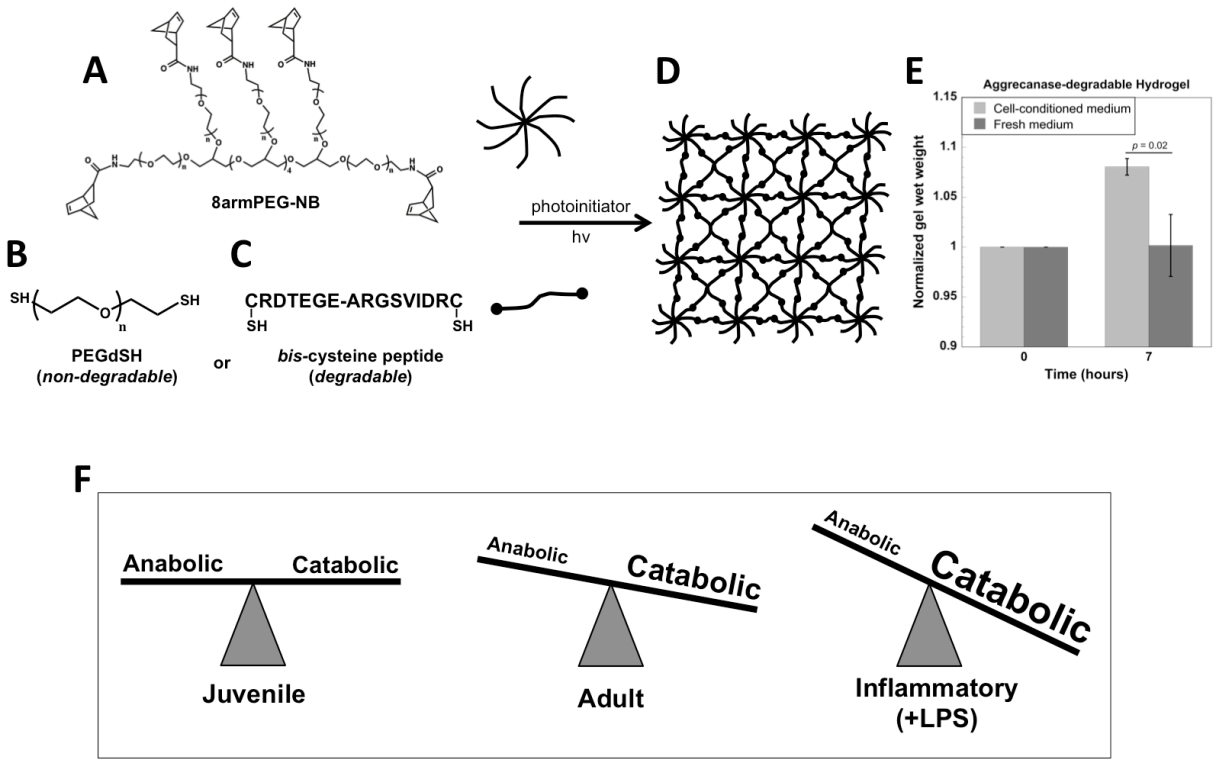

Figure 6.1 Schematic of hydrogel formation and cell sources. (A) 8-arm PEG-amide-norbornene (8armPEG-NB, 20 kDa) is crosslinked with (B) non-degradable PEG-dithiol (PEGdSH, 1000 Da), or (C) degradable peptide (CRDTEGE-ARGSVIDRC, 1767 Da) in the presence of photoinitiator and 365 nm light to create (D) a 3D crosslinked hydrogel network that cells can be encapsulated within. (E) Hydrogel degradation was demonstrated in the presence of adult cell-conditioned medium. (F) Chondrocytes were isolated from juvenile and adult bovine cartilage, and adult chondrocytes were additionally stimulated with LPS, to provide cell sources with different metabolic activities.

6.4.2 Characterization of cell-laden hydrogels: viability, modulus and cellularity

Chondrocytes from cell sources with different metabolic activities (Fig. 6.1F) were encapsulated into PEG hydrogels. Chondrocyte viability qualitatively remained high throughout the culture period and was similar for each cell source and hydrogel formulation. The addition of LPS to the culture medium did not adversely affect cell viability throughout the study. Representative confocal microscopy images are shown at week 3 (Fig. 6.2A), which were similar throughout the study. At 12 weeks hydrogel shape and size were visibly similar for all conditions (Fig. 6.2B), confirmed by normalized hydrogel volume (Fig. 6.2C), which increased ($p < 0.0001$) with time for all conditions. Mean hydrogel volume was consistently lower in the degradable hydrogels compared to non-degradable hydrogels for the same cell source with the exception of week 12 for the adult chondrocytes when both were similar. LPS led to increased ($p < 0.001$) hydrogel volume compared to the untreated hydrogel for the adult cell source at weeks 6 and 9 reaching similar values for all hydrogels with adult cells by week 12. Hydrogel modulus (Fig. 6.2D), which measured 13 ± 3 kPa at day 1, decreased ($p < 0.0002$) with time by ~50% for enzymatically degradable hydrogels regardless of cell source and treatment, but doubled ($p = 0.0001$) for juvenile cells in non-degradable hydrogels over 12 weeks. Cell number per construct (Fig. 6.2E) was affected by time and condition ($p < 0.0001$ for both). For juvenile chondrocytes in degradable hydrogels, the number of cells per construct was maintained throughout the culture period, while the other conditions showed an overall increase in cell number by week 12.

6.4.3 sGAG and aggrecan production and deposition

Cumulative sGAG production (Fig. 6.3A) is shown as the amount in the hydrogels at 12 weeks normalized to cell number and the cumulative amount released to the medium throughout 12 weeks of culture, with the latter normalized to the corresponding cell number at each time point. The amount in the constructs on a cellular basis was lower in the enzymatically degradable hydrogels ($p < 0.0001$ for juvenile cells, $p < 0.006$ for adult cells), which is supported

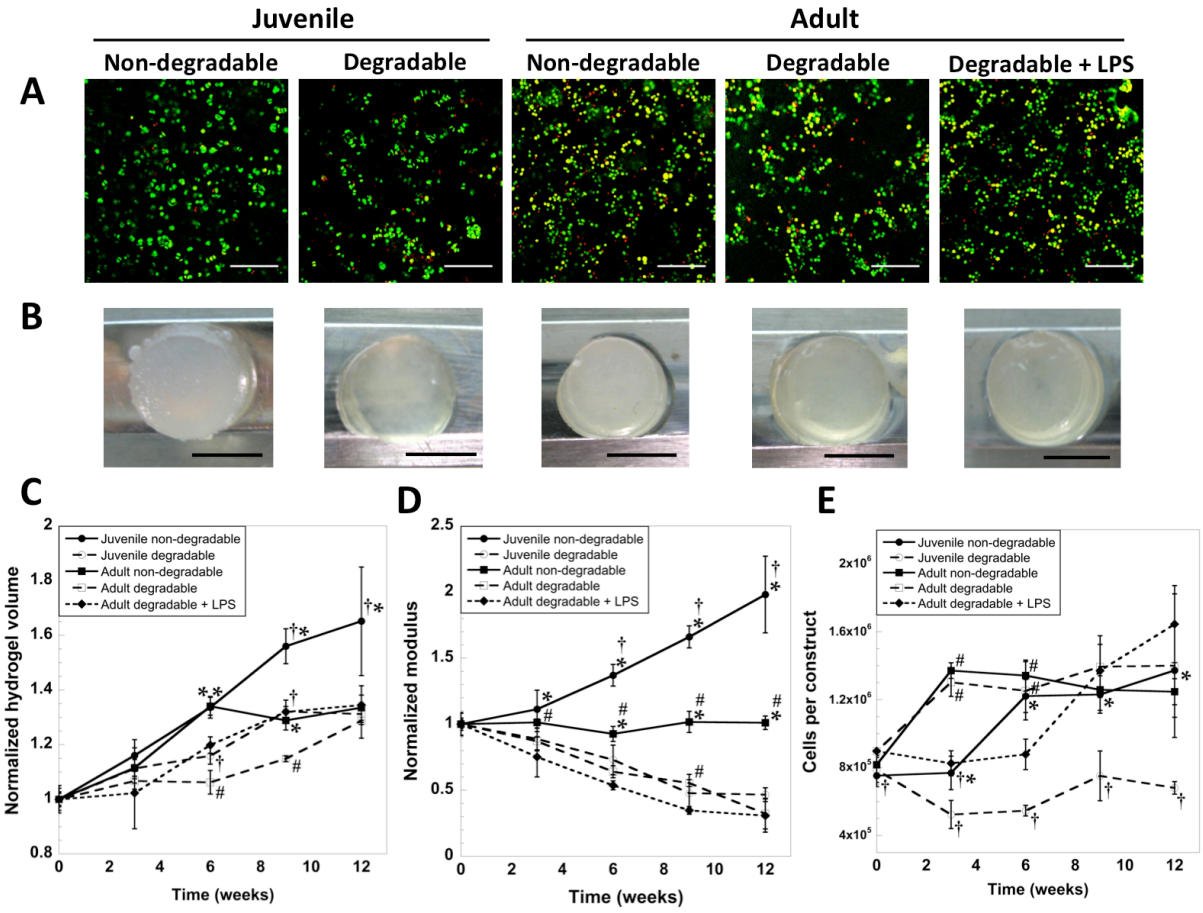

Figure 6.2 (A) Viability of encapsulated cells after 3 weeks of culture in non-degradable or enzymatically degradable hydrogels. Live cells are green, dead cells are red. Scale bars are 200 μm. (B) Representative photographs of hydrogels taken at 12 weeks. Scale bars are 5mm. (C) Hydrogel volume and (D) compressive modulus normalized to measurements from 1 day after encapsulation. (E) Cell number normalized to lyophilized hydrogel dry weight. * indicates significantly different from degradable hydrogels (at same cell age). † indicates significantly different from adult cells (same hydrogel condition). # indicates significantly different from LPS condition (adult cells only) ($p < 0.05$). Error bars are standard deviation ($n = 3$).

by the Safranin-O staining for sGAG (Fig. 6.3B). However, total sGAG released to the medium was elevated in the enzymatically degradable hydrogels for juvenile cells ($p = 0.004$), but total sGAG release was similar for adult chondrocytes. LPS treatment led to a similar amount of sGAG in the constructs per cell, but the amount released was significantly lower ($p < 0.0001$) compared to no treatment. Spatially sGAG deposition was present throughout the constructs in the non-degradable hydrogels for both cell sources. In the degradable hydrogels, sGAG was more localized to the regions adjacent to the cells for the juvenile cell source and was only

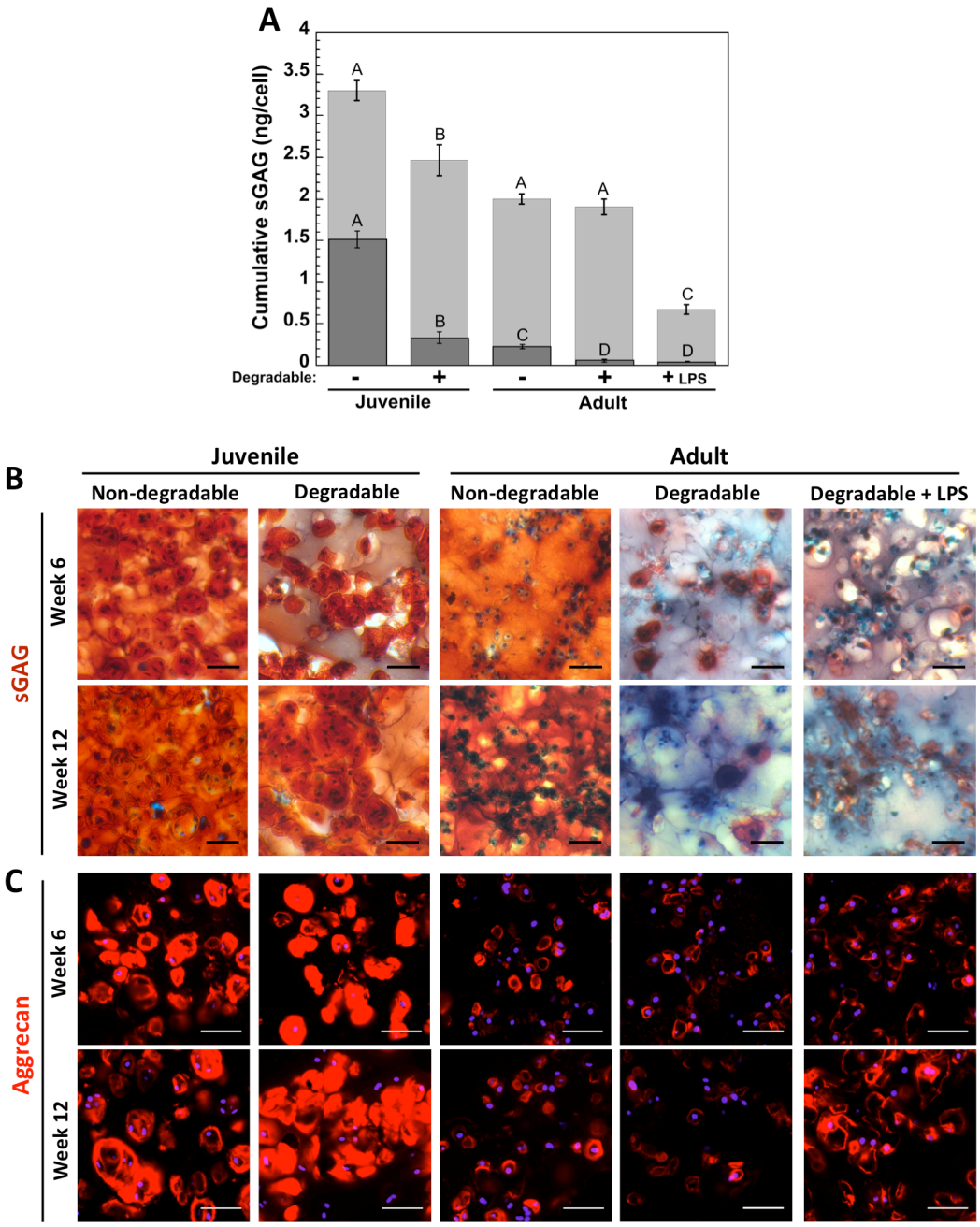

Figure 6.3 (A) Cumulative sGAG per cell produced during 12 weeks of culture, shown as amount present in the constructs at 12 weeks (■), and cumulative amount released to the medium throughout 12 weeks (■). Letter groupings show statistical similarities (same letter) and differences (different letters) ($p < 0.05$). Top letters are for total sGAG (constructs + medium), lower letters are for sGAG in constructs only. Error bars are standard deviation ($n = 3$). (B) Immunohistochemical visualization of aggrecan (red) in hydrogels at weeks 6 and 12. Nuclei are blue, scale bars are 50 μm. (C) Histological visualization of sulfated GAG (sGAG, orange-red) at weeks 6 and 12 with Safranin-O/Fast Green. Background proteins are blue, nuclei are dark blue-purple, scale bars are 50 μm.

detected pericellularly for the adult cell source. Aggrecan deposition (Fig. 6.3C) was most prevalent for juvenile cells, where the enzymatically degradable hydrogels supported matrix connectivity at 12 weeks. For adult cells, aggrecan deposition was restricted to pericellular regions for both hydrogels and did not appear to be affected by LPS.

6.4.4 Collagen production, deposition and degradation

Cumulative collagen production is shown as the amount present in the hydrogels at 12 weeks normalized to cell number and the cumulative amount released to the medium throughout 12 weeks of culture, with the latter normalized to corresponding cell number at each time point (Fig. 6.4A). The amount present in the constructs on a per cell basis was highest for juvenile cells in non-degrading hydrogels ($p < 0.0003$), but enzymatically degradable hydrogels showed greater collagen release to the medium by juvenile cells ($p < 0.0001$). Collagen II deposition (Fig. 6.4B) was most prevalent for juvenile cells, where the enzymatically degradable hydrogels supported matrix connectivity at 12 weeks. For adult cells, collagen II deposition was restricted pericellularly for both hydrogels and did not appear to be affected by LPS. C1,2C (degraded collagen) was present in all conditions and appeared to be greater in the adult cells for the non-degradable hydrogels especially at week 6, but greater in the juvenile cells for the degradable hydrogels. C1,2C appeared elevated at week 6 with LPS treatment, but no obvious differences were observed by week 12.

Collagens I and X were examined in the constructs at weeks 6 and 12 (Fig. 6.5A, B). Collagen I was restricted pericellularly in all conditions with the most intense staining in non-degradable hydrogels, and fainter staining in degradable hydrogels for both cell sources. Collagen X staining was most prominent in the non-degrading hydrogels with juvenile cells at week 12, but its deposition was minimal in enzymatically degradable hydrogels with both cell sources. LPS did not appear to affect collagen I or X deposition.

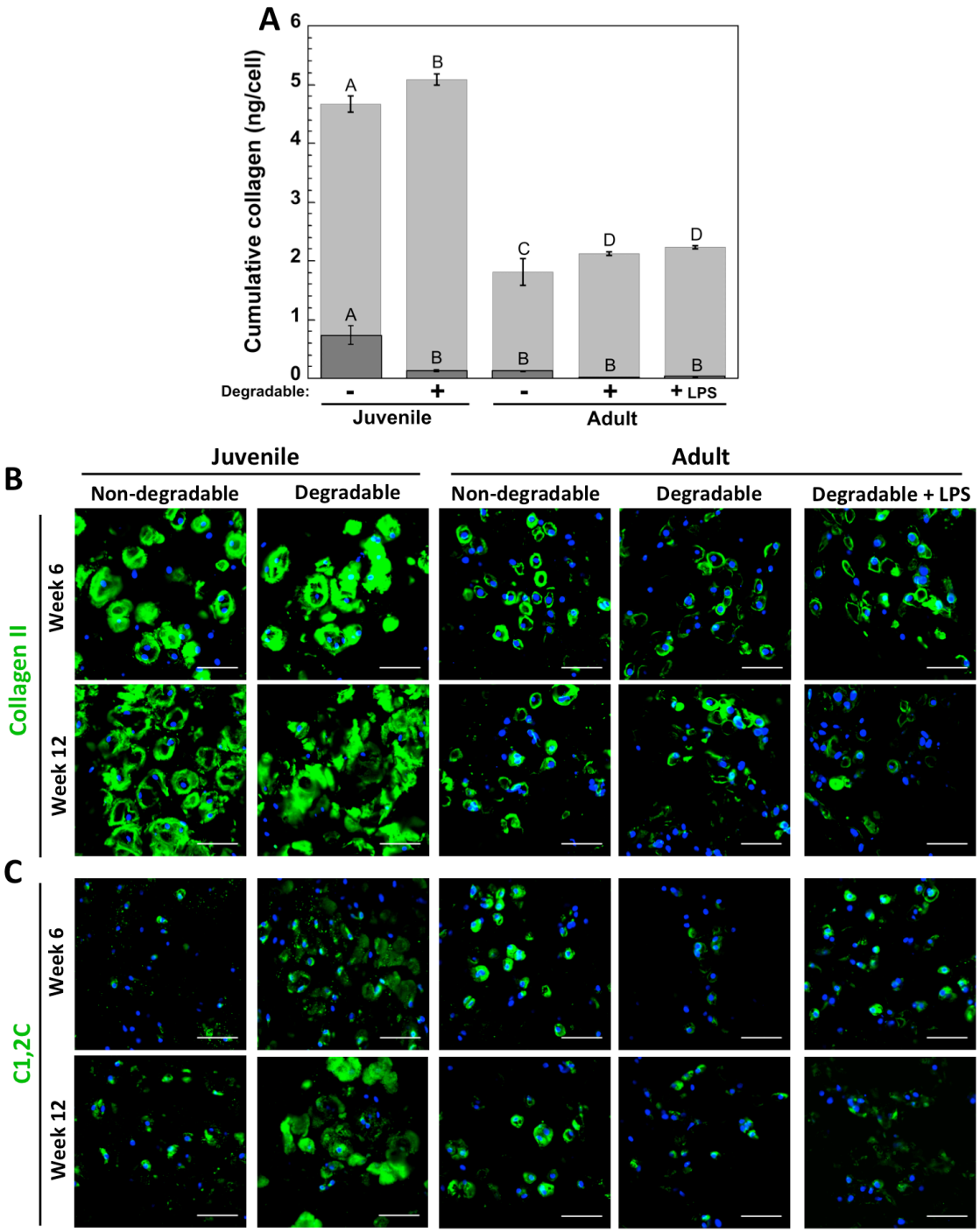

Figure 6.4 (A) Cumulative collagen per cell produced during 12 weeks of culture, shown as amount present in the constructs at 12 weeks (■), and cumulative amount released to the medium throughout 12 weeks (■). Letter groupings show statistical similarities (same letter) and differences (different letters) ($p < 0.05$). Top letters are for total collagen (constructs + medium), lower letters are for collagen in constructs only. Error bars are standard deviation ($n = 3$). (B) Immunohistochemical visualization of collagen II (green) and (C) collagenase-generated collagen neoepitope C1,2C (green) in hydrogels at weeks 6 and 12. Nuclei are blue, scale bars are 50 μm.

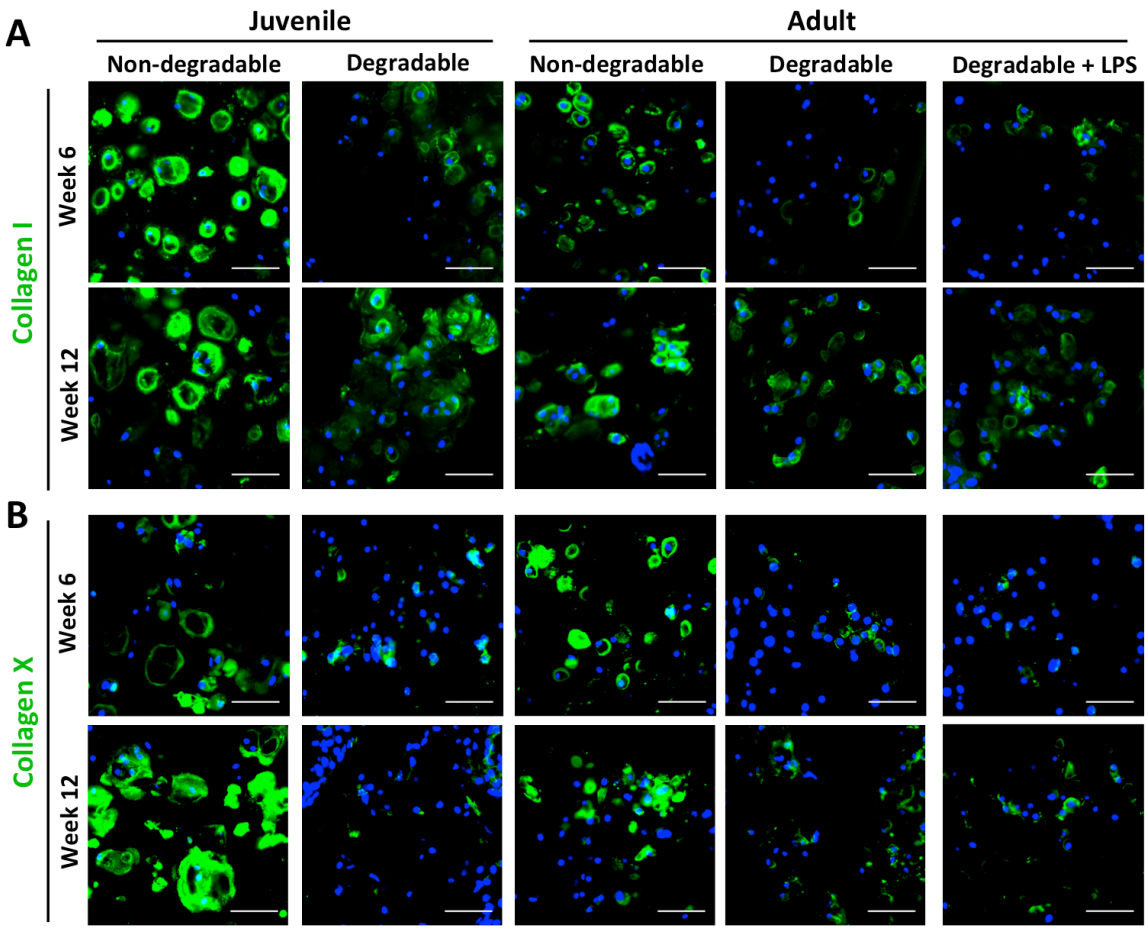

Figure 6.5 (A) Immunohistochemical visualization of collagen I (green) and (B) collagen X (green) in hydrogels at weeks 6 and 12. Nuclei are blue, scale bars are 50 μm.

6.4.5 Matrix degrading enzyme activity and IL-6 secretion

Total aggrecanase-1 and generic MMP activities are shown as the cumulative activity measured over all time points for the constructs and culture medium (Fig. 6.6A, B), and activities at each time interval are shown in figures 6.S1 and 6.S2. For juvenile cells, the degradable hydrogels led to lower ($p < 0.0001$) aggrecanase-1 and total MMP activity measured in the constructs, but greater ($p < 0.0001$) activity in the culture medium when compared to the non-degradable hydrogels. Aggrecanase-1 and total MMP activities measured in the constructs were higher ($p < 0.0001$) for the adult cells compared to juvenile cells. For adult cells, aggrecanase-1 activity was not affected by hydrogel degradation. MMP activity, however, was

lower in the constructs of the degradable hydrogels with adult cells. LPS led to the highest aggrecanase-1 and MMP activities measured in the medium ($p < 0.004$ and $p < 0.0001$, respectively). However in the constructs, aggrecanase-1 and MMP activities were lower ($p < 0.0001$) with LPS treatment. IL-6 secretion is shown as the cumulative quantity measured in the culture medium over 12 weeks (Fig. 6.6C) and the quantities measured at each time interval are shown in figure 6.S3. There was more ($p < 0.0001$) IL-6 produced by adult cells than juvenile cells, but hydrogel degradation did not affect IL-6 secretion. LPS stimulated the highest ($p < 0.0001$) amount of IL-6 secretion.

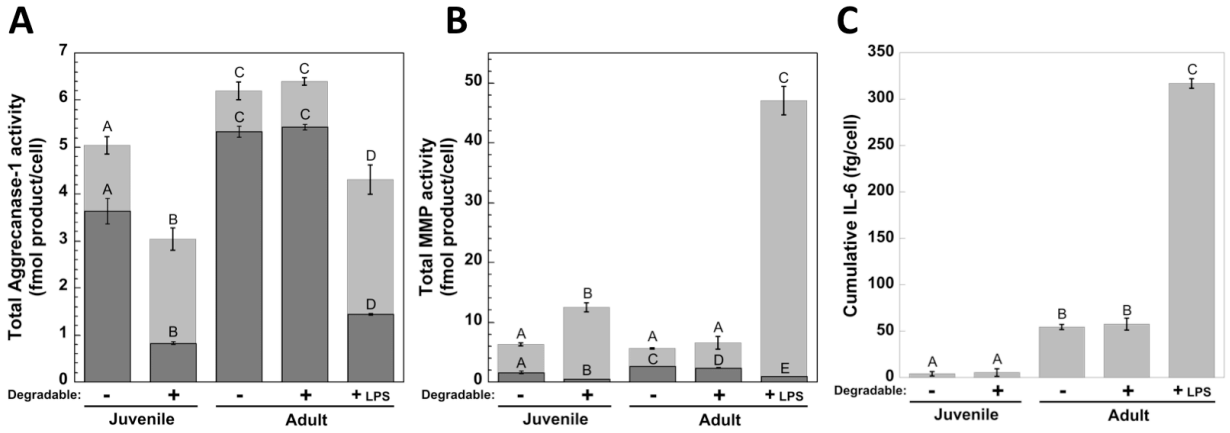

Figure 6.6 Total activity of (A) Aggrecanase-1, and (B) Generic MMPs measured per cell, shown as the additive activity measured in both the constructs (■) and culture medium (■) at all time points throughout 12 weeks. (C) Cumulative IL-6, shown as the additive quantity measured in the medium throughout 12 weeks. Letter groupings show statistical similarities (same letter) and differences (different letters) ($p < 0.05$). Top letters are for total medium activity, lower letters are for total activity in constructs. Error bars are standard deviation ($n = 3$).

6.5 Discussion

A novel aggrecanase-degradable hydrogel was developed and tested with chondrocytes exhibiting different anabolic and catabolic characteristics. We demonstrate that hydrogel degradation occurs in the presence of cell-conditioned medium, indicating that cells are able to degrade the hydrogel. Regardless of chondrocyte characteristics, enzymatically degradable hydrogels promoted cartilage-specific matrix deposition rich in aggrecan and collagen II with

reduced collagen I and minimal collagen X. We confirmed that degradation of the aggrecanase-sensitive hydrogel, which leads to exposed peptide fragments, did not appear to affect chondrocyte catabolism or elevate chondrocyte secretion of pro-inflammatory cytokines. Overall, we present a new and promising enzyme-degradable hydrogel for cartilage tissue engineering.

Juvenile chondrocytes, representing a cell source that in native tissue exhibits a homeostatic balance between anabolic and catabolic activity [39], were encapsulated in aggrecanase-sensitive hydrogels and non-degradable hydrogels and matrix elaboration was evaluated. Collagen and sGAGs were abundantly produced and deposited in the hydrogels. In non-degrading hydrogels, matrix accumulated pericellularly resulting in a two-fold increase in modulus by twelve weeks. Hydrogel degradation, however, led to higher matrix release concomitant with lower matrix retention within hydrogels, which is consistent with the decrease in modulus over time. This finding suggests that bulk degradation of the hydrogel occurred whereby enzymes secreted by juvenile chondrocytes are capable of diffusing through the hydrogel, which is evident by the presence of catabolic enzymes in the culture medium. Although matrix deposition within the hydrogel was lower with degradation, the quality of the engineered tissue was markedly improved. Most notably, the degradable hydrogels promoted an engineered tissue that was more consistent with hyaline cartilage, while the non-degradable hydrogels had collagens I, II and X present, which is more characteristic of hypertrophic cartilage. In addition, connectivity of deposited aggrecan and collagen II was evident by 12 weeks in the degradable hydrogel, but not in the non-degradable hydrogel. Because aggrecan and collagen molecules are very large, connectivity can only occur after reverse gelation happens when a sufficient number of crosslinks have been broken and the polymer dissolves. These observations point towards a combination of local and bulk degradation occurring in the aggrecanase degradable hydrogels with juvenile chondrocytes.

Adult chondrocytes representing a cell source with lower anabolic, but higher catabolic activity compared to juvenile chondrocytes [6,39] were assessed in aggrecanse-degradable and non-degradable hydrogels for matrix elaboration. As expected, cumulative sGAG and collagen synthesis was lower in the adult chondrocytes compared to the juvenile chondrocytes. In the non-degrading hydrogels, modulus was maintained over 12 weeks for adult chondrocytes, but lower when compared to the juvenile chondrocytes, which is consistent with less matrix deposition in the hydrogel. Nonetheless, the degradable hydrogels did improve the quality of the engineered tissue similar to that for the juvenile chondrocytes resulting in predominately hyaline-like cartilage deposition, but a hypertrophic-like cartilage deposition in the non-degradable hydrogels. Interestingly, degradation impacted the spatial distribution of sGAGs resulting in few sGAG detected in the extracellular space of the hydrogel. While most sGAG molecules in cartilage are attached to the aggrecan core protein, the sGAG-rich domain in aggrecan is readily degraded [29], releasing smaller sGAG-laden aggrecan fragments into the extracellular space [40] where they can either remain within or diffuse out of the hydrogel. We attribute the lack of sGAG staining in the extracellular space to rapid diffusion of the sGAG molecules out of the hydrogel due to increases in mesh size that results from hydrogel degradation. This observation is further confirmed by the large of amount of sGAG released to the culture medium. Tissue connectivity was not observed with the adult cells, which is attributed to their lower matrix synthesis rates, resulting in an overall poorer tissue elaboration by adult chondrocytes when compared to the juvenile chondrocytes.

As crosslinks in the aggrecanase-sensitive hydrogels are cleaved, cells will be exposed to peptide fragments for some period of time until a sufficient number of crosslinks are broken to release the polymer chains. ECM fragments have been shown to elicit catabolic responses in chondrocytes. For example, degraded fibronectin fragments have been shown to stimulate aggrecanase catabolism of aggrecan [41] and aggrecanase activity is elevated in osteoarthritis [42,43]. Therefore, it was important to determine whether hydrogel degradation and exposure to

peptide fragments negatively affect the encapsulated cells by eliciting an elevated catabolic and/or inflammatory response. Aggrecanase-degradable hydrogels did not increase aggrecanase activity for either adult or juvenile chondrocytes. Aggrecanase activity, however, was elevated for adult compared to juvenile chondrocytes, which is consistent with previous observations [6] and attributed to donor age and not the hydrogel environment. Generic MMP activity was assessed to probe for more general cartilage catabolism, which is necessary for tissue homeostasis, but can be increased in disease and inflammatory states [26]. Hydrogel degradability increased MMP activity in juvenile chondrocytes, but not adult chondrocytes. This finding is supported by the intense staining for MMP-degraded C1,2C collagen fragments in the degradable hydrogels with juvenile chondrocytes, especially at week 12. Pericellular collagen II deposition was dense at 6 weeks, and it has been suggested that cells may have a mechanism to activate MMPs when matrix is dense or cells are physically confined [24], therefore the increased MMP activity may be attributed to elevated matrix deposition and perhaps not to the hydrogel itself, which is supported by the fact that MMP activity was only elevated compared to non-degradable hydrogels after 6 weeks (Fig. 6.S2). IL-6, a pro-inflammatory cytokine, was assessed as an indicator for an inflammatory response, which has been shown to cause proteoglycan release from human articular cartilage [44], to be upregulated with osteoarthritis [45], and to lead to increases in aggrecanase-mediated degradation of aggrecan [46]. While IL-6 secretion was increased for adult compared to juvenile chondrocytes, it was unaffected by hydrogel degradation. Taken together, these findings suggest that the aggrecanase-degradable hydrogel does not have adverse effects on the encapsulated cells. However, it is important to note that aggrecanase-1 (ADAMTS-4) activity was measured in this study, but aggrecanase-2 (ADAMTS-5) is also secreted by chondrocytes and elevated in OA [44]. Aggrecanase-2 is capable of cleaving the E_{373}-A_{374} site on aggrecan [47] similar to aggrecanse-1, but at a much slower rate [48] and therefore may have been detected by the enzyme activity assay. We also recognize that the generic MMP assay does not differentiate between different MMPs and

therefore changes in the type of MMP activity may have occurred in the degradable hydrogel, but which was not detected.

Adult chondrocytes were exposed to LPS to represent a cell source with even higher catabolic activity relative to anabolic activity [49,50]. LPS led to a significant up-regulation of MMP activity and interleukin-6 secretion, confirming its inflammatory effect on chondrocytes. In addition, LPS led to decreased sGAGs synthesis, which is consistent with previous observations [51]. Interestingly though, LPS did not affect the amount of sGAGs retained in the hydrogel nor the spatial distribution of sGAGs or aggrecan. LPS also did not affect total collagen production or the quality of the engineered tissue with respect to collagen type. The construct modulus, however, was consistently lower than degradable hydrogels with unstimulated adult chondrocytes, but this difference was only significant at 9 weeks. It is interesting to note that C1,2C staining appeared more intense at the six week time point, which is consistent with the high MMP activity and IL-6 secretion. IL-6 secretion did drop by week 9 (Fig. 6.S3), suggesting that the inflammatory effect of LPS may not have been sustained. Interestingly, aggrecanase was down-regulated by LPS, which may in part be related to the lower sGAG production. Previous work showed that LPS stimulation upregulated aggrecanase-1 gene expression by chondrocytes [50] with 1000 ng ml^{-1} LPS, which is 100-fold higher than the concentration used in this study. It is possible that cells adapted to exogenous LPS with time, which is suggested by the changes in IL-6 secretion over time.

6.6 Conclusions

The presented work details a novel aggrecanase-sensitive hydrogel showing promise for cartilage tissue engineering by preserving the chondrocyte phenotype and promoting a hyaline-like engineered cartilage tissue by both juvenile and adult chondrocytes with minimal collagens I and X. Although hydrogel degradation led to a 2-fold decrease in compressive modulus over twelve weeks, the decrease was much less dramatic when compared to hydrolytically and bulk degrading PEG hydrogels where an 8-fold decrease in modulus was reported after only four

weeks [52]. In this study, hydrogel degradation did not increase hydrogel volume, which strongly points towards a degradation behavior that is more localized (i.e., around the cell) and distinctly different from traditional hydrolytically degrading hydrogels. The efficacy of the aggrecanase-sensitive hydrogel was dependent on the cell source, where juvenile chondrocytes produced an engineered tissue exhibiting matrix connectivity, which was not evident in adult cells and inflammatory stimulated cells with increased catabolic activity and decreased anabolic activity. Regardless of cell source, degradable hydrogels in general retained less matrix than non-degradable hydrogels, which is attributed to a rapid degradation rate relative to the rate of matrix production and deposition. One of the promising attributes of this type of hydrogel system is that degradation behavior and rate can be further optimized by increasing the initial hydrogel crosslinking density or by making slight changes to the peptide sequence to alter the degradation kinetics [18]. This hydrogel platform is nonetheless encouraging, considering that within native cartilage, the half-lives of aggrecan and collagen molecules are on the order of 15-100 days to 100 years, respectively [27,53,54]. Although this hydrogel was designed as an aggrecanase-sensitive hydrogel, the aggrecaanse targeted sequence E_{373}-A_{374} on aggrecan can be cleaved by MMPs including MMP-8, but with decreased kinetics compared to aggrecanases [55]. We also recognize that mechanical stimulation, which is important in cartilage homeostasis [14,56–58], can also influence expression and production of catabolic enzymes [59,60] and therefore may affect tissue development in these hydrogels. Nonetheless, we demonstrate the promise for aggrecanase-sensitive hydrogels in cartilage tissue engineering and future efforts will focus on further tailoring the degradation rates and localization to improve matrix elaboration, matrix deposition, and overall modulus for cells from patients that span a wide range of ages.

6.7 Acknowledgements

This research was supported by NIH grant # 1R01AR065441 and # R21AR061011, a fellowship from the National Science Foundation Graduate Research Fellowship Program (NSF

GRFP), a National Institute of Health (NIH) Pharmaceutical Biotechnology Training Grant, and a Chancellor's Fellowship from the University of Colorado. The authors would like to thank Stanley Chu for his assistance as a co-author on the manuscript.

6.8 Supplementary Figures

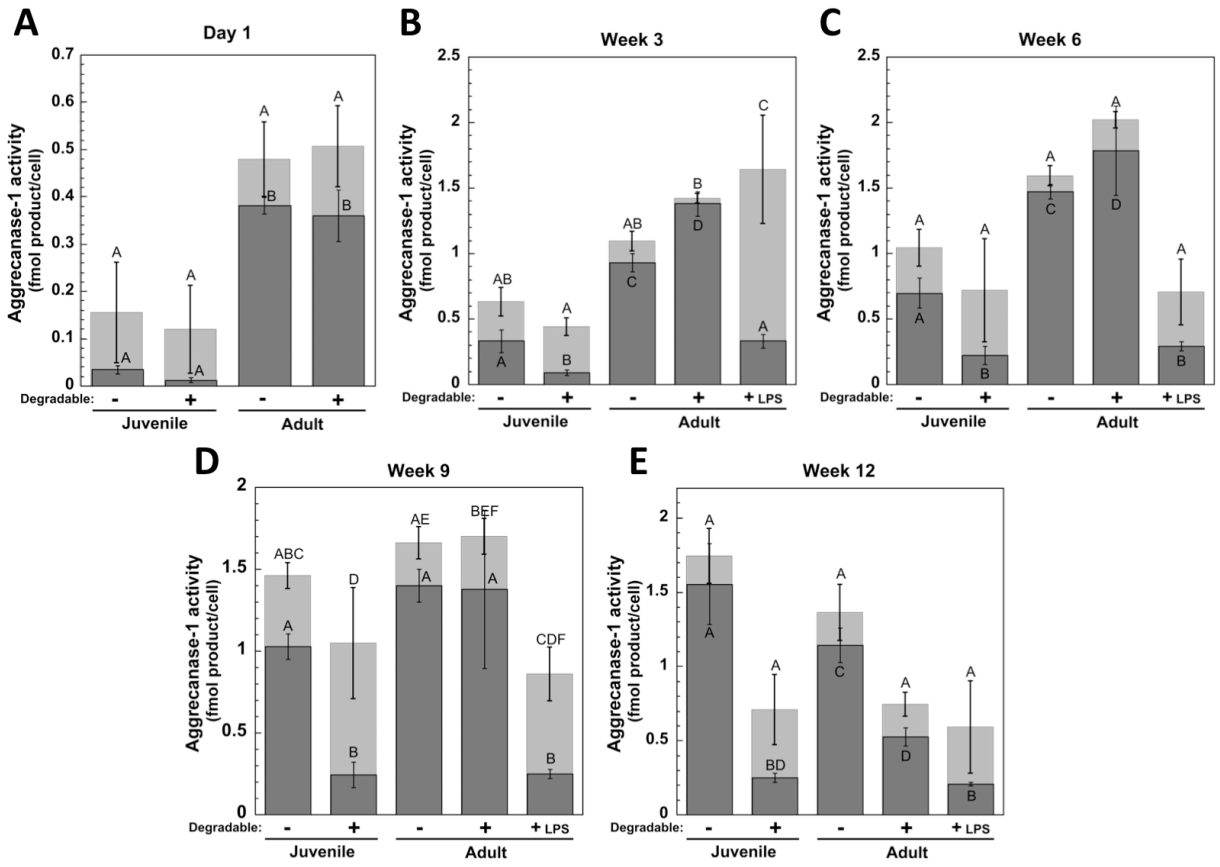

Figure 6.S1 Aggrecanase-1 activity per cell, shown as the activity measured in both the constructs (■) and culture medium (■) at (A) 1 day, and (B) 3, (C) 6, (D) 9, and (E) 12 weeks, where conditioned culture medium was pooled in 3 week increments. Letter groupings show statistical similarities (same letter) and differences (different letters) ($p < 0.05$). Top letters are for activity in the medium, lower letters are for activity in constructs. Error bars are standard deviation ($n = 3$).

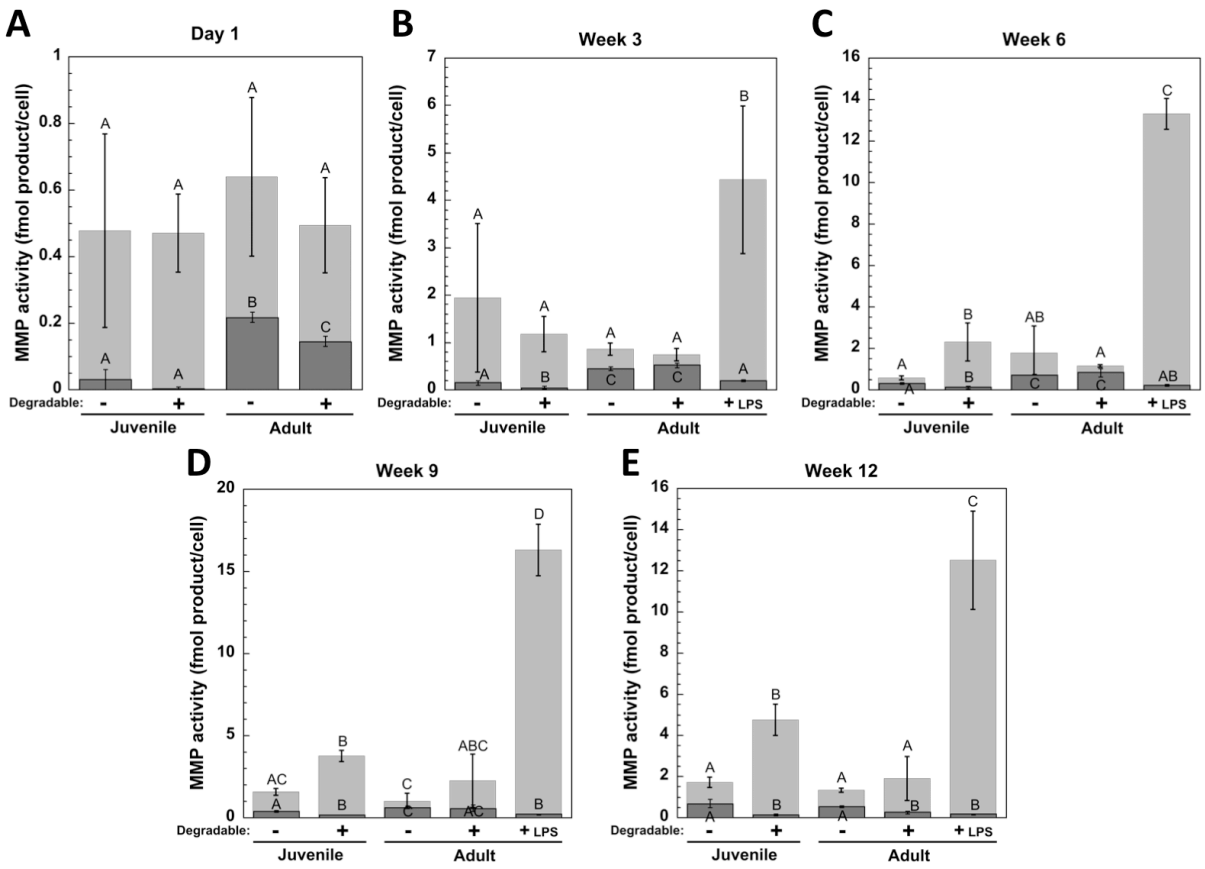

Figure 6.S2 MMP activity per cell, shown as the activity measured in both the constructs (■) and culture medium (■) at (A) 1 day, and (B) 3, (C) 6, (D) 9, and (E) 12 weeks, where conditioned culture medium was pooled in 3 week increments. Letter groupings show statistical similarities (same letter) and differences (different letters) ($p < 0.05$). Top letters are for activity in the medium, lower letters are for activity in constructs. Error bars are standard deviation (n = 3).

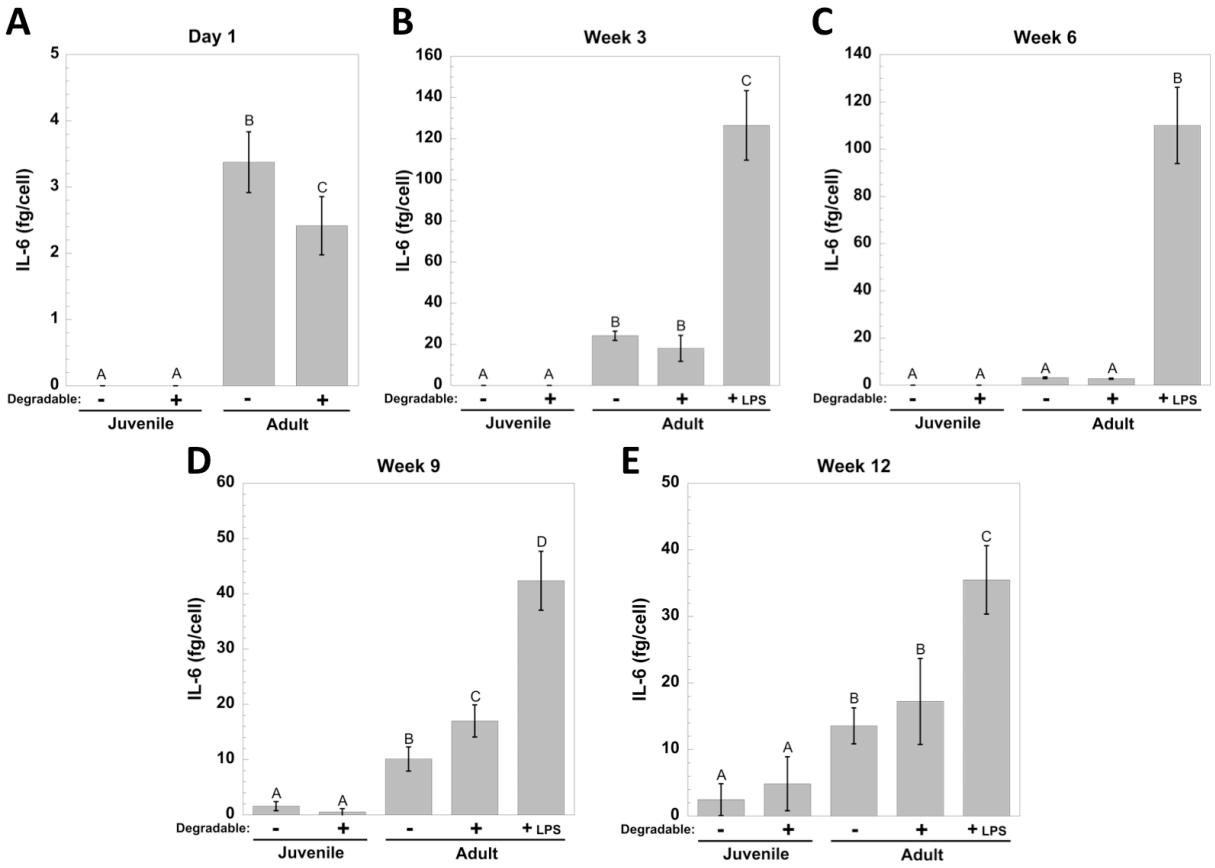

Figure 6.S3 IL-6 produced per cell and released to the culture medium at (A) 1 day, and (B) 3, (C) 6, (D) 9, and (E) 12 weeks, where conditioned culture medium was pooled in 3 week increments. Letter groupings show statistical similarities (same letter) and differences (different letters) ($p < 0.05$). Error bars are standard deviation ($n = 3$).

6.9 References

[1] Gillogly SD, Myers TH. Treatment of full-thickness chondral defects with autologous chondrocyte implantation. Orthop Clin North Am 2005;36:433–46.

[2] Richardson JB, Caterson B, Evans EH, Ashton BA, Roberts S. Repair of human articular cartilage after implantation of autologous chondrocytes. J Bone Jt Surgery-British Vol 1999;81B:1064–8.

[3] Vanlauwe J, Almqvist F, Bellemans J, Huskin J-P, Verdonk R, Victor J. Repair of symptomatic cartilage lesions of the knee: the place of autologous chondrocyte implantation. Acta Orthop Belg 2007;73:145–58.

[4] Bartlett W, Skinner JA, Gooding CR, Carrington RWJ, Flanagan AM, Briggs TWR, et al. Autologous chondrocyte implantation versus matrix-induced autologous chondrocyte

implantation for osteochondral defects of the knee: a prospective, randomised study. J Bone Joint Surg Br 2005;87:640–5.

[5] Kon E, Verdonk P, Condello V, Delcogliano M, Dhollander A, Filardo G, et al. Matrix-Assisted Autologous Chondrocyte Transplantation for the Repair of Cartilage Defects of the Knee Systematic Clinical Data Review and Study Quality Analysis. Am J Sports Med 2009;37:156S–166S.

[6] Skaalure SC, Milligan IL, Bryant SJ. Age impacts extracellular matrix metabolism in chondrocytes encapsulated in degradable hydrogels. Biomed Mater 2012;7.

[7] Farnsworth NL, Antunez LR, Bryant SJ. Dynamic compressive loading differentially regulates chondrocyte anabolic and catabolic activity with age. Biotechnol Bioeng 2013;110:2046–57.

[8] Bryant SJ, Durand KL, Anseth KS. Manipulations in hydrogel chemistry control photoencapsulated chondrocyte behavior and their extracellular matrix production. J Biomed Mater Res Part A 2003;67A:1430–6.

[9] Bryant SJ, Anseth KS. Hydrogel properties influence ECM production by chondrocytes photoencapsulated in poly(ethylene glycol) hydrogels. J Biomed Mater Res 2002;59:63–72.

[10] Bryant SJ, Chowdhury TT, Lee DA, Bader DL, Anseth KS. Crosslinking density influences chondrocyte metabolism in dynamically loaded photocrosslinked poly(ethylene glycol) hydrogels. Ann Biomed Eng 2004;32:407–17.

[11] Nicodemus GD, Skaalure SC, Bryant SJ. Gel structure has an impact on pericellular and extracellular matrix deposition, which subsequently alters metabolic activities in chondrocyte-laden PEG hydrogels. Acta Biomater 2011;7:492–504.

[12] Bryant SJ, Bender RJ, Durand KL, Anseth KS. Encapsulating Chondrocytes in degrading PEG hydrogels with high modulus: Engineering gel structural changes to facilitate cartilaginous tissue production. Biotechnol Bioeng 2004;86:747–55.

[13] Anseth KS, Bryant SJ. Controlling the spatial distribution of ECM components in degradable PEG hydrogels for tissue engineering cartilage. J Biomed Mater Res Part A 2003;64A:70–9.

[14] Roberts JJ, Nicodemus GD, Greenwald EC, Bryant SJ. Degradation Improves Tissue Formation in (Un)Loaded Chondrocyte-laden Hydrogels. Clin Orthop Relat Res 2011.

[15] West JL, Hubbell JA. Polymeric Biomaterials with Degradation Sites for Proteases Involved in Cell Migration. Macromolecules 1999;32:241–4.

[16] Fairbanks BD, Schwartz MP, Halevi AE, Nuttelman CR, Bowman CN, Anseth KS. A Versatile Synthetic Extracellular Matrix Mimic via Thiol-Norbornene Photopolymerization. Adv Mater 2009;21:5005–10.

[17] Lutolf MP, Lauer-Fields JL, Schmoekel HG, Metters AT, Weber FE, Fields GB, et al. Synthetic matrix metalloproteinase-sensitive hydrogels for the conduction of tissue regeneration: engineering cell-invasion characteristics. Proc Natl Acad Sci U S A 2003;100:5413–8.

[18] Patterson J, Hubbell JA. Enhanced proteolytic degradation of molecularly engineered PEG hydrogels in response to MMP-1 and MMP-2. Biomaterials 2010;31:7836–45.

[19] West JL, Lee SH, Miller JS, Moon JJ. Proteolytically degradable hydrogels with a fluorogenic substrate for studies of cellular proteolytic activity and migration. Biotechnol Prog 2005;21:1736–41.

[20] Lévesque SG, Shoichet MS. Synthesis of enzyme-degradable, peptide-cross-linked dextran hydrogels. Bioconjug Chem 2007;18:874–85.

[21] Vernerey FJ, Greenwald EC, Bryant SJ. Triphasic mixture model of cell-mediated enzymatic degradation of hydrogels. Comput Methods Biomech Biomed Engin 2012;15:1197–210.

[22] Dhote V, Vernerey FJ. Mathematical model of the role of degradation on matrix development in hydrogel scaffold. Biomech Model Mechanobiol 2013.

[23] Bahney CS, Hsu C-W, Yoo JU, West JL, Johnstone B. A bioresponsive hydrogel tuned to chondrogenesis of human mesenchymal stem cells. FASEB J 2011;25:1486–96.

[24] Park Y, Lutolf MP, Hubbell JA, Hunziker EB, Wong M. Bovine primary chondrocyte culture in synthetic matrix metalloproteinase-sensitive poly(ethylene glycol)-based hydrogels as a scaffold for cartilage repair. Tissue Eng 2004;10:515–22.

[25] Roberts JJ, Bryant SJ. Comparison of photopolymerizable thiol-ene PEG and acrylate-based PEG hydrogels for cartilage development. Biomaterials 2013;34:9969–79.

[26] Manicourt DH, Devogelaer JP, Thonar EJMA. Products of Cartilage Metabolism. In: Seibel MJ, Robins SP, Bilezikian JP, editors. Dyn. Bone Cartil. Metab., vol. 1, Burlington: Elsevier; 2006, p. 421–49.

[27] Knudson CB, Knudson W. Cartilage proteoglycans. Semin Cell Dev Biol 2001;12:69–78.

[28] Buckwalter JA, Rosenberg LC. Electron-Microscopic Studies of Cartilage Proteoglycans - Direct Evidence for the Variable Length of the Chondroitin Sulfate-Rich Region of Proteoglycan Subunit Core Protein. J Biol Chem 1982;257:9830–9.

[29] Caterson B, Flannery CR, Hughes GE, Little CB. Mechanisms involved in cartilage proteoglycan catabolism. Matrix Biol 2000;19:333–44.

[30] Durigova M, Nagase H, Mort JS, Roughley PJ. MMPs are less efficient than ADAMTS5 in cleaving aggrecan core protein. Matrix Biol 2011;30:145–53.

[31] Lark MW, Gordy JT, Weidner JR, Ayala J, Kimura JH, Williams HR, et al. Cell-mediated Catabolism of Aggrecan. J Biol Chem 1995;270:2550–6.

[32] Ilic MZ, Handley CJ, Robinson HC, Mok MT. Mechanism of Catabolism of Aggrecan by Articular Cartilage. Arch Biochem Biophys 1992;294:115–22.

[33] Flannery CR, Little CB, Caterson B. Molecular cloning and sequence analysis of the aggrecan interglobular domain from porcine, equine, bovine and ovine cartilage: comparison of proteinase-susceptible regions and sites of keratan sulfate substitution. Matrix Biol 1998;16:507–11.

[34] Lutolf MP, Raeber GP, Zisch AH, Tirelli N, Hubbell JA. Cell-Responsive Synthetic Hydrogels. Adv Mater 2003;15:888–92.

[35] Shih H, Lin C-C. Visible Light-Mediated Thiol-Ene Hydrogelation Using Eosin-Y as the Only Photoinitiator. Macromol Rapid Commun 2013;34:269–73.

[36] Kim YJ, Sah RLY, Doong JYH, Grodzinsky AJ. Fluorometric Assay of DNA in Cartilage Explants Using Hoechst-33258. Anal Biochem 1988;174:168–76.

[37] Woessner JF. Determination of Hydroxyproline in Tissue and Protein Samples Containing Small Proportions of This Imino Acid. Arch Biochem Biophys 1961;93:440–7.

[38] Templeton DM. The Basis and Applicability of the Dimethylmethylene Blue Binding Assay for Sulfated Glycosaminoglycans. Connect Tissue Res 1988;17:23–32.

[39] Martin JA, Buckwalter JA. Aging, articular cartilage chondrocyte senescence and osteoarthritis. Biogerontology 2002;3:257–64.

[40] Mok SS, Masuda K, Hauselmann HJ, Aydelotte MB, Thonar EJMA. Aggrecan Synthesized by Mature Bovine Chondrocytes Suspended in Alginate - Identification of 2 Distinct Metabolic Matrix Pools. J Biol Chem 1994;269:33021–7.

[41] Homandberg GA, Davis G, Maniglia C, Shrikhande A. Cartilage chondrolysis by fibronectin fragments causes cleavage of aggrecan at the same site as found in osteoarthritic cartilage. Osteoarthr Cartil 1997;5:450–3.

[42] Struglics A, Larsson S, Hansson M, Lohmander LS. Western blot quantification of aggrecan fragments in human synovial fluid indicates differences in fragment patterns between joint diseases. Osteoarthr Cartil 2009;17:497–506.

[43] Nagase H, Kashiwagi M. Aggrecanases and cartilage matrix degradation. Arthritis Res Ther 2003;5:94–103.

[44] Martel-Pelletier J, Boileau C, Pelletier J-P, Roughley PJ. Cartilage in normal and osteoarthritis conditions. Best Pract Res Clin Rheumatol 2008;22:351–84.

[45] Middleton J, Manthey A, Tyler J. Insulin-like growth factor (IGF) receptor, IGF-I, interleukin-1 beta (IL-1 beta), and IL-6 mRNA expression in osteoarthritic and normal human cartilage. J Histochem Cytochem 1996;44:133–41.

[46] Flannery CR, Little CB, Hughes CE, Curtis CL, Caterson B, Jones SA. IL-6 and its soluble receptor augment aggrecanase-mediated proteoglycan catabolism in articular cartilage. Matrix Biol 2000;19:549–53.

[47] Edwards DR, Porter S, Clark IM, Kevorkian L. The ADAMTS metalloproteinases. Biochem J 2005;386:15–27.

[48] Tortorella MD, Liu R-Q, Burn T, Newton RC, Arner E. Characterization of human aggrecanase 2 (ADAM-TS5): substrate specificity studies and comparison with aggrecanase 1 (ADAM-TS4). Matrix Biol 2002;21:499–511.

[49] Lee MS, Ikenoue T, Trindade MCD, Wong N, Goodman SB, Schurman DJ, et al. Protective effects of intermittent hydrostatic pressure on osteoarthritic chondrocytes activated by bacterial endotoxin in vitro. J Orthop Res 2003;21:117–22.

[50] Patel L, Sun W, Glasson SS, Morris EA, Flannery CR, Chockalingam PS. Tenascin-C induces inflammatory mediators and matrix degradation in osteoarthritic cartilage. BMC Musculoskelet Disord 2011;12.

[51] Morales TI, Wahl LM, Hascall VC. The Effect of Bacterial Lipopolysaccharides on the Biosynthesis and Release of Proteoglycans from Calf Articular Cartilage Cultures. J Biol Chem 1984;259:6720–9.

[52] Roberts JJ, Nicodemus GD, Greenwald EC, Bryant SJ. Degradation Improves Tissue Formation in (Un)Loaded Chondrocyte-laden Hydrogels. Clin Orthop Relat Res 2011.

[53] Mok SS, Masuda K, Hauselmann HJ, Aydelotte MB, Thonar EJMA. Aggrecan Synthesized by Mature Bovine Chondrocytes Suspended in Alginate - Identification of 2 Distinct Metabolic Matrix Pools. J Biol Chem 1994;269:33021–7.

[54] Hauselmann HJ, Masuda K, Hunziker EB, Neidhart M, Mok SS, Michel BA, et al. Adult human chondrocytes cultured in alginate form a matrix similar to native human articular cartilage. Am J Physiol Physiol 1996;271:C742–C752.

[55] Buttner FH, Hughes CE, Margerie D, Lichte A, Tschesche H, Caterson B, et al. Membrane type 1 matrix metalloproteinase (MT1-MMP) cleaves the recombinant aggrecan substrate rAgg1mut at the “aggrecanase” and the MMP sites. Biochem J 1998;333:159–65.

[56] Roberts JJ, Nicodemus GD, Giunta S, Bryant SJ. Incorporation of biomimetic matrix molecules in PEG hydrogels enhances matrix deposition and reduces load-induced loss of chondrocyte-secreted matrix. J Biomed Mater Res Part A 2011;97A:281–91.

[57] Guilak F, Butler DL, Goldstein SA. Functional tissue engineering - The role of biomechanics in articular cartilage repair. Clin Orthop Relat Res 2001:S295–S305.

[58] Darling EM, Athanasiou KA. Biomechanical strategies for articular cartilage regeneration. Ann Biomed Eng 2003;31:1114–24.

[59] Nicodemus GD, Bryant SJ. Mechanical loading regimes affect the anabolic and catabolic activities by chondrocytes encapsulated in PEG hydrogels. Osteoarthr Cartil 2010;18:126–37.

[60] De Croos JNA, Dhaliwal SS, Grynpas MD, Pilliar RM, Kandel RA. Cyclic compressive mechanical stimulation induces sequential catabolic and anabolic gene changes in chondrocytes resulting in increased extracellular matrix accumulation. Matrix Biol 2006;25:323–31.

Chapter 7

A Combined Experimental-computational Approach for Controlling Reaction- and Diffusion-dominated Degradation of Enzymatically Degradable Hydrogels

(In preparation)

7.1 Abstract

Cell-mediated enzymatically degradable hydrogel scaffolds are attractive cell carriers for tissue engineering applications, where new tissue can elaborate macroscopically within a hydrogel as the hydrogel degrades by cell-secreted enzymes. This type of degradation however is complex because scaffold degradation can vary in both space and time depending on the diffusivity of the enzyme in the hydrogel and its reactivity leading to degradation that occurs throughout the hydrogel, locally restricted around the cell, or a combination. The overall aim of this work was to apply both experimental and computational approaches to characterize the degradation behavior of enzyme-degradable hydrogels, but without the complexity of cells and their associated matrix synthesis. The specific aims were to first characterize the degradation front in an acellular 1D system and then to model cells in 3D using enzyme-releasing microspheres. It was demonstrated that reaction- or diffusion-dominated degradation (localized or bulk, respectively) could be controlled by simply varying the initial hydrogel crosslinking density, and that a critical parameter is the ratio of the hydrogel mesh size to the enzyme radius of gyration for a given system. Specific ranges of this ratio, depending on the kinetic parameters, were identified to lead to either reaction- or diffusion-dominated degradation, providing an important tool to aid hydrogel design. By understanding how hydrogel structure, along with degradation kinetics, affects degradation characteristics, these observations can be

applied to the design of a wide variety of enzymatically degradable scaffolds using any cell source.

7.2 Introduction

Biodegradable hydrogel scaffolds that degrade by cell-mediated mechanisms show promise for tissue regeneration using a variety of cell sources. Crosslinked hydrogels are promising cell carriers [1,2] because their elasticity and highly swollen environment mimics that of most native tissues and permits extracellular matrix (ECM) and nutrient transport while physically entrapping cells into the crosslinked network [1,3–5]. Hydrogels can function as a vehicle to deliver any appropriate cell type to diseased or damaged tissue in an effort to regenerate healthy, functional tissues. However, long-term presence of hydrogel scaffolds can induce the foreign body reaction initiating an adverse inflammatory response [6], and inhibit cellular migration, infiltration and ECM deposition [7], which are crucial for effective tissue regeneration. Therefore scaffold biodegradation is necessary. However, degradation rates must be matched to the rate of matrix deposition by the specific cell source in order to maintain overall mechanical integrity of the implant, and prevent encapsulated cells and new ECM from being lost from the scaffold. These criteria present a significant design challenge.

A wide variety of biodegradable hydrogels have been developed in recent decades, and hydrolytically degradable scaffolds have shown promise in some applications but provide little control over degradation. Several synthetic chemistries were introduced that contain hydrolytically labile esters, permitting bulk hydrolytic degradation [4]. Of these materials, (meth)acrylated poly(ethylene glycol) (PEG)-poly(lactic acid) showed advantages over non-degrading materials in facilitating regeneration of a wide variety of tissues including bone, nervous tissue, and cartilage [8–11]. Some degree of control over degradation rates is possible by incorporating different numbers of poly(lactic acid) repeats, but hydrogels ultimately degrade at rates independent of the encapsulated cell type. Degradation in these systems is characterized by an exponential drop in compressive modulus with time concomitant with an

exponential increase in swelling [12]. As most extracellular matrix molecules are much larger than the mesh size of the hydrogel even as crosslinks are cleaved, matrix elaboration typically does not occur until reverse gelation (i.e., dissolution of the hydrogel). As a result, hydrogel mechanical properties often decrease with culture time, which was observed with PEG-poly(lactic acid) hydrogels and encapsulated chondrocytes resulting in an 8-fold decrease in compressive modulus by 4 weeks [10].

Synthetic photopolymerizable hydrogels that degrade by cell-mediated mechanisms are promising for tissue regeneration by encapsulated cells because the cell source can provide both spatial and temporal control over degradation. While cell-mediated degradation can occur in natural hydrogels such as collagen and fibrin, it is difficult to form reproducible or mechanically robust hydrogels with these materials [1]. Natural materials however can be synthetically modified to permit crosslinking, providing more control over degradation. For example, chondroitin sulfate, which is degradable by chondroitinase, was methacrylated to permit crosslinking and was used to encapsulate chondrocytes [13,14]. Hyaluronic acid, which is degradable by hyaluronidase, has been similarly modified with methacrylates, thiols, or hydrazides to permit crosslinking [15–18] and was investigated as a carrier for various cell types. Synthetic materials such as PEG are appealing as a 'blank slate' that can be further functionalized with bioactive moieties [19], such as short enzymatically-sensitive peptide sequences incorporated into the crosslinks. These hydrogels were first introduced by West and Hubbell [20] who incorporated collagenase-sensitive and plasmin-sensitive peptide substrates to encourage cell migration, which led to the development of a variety of hydrogels incorporating matrix metalloproteinase (MMP)-degradable peptides to encourage cell migration and improve tissue engineering outcomes using encapsulated cells [21–26]. In these systems, engineering accelerated peptide degradation kinetics was found to increase hydrogel degradation rates [26], but the ability to tailor these hydrogels and exert control over degradation has so far not been well characterized.

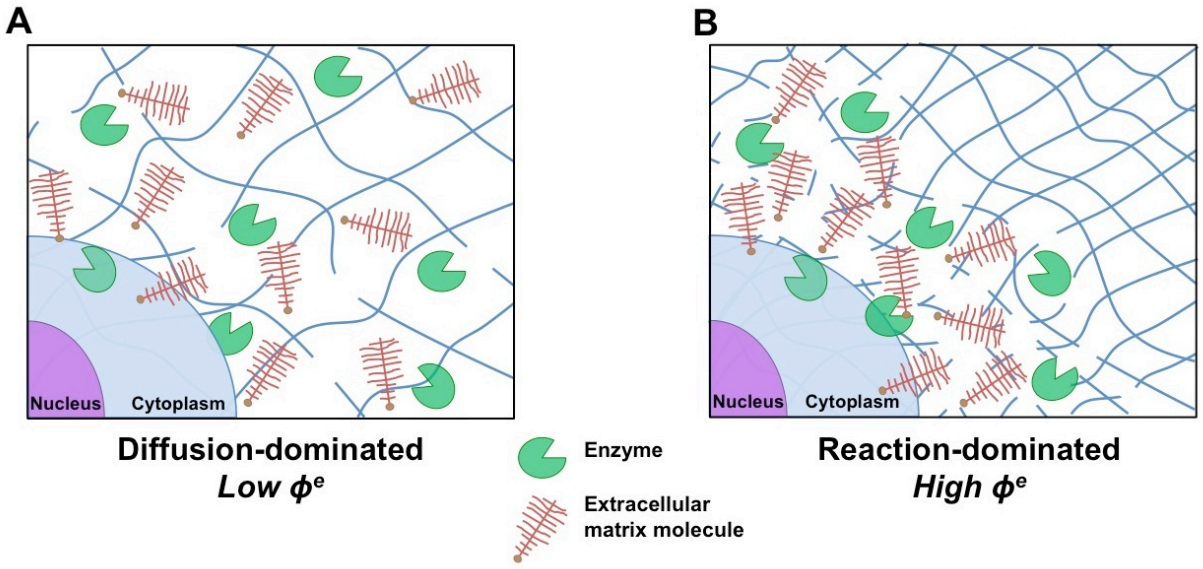

Figure 7.1 Schematic of enzymatic degradation and matrix diffusion within (A) a loosely crosslinked hydrogel where both enzyme and matrix can freely diffuse, making it a diffusion-dominated system, and (B) a tightly crosslinked hydrogel where enzyme and matrix diffusion are restricted, making it a reaction-dominated system.

In addition to peptide degradation kinetic parameters, the hydrogel network structure affects the rate *and* spatial localization of degradation, as suggested by computational models. Computational simulations of matrix elaboration by chondrocytes encapsulated within enzymatically degradable hydrogels revealed that the hydrogel crosslink density was an important factor affecting degradation [27,28], which could be diffusion-dominated when cell-secreted enzyme diffuses freely through the hydrogel network (Fig. 7.1A), or reaction-dominated when enzyme diffusion is restricted by the hydrogel crosslinks (Fig. 7.1B). The dimensionless parameter ϕ^e was introduced previously [27,28] to describe the ratio of reaction rate (numerator) to diffusion rate (denominator) in a spherical coordinate system where the degradation rate is approximated by first order kinetics with respect to enzyme concentration:

$$\phi^e = \frac{k_{cat} r_e^2}{\mathcal{D}_r} \quad (1)$$

In this equation, k_{cat} is the substrate-specific overall enzyme rate constant, r_e is the enzyme radius of gyration, and $\mathcal{D}_r$ is the enzyme diffusivity within the crosslinked hydrogel, referred to

as the restricted diffusivity. For cartilage tissue engineering, computational simulations predicted that reaction-dominated localized degradation (high ϕ^e) would encourage matrix deposition and elaboration beginning immediately surrounding the cell and continuing to grow radially outward [27]. As a result, overall modulus is maintained throughout the process of scaffold degradation and tissue regeneration, which is especially important for tissues within a mechanical environment. In order to design a hydrogel system with high ϕ^e, it is necessary to identify the most important system parameters to control experimentally.

In this work we aimed to implement a joint experimental-computational approach to characterize and thereby determine how to control localized cell-mediated degradation in order to guide hydrogel design for tissue engineering using encapsulated cells. The degradation front, which describes the evolving hydrogel crosslink density with both distance and time progressing from an enzyme source, was examined in one dimension, and then hydrogel degradation was modeled in 3D with cell-simulating microspheres. Previously developed [27,28] computational models were used to predict experimental outcomes and fit kinetic parameters, validating their utility as an effective tool for degradable hydrogel design. To model enzyme secretion from encapsulated cells, but removing the complicating factor of matrix deposition, we entrapped collagenase type II, which degrades collagens I-III [29], into poly(DL-lactide-*co*-glycolide) (PLGA) microspheres that surface erode slowly in aqueous solution, releasing the enzyme encapsulant when embedded in a hydrogel network [30,31]. For the hydrogel system, we chose to use 8-arm PEG macromer that can be crosslinked with *bis*-cysteine peptides using thiol-norbornene chemistry [32], which can be radically photopolymerized *in situ* via a homogeneous step-growth network. The peptide sequence CVPLS-LYSGC (dash indicates site of cleavage) was used for these studies, where the sequence VPLS-LYSG is degraded very efficiently (k_{cat}/K_M > 20,000 $M^{-1}s^{-1}$) by MMP-2, -7, and -9, and less efficiently by MMP-1, -3, and -14 [26,33]. By qualitatively and quantitatively characterizing how hydrogel structure affects localized degradation, specifically by distinguishing diffusion- from reaction-dominated

degradation, new enzymatically degradable hydrogels can be designed to match matrix elaboration by any cell type for tissue engineering.

7.3 Materials and Methods

7.3.1 Materials

8-arm PEG amine (MW 10,000 and 20,000) was from JenKem Technology USA (Allen, TX). 0-(7-azabenzotriazol-1-yl)-N,N,N',N'-tetramethyluronium hexafluorophosphate (HATU) and N,N'-diisopropylethylamine (DIEA) were from Chem-Impex International, Inc. (Wood Dale, IL). Collagenase type II from *Clostridium histolyticum* was from Worthington Biochemical (Lakewood, NJ). Ethyl ether and N,N-dimethylformamide (DMF) were from Fisher Scientific (Fair Lawn, NJ). Regenerated Cellulose 1000 MWCO dialysis tubing was from Spectrum Labs (Rancho Dominguez, CA). MMP-degradable peptide (CVPLS-LYSGC) was from GenScript (Piscataway, NJ). Irgacure 2959 was from Ciba Specialty Chemicals (Tarrytown, NY). Phosphate-buffered saline with calcium and magnesium (PBS), penicillin-streptomycin (P/S), fungizone, gentamicin, and NanoOrange protein quantitation kit were from Invitrogen (Carlsbad, CA). 5-norbornene-2-carboxylic acid, PEG-dithiol, Coomassie, 4-mercaptoethanol, polyvinyl alcohol (PVA, MW 30,000-70,000), sucrose, and bovine serum albumin (BSA) were from Sigma-Aldrich (St. Louis, MO). Generic MMP SensoLyte™ assay kit was from Anaspec (Fremont, CA). 4-20% TGX polyacrylamide and 10% gelatin gels, buffers, Kaleidoscope protein MW standards, Laemmli buffer, and gel electrophoresis supplies were from BioRad Laboratories (Hercules, CA). NHS-Fluorescein, AlexaFluor-546 C5 maleimide, and methylene chloride were from Thermo Fisher Scientific (Fair Lawn, NJ). 50:50 poly(DL-lactide-*co*-glycolide) (PLGA), 1.13 inherent viscosity, was from Durect (Birmingham, Alabama).

7.3.2 Collagenase type II characterization

Michaelis-Menten enzyme kinetic parameters k_{cat} (substrate turnover rate) and K_M (Michaelis-Menten constant) for collagenase type II were estimated using an activity assay for generic MMPs (probes for MMP-1- 3, 7-10, and 12-14 simultaneously). Collagenase was

incubated with substrate up to 1 h at 37 °C, taking periodic readings to generate kinetic data (supplemental Fig. S1A). The slope of the first 20 minutes was used to estimate reaction velocity, which was plotted with a Lineweaver-Burk transformation [34] in order to estimate kinetic parameters (Fig. S1B).

The average molecular weight of collagenase was determined with gel electrophoresis (Fig. S1C). Briefly, collagenase solutions were diluted 1:1 in Laemmli buffer with 5% 4-mercaptoethanol and boiled 10 minutes, then run (with Kaleidoscope protein MW standards) on a 4-20% polyacrylamide gel for 50 min at 200V. The gel was stained 5 min with 0.3% Coomassie in 45% methanol and 10% acetic acid, destained with 40% methanol and 10% acetic acid, followed by DI H_20 rinses and imaging using the BioRad VersaDoc 4000MP system. The weighted average molecular weight of collagenase II was determined to be 54 kDa by integrating band intensities and comparing to the molecular weight standards (ImageJ). Collagenase activity was characterized with a gelatin zymogram (Fig. 7.S1D). Briefly, collagenase was run on a 10% gelatin gel for 90 min at 125V, incubated 30 min each in renaturing and developing buffers, and developed in fresh developing buffer overnight. The gel was stained with Coomassie for 30 min and destained as described above.

7.3.3 Fluorescent labeling of collagenase

Collagenase type II was labeled with NHS-Fluorescein by reacting fluorescein at 15x molar excess in 100 mM sodium bicarbonate buffer, pH 8 for 1 h at room temperature. Labeled collagenase was dialyzed against PBS for 2-3 days and lyophilized. A NanoDrop 1000 spectrophotometer (Thermo Fisher Scientific, Fair Lawn, NJ) was used to determine that on average, 4 moles of fluorescein were added to each mole of collagenase.

7.3.4. Microsphere synthesis

PLGA microspheres were synthesized via a double emulsion technique [31,35]. Microspheres were loaded with three different protein encapsulants: BSA, collagenase type II, and fluorescein-collagenase, or no protein (PBS alone) to make ‘blank’ particles. Per batch, 150

mg PLGA was dissolved in 1 ml methylene chloride, and 20 mg protein encapsulant was dissolved in 100 ul PBS, added to PLGA solution, and probe sonicated 15 seconds to create the first emulsion (Microson 2000 Ultrasonic Cell disruptor, Misonix, Farmingdale, NY). Emulsion was transferred to 1 ml of 10% PVA, 30% sucrose solution and vortexed 15 seconds to create the second emulsion, which was transferred to 200 ml of 0.25% PVA, 3% sucrose solution and stirred for 4 h. Microspheres were recovered by centrifugation, washed several times in DI H_20, and lyophilized.

To quantify protein release over time, collagenase or 'blank' microspheres were suspended at 20 mg ml^{-1} in PBS and maintained at 37 °C, and sampled up to 100 h by briefly centrifuging, removing sample volume, and replacing sample volume with fresh PBS. Protein release was determined with the NanoOrange protein quantitation kit, and 'blank' microsphere samples at each time point were subtracted from collagenase.

7.3.5 Macromer synthesis

8-arm PEG amine (MW 10,000 and 20,000) were reacted with norbornene acid to synthesize 8-arm PEG-amide-norbornene (8armPEG10K-NB and 8armPEG20K-NB) [32,36,37]. Briefly, norbornene acid (8x molar excess compared to amine-terminated PEG arms) in DMF was pre-reacted for 5 minutes under argon with HATU (4x excess) and DIEA (4x excess) at room temperature. The pre-reacted mixture was combined with 8-arm PEG amine in DMF, and the reaction proceeded overnight under argon at room temperature. 8armPEG-NB was recovered by precipitation in ethyl ether, and purified by dialyzing against DI H_20 for 2-3 days. Dialyzed 8armPEG-NB was filtered (0.2 μm) and lyophilized. ^{1}H-NMR spectroscopy determined norbornene conjugation (δ = 5.9 - 6.3 ppm) per 8-arm PEG molecule (δ = 3.4 – 3.9 ppm). On average, 100% of amine-terminated PEG arms were conjugated with norbornene (for both 8armPEG10K-NB and 8armPEG20K-NB).

7.3.6 Hydrogel formation and characterization

Macromer solutions were formed with varying weight % (wt%) of 8armPEG10K-NB and 8armPEG20K-NB in PBS-antis (PBS supplemented with 1% P/S, 0.5 μg ml^{-1} fungizone, and 20 μg ml^{-1} gentamicin), and thiol:norbornene molar ratios were varied to create hydrogels with a range of crosslink densities (Table 7.1). For 1-d diffusion, PEG-dithiol (1000 MW) was used as a non-degradable crosslinker. For all other experiments, degradable (CVPLS-LYSGC peptide) crosslinker was used. Hydrogels were formed by photopolymerizing with 0.05 wt% Irgacure 2959 for 8 min with 365 nm light (6 mW cm^{-2}).

Table 7.1. Hydrogel formulations

Experiment	Name	8arm PEG MW	wt%	thiol:norbornene
1-d diffusion	high crosslinking	10,000	15	1:1
1-d degradation	high Φ^e	10,000	15	1:1
1-d degradation	intermediate Φ^e	20,000	10	0.8:1
1-d degradation	low Φ^e	20,000	5	0.5:1
3-d hydrogels	high crosslinking	10,000	15	1:1
3-d hydrogels	low crosslinking	20,000	5	0.9:1

To characterize hydrogels (lacking microspheres) in order to estimate $\mathcal{D}_r$ and thereby calculate ϕ^e for each hydrogel formulation, thin cylindrical discs were formed between two glass slides (8 mm diameter x 1 mm height) and swelled in PBS-antis overnight at 37 °C. Shear modulus was determined on an ARES Rheometer (TA Instruments, New Castle, DE) with parallel plate geometry that can apply varying strain and frequency. Both strain and frequency sweeps were conducted to validate that measurements were in the linear viscoelastic regime, and shear modulus was measured at 10% strain and 1 rad sec^{-1}. *Q* is the hydrogel volumetric swelling ratio, which is the swollen hydrogel volume divided by dry hydrogel volume. This was calculated from the swollen and lyophilized hydrogel masses, M_s and M_d, respectively, using the polymer density ρ_p (1.07 g ml^{-1}) and solvent density ρ_s (1 g ml^{-1}):

$$Q = 1 + \frac{\rho_p}{\rho_s}\left(\frac{M_s}{M_d} - 1\right) \quad (2)$$

Hydrogel crosslink density ρ_x, which must be known in order to estimate the mesh size and $\mathcal{D}_r$, was calculated from swelling ratio Q and the shear modulus G using rubber elasticity theory [38]. The relationship between crosslink density and the number of bonds between crosslinks n (where PEG has 3 bonds per repeat unit) was used to estimate the mesh size ξ [3,38–40]:

$$\rho_x = \frac{GQ^{1/3}}{RT} = \frac{3\rho_p}{nM_r} \quad (3)$$

$$\xi = Q^{1/3} L C_n^{1/2} n^{1/2} \quad (4)$$

Where C_n is the polymer characteristic ratio, L is the average bond length, and M_r is the molecular weight of one PEG repeat unit (Table 7.2) [3]. R is the gas constant and T is temperature in Kelvin. Enzyme diffusivity $\mathcal{D}_r$ depends on multiple parameters including ξ, the enzyme radius of gyration r_e, and the free diffusivity of enzyme in water $\mathcal{D}_\infty$, where $\mathcal{D}_\infty$ is calculated as:

$$\mathcal{D}_\infty = \frac{k_B T}{6\pi r_e \overline{\mu_f}} \quad (5)$$

k_B is the Boltzmann constant (1.38×10^{-23} J K^{-1}), and $\overline{\mu_f}$ is the solvent viscosity. Here we used 0.000692 kg m^{-1} s^{-1} for the viscosity of water at 37 °C [41]. When enzyme diffusion is restricted by a crosslinked hydrogel, the following equation is used for $\mathcal{D}_r$ [42]:

$$\mathcal{D}_r = \mathcal{D}_\infty \left(1 - \frac{r_e}{\xi}\right) \exp\left(\frac{-Y}{Q-1}\right) \quad (6)$$

In this equation, Y is a parameter relating the critical volume for solute translation to the average free volume per molecule, which is reasonably approximated as 1 [42,43]. Therefore, the restricted diffusivity $\mathcal{D}_r$ for an enzyme of known radius r_e in hydrogels with varying swelling ratio Q and mesh size ξ can be determined, and used to calculate ϕ^e (equation 1).

Table 7.2. Model constants used for PEG hydrogel [3]

Parameter	variable	value	unit
Characteristic ratio	C_n	4	
Average bond length	L	1.47	Å
MW of PEG repeat unit	M_r	44	Da
Polymer density	ρ_p	1.07	g/ml

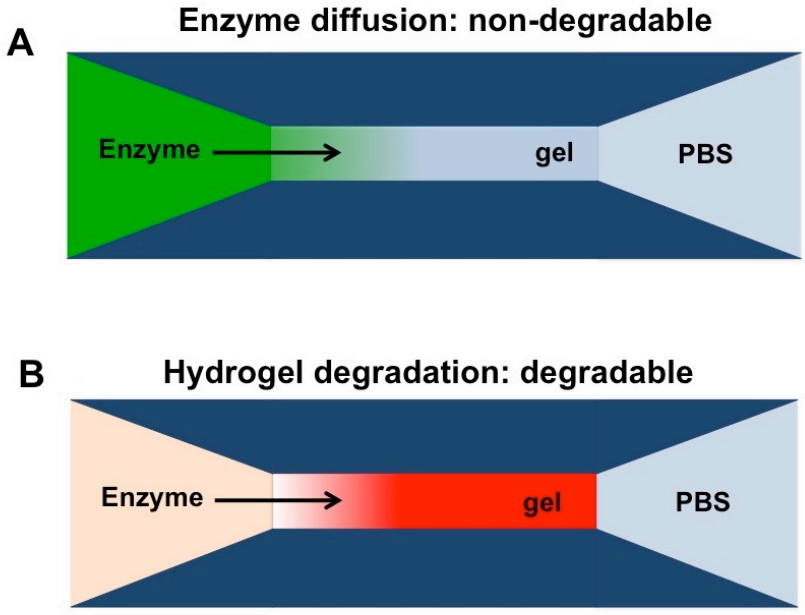

Figure 7.2 (A) Schematic of 1-dimensional diffusion experiment. A 1 mm-thick rectangular PEG hydrogel between two glass slides is exposed to PBS from one side and fluorescein-collagenase type II (0.25 mg ml^{-1}) from the opposite side. The hydrogel is non-degradable. (B) Schematic of 1-dimensional degradation experiments. A 1 mm-thick rectangular PEG hydrogel between two glass slides is exposed to PBS from one side and collagenase type II from the opposite side. Degradable PEG hydrogels are fluorescently labeled.

7.3.7 1-dimensional experiments

Enzyme diffusion and hydrogel degradation were observed in a 1-dimensional system (Fig. 7.2). Rectangular hydrogels (5 x 25 mm) were photopolymerized between glass slides in a 1 mm-thick silicone mold with two solution reservoirs. Reservoirs were filled with PBS-antis to swell overnight, after which collagenase type II was added to one reservoir. Hydrogels were maintained at 37 °C. To observe enzyme diffusion in a non-degradable hydrogel (Fig. 7.2A), fluorescein-collagenase was added to the enzyme reservoir at 0.25 mg ml^{-1} and replenished at each time point. Fluorescence images were acquired on the BioRad VersaDoc 4000 MP and fluorescent intensity profiles versus distance were analyzed using ImageJ software.

To observed hydrogel degradation in the 1-dimensional system (Fig. 7.2B), hydrogels were fluorescently labeled by adding 0.01 mM thiol-reactive AlexaFluor-546 C5 maleimide to the

macromer solution before polymerization. Three collagenase type II concentrations were used: 25 ng ml^{-1} for low ϕ^e, 200 ng ml^{-1} for intermediate ϕ^e, and 1000 ng ml^{-1} for high ϕ^e, and enzyme was replenished daily.

7.3.8 3-dimensional microsphere experiments

Hydrogel degradation by encapsulated collagenase-laden microspheres was examined visually and quantitatively. Collagenase type II and BSA microspheres were mixed with macromer (Table 7.1) and 0.01 mM AlexaFluor-546 C5 maleimide at 25 mg ml^{-1} and photopolymerized into cylindrical constructs (5 mm diameter, 1 mm height). Fluorescein-collagenase microspheres were entrapped into fluorescent hydrogels at 50 mg ml^{-1}. Images were acquired starting immediately after polymerization using a confocal laser-scanning microscope (CLSM, Zeiss LSM 510, Thornwood, NY) at 100x magnification. ImageJ software was used to quantitatively assess degradation. For the high crosslink density hydrogels, microsphere void space diameters were measured (n = 800-1300 measurements per time point), and the non-parametric Kolmogorov-Smirnov test was used to determine whether microsphere size distributions changed after 7 days (α = 0.05). For the low crosslink density hydrogels, total fluorescence was measured over time (n = 24 images per time point).

Wet weight and compressive modulus were measured for microsphere-laden hydrogels. Collagenase or BSA microspheres were mixed with macromer at 25 mg ml^{-1} and photopolymerized into cylindrical constructs (5 mm diameter x 5 mm height). Measurements were taken starting immediately after polymerization. Hydrogels were assessed for wet weight and compressive modulus up to 100 h (n = 3-4), replacing PBS-antis daily. Hydrogels were compressed to 15% strain at a strain rate of 0.5 mm min^{-1} to obtain stress-strain curves (MTS Synergie 100, 10N). The compressive modulus was estimated as the slope of the linear region of stress-strain curves.

7.3.9 Computational modeling

A multiphasic finite element model was previously developed [27,28,44] to describe hydrogel degradation and its effects on hydrogel properties such as crosslinking density and mesh size, which can vary in both space and time, depending on the characteristics and type of degradation. The model predicts enzyme transport in degrading hydrogels and the effects on local degradation kinetics. Using the experimentally determined initial hydrogel properties (derived from measurements for Q and G), the model was fit to experimental data for the 1-dimensional diffusion experiment in order to estimate the enzyme radius of gyration r_e. This value was subsequently used to fit the model to the 1-dimensional degradation experiments in order to calculate k_{cat} and K_M for the specific enzyme-substrate pair, using the experimentally estimated values (Figure 7.S1) as an initial guess.

7.4 Results and Discussion

Reaction- and diffusion-dominated degradation of enzymatically sensitive 8-arm PEG hydrogels were characterized quantitatively and qualitatively with the goal of better defining scaffold design parameters for cell-laden enzymatically degradable hydrogels for use in tissue engineering. While cell-mediated scaffold degradation provides the opportunity to spatially and temporally control degradation, this mode of degradation is complex, necessitating characterization with a combined experimental-computational approach. In order to understand how hydrogel structure affects degradation, the degradation front was first characterized in a simple 1-dimensional system. In an attempt to understand cell-mediated degradation in 3 dimensions, but in the absence of matrix deposition, PLGA microspheres were loaded with collagenase type II enzyme, serving as a model for enzyme-secreting cells. These microspheres were embedded into enzymatically degradable hydrogels with the peptide crosslinker CVPLS-LYSGC, where hydrogel formulation and thereby crosslink density were varied to assess the effect on degradation characteristics. It was determined that the high crosslink density hydrogels resulted in reaction-dominated degradation, and the low crosslink density hydrogels supported diffusion-dominated degradation, which was predicted by the

computational model. By connecting these qualitative observations to the dimensionless parameter ϕ^e, our findings can be applied universally to cell-mediated degradable hydrogels with knowledge of several variables that can be easily measured or estimated.

7.4.1 Collagenase diffusivity within hydrogels

Diffusion of fluorescently labeled collagenase through a highly crosslinked, but non-degrading hydrogel was monitored using the set-up described in (Fig. 7.2A) and assumed to represent 1-dimensional diffusion. Diffusion of collagenase was monitored up to 148 hours (Fig. 7.3). Fluorescence measurements were normalized to concentration and plotted as a function of time. The computational model was used to fit the data to estimate collagenase diffusivity within this crosslinked hydrogel (Fig. 7.3B), as well as determine the average enzyme radius of gyration (Fig. 7.3C).

This system used a bacterially-derived collagenase type II enzyme that degrades collagens I-III [29], which was characterized for kinetic parameters and average MW (Fig. 7.S1) in order to universally apply the observed results. While we chose to use this enzyme as a model system, it provides an effective example of enzymatic degradation of hydrogels with peptide crosslinks, therefore the overall conclusions can be applied to different systems if the enzyme kinetics are known. Because collagenase type II is not a single enzyme but a mixture of several of different sizes, we made a simplification by measuring an average or 'overall' enzyme radius of gyration. By comparing the experimental diffusion data to the computed model, the discrepancies in the curves can be explained by the fact that some population of the enzyme has a radius > 65 Å, which would exhibit more restricted diffusion, and some population has a radius < 65 Å, which would more easily diffuse. However, the model was a good fit for the experimental data, and the resulting estimates for ϕ^e made sense when plotted against the ξ/r_e ratio, supporting the robustness of the presented observations.

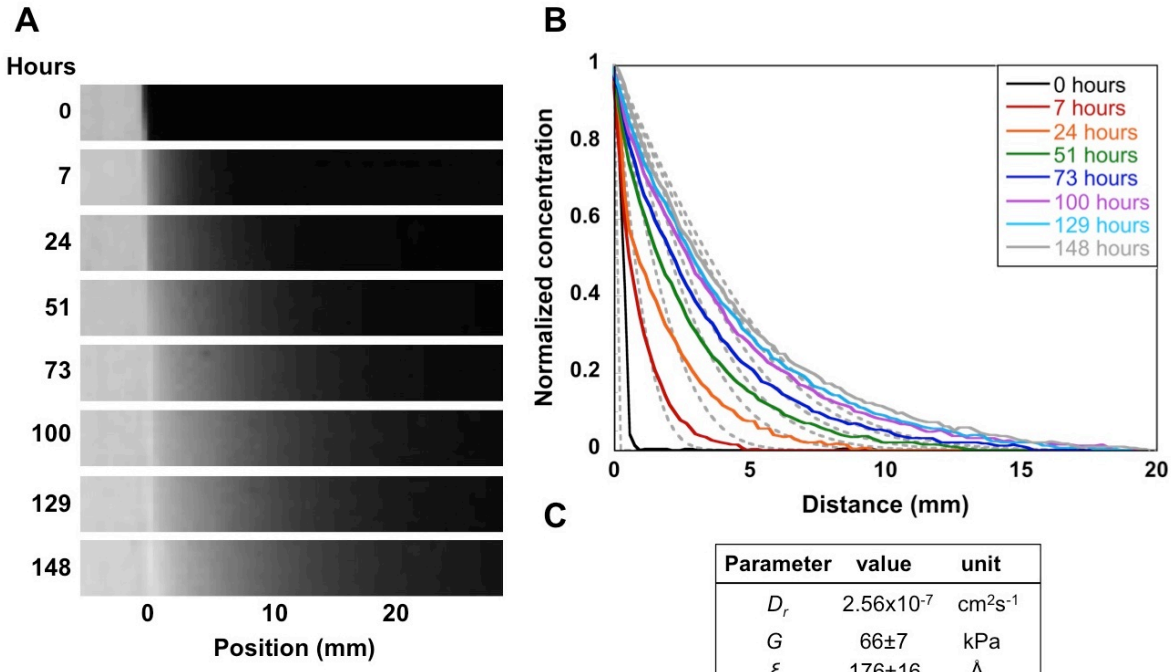

Figure 7.3 (A) Fluorescent images of enzyme infiltration into the PEG hydrogel with time. (B) Experimental data for enzyme concentration versus distance (profiles shown in color), fitted to the diffusion equation (model plots shown as gray dashed lines). (C) Table of the hydrogel properties: G (shear modulus) and ξ (mesh size); and parameters calculated from the diffusion model: $\mathcal{D}_r$ (enzyme diffusivity) and r_e (enzyme radius of gyration).

7.4.2 The hydrogel degradation front

Degradable hydrogels formed at three different crosslink densities were fluorescently labeled and degradation was monitored using the set-up shown in Fig. 2B, and assumed to represent 1-dimensional diffusion. The three hydrogel formulations were assessed for their initial properties in order to estimate ϕ^e (Fig. 7.4A), and to apply the computational model to predict the evolving degradation front (Fig. 7.4B). The degradation front describes the changing hydrogel crosslink density as a function of distance emanating from an enzyme source. The model predictions were compared to experimental data (Fig. 7.4C) determined from monitoring hydrogel fluorescence up to 148 h (Fig. 7.4D). Fluorescence measurements were normalized to the initial fluorescence (directly related to the initial crosslink density) and plotted versus

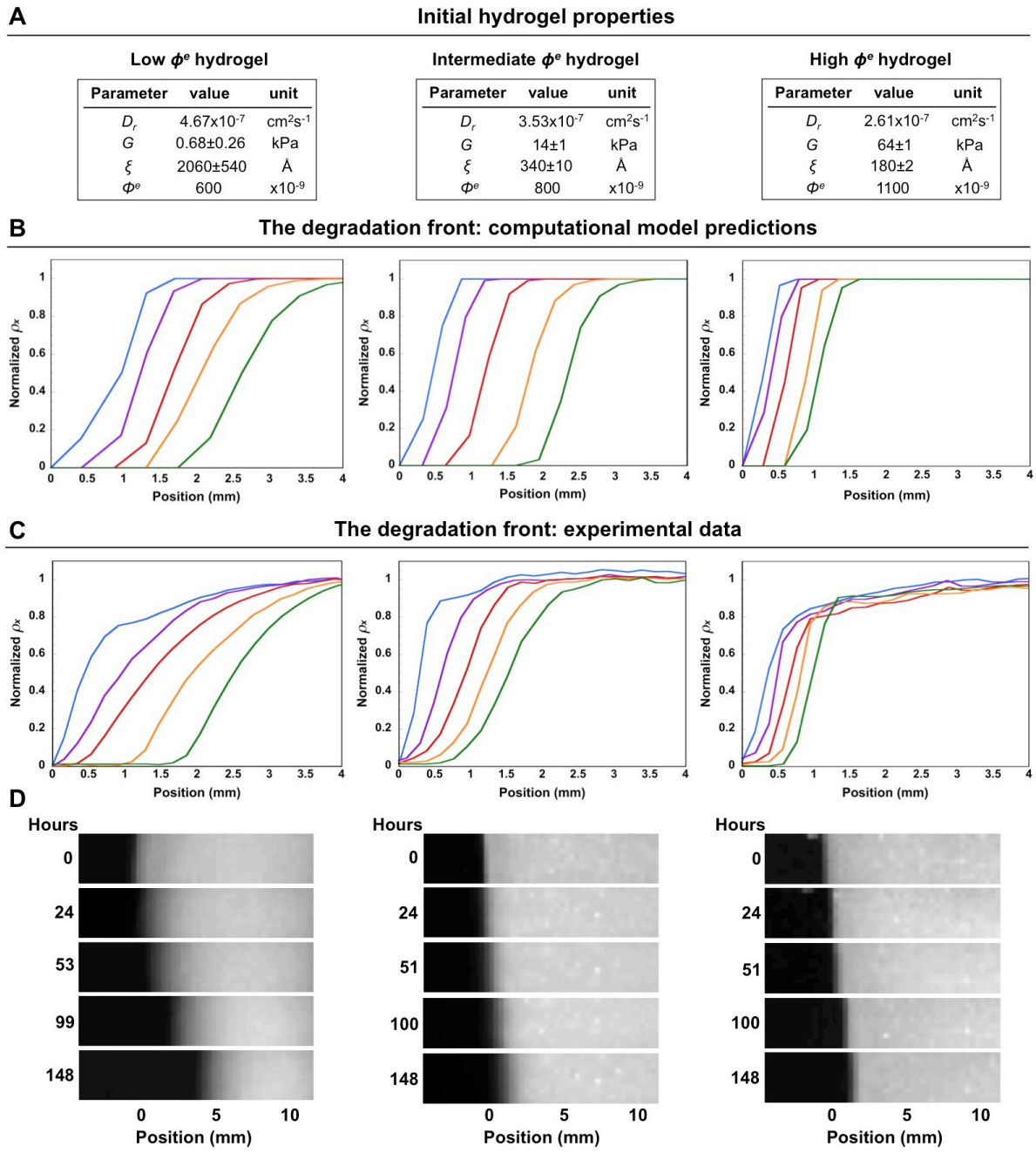

Figure 7.4 (A) Initial parameters for three distinct degradable hydrogel formulations: $\mathcal{D}_r$ (restricted enzyme diffusivity), G (shear modulus), ξ (mesh size), and ϕ^e. (B) Degradation fronts predicted by the computational model for three hydrogel formulations exposed to varied collagenase type II concentrations: Low ϕ^e hydrogel (25 ng ml^{-1} collagenase type II), intermediate ϕ^e hydrogel (200 ng ml^{-1}collagenase type II), and high ϕ^e hydrogel (1000 ng ml^{-1} collagenase type II) Time points for each degradation profile (0, 24, 51, 100, and 148 h) progress from left to right. (C) Experimentally determined data for hydrogel degradation fronts, and (D) fluorescent images of PEG hydrogel degradation with time. Experimental data are shown as plots for normalized crosslink density ρ_x versus distance. Each profile is the average of three traces of fluorescence vs. distance (ImageJ).

distance to represent the degradation front. The model qualitatively predicted the experimental results, where the discrepancies are attributed to system non-idealities and assumptions (for example, modeling the enzyme as one distinct size, when it is in fact polydisperse). From the 1-dimensional degradation experiments, the computational model was able to fit values of k_{cat} and K_M, which were close to the original estimates at 0.71 s^{-1} and 19 μM, respectively (Fig. 7.S1). The ability to determine kinetic parameters specific to this system's enzyme-substrate pair from a simple 1-dimensional degradation experiment further reveals the power of the computational model, making more expensive kinetic characterizations (such as those using custom FRET-labeled peptides) unnecessary.

Plots for low, high, and intermediate ϕ^e are shown demonstrating a diffusion-dominated system, a reaction-dominated system, and an intermediate system, respectively. The parameter ϕ^e varied as a function of diffusivity, which depends on the hydrogel crosslink density and mesh size. In order to generalize these qualitative observations to any hydrogel formulation, equation (6) was simplified to remove the exponential term, permitting $\mathcal{D}_r$ to be expressed in terms of mesh size ξ as the only variable, which was used to plot the theoretical ϕ^e versus mesh size (Fig. 7.5). The mesh size ξ normalized to the enzyme size r_e is a crucial parameter affecting ϕ^e, as demonstrated in Fig. 7.5A. The three calculated ϕ^e values that match the different degradation fronts are plotted with the curve, making it clear that there are two distinct regimes, marked with gray boxes, that lead to either reaction- or diffusion-dominated degradation. Because ϕ^e values also vary with k_{cat}, and only one degradable system was used in this study, the effect of varying k_{cat} is shown in Fig. 7.5B. When k_{cat} is small, ξ/r_e must also be small in order to achieve reaction-dominated degradation. When k_{cat} is large, ξ/r_e can be larger and still achieve reaction-dominated degradation because the enzyme reaction rate is very fast.

Three hydrogel formulations were investigated within a range of shear moduli that span a range of tissue engineering applications, which also spanned diffusion-dominated and

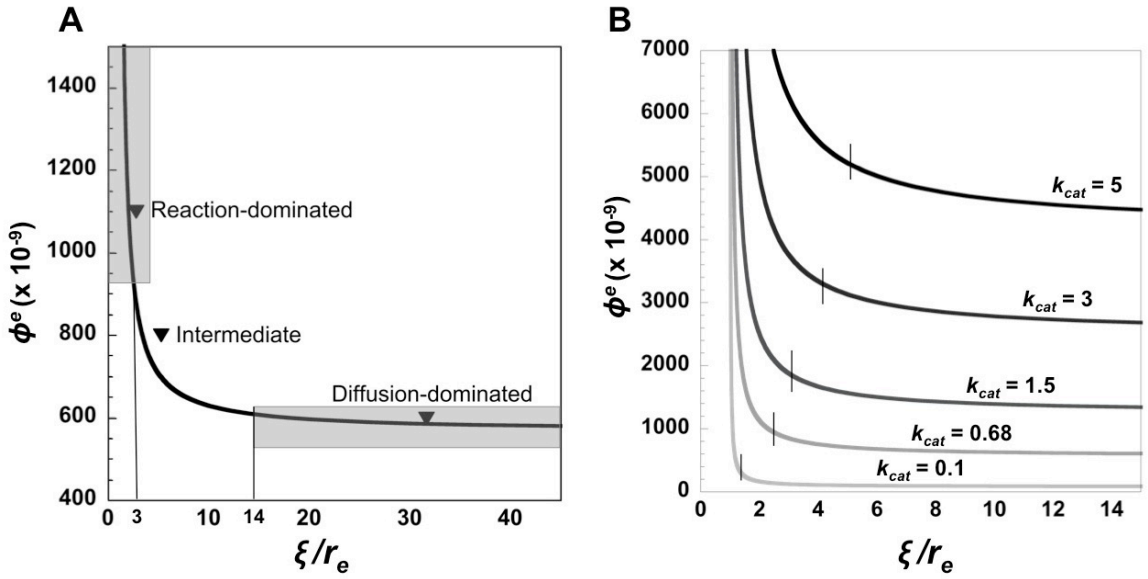

Figure 7.5 (A) ϕ^e plotted versus the ratio between mesh size and enzyme radius of gyration, ξ/r_e, for the collagenase type II-degradable system. The calculated ϕ^e for each of the three degradation front experiments (Fig. 4) are plotted (triangles). Gray areas shade the plot regions that are considered either reaction- or diffusion-dominated, based on experimental observations. (B) ϕ^e plotted versus the ratio between mesh size and enzyme radius of gyration, ξ/r_e, for k_{cat} values between 0.1 and 5 s^{-1}. Markings on the plots indicate the 'cutoff' points where the tangent slope is equivalent to the slope at ξ/r_e = 3 from (A).

reaction-dominated degradation characteristics. Diffusion-dominated degradation is characterized by enzyme diffusing easily through a hydrogel with large mesh size, so that degradation occurs in bulk. The free diffusivity (not through a hydrogel) of collagenase type II in water was calculated as 5.06 x 10^{-7} cm^2 s^{-1}, and diffusivity in the low crosslink density hydrogel was 4.67 x 10^{-7} cm^2 s^{-1}, therefore it is not surprising that enzyme diffusion was minimally restricted in these hydrogels. Reaction-dominated degradation is characterized by restricted enzyme diffusion, where the network must be degraded before the enzyme can diffuse further into the material. While the degradation front was much sharper in high crosslink density hydrogels, the mesh size was still almost three times the size of the enzyme.

A ϕ^e value was calculated for each hydrogel, providing a quantitative means to evaluate qualitative observations of the degradation front. If diffusivity is at its maximum unrestricted

value of 5.06 x 10^{-7} cm^2 s^{-1}, ϕ^e is 565 x 10^{-9}, which is close to the low ϕ^e hydrogel at 600 x 10^{-9}. The high ϕ^e hydrogel was not as close to an estimated upper limit, calculated as 8000 x 10^{-9} when the mesh size is 70 Å (compared to 65 Å enzyme radius of gyration). For tissue engineering purposes, it is not practical to create materials with such a high ϕ^e value because dramatic restriction of enzyme diffusion will also limit nutrient and matrix diffusion, which can be detrimental for tissue engineering outcomes [45–47]. However, it was promising that reaction-dominated degradation characteristics were observed in a system where the mesh size was several times larger than the enzyme, which is expected to also allow nutrient diffusion.

We extended the applicability of observations within our model system by investigating how varying k_{cat} values, which describe the enzyme rate constant, affect ϕ^e. While only one enzyme-peptide pair was used in these studies with one specific k_{cat} value, others have investigated the effects of varying degradation kinetics [26], where higher k_{cat} values resulted in faster-degrading hydrogels. Plots of theoretical ϕ^e versus ξ/r_e for varying k_{cat} values within a range of reported values for MMPs [22,26,48] were generated, showing that the 'cutoff' value for ξ/r_e depended on k_{cat}, where reaction-dominated degradation should be possible in a hydrogel where the mesh size is 5x or more the size of the enzyme when the enzyme rate constant sufficiently high. This may prove important when designing enzymatically degradable hydrogels for a specific tissue engineering application – for example if a low modulus, loosely crosslinked network is desirable, but localized reaction-dominated degradation is also required, this scenario is possible to achieve if enzyme kinetic rates can be engineered to be very high.

7.4.3 3D hydrogel degradation with collagenase microspheres

Collagenase-laden PLGA microspheres release enzyme over time, simulating the release of enzyme from cells. Microspheres were embedded in fluorescently labeled hydrogels of high and low crosslink density, and degradation was visually monitored, compared to BSA-laden microspheres in a high crosslink density hydrogel (Fig. 7.6, 7.7). Degradation was locally restricted in high crosslink density hydrogels (reaction-dominated), whereas it was more bulk in

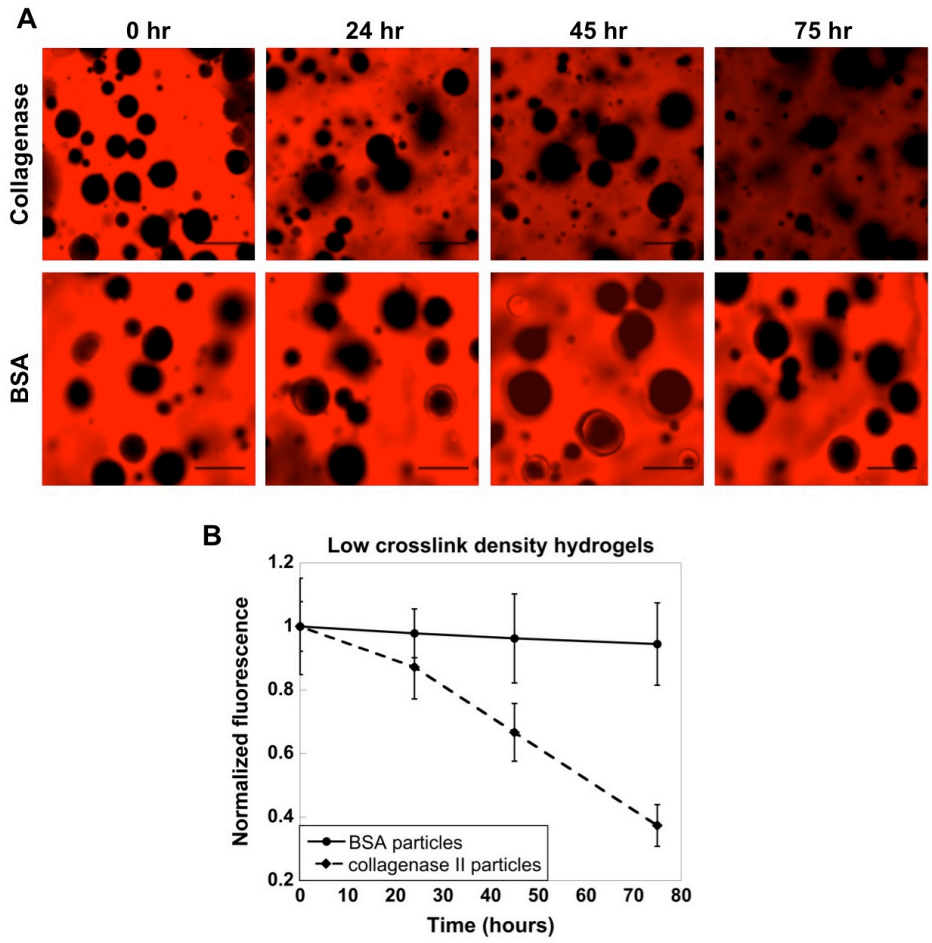

Figure 7.6 (A) Representative images of fluorescently labeled (red) degradable PEG hydrogels with entrapped collagenase II microspheres in low crosslink density hydrogels, or BSA microspheres in high crosslink density hydrogels, between 0 and 75 hours after hydrogel formation. Scale bars are 200 μm. (B) Average overall image fluorescence as a function of time. Error bars are standard deviation for n = 24 images per condition.

lower crosslink density hydrogels (diffusion-dominated). Total fluorescence was measured for each image over time for the low crosslink density hydrogels (Fig. 7.6) and decreased steadily with time. To assess localized degradation, the diameter of microsphere void spaces was measured initially after formation and after 7 days of degradation (Fig. 7.7), revealing that the size of void spaces increased significantly with time ($p < 0.000001$) due to localized degradation with collagenase microspheres.

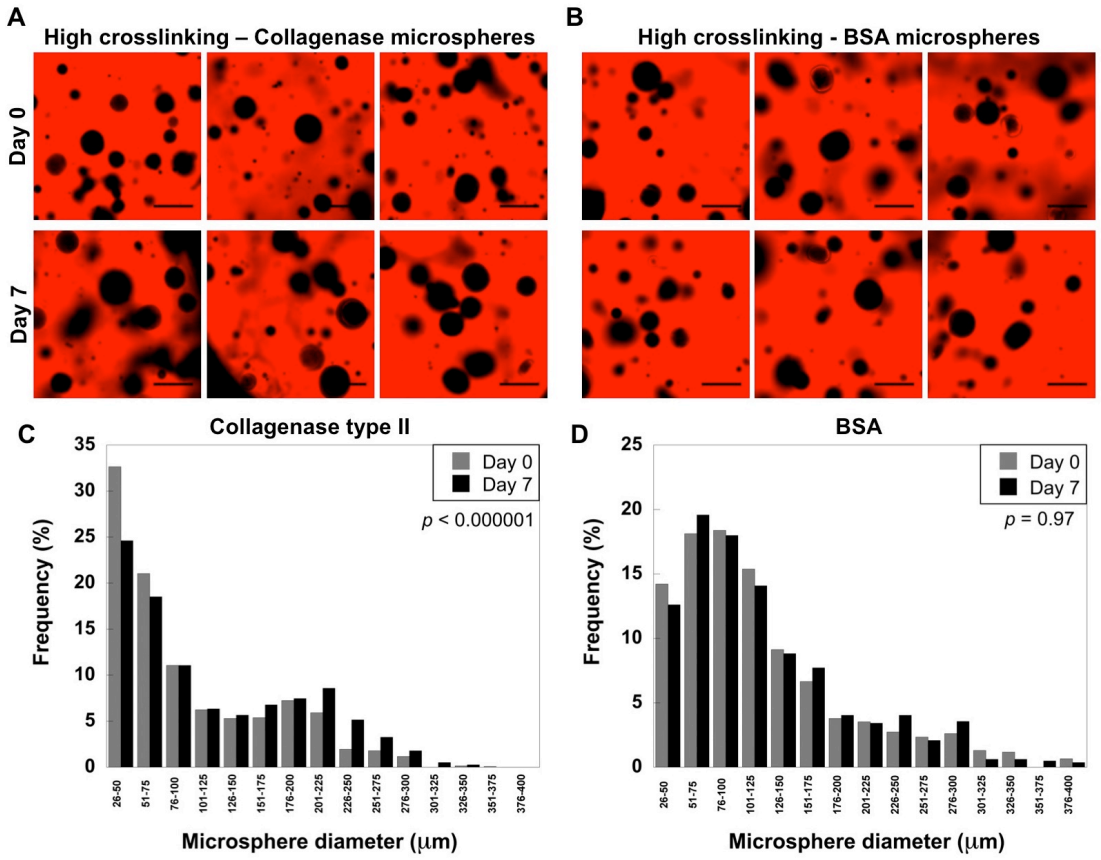

Figure 7.7 Representative images of fluorescently labeled (red) degradable high crosslink density PEG hydrogels with entrapped (A) collagenase microspheres or (B) BSA microspheres at days 0 and 7. Three images are shown for each time point. Scale bars are 200 μm. Microsphere void space diameter distributions for (C) collagenase microspheres or (D) BSA microspheres at days 0 and 7. The *p*-value for the probability that distributions were the same at days 0 and 7 are shown on the plots. Distributions were determined from n = 800-1300 diameter measurements per time point.

Collagenase type II was fluorescently labeled and incorporated into microspheres in order to observe the release and distribution of enzyme in the different crosslink density hydrogels. Release of fluorescently-labeled collagenase from microspheres within fluorescently labeled hydrogels that were degrading was monitored over time in low (Fig. 7.8) and high (Fig. 7.9) crosslink density hydrogels, revealing that collagenase type II was diffusely distributed throughout the low crosslink density hydrogels from hours 9-21, and that it required longer times (45-72 h) to become diffusely distributed in high crosslink density hydrogels, supporting that enzyme diffusivity is elevated in low crosslink density hydrogels. This also might suggest that a

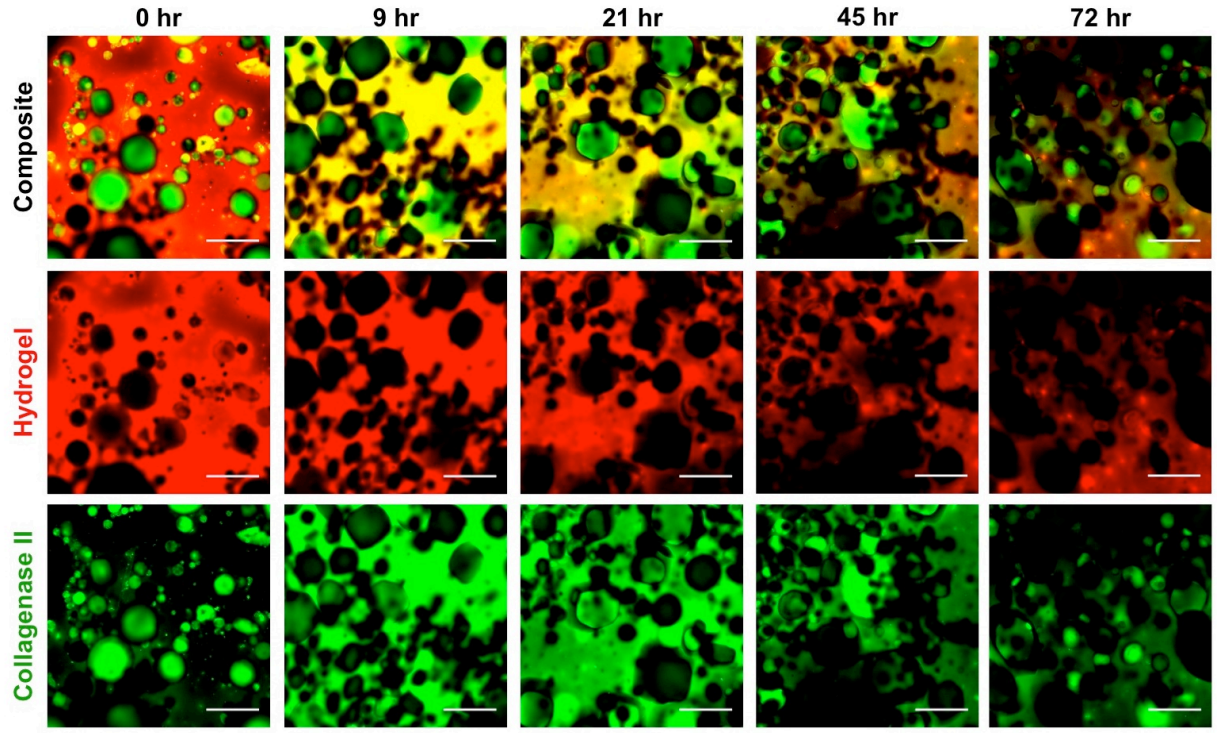

Figure 7.8 Representative images of fluorescently labeled (red) degradable PEG hydrogels with entrapped fluorescein-collagenase type II (green) microspheres in high crosslink density hydrogels, between 0 and 72 hours after hydrogel formation. Scale bars are 200 μm.

threshold concentration of enzyme is necessary to cleave the substrate, because the enzyme was observed throughout the hydrogel even though degradation was most pronounced surrounding the microspheres in the high crosslink density hydrogels. This supports the previous discussion on the effects of k_{cat}, where when k_{cat} is high, enzyme concentration can be lower and still maintain a high rate of reaction.

Bulk properties of degrading hydrogels with enzyme-secreting microspheres were measured in order to compare the macroscopic effects of reaction- versus diffusion-dominated degradation. Enzyme release from the microspheres was characterized by a rapid burst release followed by slow yet steady sustained release of enzyme (Fig. 7.10A), which is consistently observed for PLGA microspheres [49]. Nonetheless, the degradation profiles in the different hydrogels were distinct, and cells, which the microspheres are intended to model, are complex

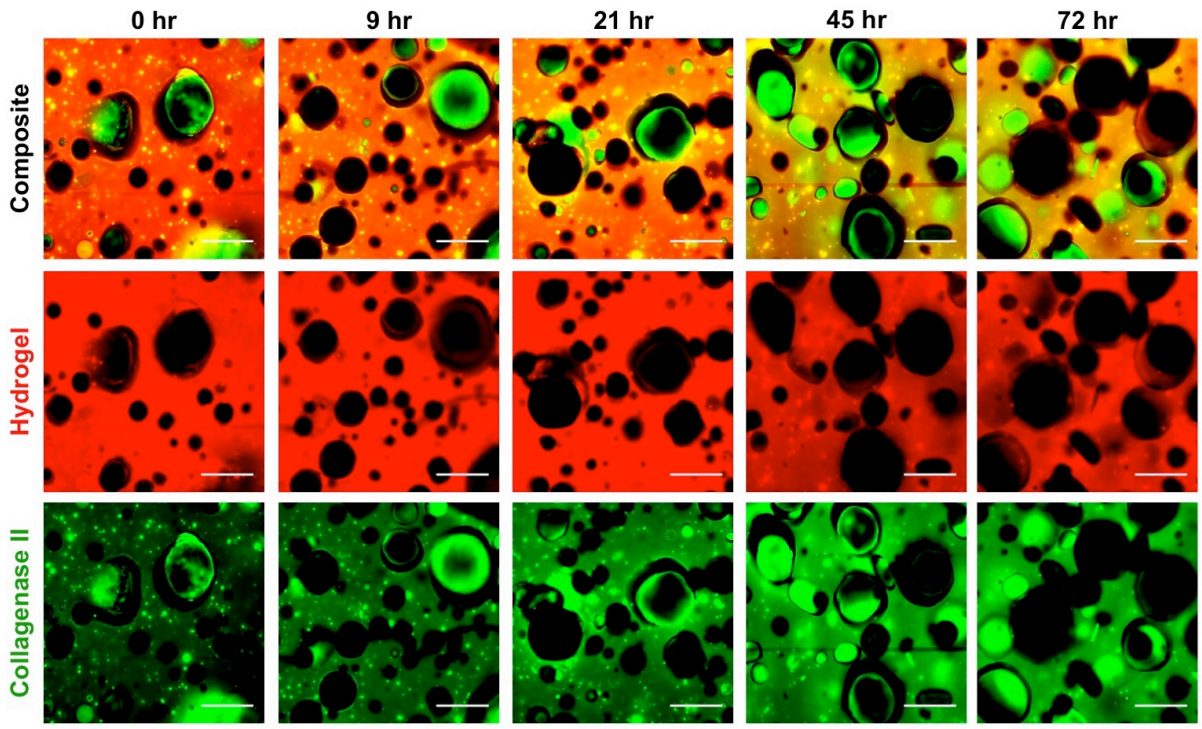

Figure 7.9 Representative images of fluorescently labeled (red) degradable PEG hydrogels with entrapped fluorescein-collagenase type II (green) microspheres in low crosslink density hydrogels, between 0 and 72 hours after hydrogel formation. Scale bars are 200 μm.

and unlikely to produce enzyme at a steady and consistent rate. Normalized compressive modulus (Fig. 7.10B, C) and wet weight (Fig 7.10D, E) were measured over time for low and high crosslink density hydrogels with collagenase type II or BSA loaded microspheres. In a low crosslink density, diffusion-dominated system with collagenase microspheres, hydrogels swelled considerably and dropped rapidly in compressive modulus, which is characteristic of bulk degrading hydrogels [12]. In comparison, the high crosslink density, reaction-dominated system was characterized by little swelling and a slower, steady drop in modulus, which we believe is unique to localized degradation. A 50% drop in compressive modulus was observed for BSA-laden microspheres in low crosslink density hydrogels, which may be attributed to the surface erosion of PLGA particles. These microspheres are rigid, therefore may contribute to overall scaffold mechanics when encapsulated within hydrogels, however as they erode void spaces

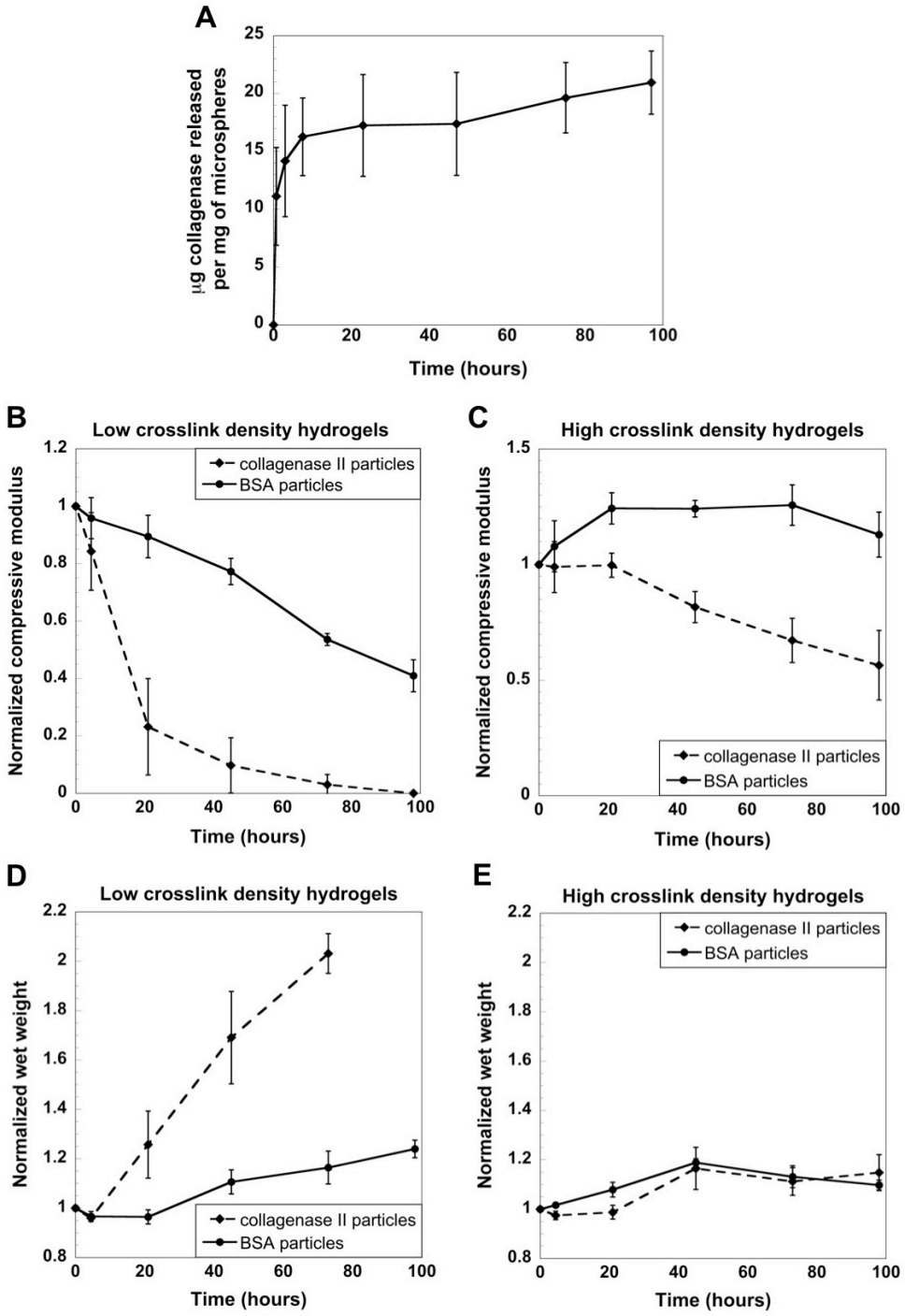

Figure 7.10 (A) Average enzyme release over time from collagenase II microspheres in PBS. Error bars are standard deviation for *n* = 3 sample replicates. (B, D) Average compressive modulus or (C, E) wet weight normalized to initial values measured immediately after hydrogel formation for (B, C) low or (D, E) high crosslink density hydrogels with entrapped collagenase II or BSA microspheres. Error bars are standard deviation for *n* = 3-4 hydrogel replicates.

are created which will weaken the overall hydrogel. This phenomenon would be more pronounced in a more loosely crosslinked hydrogel. The difference between BSA particles and collagenase particles was still dramatic suggesting the change in modulus was dominated by enzymatic degradation.

Overall, we demonstrated a system that models cell-mediated enzymatic degradation so that hydrogel degradation could be characterized without the complication of cells producing matrix. Within a collagenase type II-degraded system, it was shown that either reaction- or diffusion-dominated degradation could be controlled by the hydrogel properties, and by relating observations to dimensionless parameters and validating the use of the computational model, these results could have wide applicability. A limitation of the presented work is that it is a very simplified model of enzyme release from cells, where cellular release of enzyme and regulation of enzyme activity are very complex processes. Most enzymes are regulated by Tissue Inhibitors of MetalloProteinases (TIMPs), a family of protein inhibitors for MMPs [50–53] that have also shown ability to inhibit other enzyme types such as aggrecanases [54,55]. These proteins are released by cells in order to regulate local extracellular enzyme activity, however the mechanisms that determine their release are still unclear, necessitating future work to explore how TIMPs may affect cell-mediated hydrogel degradation.

7.5 Conclusions

A model experimental system was developed in order to investigate cell-mediated enzymatic hydrogel degradation within an acellular system in order to characterize the parameters that affect hydrogel degradation. The purpose was to elucidate the key parameters that determine whether degradation is reaction- or diffusion-dominated, so that scaffolds can be carefully and rationally designed for a wide variety of tissue engineering applications. The dimensionless parameter ϕ^e relates the enzyme reaction rate to diffusion rate within porous networks, and it was identified that the network mesh size, and its ratio to the enzyme radius of gyration, is possibly the most important parameter determining reaction-or diffusion-dominated

degradation. By comparing theoretical relationships and computational models to experimental measurements and qualitative observations, we have established an important link between ϕ^e and the degradation characteristics, and generalized these observations to systems with different mesh sizes and kinetic parameters. The ultimate aim is to assist experimentalists in rationally using the tools available to them: scaffold and peptide design primarily, in order to engineer the degradation characteristics required to engineer a variety of tissues using encapsulated cells.

7.6 Acknowledgements

This research was supported by NIH grant # 1R01AR065441 and # R21AR061011, a fellowship from the National Science Foundation Graduate Research Fellowship Program (NSF GRFP), a National Institute of Health (NIH) Pharmaceutical Biotechnology Training Grant, and a Chancellor's Fellowship from the University of Colorado. The authors would like to thank Umut Akalp and Dr. Franck Vernerey for their assistance in conducting the computational modeling and for co-authoring the manuscript.

7.7 Supplementary Figures

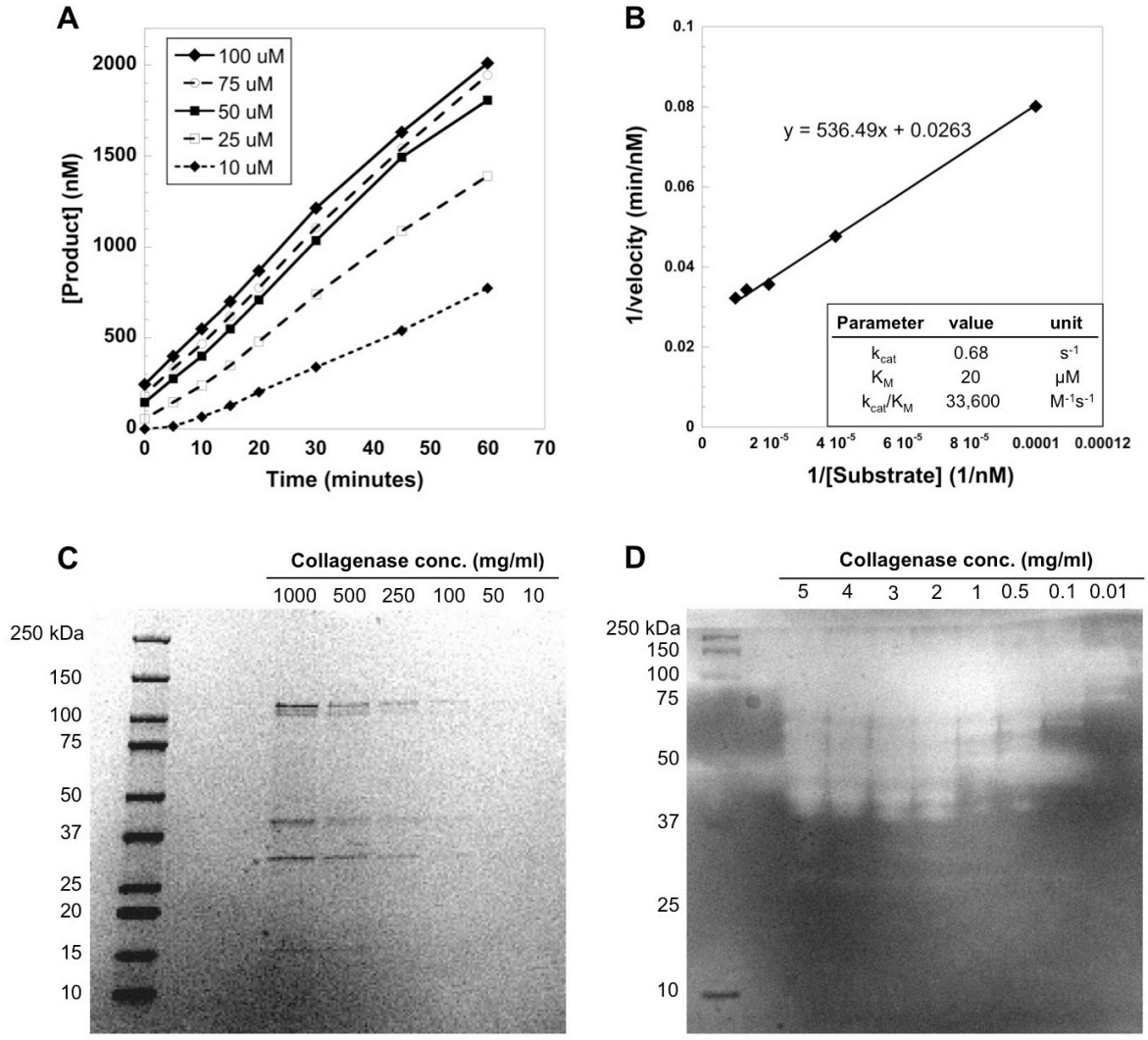

Figure 7.S1 (A) Rates of cleavage of an MMP-specific FRET substrate by collagenase II with different substrate concentrations from 10 to 100 µM. (B) Lineweaver-Burk plot of reciprocal-reaction velocity versus reciprocal-substrate concentration in order to estimate Michaelis-Menten kinetic parameters (shown on plot). (C) Polyacrylamide gel electrophoresis and Coomassie protein stain of various collagenase II concentrations. (D) Gelatin zymogram with Coomassie protein stain of various collagenase type II concentrations.

7.8 References

[1] Nicodemus GD, Bryant SJ. Cell encapsulation in biodegradable hydrogels for tissue engineering applications. Tissue Eng Part B-Reviews 2008;14:149–65.

[2] Slaughter B V, Khurshid SS, Fisher OZ, Khademhosseini A, Peppas NA. Hydrogels in regenerative medicine. Adv Mater 2009;21:3307–29.

[3] Bryant SJ, Anseth KS. Photopolymerization of Hydrogel Scaffolds. In: Ma PX, Elisseeff JH, editors. Scaffolding Tissue Eng., Boca Raton, FL: CRC Press, Inc.; 2006, p. 71–90.

[4] Ifkovits JL, Burdick JA. Review: photopolymerizable and degradable biomaterials for tissue engineering applications. Tissue Eng 2007;13:2369–85.

[5] Anseth KS, Kloxin AM, Kloxin CJ, Bowman CN. Mechanical Properties of Cellularly Responsive Hydrogels and Their Experimental Determination. Adv Mater 2010;22:3484–94.

[6] Lynn AD, Blakney AK, Kyriakides TR, Bryant SJ. Temporal progression of the host response to implanted poly(ethylene glycol)-based hydrogels. J Biomed Mater Res Part A 2011;96A:621–31.

[7] Nicodemus GD, Skaalure SC, Bryant SJ. Gel structure has an impact on pericellular and extracellular matrix deposition, which subsequently alters metabolic activities in chondrocyte-laden PEG hydrogels. Acta Biomater 2011;7:492–504.

[8] Benoit DSW, Durney AR, Anseth KS. Manipulations in Hydrogel Degradation Behavior Enhance Osteoblast Function and Mineralized Tissue Formation. Tissue Eng 2006;12:1663–73.

[9] Mahoney MJ, Anseth KS. Three-dimensional growth and function of neural tissue in degradable polyethylene glycol hydrogels. Biomaterials 2006;27:2265–74.

[10] Roberts JJ, Nicodemus GD, Greenwald EC, Bryant SJ. Degradation Improves Tissue Formation in (Un)Loaded Chondrocyte-laden Hydrogels. Clin Orthop Relat Res 2011.

[11] Anseth KS, Bryant SJ. Controlling the spatial distribution of ECM components in degradable PEG hydrogels for tissue engineering cartilage. J Biomed Mater Res Part A 2003;64A:70–9.

[12] Anseth KS, Metters AT, Bryant SJ, Martens PJ, Elisseeff JH, Bowman CN. In situ forming degradable networks and their application in tissue engineering and drug delivery. J Control Release 2002;78:199–209.

[13] Bryant SJ, Davis-Arehart KA, Luo N, Shoemaker RK, Arthur JA, Anseth KS. Synthesis and Characterization of Photopolymerized Multifunctional Hydrogels: Water-Soluble Poly(Vinyl Alcohol) and Chondroitin Sulfate Macromers for Chondrocyte Encapsulation. Macromolecules 2004;37:6726–33.

[14] Li Q, Williams CG, Sun DDN, Wang J, Leong K, Elisseeff JH. Photocrosslinkable polysaccharides based on chondroitin sulfate. J Biomed Mater Res Part A 2004;68A:28–33.

[15] Burdick JA, Prestwich GD. Hyaluronic Acid Hydrogels for Biomedical Applications. Adv Mater 2011;23:H41–H56.

[16] Burdick JA, Chung C, Jia XQ, Randolph MA, Langer R. Controlled degradation and mechanical behavior of photopolymerized hyaluronic acid networks. Biomacromolecules 2005;6:386–91.

[17] Shu XZ, Liu Y, Luo Y, Roberts MC, Prestwich GD. Disulfide Cross-Linked Hyaluronan Hydrogels. Biomacromolecules 2002;3:1304–11.

[18] Prestwich GD, Marecak DM, Marecek JF, Vercruysse KP, Ziebell MR. Controlled chemical modification of hyaluronic acid: synthesis, applications, and biodegradation of hydrazide derivatives. J Control Release 1998;53:93–103.

[19] Zhu JM. Bioactive modification of poly(ethylene glycol) hydrogels for tissue engineering. Biomaterials 2010;31:4639–56.

[20] West JL, Hubbell JA. Polymeric Biomaterials with Degradation Sites for Proteases Involved in Cell Migration. Macromolecules 1999;32:241–4.

[21] Park Y, Ph D, Lutolf MP, Hubbell JA, Hunziker EB, Wong M, et al. Bovine Primary Chondrocyte Culture in Synthetic Matrix Hydrogels as a Scaffold for Cartilage Repair 2004;10.

[22] Lutolf MP, Lauer-Fields JL, Schmoekel HG, Metters AT, Weber FE, Fields GB, et al. Synthetic matrix metalloproteinase-sensitive hydrogels for the conduction of tissue regeneration: engineering cell-invasion characteristics. Proc Natl Acad Sci U S A 2003;100:5413–8.

[23] Lutolf MP, Raeber GP, Zisch AH, Tirelli N, Hubbell JA. Cell-Responsive Synthetic Hydrogels. Adv Mater 2003;15:888–92.

[24] West JL, Lee SH, Miller JS, Moon JJ. Proteolytically degradable hydrogels with a fluorogenic substrate for studies of cellular proteolytic activity and migration. Biotechnol Prog 2005;21:1736–41.

[25] Bahney CS, Hsu C-W, Yoo JU, West JL, Johnstone B. A bioresponsive hydrogel tuned to chondrogenesis of human mesenchymal stem cells. FASEB J 2011;25:1486–96.

[26] Patterson J, Hubbell JA. Enhanced proteolytic degradation of molecularly engineered PEG hydrogels in response to MMP-1 and MMP-2. Biomaterials 2010;31:7836–45.

[27] Dhote V, Vernerey FJ. Mathematical model of the role of degradation on matrix development in hydrogel scaffold. Biomech Model Mechanobiol 2013;13:167–83.

[28] Vernerey FJ, Greenwald EC, Bryant SJ. Triphasic mixture model of cell-mediated enzymatic degradation of hydrogels. Comput Methods Biomech Biomed Engin 2012;15:1197–210.

[29] French MF, Bhown A, Van Wart HE. Identification of Clostridium histolyticum Collagenase Hyperreactive Sites in Type I, II, and III Collagens: Lack of Correlation with Local Triple Helical Stability. J Protein Chem 1992;11:83–97.

[30] Sandor M, Enscore D, Weston P, Mathiowitz E. Effect of protein molecular weight on release from micron-sized PLGA microspheres. J Control Release 2001;76:297–311.

[31] Cohen S, Yoshioka T, Lucarelli M, Hwang LH, Langer R. Controlled Delivery Systems for Proteins Based on Poly(Lactic Glycolic Acid) Microspheres. Pharm Res 1991;8:713–20.

[32] Fairbanks BD, Schwartz MP, Halevi AE, Nuttelman CR, Bowman CN, Anseth KS. A Versatile Synthetic Extracellular Matrix Mimic via Thiol-Norbornene Photopolymerization. Adv Mater 2009;21:5005–10.

[33] Turk BE, Huang LL, Piro ET, Cantley LC. Determination of protease cleavage site motifs using mixture-based oriented peptide libraries. Nat Biotechnol 2001;19:661–7.

[34] Lineweaver H, Burk D. The Determination of Enzyme Dissociation Constants. J Am Chem Soc 1934;56:658–66.

[35] Ashton RS, Banerjee A, Punyani S, Schaffer DV, Kane RS. Scaffolds based on degradable alginate hydrogels and poly(lactide-co-glycolide) microspheres for stem cell culture. Biomaterials 2007;28:5518–25.

[36] Roberts JJ, Bryant SJ. Comparison of photopolymerizable thiol-ene PEG and acrylate-based PEG hydrogels for cartilage development. Biomaterials 2013;34:9969–79.

[37] Shih H, Lin C-C. Visible Light-Mediated Thiol-Ene Hydrogelation Using Eosin-Y as the Only Photoinitiator. Macromol Rapid Commun 2013;34:269–73.

[38] Gould ST, Darling NJ, Anseth KS. Small peptide functionalized thiol-ene hydrogels as culture substrates for understanding valvular interstitial cell activation and de novo tissue deposition. Acta Biomater 2012;8:3201–9.

[39] Peppas NA, Barr-Howell BD. Characterization of the cross-linked structure of hydrogels. In: Peppas NA, editor. Hydrogels Med. Pharmacy, Vol. I Fundam., Boca Raton, FL: CRC Press, Inc.; 1986, p. 27–56.

[40] Canal T, Peppas NA. Correlation between mesh size and equilibrium degree of swelling of polymeric networks. J Biomed Mater Res 1989;23:1183–93.

[41] Korson L, Drost-Hansen W, Millero FJ. Viscosity of Water at Various Temperatures. J Phys Chem 1969;73:34–9.

[42] Lustig SR, Peppas NA. Solute diffusion in swollen membranes. IX. Scaling laws for solute diffusion in gels. J Appl Polym Sci 1988;36:735–47.

[43] Amsden B. Solute Diffusion within Hydrogels. Mechanisms and Models. Macromolecules 1998;31:8382–95.

[44] Dhote V, Skaalure S, Akalp U, Roberts J, Bryant SJ, Vernerey FJ. On the role of hydrogel structure and degradation in controlling the transport of cell-secreted matrix molecules for engineered cartilage. J Mech Behav Biomed Mater 2013;19:61–74.

[45] Drury JL, Mooney DJ. Hydrogels for tissue engineering: scaffold design variables and applications. Biomaterials 2003;24:4337–51.

[46] Brandl F, Sommer F, Goepferich A. Rational design of hydrogels for tissue engineering: Impact of physical factors on cell behavior. Biomaterials 2007;28:134–46.

[47] Nicodemus GD, Skaalure SC, Bryant SJ. Gel structure has an impact on pericellular and extracellular matrix deposition, which subsequently alters metabolic activities in chondrocyte-laden PEG hydrogels. Acta Biomater 2011;7:492–504.

[48] Nagase H, Fields GB. Human matrix metalloproteinase specificity studies using collagen sequence-based synthetic peptides. Biopolymers 1996;40:399–416.

[49] Allison SD. Analysis of initial burst in PLGA microparticles. Expert Opin Drug Deliv 2008;5:615–28.

[50] Nagase H, Visse R, Murphy G. Structure and function of matrix metalloproteinases and TIMPs. Cardiovasc Res 2006;69:562–73.

[51] Woessner JF. Matrix Metalloproteinases and Their Inhibitors in Connective Tissue Remodeling. Faseb J 1991;5:2145–54.

[52] Murphy G, Baker AH, Edwards DR. Metalloproteinase inhibitors: biological actions and therapeutic opportunities. J Cell Sci 2002;115:3719–27.

[53] Gomez DE, Alonso DF, Yoshiji H, Thorgeirsson UP. Tissue inhibitors of metalloproteinases: structure, regulation and biological functions. Eur J Cell Biol 1997;74:111–22.

[54] Brew K, Kashiwagi M, Tortorella M, Nagase H. TIMP-3 is a potent inhibitor of aggrecanase 1 (ADAM-TS4) and aggrecanase 2 (ADAM-TS5). J Biol Chem 2001;276:12501–4.

[55] Edwards DR, Porter S, Clark IM, Kevorkian L. The ADAMTS metalloproteinases. Biochem J 2005;386:15–27.

Chapter 8

Conclusions and Recommendations

8.1 Conclusions

This thesis advances research into the effects of chondrocyte donor age on cartilage regeneration potential within various degradable scaffold environments, including a novel cell-mediated degradable hydrogel that was introduced within this thesis. Cell-based therapies for cartilage regeneration are the current state-of-the-art in clinical practice [1], which use autologous chondrocytes harvested from the patient [2,3], however these treatments are most successful in younger patients [3,4], despite that the clinical need for cartilage regeneration is most pressing for older patients [5]. In an effort to expand these treatments to patients of a wider age range, the effect of cell donor age was assessed in a tissue engineering environment. In this thesis, PEG-based degradable materials were used, because they are photopolymerizable and injectable, thus providing temporal and spatial control over hydrogel formation, the chemistry is easily tailored to introduce different degradable functionalities [6,7], and because they support cartilage-specific matrix production [8–12]. Degradable hydrogels were used because scaffold degradation is necessary to permit macroscopic tissue elaboration, and long-term scaffold presence can elicit an adverse immune response, however scaffold degradation must match matrix production, which is a significant design challenge.

Because chondrocytes isolated from skeletally immature (juvenile) donors are most commonly investigated in cartilage tissue engineering research, initial work (chapter 3) aimed to compare tissue metabolism of juvenile bovine chondrocytes to adult bovine chondrocytes isolated from skeletally mature donors. This work was conducted within radically photoinitiated chain-growth PEG-poly(lactic acid)-dimethacrylate (PEG-PLA) hydrogels (mixed with a small

amount of PEG-dimethacrylate to slow degradation), which form relatively heterogeneous networks that degrade by bulk hydrolytic degradation [13,14]. PEG-PLA hydrogels supported cartilage-specific matrix formation by both juvenile and adult encapsulated chondrocytes, characterized by aggrecan and collagen II deposition, however matrix was only deposited pericellularly. Juvenile chondrocytes produced more collagen per wet weight than adult chondrocytes, which was expected, yet adult chondrocytes produced more sGAG per wet weight, which is promising because it suggests that tissue engineering using chondrocytes from adult donors may be possible. Adult chondrocyte construct cellularity was higher than juvenile chondrocytes over the course of the study, which is similarly promising. This phenomenon was also observed within cell-mediated degradable scaffolds, investigated in chapter 6. Our current hypothesis is that chondrocytes isolated from adult donors are simply more resilient to changes in their environment due to surviving for years within a mechanically dynamic environment. While the hydrogel degradation characteristics were not fully characterized in this work, hydrogel swelling and softening were observed over the course of the 4 week culture period, which was assumed to contribute to the observed loss of scaffold cellularity which began after 1 week, when scaffold swelling became more pronounced. It was also hypothesized that this led to loss of extracellular matrix from the scaffolds, because the only matrix that remained was located pericellularly. One of the most interesting observations from this study was that aggrecanase-mediated aggrecan degradation within the interglobular domain (IGD) was elevated by adult compared to juvenile chondrocytes, and that evidence of MMP-mediated aggrecan degradation was also apparent by both cell types. This work confirmed that cell donor age impacts extracellular matrix metabolism within degradable hydrogels, motivating the need to improve hydrogel systems to support matrix elaboration by cells from older donors.

Chapters 4 and 5 aimed to modify the degradable PEG hydrogel culture platform in order to better mimic the native tissue environment, which was hypothesized to promote matrix production as well as retention within degradable scaffolds. Chapter 4 investigated entrapping

hyaluronic acid (HA), which is a native component of cartilage ECM involved in aggrecan organization [15,16] that can also mediate chondrocyte metabolic behavior [17,18]. HA was physically entrapped into PEG-PLA hydrogels to form semi-interpenetrating networks with encapsulated adult chondrocytes. HA of two different concentrations and molecular weights were investigated, because high MW HA can promote matrix production and tissue healing, whereas low MW HA can decrease matrix retention and induce an inflammatory response [19]. Within hydrolytically degradable hydrogels, entrapped HA release was characterized, and about 90% of the initially entrapped amount was released by 4 weeks. HA was found to improve matrix deposition within constructs at 8 days, regardless of MW, and increased overall matrix production by 4 weeks in a dose-dependent manner, however the majority of the produced matrix was released to the culture medium. This phenomenon was attributed mainly to the bulk degrading scaffolds, which was also deemed responsible for the loss of entrapped HA. However, HA presence within scaffolds proved beneficial to adult chondrocytes, and high MW HA was most beneficial because the low MW HA increased catabolic activity at 15 days. Further investigations should aim to improve HA retention within scaffolds, potentially by incorporating HA-binding peptides [20], but HA overall was demonstrated as a potentially powerful tool to stimulate matrix production by adult chondrocytes.

Chapter 5 investigated mimicking the native osmotic environment in cartilage, which is elevated (350-450 mOsm) compared to standard chondrocyte culture medium (330 mOsm) [21]. Elevating the culture medium was previously shown to improve adult chondrocyte survival during encapsulation, and to stimulate matrix production in short-term experiments [21–23], therefore it was hypothesized that long-term elevated osmolarity might improve matrix production. Adult chondrocytes were encapsulated in PEG-PLA hydrogels and cultured in either standard 330 mOsm culture medium, or elevated medium adjusted to 400 mOsm, for 4 weeks. Elevated osmolarity improved matrix deposition (sGAGs and collagen) within the constructs after 1 day, however the standard lower osmolarity medium increased overall collagen

production after 4 weeks. This result suggested that longer-term, after chondrocytes produce and deposit their own pericellular matrix rich in negatively charged sGAGs that locally attract cations, they are able to regulate their immediate extracellular osmolarity [21]. This has important implications for long-term culture experiments, where it may be beneficial to increase the medium osmolarity in the first few days, but standard lower osmolarity medium was sufficient and actually an improvement throughout longer-term culture. Most of the matrix that was produced over 4 weeks, however, was measured in the culture medium, similar to the experiment with entrapped HA. The loss of newly produced matrix was mainly attributed to the bulk hydrolytically degradable scaffolds, which did not seem well suited to encourage matrix elaboration by either juvenile or adult chondrocytes.

Chapters 6 and 7 aimed to investigate cartilage tissue engineering in cell-mediated degradable PEG hydrogels, which were hypothesized to be an improvement over bulk hydrolytic degradation because degradation is dictated by enzyme-secreting cells instead of occurring homogeneously throughout the scaffold. Radically photoinitiated step-growth PEG-based thiol-norbornene hydrogels, which form more homogeneous network structures where crosslinks can be any dithiol molecule such as a *bis*-cysteine peptide [24], were used to enable cell-mediated degradation. A novel aggrecanase-degradable hydrogel was introduced, incorporating a peptide crosslinker that mimicked the same sequence in aggrecan that was shown to be cleaved by adult chondrocytes in chapter 3. Both juvenile and adult chondrocytes were encapsulated in either aggrecanase-degradable or non-degradable PEG thiol-norbornene hydrogels, and cultured up to 12 weeks. In one additional condition, adult chondrocytes in degradable hydrogels were subjected to inflammatory stimulation by adding lipopolysaccharide to the culture medium, which increased MMP activity and IL-6 production but was promising because cartilaginous matrix deposition was still observed even in this inflammatory environment. The degradable hydrogel modulus decreased steadily over time, but significant swelling was not observed, although sGAG and collagen loss were still most pronounced in degradable

hydrogels. It was encouraging that juvenile chondrocytes produced large quantities of aggrecan and collagen II, and matrix connectivity was improved for juvenile chondrocytes in degradable hydrogels. It was further encouraging that the degradable hydrogels seemed to promote the chondrocyte phenotype and inhibited deposition of fibrocartilage-specific collagen I and hypertrophic collagen X, and degradable hydrogels were not found to increase aggrecanase activity or IL-6 secretion, supporting the use of this system for cartilage tissue engineering. However, degradation was still not matched to matrix deposition, especially for adult chondrocytes that exhibit lowered anabolic and elevated catabolic activity compared to juvenile cells, therefore further tuning of degradation is necessary.

Chapter 7 aimed to characterize cell-mediated scaffold degradation in an attempt to elucidate which parameters are important to control in order to achieve either reaction- or diffusion-dominated degradation, where the former is characterized by localized degradation surrounding cells, and the latter is more similar to bulk degradation. A simple, acellular model system was explored using collagenase type II enzyme and a peptide crosslinker that exhibited rapid degradation kinetics with collagenase type II. The degradation front was observed in one dimension in hydrogels of three different crosslink densities, exhibiting both reaction- and diffusion-dominated degradation, characterized by either a sharp or wide degradation front, respectively, as well as an intermediate form of degradation. The dimensionless parameter ϕ^e was calculated, which describes the ratio between the enzyme reaction rate and the enzyme diffusion rate. ϕ^e was calculated for the three distinct hydrogels, and plotted against the theoretical ϕ^e as a function of the ratio of hydrogel mesh size to the enzyme size. This made it clear that there are two distinct regimes, or ranges of mesh/enzyme size (specific to the kinetic parameters), that determine whether degradation is reaction- or diffusion-dominated, which is an important tool for hydrogel design. The system was further characterized in 3 dimensions, where enzyme-loaded PLGA microspheres, which served as a model for enzyme-secreting cells, were embedded into degradable hydrogels, and degradation was visually monitored,

reflecting the results from 1-dimensional observations, as well as quantified. In the low crosslinked hydrogels, the modulus decreased rapidly while hydrogels swelled considerably, reflective of bulk degradation. In the highly crosslinked hydrogels, the modulus decreased slowly and little swelling was observed, more indicative of localized degradation. These findings show that careful control of the initial hydrogel properties can be an experimental tool to dictate the degradation characteristics in cell-mediated degradable hydrogels.

The findings of this thesis overall support the importance of examining the effects of cell donor age on cartilage regeneration within degradable hydrogels, if tissue engineering research is intended to advance cell-based therapies that can be clinically applied. We 1) established that cellular metabolism varies with donor age in degradable hydrogels, 2) culture medium osmolarity and hyaluronic acid can be effective tools to increase matrix production by chondrocytes, and 3) cell-mediated degradable hydrogels are a promising platform for cartilage tissue engineering that present an opportunity to better tune degradation to matrix production by different cell sources. Scaffold degradation and careful characterization of the cell source and the effects of age were demonstrated as important factors to consider when designing tunable degradable scaffolds for cartilage tissue engineering, where bioactive factors can be further incorporated in order to promote matrix production by cells from older donors.

8.2 Recommendations

This thesis demonstrated that cells from different aged donors exhibited different metabolic activities within degradable PEG hydrogels, but that hydrogel degradation can be tuned to match the specific cell source. The PEG hydrogel platform best suited for future investigations is the photopolymerizable thiol-norbornene step growth hydrogel system [24–26]. Hydrogel degradation can be easily tailored in this system by incorporating enzymatically degradable peptide sequences with different degradation kinetics, and we demonstrated that controlling the initial crosslink density is an effective tool to specify degradation behavior. The 8-arm PEG hydrogel system is especially beneficial because not all arms must necessarily be

reacted in order to form a hydrogel network, meaning that some of the free thiol-reactive arms can be used to tether growth factors, matrix molecules, or adhesive peptides. Because it was also recently observed that that radical damage to cartilage cells during photopolymerization was decreased in thiol-norbornene compared to diacrylate hydrogels [27], this hydrogel platform is an ideal system to develop new cartilage tissue engineering strategies.

8.2.1 Mimicking the native environment for in vitro culture

In order to investigate tissue engineering therapies that are clinically relevant and can ultimately be translated to clinical application, *in vitro* studies should aim to match the physiological environment as closely as possible. Two physiological factors that merit further study are extracellular osmolarity and oxygen concentration. Several studies, including the work presented in chapter 5, showed that mimicking elevated cartilage osmolarity improved chondrocyte survival and matrix production in the short term [21–23], however we demonstrated that these benefits diminished longer-term after chondrocytes deposited a pericellular matrix. For *in vitro* culture, it may be most beneficial to apply elevated osmolarity for the first several days of culture, and either switch directly to standard culture medium or slowly decrease osmolarity over time. Another important factor which is not effectively mimicked in standard *in vitro* culture is oxygen concentration, because cartilage tissue is hypoxic, with oxygen concentrations between 1 and 7% [28]. However, hypoxic chambers can be used, or incubators can be modified to control the oxygen levels similarly to how CO_2 levels are controlled. The benefit of these systems has been demonstrated, showing that chondrocytes cultured in a 5% oxygen environment produced more cartilaginous matrix compared to standard 21% oxygen [29]. Therefore the benefits of mimicking the native environment are twofold, in that cartilage matrix production can be enhanced, while also providing a better experimental model for the *in vivo* environment.

8.2.2 Autologous stem cells

Another potential autologous cell source for cell-based tissue engineering is mesenchymal stem cells (MSCs). MSCs can be harvested non-invasively from the patient's bone marrow and expanded in 2-dimensional culture, and they have the capacity to differentiate into chondrocytes within appropriate chondrogenic environments [63]. MSCs could be an effective cell source for autologous tissue engineering, but only if their differentiation is highly controlled, and hypertrophic differentiation is suppressed [64]. Because the aggrecanase-degradable hydrogels were effective in promoting the chondrocyte phenotype and decreasing fibrocartilage and hypertrophic cartilage phenotypes, this tissue engineering platform could be effective to encourage MSC differentiation, especially if combined with growth factors.

Another future focus of autologous cell-based tissue engineering could be implementation of osteoarthritic chondrocytes, which would likely need to be stimulated or reprogrammed in order to produce healthy new cartilage. The fact that encapsulated adult chondrocytes stimulated with inflammatory LPS (chapter 6) were able to deposit cartilaginous tissue was promising for eventual implementation of these therapies within patients whose joints are inflamed. Pluripotent stem cells were recently induced from osteoarthritic chondrocytes, which then underwent chondrogenic differentiation [65], showing that tissue engineering could feasibly be implemented using cells from osteoarthritic patients.

8.2.3 Growth factors to stimulate matrix production

This thesis demonstrated that chondrocytes isolated from adult donors produced much less cartilaginous matrix than cells from juvenile donors. In order to effectively regenerate cartilage using adult chondrocytes, these cells will need to be anabolically stimulated to produce more extracellular matrix. Growth factors and extracellular matrix molecules have been incorporated into scaffolds in a variety of ways in order to mimic native cartilage and increase cartilaginous matrix production. The main growth factors that can induce chondrogenic differentiation and/or increase matrix production are TGF-β1-3, BMP-2, -4, -6, -7, -13, and -14, bFGF, and IGF-1 [28,30], where certain combinations, such as TGF-β1 with BMP-2, are

particularly effective [30,31]. Covalently tethering active growth factors is particularly feasible in the thiol-norbornene PEG hydrogel platform [32,33], therefore this strategy merits further investigation, especially using encapsulated adult chondrocytes or mesenchymal stem cells that can differentiate into chondrocytes.

8.2.4 Catabolic inhibitors

While catabolism is necessary, catabolic inhibitors could be carefully implemented in order to control the balance between anabolic and catabolic activity for chondrocytes from adult, aged, or osteoarthritic patients. Tissue inhibitors of metalloproteinases (TIMPs) are a family of protein inhibitors for MMPs, [34–36], where TIMP-1-4 have been characterized so far, and TIMP-1 and TIMP-2 showed activity against every MMP [37]. TIMP-3 effectively inhibits aggrecanase-1 and -2 [38,39], and there are a variety of synthetic inhibitors that have been developed, however they are not nearly as effective as TIMP-3 [40,41]. The Burdick group [42] recently demonstrated a hyaluronic acid-based hydrogel that controllably releases physically sequestered TIMP-3 in response to MMP activity. Incorporating TIMPs into hydrogels exogenously, by entrapment, or by tethering similar to what was demonstrated for TGF-β1 [33] could provide an additional mechanism to control catabolic activity within degradable PEG hydrogels.

8.2.5 Creating a 'toolbox' of enzymatically sensitive peptides

While just one cartilage-specific enzymatically cleavable peptide crosslinker was introduced within this thesis (chapter 6), it could be advantageous to design a 'toolbox' of different peptides with a variety of degradation kinetics. Because aggrecan is degraded *in vivo* much more quickly than collagen [15,43,44], it was targeted as an appropriate substrate for degradation by chondrocytes. The aggrecanase-degraded site in the interglobular domain (IGD), with the sequence TEGE-ARGS, was initially investigated because it has been well characterized, and because aggrecanases cleave aggrecan much more efficiently than MMPs [45–47]. Degradation at the other site within the bovine IGD with the sequence IPES-FFGV,

which is MMP-specific, is more associated with normal tissue homeostasis [48,49], therefore it might be another appropriate target to mimic with a degradable peptide crosslinker. Catabolism of aggrecan within the sGAG-bearing region of the core protein may present additional effective targets because these sites are degraded by aggrecanases more efficiently than the site in the IGD [41]. What is particularly interesting is that these specific sites have amino acid sequences (in bovine aggrecan) that are similar to that in the IGD (IGD: TEGE-ARGS; sGAG region: TAQE-AGEG, VSQE-LGQR, GELE-GRGD, and KEEE-GLGS) [41,47], meaning that trying different combinations of specific amino acids with similar side-group patterns (for example, R and Q both contain amine groups) could result in populating our toolbox with peptides that have a variety of degradation kinetics. A complicating factor is that aggrecanase-mediated degradation of the aggrecan core protein in the sGAG-bearing regions may be dependent on presence of sGAGs [50,51], therefore carefully validating degradation of these peptides will be crucial.

Although degradation of collagen *in vivo* can be very slow, it may be beneficial to have a toolbox that contains both slow- and fast-degrading peptides. Additionally, it is possible that creating hydrogels with a combination of degradable peptides might be most effective, where fast-degrading peptides might be necessary to encourage initial matrix formation, but slower degrading peptides could facilitate later-stage extracellular matrix assembly. Indeed, MMP-mediated degradation of a collagen-specific peptide was already demonstrated with chondrocytes [52], and the degradation kinetics of these types of substrates can be varied by introducing amino acid point mutations [53], or introducing synthetic, non-natural amino acids such as norvaline [54]. Therefore, there is a wide range of possible targets that can be engineered to facilitate cell-mediated hydrogel degradation.

8.2.6 Investigating cell-mediated degradation in a mechanically relevant environment

Mechanical loading can either stimulate or inhibit catabolism. This could be important for either trying to control the balance of anabolic and catabolic behavior, or to simply model

chondrocyte metabolism and matrix elaboration that might occur once a cell-laden material is injected into a patient's joint and the patient is able to move or undergo physical therapy regimes. Because cartilage exists *in vivo* in a highly dynamic mechanical environment, many groups have attempted to replicate these environments for stem cells or chondrocytes in three-dimensional culture, which can improve chondrogenic differentiation and cartilaginous matrix production [55–57], however the effect on catabolic activity is highly complex, as different mechanical regimes, as well as the age of the cell donor, can either increase or decrease catabolism [58–62]. A challenge with mechanical loading of degradable scaffolds is that it can potentially accelerate degradation by increasing fluid flow and/or stimulating catabolic enzyme production, which is hard to predict and can lead to premature scaffold dissolution. Because the aggrecanase-degradable hydrogels demonstrated in chapter 6 degraded much more slowly than hydrolytically degradable hydrogels [10], the cell-mediated degradable platform may be much better suited to studying under mechanical loading. Future studies should aim to characterize how different loading regimes affect catabolic behavior, degradation kinetics, and matrix elaboration by cells from different aged donors, which could be used to further develop computational models that predict tissue formation by cells in different hydrogel environments.

8.3 Long-term Project Goals

The long-term goal of this project is to develop a tunable hydrogel system that can be tailored to autologous cells isolated from patients of any age, and this could eventually be expanded to osteoarthritic patients as well. Because aging, scaffold degradation, and matrix production are all highly complex, there is a need to develop computational tools that experimentalists or clinicians can use to predict an appropriate hydrogel environment to encapsulate cells from specific patients or donors. In order to do this, the cellular characteristics that must be quantified include matrix and enzyme production rates, which would serve as inputs into a computational model. Through collaboration with Dr. Franck Vernerey, progress has been made towards developing a predictive computational model [66–68], but much more

work is needed to calibrate the model predictions to experimental results, especially in light of even more complex phenomena introduced within this concluding chapter (catabolic inhibitors, mechanical loading, and osteoarthritic chondrocytes, for example). The ultimate goal is to develop a computational model that can predict an optimal patient-specific hydrogel with degradation characteristics that match the rates and localization of matrix production, and that maintains overall scaffold mechanical integrity throughout the process of tissue regeneration, inhibits hypertrophy, and prevents loss of newly synthesized matrix. While these may seem to be lofty goals, significant progress has already been made and hydrogel systems will only continue to improve, towards implementing a personalized medicine approach to cartilage tissue engineering.

8.4 References

[1] Perera JR, Gikas PD, Bentley G. The present state of treatments for articular cartilage defects in the knee. Ann R Coll Surg Engl 2012;94:381–7.

[2] Gillogly SD, Myers TH. Treatment of full-thickness chondral defects with autologous chondrocyte implantation. Orthop Clin North Am 2005;36:433–46.

[3] Bartlett W, Skinner JA, Gooding CR, Carrington RWJ, Flanagan AM, Briggs TWR, et al. Autologous chondrocyte implantation versus matrix-induced autologous chondrocyte implantation for osteochondral defects of the knee: a prospective, randomised study. J Bone Joint Surg Br 2005;87:640–5.

[4] Bekkers JEJ, Inklaar M, Saris DBF. Treatment selection in articular cartilage lesions of the knee: a systematic review. Am J Sports Med 2009;37 Suppl 1:148S–55S.

[5] Hootman JM, Helmick CG. Projections of US prevalence of arthritis and associated activity limitations. Arthritis Rheum 2006;54:226–9.

[6] Zhu JM. Bioactive modification of poly(ethylene glycol) hydrogels for tissue engineering. Biomaterials 2010;31:4639–56.

[7] Kloxin AM, Kloxin CJ, Bowman CN, Anseth KS. Mechanical Properties of Cellularly Responsive Hydrogels and Their Experimental Determination. Adv Mater 2010;22:3484–94.

[8] Bryant SJ, Anseth KS. Hydrogel properties influence ECM production by chondrocytes photoencapsulated in poly(ethylene glycol) hydrogels. J Biomed Mater Res 2002;59:63–72.

[9] Anseth KS, Bryant SJ. Controlling the spatial distribution of ECM components in degradable PEG hydrogels for tissue engineering cartilage. J Biomed Mater Res Part A 2003;64A:70–9.

[10] Roberts JJ, Nicodemus GD, Greenwald EC, Bryant SJ. Degradation Improves Tissue Formation in (Un)Loaded Chondrocyte-laden Hydrogels. Clin Orthop Relat Res 2011.

[11] Bryant SJ, Durand KL, Anseth KS. Manipulations in hydrogel chemistry control photoencapsulated chondrocyte behavior and their extracellular matrix production. J Biomed Mater Res Part A 2003;67A:1430–6.

[12] Bryant SJ, Bender RJ, Durand KL, Anseth KS. Encapsulating Chondrocytes in degrading PEG hydrogels with high modulus: Engineering gel structural changes to facilitate cartilaginous tissue production. Biotechnol Bioeng 2004;86:747–55.

[13] Anseth KS, Metters AT, Bryant SJ, Martens PJ, Elisseeff JH, Bowman CN. In situ forming degradable networks and their application in tissue engineering and drug delivery. J Control Release 2002;78:199–209.

[14] Anseth KS, Metters AT, Bowman CN. Fundamental studies of a novel, biodegradable PEG-b-PLA hydrogel. Polymer (Guildf) 2000;41:3993–4004.

[15] Knudson CB, Knudson W. Cartilage proteoglycans. Semin Cell Dev Biol 2001;12:69–78.

[16] Roughley PJ. The structure and function of cartilage proteoglycans. Eur Cell Mater 2006;12:92–101.

[17] Kawasaki K, Ochi M, Uchio Y, Adachi N, Matsusaki M. Hyaluronic acid enhances proliferation and chondroitin sulfate synthesis in cultured chondrocytes embedded in collagen gels. J Cell Physiol 1999;179:142–8.

[18] Allison DD, Grande-Allen KJ. Review. Hyaluronan: A powerful tissue engineering tool. Tissue Eng 2006;12:2131–40.

[19] Stern R, Asari AA, Sugahara KN. Hyaluronan fragments: An information-rich system. Eur J Cell Biol 2006;85:699–715.

[20] Roberts JJ, Elder RM, Neumann AJ, Jayaraman A, Bryant SJ. Interaction of Hyaluronan Binding Peptides with Glycosaminoglycans in Poly(ethylene glycol) Hydrogels. Biomacromolecules 2014.

[21] Urban JPG, Hall AC, Gehl KA. Regulation of Matrix Synthesis Rates by the Ionic and Osmotic Environment of Articular Chondrocytes. J Cell Physiol 1993;154:262–70.

[22] Villanueva I, Bishop NL, Bryant SJ. Medium Osmolarity and Pericellular Matrix Development Improves Chondrocyte Survival When Photoencapsulated in Poly(Ethylene Glycol) Hydrogels at Low Densities. Tissue Eng Part A 2009;15:3037–48.

[23] Amin AK, Huntley JS, Bush PG, Simpson AHRW, Hall AC. Osmolarity influences chondrocyte death in wounded articular cartilage. J Bone Jt Surgery-American Vol 2008;90A:1531–42.

[24] Fairbanks BD, Schwartz MP, Halevi AE, Nuttelman CR, Bowman CN, Anseth KS. A Versatile Synthetic Extracellular Matrix Mimic via Thiol-Norbornene Photopolymerization. Adv Mater 2009;21:5005–10.

[25] Gould ST, Darling NJ, Anseth KS. Small peptide functionalized thiol-ene hydrogels as culture substrates for understanding valvular interstitial cell activation and de novo tissue deposition. Acta Biomater 2012;8:3201–9.

[26] Aimetti AA, Machen AJ, Anseth KS. Poly(ethylene glycol) hydrogels formed by thiol-ene photopolymerization for enzyme-responsive protein delivery. Biomaterials 2009;30:6048–54.

[27] Roberts JJ, Bryant SJ. Comparison of photopolymerizable thiol-ene PEG and acrylate-based PEG hydrogels for cartilage development. Biomaterials 2013.

[28] Vinatier C, Mrugala D, Jorgensen C, Guicheux J, Noel D. Cartilage engineering: a crucial combination of cells, biomaterials and biofactors. Trends Biotechnol 2009;27:307–14.

[29] Domm C, Schünke M, Christesen K, Kurz B. Redifferentiation of dedifferentiated bovine articular chondrocytes in alginate culture under low oxygen tension. Osteoarthritis Cartilage 2002;10:13–22.

[30] Nesic D, Whiteside R, Brittberg M, Wendt D, Martin I, Mainil-Varlet P. Cartilage tissue engineering for degenerative joint disease. Adv Drug Deliv Rev 2006;58:300–22.

[31] Mollon B, Kandel R, Chahal J, Theodoropoulos J. The clinical status of cartilage tissue regeneration in humans. Osteoarthritis Cartilage 2013;21:1824–33.

[32] McCall JD, Anseth KS. Thiol-ene photopolymerizations provide a facile method to encapsulate proteins and maintain their bioactivity. Biomacromolecules 2012;13:2410–7.

[33] McCall JD, Luoma JE, Anseth KS. Covalently tethered transforming growth factor beta in PEG hydrogels promotes chondrogenic differentiation of encapsulated human mesenchymal stem cells. Drug Deliv Transl Res 2012;2:305–12.

[34] Nagase H, Visse R, Murphy G. Structure and function of matrix metalloproteinases and TIMPs. Cardiovasc Res 2006;69:562–73.

[35] Woessner JF. Matrix Metalloproteinases and Their Inhibitors in Connective Tissue Remodeling. Faseb J 1991;5:2145–54.

[36] Murphy G, Baker AH, Edwards DR. Metalloproteinase inhibitors: biological actions and therapeutic opportunities. J Cell Sci 2002;115:3719–27.

[37] Gomez DE, Alonso DF, Yoshiji H, Thorgeirsson UP. Tissue inhibitors of metalloproteinases: structure, regulation and biological functions. Eur J Cell Biol 1997;74:111–22.

[38] Brew K, Kashiwagi M, Tortorella M, Nagase H. TIMP-3 is a potent inhibitor of aggrecanase 1 (ADAM-TS4) and aggrecanase 2 (ADAM-TS5). J Biol Chem 2001;276:12501–4.

[39] Edwards DR, Porter S, Clark IM, Kevorkian L. The ADAMTS metalloproteinases. Biochem J 2005;386:15–27.

[40] Shiozaki M, Maeda K, Miura T, Kotoku M, Yamasaki T, Matsuda I, et al. Discovery of (1S,2R,3R)-2,3-Dimethyl-2-phenyl-1-sulfamidocyclopropanecarboxylates: Novel and Highly Selective Aggrecanase Inhibitors. J Med Chem 2011;54:2839–63.

[41] Nagase H, Kashiwagi M. Aggrecanases and cartilage matrix degradation. Arthritis Res Ther 2003;5:94–103.

[42] Purcell BP, Lobb D, Charati MB, Dorsey SM, Wade RJ, Zellars KN, et al. Injectable and bioresponsive hydrogels for on-demand matrix metalloproteinase inhibition. Nat Mater 2014.

[43] Mok SS, Masuda K, Hauselmann HJ, Aydelotte MB, Thonar EJMA. Aggrecan Synthesized by Mature Bovine Chondrocytes Suspended in Alginate - Identification of 2 Distinct Metabolic Matrix Pools. J Biol Chem 1994;269:33021–7.

[44] Hauselmann HJ, Masuda K, Hunziker EB, Neidhart M, Mok SS, Michel BA, et al. Adult human chondrocytes cultured in alginate form a matrix similar to native human articular cartilage. Am J Physiol Physiol 1996;271:C742–C752.

[45] Durigova M, Nagase H, Mort JS, Roughley PJ. MMPs are less efficient than ADAMTS5 in cleaving aggrecan core protein. Matrix Biol 2011;30:145–53.

[46] Lark MW, Gordy JT, Weidner JR, Ayala J, Kimura JH, Williams HR, et al. Cell-mediated Catabolism of Aggrecan. J Biol Chem 1995;270:2550–6.

[47] Ilic MZ, Handley CJ, Robinson HC, Mok MT. Mechanism of Catabolism of Aggrecan by Articular Cartilage. Arch Biochem Biophys 1992;294:115–22.

[48] Fosang AJ, Last K, Stanton H, Weeks DB, Campbell IK, Hardingham TE, et al. Generation and novel distribution of matrix metalloproteinase-derived aggrecan fragments in porcine cartilage explants. J Biol Chem 2000;275:33027–37.

[49] Sandy JD. A contentious issue finds some clarity: on the independent and complementary roles of aggrecanase activity and MMP activity in human joint aggrecanolysis. Osteoarthritis Cartilage 2006;14:95–100.

[50] Tortorella MD, Pratta M, Liu R-Q, Austin J, Ross OH, Abbaszade I, et al. Sites of Aggrecan Cleavage by Recombinant Human Aggrecanase-1 (ADAMTS-4). J Biol Chem 2000;275:18566–73.

[51] Pratta MA, Tortorella MD, Arner EC. Age-related changes in aggrecan glycosylation affect cleavage by aggrecanase. J Biol Chem 2000;275:39096–102.

[52] Wong M, Park Y, Lutolf MP, Hubbell JA, Hunziker EB. Bovine primary chondrocyte culture in synthetic matrix metalloproteinase-sensitive poly(ethylene glycol)-based hydrogels as a scaffold for cartilage repair. Tissue Eng 2004;10:515–22.

[53] Nagase H, Fields GB. Human matrix metalloproteinase specificity studies using collagen sequence-based synthetic peptides. Biopolymers 1996;40:399–416.

[54] Nagase H, Fields CG, Fields GB. Design and Characterization of a Fluorogenic Substrate Selectively Hydrolyzed by Stromelysin-1 (Matrix Metalloproteinase-3). J Biol Chem 1994;269:20952–7.

[55] Waldman SD, Couto DC, Grynpas MD, Pilliar RM, Kandel RA. A single application of cyclic loading can accelerate matrix deposition and enhance the properties of tissue-engineered cartilage. Osteoarthr Cartil 2006;14:323–30.

[56] Mauck RL, Seyhan SL, Ateshian GA, Hung CT. Influence of seeding density and dynamic deformational loading on the developing structure/function relationships of chondrocyte-seeded agarose hydrogels. Ann Biomed Eng 2002;30:1046–56.

[57] Bian L, Zhai DY, Zhang EC, Mauck RL, Burdick JA. Dynamic Compressive Loading Enhances Cartilage Matrix Synthesis and Distribution and Suppresses Hypertrophy in hMSC-Laden Hyaluronic Acid Hydrogels. Tissue Eng Part A 2012;18:715–24.

[58] Blain EJ. Mechanical regulation of matrix metalloproteinases. Front Biosci 2007;12:507–27.

[59] Bryant SJ, Nicodemus GD. Mechanical loading regimes affect the anabolic and catabolic activities by chondrocytes encapsulated in PEG hydrogels. Osteoarthr Cartil 2010;18:126–37.

[60] De Croos JNA, Dhaliwal SS, Grynpas MD, Pilliar RM, Kandel RA. Cyclic compressive mechanical stimulation induces sequential catabolic and anabolic gene changes in chondrocytes resulting in increased extracellular matrix accumulation. Matrix Biol 2006;25:323–31.

[61] Kisiday JD, Lee JH, Siparsky PN, Frisbie DD, Flannery CR, Sandy JD, et al. Catabolic Responses of Chondrocyte-Seeded Peptide Hydrogel to Dynamic Compression. Ann Biomed Eng 2009;37:1368–75.

[62] Farnsworth NL, Antunez LR, Bryant SJ. Dynamic compressive loading differentially regulates chondrocyte anabolic and catabolic activity with age. Biotechnol Bioeng 2013;110:2046–57.

[63] Tuan RS. Stemming cartilage degeneration: adult mesenchymal stem cells as a cell source for articular cartilage tissue engineering. Arthritis Rheum 2006;54:3075–8.

[64] Ichinose S, Yamagata K, Sekiya I, Muneta T, Tagami M. Detailed examination of cartilage formation and endochondral ossification using human mesenchymal stem cells. Clin Exp Pharmacol Physiol 2005;32:561–70.

[65] Wei Y, Zeng W, Wan R, Wang J, Zhou Q, Qiu S, et al. Chondrogenic Differentiation of Induced Pluripotent Stem Cells from Osteoarthritc Chondrocytes in Alginate Matrix. Eur Cell Mater 2012;23:1–12.

[66] Vernerey FJ, Greenwald EC, Bryant SJ. Triphasic mixture model of cell-mediated enzymatic degradation of hydrogels. Comput Methods Biomech Biomed Engin 2012;15:1197–210.

[67] Dhote V, Skaalure S, Akalp U, Roberts J, Bryant SJ, Vernerey FJ. On the role of hydrogel structure and degradation in controlling the transport of cell-secreted matrix molecules for engineered cartilage. J Mech Behav Biomed Mater 2013;19:61–74.

[68] Dhote V, Vernerey FJ. Mathematical model of the role of degradation on matrix development in hydrogel scaffold. Biomech Model Mechanobiol 2013.

Chapter 9

Bibliography

Chapter 1

[1] Mansour JM. Biomechanics of Cartilage. In: Oatis CA, editor. Kinesiol. Mech. pathomechanics Hum. Mov., Baltimore, MD: Lippincott Williams & Wilkins; 2003, p. 66–75.

[2] Manicourt DH, Devogelaer JP, Thonar EJMA. Products of Cartilage Metabolism. In: Seibel MJ, Robins SP, Bilezikian JP, editors. Dyn. Bone Cartil. Metab., vol. 1, Burlington: Elsevier; 2006, p. 421–49.

[3] Buckwalter JA, Woo SL, Goldberg VM, Hadley EC, Booth F, Oegema TR, et al. Soft-tissue aging and musculoskeletal function. J Bone Jt Surg Am 1993;75:1533–48.

[4] Hootman JM, Helmick CG. Projections of US prevalence of arthritis and associated activity limitations. Arthritis Rheum 2006;54:226–9.

[5] Ateshian GA, Hung CT. Functional Properties of Native Articular Cartilage. In: Guilak F, Butler DL, Goldstein SA, Mooney DJ, editors. Funct. Tissue Eng., New York: Springer-Verlag; 2003, p. 46–68.

[6] Martel-Pelletier J, Boileau C, Pelletier J-P, Roughley PJ. Cartilage in normal and osteoarthritis conditions. Best Pract Res Clin Rheumatol 2008;22:351–84.

[7] Hardingham TE, Fosang AJ. Proteoglycans - Many Forms and Many Functions. Faseb J 1992;6:861–70.

[8] Hardingham TE. Proteoglycans and Glycosaminoglycans. In: Seibel MJ, Robins SP, Bilezikian JP, editors. Dyn. bone Cartil. Metab., Burlington: Elsevier Science; 2006, p. 85–98.

[9] Guilak F, Alexopoulos LG, Upton ML, Youn I, Choi JB, Cao L, et al. The pericellular matrix as a transducer of biomechanical and biochemical signals in articular cartilage. Ann New York Acad Sci Skelet Dev Remodel Heal Dis Aging 2006;1068:498–512.

[10] Engel J, Furthmayr H, Odermatt E, von der Mark H, Aumailley M, Fleischmajer R, et al. Structure and macromolecular organization of type VI collagen. Ann N Y Acad Sci 1985;460:25–37.

[11] Eyre D. Collagen of articular cartilage. Arthritis Res 2002;4:30–5.

[12] Vondermark K, Kirsch T, Nerlich A, Kuss A, Weseloh G, Gluckert K, et al. Type-X Collagen-Synthesis in Human Osteoarthritic Cartilage - Indication of Chondrocyte Hypertrophy. Arthritis Rheum 1992;35:806–11.

[13] Eyre DR, Wu JJ. Collagen of fibrocartilage: a distinctive molecular phenotype in bovine meniscus. FEBS Lett 1983;158:265–70.

[14] Mandelbaum BR, Browne JE, Fu F, Micheli L, Mosely JBJ, Erggelet C, et al. Articular Cartilage Lesions of the Knee. Am J Sport Med 1998;26:853–61.

[15] Paulsson M, Morgelin M, Wiedemann H, Beardmore-Gray M, Dunham D, Hardingham T, et al. Extended and globular protein domains in cartilage proteoglycans. Biochem J 1987;245:763–72.

[16] Buckwalter JA, Rosenberg LC. Electron-Microscopic Studies of Cartilage Proteoglycans - Direct Evidence for the Variable Length of the Chondroitin Sulfate-Rich Region of Proteoglycan Subunit Core Protein. J Biol Chem 1982;257:9830–9.

[17] Knudson CB, Knudson W. Cartilage proteoglycans. Semin Cell Dev Biol 2001;12:69–78.

[18] Hall AC, Horwitz ER, Wilkins RJ. The cellular physiology of articular cartilage. Exp Physiol 1996;81:535–45.

[19] Urban JPG, Hall AC, Gehl KA. Regulation of Matrix Synthesis Rates by the Ionic and Osmotic Environment of Articular Chondrocytes. J Cell Physiol 1993;154:262–70.

[20] Roughley PJ. The structure and function of cartilage proteoglycans. Eur Cell Mater 2006;12:92–101.

[21] Knudson CB. Hyaluronan Receptor-Directed Assembly of Chondrocyte Pericellular Matrix. J Cell Biol 1993;120:825–34.

[22] Martin JA, Buckwalter JA. Aging, articular cartilage chondrocyte senescence and osteoarthritis. Biogerontology 2002;3:257–64.

[23] Nesic D, Whiteside R, Brittberg M, Wendt D, Martin I, Mainil-Varlet P. Cartilage tissue engineering for degenerative joint disease. Adv Drug Deliv Rev 2006;58:300–22.

[24] Forsyth CB, Cole A, Murphy G, Bienias JL, Im HJ, Loeser RF. Increased matrix metalloproteinase-13 production with aging by human articular chondrocytes in response to catabolic stimuli. Journals Gerontol Ser a-Biological Sci Med Sci 2005;60:1118–24.

[25] Mok SS, Masuda K, Hauselmann HJ, Aydelotte MB, Thonar EJMA. Aggrecan Synthesized by Mature Bovine Chondrocytes Suspended in Alginate - Identification of 2 Distinct Metabolic Matrix Pools. J Biol Chem 1994;269:33021–7.

[26] Hauselmann HJ, Masuda K, Hunziker EB, Neidhart M, Mok SS, Michel BA, et al. Adult human chondrocytes cultured in alginate form a matrix similar to native human articular cartilage. Am J Physiol Physiol 1996;271:C742–C752.

[27] Wu W, Billinghurst RC, Pidoux I, Antoniou J, Zukor D, Tanzer M, et al. Sites of collagenase cleavage and denaturation of type II collagen in aging and osteoarthritic articular cartilage and their relationship to the distribution of matrix metalloproteinase 1 and matrix metalloproteinase 13. Arthritis Rheum 2002;46:2087–94.

[28] Edwards DR, Porter S, Clark IM, Kevorkian L. The ADAMTS metalloproteinases. Biochem J 2005;386:15–27.

[29] Caterson B, Flannery CR, Hughes GE, Little CB. Mechanisms involved in cartilage proteoglycan catabolism. Matrix Biol 2000;19:333–44.

[30] Nagase H, Kashiwagi M. Aggrecanases and cartilage matrix degradation. Arthritis Res Ther 2003;5:94–103.

[31] Fosang AJ, Last K, Stanton H, Weeks DB, Campbell IK, Hardingham TE, et al. Generation and novel distribution of matrix metalloproteinase-derived aggrecan fragments in porcine cartilage explants. J Biol Chem 2000;275:33027–37.

[32] Sandy JD. A contentious issue finds some clarity: on the independent and complementary roles of aggrecanase activity and MMP activity in human joint aggrecanolysis. Osteoarthritis Cartilage 2006;14:95–100.

[33] Fosang AJ, Last K, Maciewicz RA. Aggrecan is degraded by matrix metalloproteinases in human arthritis - Evidence that matrix metalloproteinase and aggrecanase activities can be independent. J Clin Invest 1996;98:2292–9.

[34] Fosang AJ, Last K, Knauper V, Murphy G, Neame PJ. Degradation of cartilage aggrecan by collagenase-3 (MMP-13). Febs Lett 1996;380:17–20.

[35] Durigova M, Nagase H, Mort JS, Roughley PJ. MMPs are less efficient than ADAMTS5 in cleaving aggrecan core protein. Matrix Biol 2011;30:145–53.

[36] Fosang AJ, Neame PJ, Hardingham TE, Murphy G, Hamilton JA. Cleavage of cartilage proteoglycan between G1 and G2 domains by stromelysins. J Biol Chem 1991;266:15579–82.

[37] Flannery CR, Lark MW, Sandy JD. Identification of a stromelysin cleavage site within the interglobular domain of human aggrecan. Evidence for proteolysis at this site in vivo in human articular cartilage. J Biol Chem 1992;267:1008–14.

[38] Lark MW, Gordy JT, Weidner JR, Ayala J, Kimura JH, Williams HR, et al. Cell-mediated Catabolism of Aggrecan. J Biol Chem 1995;270:2550–6.

[39] Ilic MZ, Handley CJ, Robinson HC, Mok MT. Mechanism of Catabolism of Aggrecan by Articular Cartilage. Arch Biochem Biophys 1992;294:115–22.

[40] McCormick A, Campisi J. Cellular aging and senescence. Curr Opin Cell Biol 1991;3:230–4.

[41] Carlo Jr. MD, Loeser RF. Increased oxidative stress with aging reduces chondrocyte survival: correlation with intracellular glutathione levels. Arthritis Rheum 2003;48:3419–30.

[42] Stockwell RA. The Cell Density of Human Articular and Costal Cartilage. J Anat 1967;101:753–63.

[43] Loeser RF. Molecular Mechanisms of Cartilage Destruction: Mechanics, Inflammatory Mediators, and Aging Collide. Arthritis Rheum 2006;54:1357–60.

[44] Bayliss MT, Howat S, Davidson C, Dudhia J. The organization of aggrecan in human articular cartilage - Evidence for age-related changes in the rate of aggregation of newly synthesized molecules. J Biol Chem 2000;275:6321–7.

[45] Verbruggen G, Cornelissen M, Almqvist KF, Wang L, Elewaut D, Broddelez C, et al. Influence of aging on the synthesis and morphology of the aggrecans synthesized by differentiated human articular chondrocytes. Osteoarthr Cartil 2000;8:170–9.

[46] Sztrolovics R, Alini M, Roughley PJ, Mort JS. Aggrecan degradation in human intervertebral disc and articular cartilage. Biochem J 1997;326:235–41.

[47] Sandy JD, Plaas AHK. Age-Related-Changes in the Kinetics of Release of Proteoglycans from Normal Rabbit Cartilage Explants. J Orthop Res 1986;4:263–72.

[48] Pratta MA, Tortorella MD, Arner EC. Age-related changes in aggrecan glycosylation affect cleavage by aggrecanase. J Biol Chem 2000;275:39096–102.

[49] Billinghurst RC, Dahlberg L, Ionescu M, Reiner A, Bourne R, Rorabeck C, et al. Enhanced cleavage of type II collagen by collagenases in osteoarthritic articular cartilage. J Clin Invest 1997;99:1534–45.

[50] Struglics A, Larsson S, Hansson M, Lohmander LS. Western blot quantification of aggrecan fragments in human synovial fluid indicates differences in fragment patterns between joint diseases. Osteoarthr Cartil 2009;17:497–506.

[51] Middleton J, Manthey A, Tyler J. Insulin-like growth factor (IGF) receptor, IGF-I, interleukin-1 beta (IL-1 beta), and IL-6 mRNA expression in osteoarthritic and normal human cartilage. J Histochem Cytochem 1996;44:133–41.

[52] Buckwalter JA, Mankin HJ, Grodzinsky AJ. Articular Cartilage and Osteoarthritis. AAOS Instr Course Lect 2005;54:465–80.

[53] Gelber AC. Joint Injury in Young Adults and Risk for Subsequent Knee and Hip Osteoarthritis. Ann Intern Med 2000;133:321.

[54] Lohmander LS, Ionescu M, Jugessur H, Poole AR. Changes in joint cartilage aggrecan after knee injury and in osteoarthritis. Arthritis Rheum 1999;42:534–44.

[55] Mollon B, Kandel R, Chahal J, Theodoropoulos J. The clinical status of cartilage tissue regeneration in humans. Osteoarthritis Cartilage 2013;21:1824–33.

[56] Goldberg VM, Buckwalter JA. Hyaluronans in the treatment of osteoarthritis of the knee: evidence for disease-modifying activity. Osteoarthr Cartil 2005;13:216–24.

[57] Maffulli N, Longo UG, Gougoulias N, Loppini M, Denaro V. Long-term health outcomes of youth sports injuries. Br J Sports Med 2010;44:21–5.

[58] Levy AS, Lohnes J, Sculley S, LeCroy M, Garrett W. Chondral Delamination of the Knee in Soccer Players. Am J Sports Med 1996;24:634–9.

[59] Vanlauwe J, Almqvist F, Bellemans J, Huskin JP, Verdonk R, Victor J. Repair of symptomatic cartilage lesions of the knee The place of autologous chondrocyte implantation. Acta Orthop Belg 2007;73:145–58.

[60] Bekkers JEJ, Inklaar M, Saris DBF. Treatment selection in articular cartilage lesions of the knee: a systematic review. Am J Sports Med 2009;37 Suppl 1:148S–55S.

[61] Richardson JB, Caterson B, Evans EH, Ashton BA, Roberts S. Repair of human articular cartilage after implantation of autologous chondrocytes. J Bone Jt Surgery-British Vol 1999;81B:1064–8.

[62] Gillogly SD, Myers TH. Treatment of full-thickness chondral defects with autologous chondrocyte implantation. Orthop Clin North Am 2005;36:433–46.

[63] Samuelson EM, Brown DE. Cost-effectiveness analysis of autologous chondrocyte implantation: a comparison of periosteal patch versus type I/III collagen membrane. Am J Sports Med 2012;40:1252–8.

[64] Bartlett W, Skinner JA, Gooding CR, Carrington RWJ, Flanagan AM, Briggs TWR, et al. Autologous chondrocyte implantation versus matrix-induced autologous chondrocyte implantation for osteochondral defects of the knee: a prospective, randomised study. J Bone Joint Surg Br 2005;87:640–5.

[65] Brittberg M. Cell carriers as the next generation of cell therapy for cartilage repair: a review of the matrix-induced autologous chondrocyte implantation procedure. Am J Sports Med 2010;38:1259–71.

[66] Kon E, Verdonk P, Condello V, Delcogliano M, Dhollander A, Filardo G, et al. Matrix-Assisted Autologous Chondrocyte Transplantation for the Repair of Cartilage Defects of the Knee Systematic Clinical Data Review and Study Quality Analysis. Am J Sports Med 2009;37:156S–166S.

[67] Perera JR, Gikas PD, Bentley G. The present state of treatments for articular cartilage defects in the knee. Ann R Coll Surg Engl 2012;94:381–7.

[68] Schnabel M, Marlovits S, Eckhoff G, Fichtel I, Gotzen L, Vécsei V, et al. Dedifferentiation-associated changes in morphology and gene expression in primary human articular chondrocytes in cell culture. Osteoarthritis Cartilage 2002;10:62–70.

[69] Tuan RS. Stemming cartilage degeneration: adult mesenchymal stem cells as a cell source for articular cartilage tissue engineering. Arthritis Rheum 2006;54:3075–8.

[70] Ichinose S, Yamagata K, Sekiya I, Muneta T, Tagami M. Detailed examination of cartilage formation and endochondral ossification using human mesenchymal stem cells. Clin Exp Pharmacol Physiol 2005;32:561–70.

[71] Guilak F, Awad HA, Fermor B, Leddy HA, Gimble JA. Adipose-derived adult stem cells for cartilage tissue engineering. Biorheology 2004;41:389–99.

[72] Koay EJ, Hoben GMB, Athanasiou KA. Tissue engineering with chondrogenically differentiated human embryonic stem cells. Stem Cells 2007;25:2183–90.

[73] Drukker M, Benvenisty N. The immunogenicity of human embryonic stem-derived cells. Trends Biotechnol 2004;22:136–41.

[74] Wei Y, Zeng W, Wan R, Wang J, Zhou Q, Qiu S, et al. Chondrogenic Differentiation of Induced Pluripotent Stem Cells from Osteoarthritc Chondrocytes in Alginate Matrix. Eur Cell Mater 2012;23:1–12.

[75] Darling EM, Athanasiou KA. Retaining zonal chondrocyte phenotype by means of novel growth environments. Tissue Eng 2005;11:395–403.

[76] Wakitani S, Goto T, Pineda S, Young R, Mansour J, Caplan A, et al. Mesenchymal cell-based repair of large, full-thickness defects of articular cartilage. J Bone Jt Surg 1994;76:579–92.

[77] Nicodemus GD, Bryant SJ. Cell encapsulation in biodegradable hydrogels for tissue engineering applications. Tissue Eng Part B-Reviews 2008;14:149–65.

[78] Kim IL, Mauck RL, Burdick JA. Hydrogel design for cartilage tissue engineering: A case study with hyaluronic acid. Biomaterials 2011;32:8771–82.

[79] Burdick JA, Chung C, Jia XQ, Randolph MA, Langer R. Controlled degradation and mechanical behavior of photopolymerized hyaluronic acid networks. Biomacromolecules 2005;6:386–91.

[80] Burdick JA, Prestwich GD. Hyaluronic Acid Hydrogels for Biomedical Applications. Adv Mater 2011;23:H41–H56.

[81] Shu XZ, Liu Y, Luo Y, Roberts MC, Prestwich GD. Disulfide Cross-Linked Hyaluronan Hydrogels. Biomacromolecules 2002;3:1304–11.

[82] Mauck RL, Seyhan SL, Ateshian GA, Hung CT. Influence of seeding density and dynamic deformational loading on the developing structure/function relationships of chondrocyte-seeded agarose hydrogels. Ann Biomed Eng 2002;30:1046–56.

[83] Mauck RL, Soltz MA, Wang CCB, Wong DD, Chao PHG, Valhmu WB, et al. Functional tissue engineering of articular cartilage through dynamic loading of chondrocyte-seeded agarose gels. J Biomech Eng Asme 2000;122:252–60.

[84] Kelly TAN, Ng KW, Wang CCB, Ateshian GA, Hung CT. Spatial and temporal development of chondrocyte-seeded agarose constructs in free-swelling and dynamically loaded cultures. J Biomech 2006;39:1489–97.

[85] Byers BA, Mauck RL, Chiang IE, Tuan RS. Transient exposure to transforming growth factor beta 3 under serum-free conditions enhances the biomechanical and biochemical maturation of tissue-engineered cartilage. Tissue Eng Part A 2008;14:1821–34.

[86] Athanasiou K, Agrawal C, Barber F, Burkhart S. Orthopaedic applications for PLA-PGA biodegradable polymers. Arthrosc J Arthrosc Relat Surg 1998;14:726–37.

[87] Athanasiou K. Sterilization, toxicity, biocompatibility and clinical applications of polylactic acid/ polyglycolic acid copolymers. Biomaterials 1996;17:93–102.

[88] Eyrich D, Wiese H, Maier G, Skodacek D, Appel B, Sarhan H, et al. In vitro and in vivo cartilage engineering using a combination of chondrocyte-seeded long-term stable fibrin gels and polycaprolactone-based polyurethane scaffolds. Tissue Eng 2007;13:2207–18.

[89] Slaughter BV, Khurshid SS, Fisher OZ, Khademhosseini A, Peppas NA. Hydrogels in regenerative medicine. Adv Mater 2009;21:3307–29.

[90] Nuttelman CR, Rice MA, Rydholm AE, Salinas CN, Shah DN, Anseth KS. Macromolecular monomers for the synthesis of hydrogel niches and their application in cell encapsulation and tissue engineering. Prog Polym Sci 2008;33:167–79.

[91] Ifkovits JL, Burdick JA. Review: photopolymerizable and degradable biomaterials for tissue engineering applications. Tissue Eng 2007;13:2369–85.

[92] West JL, Nguyen KT. Photopolymerizable hydrogels for tissue engineering applications. Biomaterials 2002;23:4307–14.

[93] Bryant SJ, Anseth KS. Photopolymerization of Hydrogel Scaffolds. In: Ma PX, Elisseeff JH, editors. Scaffolding Tissue Eng., Boca Raton, FL: CRC Press, Inc.; 2006, p. 71–90.

[94] Anseth KS, Kloxin AM, Kloxin CJ, Bowman CN. Mechanical Properties of Cellularly Responsive Hydrogels and Their Experimental Determination. Adv Mater 2010;22:3484–94.

[95] Bryant SJ, Durand KL, Anseth KS. Manipulations in hydrogel chemistry control photoencapsulated chondrocyte behavior and their extracellular matrix production. J Biomed Mater Res Part A 2003;67A:1430–6.

[96] Bryant SJ, Anseth KS. Hydrogel properties influence ECM production by chondrocytes photoencapsulated in poly(ethylene glycol) hydrogels. J Biomed Mater Res 2002;59:63–72.

[97] Bryant SJ, Bender RJ, Durand KL, Anseth KS. Encapsulating Chondrocytes in degrading PEG hydrogels with high modulus: Engineering gel structural changes to facilitate cartilaginous tissue production. Biotechnol Bioeng 2004;86:747–55.

[98] Lynn AD, Blakney AK, Kyriakides TR, Bryant SJ. Temporal progression of the host response to implanted poly(ethylene glycol)-based hydrogels. J Biomed Mater Res Part A 2011;96A:621–31.

[99] Nicodemus GD, Skaalure SC, Bryant SJ. Gel structure has an impact on pericellular and extracellular matrix deposition, which subsequently alters metabolic activities in chondrocyte-laden PEG hydrogels. Acta Biomater 2011;7:492–504.

[100] Mason MN, Metters AT, Bowman CN, Anseth KS. Predicting controlled-release behavior of degradable PLA-b-PEG-b-PLA hydrogels. Macromolecules 2001;34:4630–5.

[101] Gould ST, Darling NJ, Anseth KS. Small peptide functionalized thiol-ene hydrogels as culture substrates for understanding valvular interstitial cell activation and de novo tissue deposition. Acta Biomater 2012;8:3201–9.

[102] Anseth KS, Bryant SJ. Controlling the spatial distribution of ECM components in degradable PEG hydrogels for tissue engineering cartilage. J Biomed Mater Res Part A 2003;64A:70–9.

[103] Roberts JJ, Nicodemus GD, Greenwald EC, Bryant SJ. Degradation Improves Tissue Formation in (Un)Loaded Chondrocyte-laden Hydrogels. Clin Orthop Relat Res 2011.

[104] Metters AT, Anseth KS, Bowman CN. Fundamental studies of a novel, biodegradable PEG-b-PLA hydrogel. Polymer (Guildf) 2000;41:3993–4004.

[105] Anseth KS, Metters AT, Bryant SJ, Martens PJ, Elisseeff JH, Bowman CN. In situ forming degradable networks and their application in tissue engineering and drug delivery. J Control Release 2002;78:199–209.

[106] Bryant SJ, Davis-Arehart KA, Luo N, Shoemaker RK, Arthur JA, Anseth KS. Synthesis and Characterization of Photopolymerized Multifunctional Hydrogels: Water-Soluble Poly(Vinyl Alcohol) and Chondroitin Sulfate Macromers for Chondrocyte Encapsulation. Macromolecules 2004;37:6726–33.

[107] Li Q, Williams CG, Sun DDN, Wang J, Leong K, Elisseeff JH. Photocrosslinkable polysaccharides based on chondroitin sulfate. J Biomed Mater Res Part A 2004;68A:28–33.

[108] Prestwich GD, Marecak DM, Marecek JF, Vercruysse KP, Ziebell MR. Controlled chemical modification of hyaluronic acid: synthesis, applications, and biodegradation of hydrazide derivatives. J Control Release 1998;53:93–103.

[109] Chung C, Erickson IE, Mauck RL, Burdick JA. Differential behavior of auricular and articular chondrocytes in hyaluronic acid hydrogels. Tissue Eng Part A 2008;14:1121–31.

[110] Chung C, Burdick JA. Influence of Three-Dimensional Hyaluronic Acid Microenvironments on Mesenchymal Stem Cell Chondrogenesis. Tissue Eng Part A 2009;15:243–54.

[111] Stern R, Asari AA, Sugahara KN. Hyaluronan fragments: An information-rich system. Eur J Cell Biol 2006;85:699–715.

[112] Zhu JM. Bioactive modification of poly(ethylene glycol) hydrogels for tissue engineering. Biomaterials 2010;31:4639–56.

[113] West JL, Hubbell JA. Polymeric Biomaterials with Degradation Sites for Proteases Involved in Cell Migration. Macromolecules 1999;32:241–4.

[114] Park Y, Lutolf MP, Hubbell JA, Hunziker EB, Wong M, et al. Bovine Primary Chondrocyte Culture in Synthetic Matrix Hydrogels as a Scaffold for Cartilage Repair 2004;10.

[115] Lutolf MP, Lauer-Fields JL, Schmoekel HG, Metters AT, Weber FE, Fields GB, et al. Synthetic matrix metalloproteinase-sensitive hydrogels for the conduction of tissue regeneration: engineering cell-invasion characteristics. Proc Natl Acad Sci U S A 2003;100:5413–8.

[116] Lutolf MP, Raeber GP, Zisch AH, Tirelli N, Hubbell JA. Cell-Responsive Synthetic Hydrogels. Adv Mater 2003;15:888–92.

[117] West JL, Lee SH, Miller JS, Moon JJ. Proteolytically degradable hydrogels with a fluorogenic substrate for studies of cellular proteolytic activity and migration. Biotechnol Prog 2005;21:1736–41.

[118] Bahney CS, Hsu C-W, Yoo JU, West JL, Johnstone B. A bioresponsive hydrogel tuned to chondrogenesis of human mesenchymal stem cells. FASEB J 2011;25:1486–96.

[119] Patterson J, Hubbell JA. Enhanced proteolytic degradation of molecularly engineered PEG hydrogels in response to MMP-1 and MMP-2. Biomaterials 2010;31:7836–45.

[120] Fairbanks BD, Schwartz MP, Halevi AE, Nuttelman CR, Bowman CN, Anseth KS. A Versatile Synthetic Extracellular Matrix Mimic via Thiol-Norbornene Photopolymerization. Adv Mater 2009;21:5005–10.

[121] Aimetti AA, Machen AJ, Anseth KS. Poly(ethylene glycol) hydrogels formed by thiol-ene photopolymerization for enzyme-responsive protein delivery. Biomaterials 2009;30:6048–54.

[122] Park Y, Lutolf MP, Hubbell JA, Hunziker EB, Wong M. Bovine primary chondrocyte culture in synthetic matrix metalloproteinase-sensitive poly(ethylene glycol)-based hydrogels as a scaffold for cartilage repair. Tissue Eng 2004;10:515–22.

[123] Johnstone B, Bahney CS, Hsu CW, Yoo JU, West JL. A bioresponsive hydrogel tuned to chondrogenesis of human mesenchymal stem cells. Faseb J 2011;25:1486–96.

[124] Roberts JJ, Bryant SJ. Comparison of photopolymerizable thiol-ene PEG and acrylate-based PEG hydrogels for cartilage development. Biomaterials 2013.

[125] Villanueva I, Bishop NL, Bryant SJ. Medium Osmolarity and Pericellular Matrix Development Improves Chondrocyte Survival When Photoencapsulated in Poly(Ethylene Glycol) Hydrogels at Low Densities. Tissue Eng Part A 2009;15:3037–48.

[126] Amin AK, Huntley JS, Bush PG, Simpson AHRW, Hall AC. Osmolarity influences chondrocyte death in wounded articular cartilage. J Bone Jt Surgery-American Vol 2008;90A:1531–42.

[127] Vinatier C, Mrugala D, Jorgensen C, Guicheux J, Noel D. Cartilage engineering: a crucial combination of cells, biomaterials and biofactors. Trends Biotechnol 2009;27:307–14.

[128] Domm C, Schünke M, Christesen K, Kurz B. Redifferentiation of dedifferentiated bovine articular chondrocytes in alginate culture under low oxygen tension. Osteoarthritis Cartilage 2002;10:13–22.

[129] Waldman SD, Couto DC, Grynpas MD, Pilliar RM, Kandel RA. A single application of cyclic loading can accelerate matrix deposition and enhance the properties of tissue-engineered cartilage. Osteoarthr Cartil 2006;14:323–30.

[130] Bian L, Zhai DY, Zhang EC, Mauck RL, Burdick JA. Dynamic Compressive Loading Enhances Cartilage Matrix Synthesis and Distribution and Suppresses Hypertrophy in hMSC-Laden Hyaluronic Acid Hydrogels. Tissue Eng Part A 2012;18:715–24.

[131] Bryant SJ, Nicodemus GD. Mechanical loading regimes affect the anabolic and catabolic activities by chondrocytes encapsulated in PEG hydrogels. Osteoarthr Cartil 2010;18:126–37.

[132] De Croos JNA, Dhaliwal SS, Grynpas MD, Pilliar RM, Kandel RA. Cyclic compressive mechanical stimulation induces sequential catabolic and anabolic gene changes in chondrocytes resulting in increased extracellular matrix accumulation. Matrix Biol 2006;25:323–31.

[133] Kisiday JD, Lee JH, Siparsky PN, Frisbie DD, Flannery CR, Sandy JD, et al. Catabolic Responses of Chondrocyte-Seeded Peptide Hydrogel to Dynamic Compression. Ann Biomed Eng 2009;37:1368–75.

[134] Farnsworth NL, Antunez LR, Bryant SJ. Dynamic compressive loading differentially regulates chondrocyte anabolic and catabolic activity with age. Biotechnol Bioeng 2013;110:2046–57.

[135] DeLong SA, Moon JJ, West JL. Covalently immobilized gradients of bFGF on hydrogel scaffolds for directed cell migration. Biomaterials 2005;26:3227–34.

[136] McCall JD, Anseth KS. Thiol-ene photopolymerizations provide a facile method to encapsulate proteins and maintain their bioactivity. Biomacromolecules 2012;13:2410–7.

[137] McCall JD, Luoma JE, Anseth KS. Covalently tethered transforming growth factor beta in PEG hydrogels promotes chondrogenic differentiation of encapsulated human mesenchymal stem cells. Drug Deliv Transl Res 2012;2:305–12.

[138] Mann BK, Schmedlen RH, West JL. Tethered-TGF-β increases extracellular matrix production of vascular smooth muscle cells. Biomaterials 2001;22:439–44.

[139] Kawasaki K, Ochi M, Uchio Y, Adachi N, Matsusaki M. Hyaluronic acid enhances proliferation and chondroitin sulfate synthesis in cultured chondrocytes embedded in collagen gels. J Cell Physiol 1999;179:142–8.

[140] Lindenhayn K, Perka C, Spitzer R, Heilmann H, Pommerening K, Mennicke J, et al. Retention of hyaluronic acid in alginate beads: aspects for in vitro cartilage engineering. J Biomed Mater Res 1999;44:149–55.

[141] Bryant SJ, Villanueva I, Gladem SK, Kessler J. Dynamic loading stimulates chondrocyte biosynthesis when encapsulated in charged hydrogels prepared from poly(ethylene glycol) and chondroitin sulfate. Matrix Biol 2010;29:51–62.

[142] Roberts JJ, Nicodemus GD, Giunta S, Bryant SJ. Incorporation of biomimetic matrix molecules in PEG hydrogels enhances matrix deposition and reduces load-induced loss of chondrocyte-secreted matrix. J Biomed Mater Res Part A 2011;97A:281–91.

[143] Bryant SJ, Anseth KS. Hydrogel properties influence ECM production by chondrocytes photoencapsulated in poly(ethylene glycol) hydrogels. J Biomed Mater Res 2002;59:63–72.

[144] Nicodemus GD, Skaalure SC, Bryant SJ. Gel structure has an impact on pericellular and extracellular matrix deposition, which subsequently alters metabolic activities in chondrocyte-laden PEG hydrogels. Acta Biomater 2011;7:492–504.

[145] Chung C, Beecham M, Mauck RL, Burdick JA. The influence of degradation characteristics of hyaluronic acid hydrogels on in vitro neocartilage formation by mesenchymal stem cells. Biomaterials 2009;30:4287–96.

[146] Roberts JJ, Nicodemus GD, Greenwald EC, Bryant SJ. Degradation Improves Tissue Formation in (Un)Loaded Chondrocyte-laden Hydrogels. Clin Orthop Relat Res 2011.

[147] Skaalure SC, Milligan IL, Bryant SJ. Age impacts extracellular matrix metabolism in chondrocytes encapsulated in degradable hydrogels. Biomed Mater 2012;7.

[148] Tran-Khanh N, Hoemann CD, McKee MD, Henderson JE, Buschmann MD. Aged bovine chondrocytes display a diminished capacity to produce a collagen-rich, mechanically functional cartilage extracellular matrix. J Orthop Res 2005;23:1354–62.

[149] Kloxin AM, Kloxin CJ, Bowman CN, Anseth KS. Mechanical Properties of Cellularly Responsive Hydrogels and Their Experimental Determination. Adv Mater 2010;22:3484–94.

Chapter 2

[1] Gillogly SD, Myers TH. Treatment of full-thickness chondral defects with autologous chondrocyte implantation. Orthop Clin North Am 2005;36:433–46.

[2] Kon E, Verdonk P, Condello V, Delcogliano M, Dhollander A, Filardo G, et al. Matrix-assisted autologous chondrocyte transplantation for the repair of cartilage defects of the knee: systematic clinical data review and study quality analysis. Am J Sports Med 2009;37 Suppl 1:156S–66S.

[3] Bryant SJ, Anseth KS. Hydrogel properties influence ECM production by chondrocytes photoencapsulated in poly(ethylene glycol) hydrogels. J Biomed Mater Res 2002;59:63–72.

[4] Anseth KS, Bryant SJ. Controlling the spatial distribution of ECM components in degradable PEG hydrogels for tissue engineering cartilage. J Biomed Mater Res Part A 2003;64A:70–9.

[5] Roberts JJ, Nicodemus GD, Greenwald EC, Bryant SJ. Degradation Improves Tissue Formation in (Un)Loaded Chondrocyte-laden Hydrogels. Clin Orthop Relat Res 2011.

[6] Bryant SJ, Durand KL, Anseth KS. Manipulations in hydrogel chemistry control photoencapsulated chondrocyte behavior and their extracellular matrix production. J Biomed Mater Res Part A 2003;67A:1430–6.

[7] Bryant SJ, Bender RJ, Durand KL, Anseth KS. Encapsulating Chondrocytes in degrading PEG hydrogels with high modulus: Engineering gel structural changes to facilitate cartilaginous tissue production. Biotechnol Bioeng 2004;86:747–55.

[8] Zhu JM. Bioactive modification of poly(ethylene glycol) hydrogels for tissue engineering. Biomaterials 2010;31:4639–56.

[9] Kloxin AM, Kloxin CJ, Bowman CN, Anseth KS. Mechanical Properties of Cellularly Responsive Hydrogels and Their Experimental Determination. Adv Mater 2010;22:3484–94.

[10] Farnsworth NL, Antunez LR, Bryant SJ. Dynamic compressive loading differentially regulates chondrocyte anabolic and catabolic activity with age. Biotechnol Bioeng 2013;110:2046–57.

[11] Tran-Khanh N, Hoemann CD, McKee MD, Henderson JE, Buschmann MD. Aged bovine chondrocytes display a diminished capacity to produce a collagen-rich, mechanically functional cartilage extracellular matrix. J Orthop Res 2005;23:1354–62.

[12] Knudson CB, Knudson W. Cartilage proteoglycans. Semin Cell Dev Biol 2001;12:69–78.

[13] Kawasaki K, Ochi M, Uchio Y, Adachi N, Matsusaki M. Hyaluronic acid enhances proliferation and chondroitin sulfate synthesis in cultured chondrocytes embedded in collagen gels. J Cell Physiol 1999;179:142–8.

[14] Stern R, Asari AA, Sugahara KN. Hyaluronan fragments: An information-rich system. Eur J Cell Biol 2006;85:699–715.

[15] Urban JPG, Hall AC, Gehl KA. Regulation of Matrix Synthesis Rates by the Ionic and Osmotic Environment of Articular Chondrocytes. J Cell Physiol 1993;154:262–70.

[16] Villanueva I, Bishop NL, Bryant SJ. Medium Osmolarity and Pericellular Matrix Development Improves Chondrocyte Survival When Photoencapsulated in Poly(Ethylene Glycol) Hydrogels at Low Densities. Tissue Eng Part A 2009;15:3037–48.

[17] Xu X, Urban JPG, Tirlapur UK, Cui Z. Osmolarity effects on bovine articular chondrocytes during three-dimensional culture in alginate beads. Osteoarthr Cartil 2010;18:433–9.

[18] Fairbanks BD, Schwartz MP, Halevi AE, Nuttelman CR, Bowman CN, Anseth KS. A Versatile Synthetic Extracellular Matrix Mimic via Thiol-Norbornene Photopolymerization. Adv Mater 2009;21:5005–10.

[19] Vernerey FJ, Greenwald EC, Bryant SJ. Triphasic mixture model of cell-mediated enzymatic degradation of hydrogels. Comput Methods Biomech Biomed Engin 2012;15:1197–210.

[20] Dhote V, Vernerey FJ. Mathematical model of the role of degradation on matrix development in hydrogel scaffold. Biomech Model Mechanobiol 2014;13:167–83.

Chapter 3

[1] Hootman JM, Helmick CG. Projections of US prevalence of arthritis and associated activity limitations. Arthritis Rheum 2006;54:226–9.

[2] Richardson JB, Caterson B, Evans EH, Ashton BA, Roberts S. Repair of human articular cartilage after implantation of autologous chondrocytes. J Bone Jt Surgery-British Vol 1999;81B:1064–8.

[3] Gillogly SD, Myers TH. Treatment of full-thickness chondral defects with autologous chondrocyte implantation. Orthop Clin North Am 2005;36:433–46.

[4] Martin JA, Buckwalter JA. Aging, articular cartilage chondrocyte senescence and osteoarthritis. Biogerontology 2002;3:257–64.

[5] West JL, Nguyen KT. Photopolymerizable hydrogels for tissue engineering applications. Biomaterials 2002;23:4307–14.

[6] Anseth KS, Metters AT, Bryant SJ, Martens PJ, Elisseeff JH, Bowman CN. In situ forming degradable networks and their application in tissue engineering and drug delivery. J Control Release 2002;78:199–209.

[7] Elisseeff J, Anseth K, Sims D, McIntosh W, Randolph M, Yaremchuk M, et al. Transdermal photopolymerization of poly(ethylene oxide)-based injectable hydrogels for tissue-engineered cartilage. Plast Reconstr Surg 1999;104:1014–22.

[8] Nicodemus GD, Skaalure SC, Bryant SJ. Gel structure has an impact on pericellular and extracellular matrix deposition, which subsequently alters metabolic activities in chondrocyte-laden PEG hydrogels. Acta Biomater 2011;7:492–504.

[9] Sontjens SHM, Nettles DL, Carnahan MA, Setton LA, Grinstaff MW. Biodendrimer-based hydrogel scaffolds for cartilage tissue repair. Biomacromolecules 2006;7:310–6.

[10] Roberts JJ, Nicodemus GD, Greenwald EC, Bryant SJ. Degradation Improves Tissue Formation in (Un)Loaded Chondrocyte-laden Hydrogels. Clin Orthop Relat Res 2011.

[11] Anseth KS, Bryant SJ. Controlling the spatial distribution of ECM components in degradable PEG hydrogels for tissue engineering cartilage. J Biomed Mater Res Part A 2003;64A:70–9.

[12] Kloxin AM, Kloxin CJ, Bowman CN, Anseth KS. Mechanical Properties of Cellularly Responsive Hydrogels and Their Experimental Determination. Adv Mater 2010;22:3484–94.

[13] Bryant SJ, Durand KL, Anseth KS. Manipulations in hydrogel chemistry control photoencapsulated chondrocyte behavior and their extracellular matrix production. J Biomed Mater Res Part A 2003;67A:1430–6.

[14] Bryant SJ, Bender RJ, Durand KL, Anseth KS. Encapsulating Chondrocytes in degrading PEG hydrogels with high modulus: Engineering gel structural changes to facilitate cartilaginous tissue production. Biotechnol Bioeng 2004;86:747–55.

[15] Bryant SJ, Anseth KS. Hydrogel properties influence ECM production by chondrocytes photoencapsulated in poly(ethylene glycol) hydrogels. J Biomed Mater Res 2002;59:63–72.

[16] Mason MN, Metters AT, Bowman CN, Anseth KS. Predicting controlled-release behavior of degradable PLA-b-PEG-b-PLA hydrogels. Macromolecules 2001;34:4630–5.

[17] Manicourt DH, Devogelaer JP, Thonar EJMA. Products of Cartilage Metabolism. In: Seibel MJ, Robins SP, Bilezikian JP, editors. Dyn. Bone Cartil. Metab., vol. 1, Burlington: Elsevier; 2006, p. 421–49.

[18] Roughley PJ. The structure and function of cartilage proteoglycans. Eur Cell Mater 2006;12:92–101.

[19] Nesic D, Whiteside R, Brittberg M, Wendt D, Martin I, Mainil-Varlet P. Cartilage tissue engineering for degenerative joint disease. Adv Drug Deliv Rev 2006;58:300–22.

[20] McCormick A, Campisi J. Cellular aging and senescence. Curr Opin Cell Biol 1991;3:230–4.

[21] Carlo Jr. MD, Loeser RF. Increased oxidative stress with aging reduces chondrocyte survival: correlation with intracellular glutathione levels. Arthritis Rheum 2003;48:3419–30.

[22] Stockwell RA. The Cell Density of Human Articular and Costal Cartilage. J Anat 1967;101:753–63.

[23] Forsyth CB, Cole A, Murphy G, Bienias JL, Im HJ, Loeser RF. Increased matrix metalloproteinase-13 production with aging by human articular chondrocytes in response to catabolic stimuli. Journals Gerontol Ser a-Biological Sci Med Sci 2005;60:1118–24.

[24] Buckwalter JA, Woo SL, Goldberg VM, Hadley EC, Booth F, Oegema TR, et al. Soft-tissue aging and musculoskeletal function. J Bone Jt Surg Am 1993;75:1533–48.

[25] Pratta MA, Tortorella MD, Arner EC. Age-related changes in aggrecan glycosylation affect cleavage by aggrecanase. J Biol Chem 2000;275:39096–102.

[26] Verbruggen G, Cornelissen M, Almqvist KF, Wang L, Elewaut D, Broddelez C, et al. Influence of aging on the synthesis and morphology of the aggrecans synthesized by differentiated human articular chondrocytes. Osteoarthr Cartil 2000;8:170–9.

[27] Tran-Khanh N, Hoemann CD, McKee MD, Henderson JE, Buschmann MD. Aged bovine chondrocytes display a diminished capacity to produce a collagen-rich, mechanically functional cartilage extracellular matrix. J Orthop Res 2005;23:1354–62.

[28] Sawhney AS, Pathak CP, Hubbell JA. Bioerodible Hydrogels Based on Photopolymerized Poly(ethylene glycol)-co-poly(alpha-hydroxy acid) Diacrylate Macromers. Macromolecules 1993;26:581–7.

[29] Lin-Gibson S, Bencherif S, Cooper JA, Wetzel SJ, Antonucci JM, Vogel BM, et al. Synthesis and characterization of PEG dimethacrylates and their hydrogels. Biomacromolecules 2004;5:1280–7.

[30] Kim YJ, Sah RLY, Doong JYH, Grodzinsky AJ. Fluorometric Assay of DNA in Cartilage Explants Using Hoechst-33258. Anal Biochem 1988;174:168–76.

[31] Woessner JF. Determination of Hydroxyproline in Tissue and Protein Samples Containing Small Proportions of This Imino Acid. Arch Biochem Biophys 1961;93:440–7.

[32] Templeton DM. The basis and applicability of the dimethylmethylene blue binding assay for sulfated glycosaminoglycans. Connect Tissue Res 1988;17:23–32.

[33] Lee MS, Ikenoue T, Trindade MCD, Wong N, Goodman SB, Schurman DJ, et al. Protective effects of intermittent hydrostatic pressure on osteoarthritic chondrocytes activated by bacterial endotoxin in vitro. J Orthop Res 2003;21:117–22.

[34] Metters A, Anseth KS, Bowman CN. Fundamental studies of a novel, biodegradable PEG-b-PLA hydrogel. Polymer (Guildf) 2000;41:3993–4004.

[35] Hardingham T. Proteoglycans and Glycosaminoglycans. In: Seibel MJ, Robins SP, Bilezikian JP, editors. Dyn. Bone Cartil. Metab., vol. 1, Burlington: Elsevier; 2006, p. 85.

[36] Hardingham TE, Fosang AJ. Proteoglycans - Many Forms and Many Functions. Faseb J 1992;6:861–70.

[37] Knudson CB, Knudson W. Cartilage proteoglycans. Semin Cell Dev Biol 2001;12:69–78.

[38] Villanueva I, Bishop NL, Bryant SJ. Medium Osmolarity and Pericellular Matrix Development Improves Chondrocyte Survival When Photoencapsulated in Poly(Ethylene Glycol) Hydrogels at Low Densities. Tissue Eng Part A 2009;15:3037–48.

[39] Poole AR, Wu W, Billinghurst RC, Pidoux I, Antoniou J, Zukor D, et al. Sites of collagenase cleavage and denaturation of type II collagen in aging and osteoarthritic articular cartilage and their relationship to the distribution of matrix metalloproteinase 1 and matrix metalloproteinase 13. Arthritis Rheum 2002;46:2087–94.

[40] Welgus HG, Campbell EJ, Bar-Shavit Z, Senior RM, Teitelbaum SL. Human alveolar macrophages produce a fibroblast-like collagenase and collagenase inhibitor. J Clin Invest 1985;76:219–24.

[41] Rossa C, Liu M, Bronson P, Kirkwood KL. Transcriptional activation of MMP-13 by periodontal pathogenic LPS requires p38 MAP kinase. J Endotoxin Res 2007;13:85–93.

[42] Dahlberg L, Billinghurst RC, Manner P, Nelson F, Webb G, Ionescu M, et al. Selective enhancement of collagenase-mediated cleavage of resident type II collagen in cultured osteoarthritic cartilage and arrest with a synthetic inhibitor that spares collagenase 1 (matrix metalloproteinase 1). Arthritis Rheum 2000;43:673–82.

[43] Mok SS, Masuda K, Hauselmann HJ, Aydelotte MB, Thonar EJMA. Aggrecan Synthesized by Mature Bovine Chondrocytes Suspended in Alginate - Identification of 2 Distinct Metabolic Matrix Pools. J Biol Chem 1994;269:33021–7.

[44] Sandy JD, Flannery CR, Neame PJ, Lohmander LS. The Structure of Aggrecan Fragments in Human Synovial-Fluid - Evidence for the Involvement in Osteoarthritis of a

Novel Proteinase Which Cleaves the Glu-373-Ala-374 Bond of the Interglobular Domain. J Clin Invest 1992;89:1512–6.

[45] Lohmander LS, Neame PJ, Sandy JD. The Structure of Aggrecan Fragments in Human Synovial-Fluid - Evidence That Aggrecanase Mediates Cartilage Degradation in Inflammatory Joint Disease, Joint Injury, and Osteoarthritis. Arthritis Rheum 1993;36:1214–22.

[46] De Croos JNA, Dhaliwal SS, Grynpas MD, Pilliar RM, Kandel RA. Cyclic compressive mechanical stimulation induces sequential catabolic and anabolic gene changes in chondrocytes resulting in increased extracellular matrix accumulation. Matrix Biol 2006;25:323–31.

[47] Poole AR, Nelson F, Dahlberg L, Tchetina E, Kobayashi M, Yasuda T, et al. Proteolysis of the collagen fibril in osteoarthritis. Proteases Regul Biol Process 2003;70:115–23.

[48] Connelly JT, Wilson CG, Levenston ME. Characterization of proteoglycan production and processing by chondrocytes and BMSCs in tissue engineered constructs. Osteoarthr Cartil 2008;16:1092–100.

[49] Wong M, Park Y, Lutolf MP, Hubbell JA, Hunziker EB. Bovine primary chondrocyte culture in synthetic matrix metalloproteinase-sensitive poly(ethylene glycol)-based hydrogels as a scaffold for cartilage repair. Tissue Eng 2004;10:515–22.

[50] West JL, Lee SH, Miller JS, Moon JJ. Proteolytically degradable hydrogels with a fluorogenic substrate for studies of cellular proteolytic activity and migration. Biotechnol Prog 2005;21:1736–41.

[51] Fairbanks BD, Schwartz MP, Halevi AE, Nuttelman CR, Bowman CN, Anseth KS. A Versatile Synthetic Extracellular Matrix Mimic via Thiol-Norbornene Photopolymerization. Adv Mater 2009;21:5005–10.

[52] Yoo HS, Lee EA, Yoon JJ, Park TG. Hyaluronic acid modified biodegradable scaffolds for cartilage tissue engineering. Biomaterials 2005;26:1925–33.

[53] Bryant SJ, Villanueva I, Gladem SK, Kessler J. Dynamic loading stimulates chondrocyte biosynthesis when encapsulated in charged hydrogels prepared from poly(ethylene glycol) and chondroitin sulfate. Matrix Biol 2010;29:51–62.

[54] Yaeger PC, Masi TL, de Ortiz JL, Binette F, Tubo R, McPherson JM. Synergistic action of transforming growth factor-beta and insulin-like growth factor-I induces expression of type II collagen and aggrecan genes in adult human articular chondrocytes. Exp Cell Res 1997;237:318–25.

[55] Sandy JD, Gamett D, Thompson V, Verscharen C. Chondrocyte-mediated catabolism of aggrecan: aggrecanase-dependent cleavage induced by interleukin-1 or retinoic acid can be inhibited by glucosamine. Biochem J 1998;335:59–66.

[56] Nicodemus GD, Bryant SJ. The role of hydrogel structure and dynamic loading on chondrocyte gene expression and matrix formation. J Biomech 2008;41:1528–36.

[57] Kelly TAN, Ng KW, Wang CCB, Ateshian GA, Hung CT. Spatial and temporal development of chondrocyte-seeded agarose constructs in free-swelling and dynamically loaded cultures. J Biomech 2006;39:1489–97.

Chapter 4

[1] Bryant SJ, Durand KL, Anseth KS. Manipulations in hydrogel chemistry control photoencapsulated chondrocyte behavior and their extracellular matrix production. J Biomed Mater Res Part A 2003;67A:1430–6.

[2] Bryant SJ, Anseth KS. Hydrogel properties influence ECM production by chondrocytes photoencapsulated in poly(ethylene glycol) hydrogels. J Biomed Mater Res 2002;59:63–72.

[3] Bryant SJ, Chowdhury TT, Lee DA, Bader DL, Anseth KS. Crosslinking density influences chondrocyte metabolism in dynamically loaded photocrosslinked poly(ethylene glycol) hydrogels. Ann Biomed Eng 2004;32:407–17.

[4] Nicodemus GD, Skaalure SC, Bryant SJ. Gel structure has an impact on pericellular and extracellular matrix deposition, which subsequently alters metabolic activities in chondrocyte-laden PEG hydrogels. Acta Biomater 2011;7:492–504.

[5] Roberts JJ, Nicodemus GD, Greenwald EC, Bryant SJ. Degradation Improves Tissue Formation in (Un)Loaded Chondrocyte-laden Hydrogels. Clin Orthop Relat Res 2011.

[6] Bryant SJ, Bender RJ, Durand KL, Anseth KS. Encapsulating Chondrocytes in degrading PEG hydrogels with high modulus: Engineering gel structural changes to facilitate cartilaginous tissue production. Biotechnol Bioeng 2004;86:747–55.

[7] Anseth KS, Bryant SJ. Controlling the spatial distribution of ECM components in degradable PEG hydrogels for tissue engineering cartilage. J Biomed Mater Res Part A 2003;64A:70–9.

[8] Goldberg VM, Buckwalter JA. Hyaluronans in the treatment of osteoarthritis of the knee: evidence for disease-modifying activity. Osteoarthr Cartil 2005;13:216–24.

[9] Itano N, Sawai T, Yoshida M, Lenas P, Yamada Y, Imagawa M, et al. Three isoforms of mammalian hyaluronan synthases have distinct enzymatic properties. J Biol Chem 1999;274:25085–92.

[10] Buckwalter JA, Rosenberg LC. Electron-Microscopic Studies of Cartilage Proteoglycans - Direct Evidence for the Variable Length of the Chondroitin Sulfate-Rich Region of Proteoglycan Subunit Core Protein. J Biol Chem 1982;257:9830–9.

[11] Knudson CB, Knudson W. Cartilage proteoglycans. Semin Cell Dev Biol 2001;12:69–78.

[12] Roughley PJ. The structure and function of cartilage proteoglycans. Eur Cell Mater 2006;12:92–101.

[13] Chen WYJ, Abatangelo G. Functions of hyaluronan in wound repair. Wound Repair Regen 1999;7:79–89.

[14] Kawasaki K, Ochi M, Uchio Y, Adachi N, Matsusaki M. Hyaluronic acid enhances proliferation and chondroitin sulfate synthesis in cultured chondrocytes embedded in collagen gels. J Cell Physiol 1999;179:142–8.

[15] Lindenhayn K, Perka C, Spitzer RS, Heilmann HH, Pommerening K, Mennicke J, et al. Retention of hyaluronic acid in alginate beads: Aspects for in vitro cartilage engineering. J Biomed Mater Res 1999;44:149–55.

[16] Park TG, Yoo HS, Lee EA, Yoon JJ. Hyaluronic acid modified biodegradable scaffolds for cartilage tissue engineering. Biomaterials 2005;26:1925–33.

[17] Yamane S, Iwasaki N, Majima T, Funakoshi T, Masuko T, Harada K, et al. Feasibility of chitosan-based hyaluronic acid hybrid biomaterial for a novel scaffold in cartilage tissue engineering. Biomaterials 2005;26:611–9.

[18] Kim IL, Mauck RL, Burdick JA. Hydrogel design for cartilage tissue engineering: A case study with hyaluronic acid. Biomaterials 2011;32:8771–82.

[19] Burdick JA, Chung C, Jia XQ, Randolph MA, Langer R. Controlled degradation and mechanical behavior of photopolymerized hyaluronic acid networks. Biomacromolecules 2005;6:386–91.

[20] Burdick JA, Prestwich GD. Hyaluronic Acid Hydrogels for Biomedical Applications. Adv Mater 2011;23:H41–H56.

[21] Shu XZ, Liu Y, Luo Y, Roberts MC, Prestwich GD. Disulfide Cross-Linked Hyaluronan Hydrogels. Biomacromolecules 2002;3:1304–11.

[22] Shu XZ, Liu Y, Palumbo FS, Luo Y, Prestwich GD. In situ crosslinkable hyaluronan hydrogels for tissue engineering. Biomaterials 2004;25:1339–48.

[23] Prestwich GD. Hyaluronic acid-based clinical biomaterials derived for cell and molecule delivery in regenerative medicine. J Control Release 2011;155:193–9.

[24] Ghosh K, Shu XZ, Mou R, Lombardi J, Prestwich GD, Rafailovich MH, et al. Rheological characterization of in situ cross-linkable hyaluronan hydrogels. Biomacromolecules 2005;6:2857–65.

[25] Mansour JM. Biomechanics of Cartilage. In: Oatis CA, editor. Kinesiol. Mech. pathomechanics Hum. Mov., Baltimore, MD: Lippincott Williams & Wilkins; 2003, p. 66–75.

[26] Liu Y, Shu XZ, Prestwich GD. Osteochondral Defect Repair with Autologous Bone Marrow-Derived Mesenchymal Stem Cells in an Injectable, In Situ, Cross-Linked Synthetic Extracellular Matrix. Tissue Eng 2006;12:3405–16.

[27] Chung C, Burdick JA. Influence of Three-Dimensional Hyaluronic Acid Microenvironments on Mesenchymal Stem Cell Chondrogenesis. Tissue Eng Part A 2009;15:243–54.

[28] Stern R, Asari AA, Sugahara KN. Hyaluronan fragments: An information-rich system. Eur J Cell Biol 2006;85:699–715.

[29] Sahoo S, Chung C, Khetan S, Burdick J a. Hydrolytically degradable hyaluronic acid hydrogels with controlled temporal structures. Biomacromolecules 2008;9:1088–92.

[30] Chung C, Beecham M, Mauck RL, Burdick JA. The influence of degradation characteristics of hyaluronic acid hydrogels on in vitro neocartilage formation by mesenchymal stem cells. Biomaterials 2009;30:4287–96.

[31] Allison DD, Grande-Allen KJ. Review. Hyaluronan: A powerful tissue engineering tool. Tissue Eng 2006;12:2131–40.

[32] Noble PW. Hyaluronan and its catabolic products in tissue injury and repair. Matrix Biol 2002;21:25–9.

[33] Lindenhayn K, Perka C, Spitzer R, Heilmann H, Pommerening K, Mennicke J, et al. Retention of hyaluronic acid in alginate beads: aspects for in vitro cartilage engineering. J Biomed Mater Res 1999;44:149–55.

[34] Praest BM, Greiling H, Kock R. Assay of synovial fluid parameters: hyaluronan concentration as a potential marker for joint diseases. Clin Chim Acta 1997;266:117–28.

[35] Holmes MWA, Bayliss MT, Muir H. Hyaluronic-Acid in Human Articular-Cartilage - Age-Related-Changes in Content and Size. Biochem J 1988;250:435–41.

[36] Ohno S, Ohno-Nakahara M, Knudson CB, Knudson W. Induction of MMP-3 by Hyaluronan Oligosaccharides in Temporomandibular Joint Chondrocytes. J Dent Res 2005;84:1005–9.

[37] Ohno S, Im H-J, Knudson CB, Knudson W. Hyaluronan oligosaccharides induce matrix metalloproteinase 13 via transcriptional activation of NFkappaB and p38 MAP kinase in articular chondrocytes. J Biol Chem 2006;281:17952–60.

[38] Yoo HS, Lee EA, Yoon JJ, Park TG. Hyaluronic acid modified biodegradable scaffolds for cartilage tissue engineering. Biomaterials 2005;26:1925–33.

[39] Knudson CB. Hyaluronan Receptor-Directed Assembly of Chondrocyte Pericellular Matrix. J Cell Biol 1993;120:825–34.

[40] Skaalure SC, Milligan IL, Bryant SJ. Age impacts extracellular matrix metabolism in chondrocytes encapsulated in degradable hydrogels. Biomed Mater 2012;7.

[41] Farnsworth NL, Antunez LR, Bryant SJ. Dynamic compressive loading differentially regulates chondrocyte anabolic and catabolic activity with age. Biotechnol Bioeng 2013;110:2046–57.

[42] Richardson JB, Caterson B, Evans EH, Ashton BA, Roberts S. Repair of human articular cartilage after implantation of autologous chondrocytes. J Bone Jt Surgery-British Vol 1999;81B:1064–8.

[43] Gillogly SD, Myers TH. Treatment of full-thickness chondral defects with autologous chondrocyte implantation. Orthop Clin North Am 2005;36:433–46.

[44] Sawhney AS, Pathak CP, Hubbell JA. Bioerodible Hydrogels Based on Photopolymerized Poly(Ethylene Glycol)-Co-Poly(Alpha-Hydroxy Acid) Diacrylate Macromers. Macromolecules 1993;26:581–7.

[45] Lin-Gibson S, Bencherif S, Cooper JA, Wetzel SJ, Antonucci JM, Vogel BM, et al. Synthesis and characterization of PEG dimethacrylates and their hydrogels. Biomacromolecules 2004;5:1280–7.

[46] Villanueva I, Bishop NL, Bryant SJ. Medium Osmolarity and Pericellular Matrix Development Improves Chondrocyte Survival When Photoencapsulated in Poly(Ethylene Glycol) Hydrogels at Low Densities. Tissue Eng Part A 2009;15:3037–48.

[47] Ogamo A, Matsuzaki K, Uchiyama H, Nagasawa K. Preparation and Properties of Fluorescent Glycosaminoglycuronans Labeled with 5-Aminofluorescein. Carbohydr Res 1982;105:69–85.

[48] Metters AT, Anseth KS, Bowman CN. A statistical kinetic model for the bulk degradation of PLA-b-PEG-b-PLA hydrogel networks: Incorporating network non-idealities. J Phys Chem B 2001;105:8069–76.

[49] Kim YJ, Sah RLY, Doong JYH, Grodzinsky AJ. Fluorometric Assay of DNA in Cartilage Explants Using Hoechst-33258. Anal Biochem 1988;174:168–76.

[50] Woessner JF. Determination of Hydroxyproline in Tissue and Protein Samples Containing Small Proportions of This Imino Acid. Arch Biochem Biophys 1961;93:440–7.

[51] Templeton DM. The Basis and Applicability of the Dimethylmethylene Blue Binding Assay for Sulfated Glycosaminoglycans. Connect Tissue Res 1988;17:23–32.

[52] Ishida O, Tanaka Y, Morimoto I, Takigawa M, Eto S. Chondrocytes are regulated by cellular adhesion through CD44 and hyaluronic acid pathway. J Bone Miner Res 1997;12:1657–63.

[53] Evanko SP, Wight TN. Intracellular Localization of Hyaluronan in Proliferating Cells. J Histochem Cytochem 1999;47:1331–41.

[54] Von der Mark K, Kirsch T, Nerlich A, Kuss A, Weseloh G, Gluckert K, et al. Type-X Collagen-Synthesis in Human Osteoarthritic Cartilage - Indication of Chondrocyte Hypertrophy. Arthritis Rheum 1992;35:806–11.

[55] Bayliss MT, Howat S, Davidson C, Dudhia J. The organization of aggrecan in human articular cartilage - Evidence for age-related changes in the rate of aggregation of newly synthesized molecules. J Biol Chem 2000;275:6321–7.

[56] Roberts JJ, Nicodemus GD, Giunta S, Bryant SJ. Incorporation of biomimetic matrix molecules in PEG hydrogels enhances matrix deposition and reduces load-induced loss of chondrocyte-secreted matrix. J Biomed Mater Res Part A 2011;97A:281–91.

[57] Hua Q, Knudson CB, Knudson W. Internalization of Hyaluronan by Chondrocytes Occurs Via Receptor-Mediated Endocytosis. J Cell Sci 1993;106:365–75.

[58] Kvam BJ, Fragonas E, Degrassi A, Kvam C, Matulova M, Pollesello P, et al. Oxygen-Derived Free-Radical (Odfr) Action on Hyaluronan (Ha), on 2 Ha Ester Derivatives, and on the Metabolism of Articular Chondrocytes. Exp Cell Res 1995;218:79–86.

[59] Guilak F, Butler DL, Goldstein SA. Functional tissue engineering - The role of biomechanics in articular cartilage repair. Clin Orthop Relat Res 2001:S295–S305.

[60] Darling EM, Athanasiou KA. Biomechanical strategies for articular cartilage regeneration. Ann Biomed Eng 2003;31:1114–24.

[61] Bian L, Zhai DY, Zhang EC, Mauck RL, Burdick JA. Dynamic Compressive Loading Enhances Cartilage Matrix Synthesis and Distribution and Suppresses Hypertrophy in hMSC-Laden Hyaluronic Acid Hydrogels. Tissue Eng Part A 2012;18:715–24.

[62] Roberts JJ, Elder RM, Neumann AJ, Jayaraman A, Bryant SJ. Interaction of Hyaluronan Binding Peptides with Glycosaminoglycans in Poly(ethylene glycol) Hydrogels. Biomacromolecules 2014.

Chapter 5

[1] Bryant SJ, Durand KL, Anseth KS. Manipulations in hydrogel chemistry control photoencapsulated chondrocyte behavior and their extracellular matrix production. J Biomed Mater Res Part A 2003;67A:1430–6.

[2] Bryant SJ, Anseth KS. Hydrogel properties influence ECM production by chondrocytes photoencapsulated in poly(ethylene glycol) hydrogels. J Biomed Mater Res 2002;59:63–72.

[3] Roberts JJ, Nicodemus GD, Greenwald EC, Bryant SJ. Degradation Improves Tissue Formation in (Un)Loaded Chondrocyte-laden Hydrogels. Clin Orthop Relat Res 2011.

[4] Anseth KS, Bryant SJ. Controlling the spatial distribution of ECM components in degradable PEG hydrogels for tissue engineering cartilage. J Biomed Mater Res Part A 2003;64A:70–9.

[5] Tran-Khanh N, Hoemann CD, McKee MD, Henderson JE, Buschmann MD. Aged bovine chondrocytes display a diminished capacity to produce a collagen-rich, mechanically functional cartilage extracellular matrix. J Orthop Res 2005;23:1354–62.

[6] Hall AC, Horwitz ER, Wilkins RJ. The cellular physiology of articular cartilage. Exp Physiol 1996;81:535–45.

[7] Urban JPG, Hall AC, Gehl KA. Regulation of Matrix Synthesis Rates by the Ionic and Osmotic Environment of Articular Chondrocytes. J Cell Physiol 1993;154:262–70.

[8] Villanueva I, Bishop NL, Bryant SJ. Medium Osmolarity and Pericellular Matrix Development Improves Chondrocyte Survival When Photoencapsulated in Poly(Ethylene Glycol) Hydrogels at Low Densities. Tissue Eng Part A 2009;15:3037–48.

[9] Negoro K, Kobayashi S, Takeno K, Uchida K, Baba H. Effect of osmolarity on glycosaminoglycan production and cell metabolism of articular chondrocyte under three-dimensional culture system. Clin Exp Rheumatol 2008;26:534–41.

[10] Xu X, Urban JPG, Tirlapur UK, Cui Z. Osmolarity effects on bovine articular chondrocytes during three-dimensional culture in alginate beads. Osteoarthr Cartil 2010;18:433–9.

[11] Lin-Gibson S, Bencherif S, Cooper JA, Wetzel SJ, Antonucci JM, Vogel BM, et al. Synthesis and characterization of PEG dimethacrylates and their hydrogels. Biomacromolecules 2004;5:1280–7.

[12] Skaalure SC, Milligan IL, Bryant SJ. Age impacts extracellular matrix metabolism in chondrocytes encapsulated in degradable hydrogels. Biomed Mater 2012;7.

[13] Skaalure SC, Dimson SO, Pennington AM, Bryant SJ. Semi-interpenetrating networks of hyaluronic acid in degradable PEG hydrogels for cartilage tissue engineering. Acta Biomater 2014.

[14] Metters AT, Anseth KS, Bowman CN. A statistical kinetic model for the bulk degradation of PLA-b-PEG-b-PLA hydrogel networks: Incorporating network non-idealities. J Phys Chem B 2001;105:8069–76.

[15] Mason MN, Metters AT, Bowman CN, Anseth KS. Predicting controlled-release behavior of degradable PLA-b-PEG-b-PLA hydrogels. Macromolecules 2001;34:4630–5.

[16] Kim YJ, Sah RLY, Doong JYH, Grodzinsky AJ. Fluorometric Assay of DNA in Cartilage Explants Using Hoechst-33258. Anal Biochem 1988;174:168–76.

[17] Woessner JF. Determination of Hydroxyproline in Tissue and Protein Samples Containing Small Proportions of This Imino Acid. Arch Biochem Biophys 1961;93:440–7.

[18] Mobasheri A. Regulation of Na+, K+-ATPase density by the extracellular ionic and osmotic environment in bovine articular chondrocytes. Physiol Res 1999;48:509–12.

[19] Hoffmann EK, Dunham PB. Membrane Mechanisms and Intracellular Signalling in Cell Volume Regulation. Int Rev Cytol 1995;161:173–262.

[20] Lee JC, Timasheff SN. The stabilization of proteins by sucrose. J Biol Chem 1981;256:7193–201.

[21] Scott JE. Proteoglycan-fibrillar collagen interactions. Biochem J 1988;252:313–23.

[22] Jimenez SA, Ala-Kokko L, Prockop DJ, Merryman CF, Shepard N, Dodge GR. Characterization of human type II procollagen and collagen-specific antibodies and their application to the study of human type II collagen processing and ultrastructure. Matrix Biol 1997;16:29–39.

Chapter 6

[1] Gillogly SD, Myers TH. Treatment of full-thickness chondral defects with autologous chondrocyte implantation. Orthop Clin North Am 2005;36:433–46.

[2] Richardson JB, Caterson B, Evans EH, Ashton BA, Roberts S. Repair of human articular cartilage after implantation of autologous chondrocytes. J Bone Jt Surgery-British Vol 1999;81B:1064–8.

[3] Vanlauwe J, Almqvist F, Bellemans J, Huskin J-P, Verdonk R, Victor J. Repair of symptomatic cartilage lesions of the knee: the place of autologous chondrocyte implantation. Acta Orthop Belg 2007;73:145–58.

[4] Bartlett W, Skinner JA, Gooding CR, Carrington RWJ, Flanagan AM, Briggs TWR, et al. Autologous chondrocyte implantation versus matrix-induced autologous chondrocyte implantation for osteochondral defects of the knee: a prospective, randomised study. J Bone Joint Surg Br 2005;87:640–5.

[5] Kon E, Verdonk P, Condello V, Delcogliano M, Dhollander A, Filardo G, et al. Matrix-Assisted Autologous Chondrocyte Transplantation for the Repair of Cartilage Defects of the Knee Systematic Clinical Data Review and Study Quality Analysis. Am J Sports Med 2009;37:156S–166S.

[6] Skaalure SC, Milligan IL, Bryant SJ. Age impacts extracellular matrix metabolism in chondrocytes encapsulated in degradable hydrogels. Biomed Mater 2012;7.

[7] Farnsworth NL, Antunez LR, Bryant SJ. Dynamic compressive loading differentially regulates chondrocyte anabolic and catabolic activity with age. Biotechnol Bioeng 2013;110:2046–57.

[8] Bryant SJ, Durand KL, Anseth KS. Manipulations in hydrogel chemistry control photoencapsulated chondrocyte behavior and their extracellular matrix production. J Biomed Mater Res Part A 2003;67A:1430–6.

[9] Bryant SJ, Anseth KS. Hydrogel properties influence ECM production by chondrocytes photoencapsulated in poly(ethylene glycol) hydrogels. J Biomed Mater Res 2002;59:63–72.

[10] Bryant SJ, Chowdhury TT, Lee DA, Bader DL, Anseth KS. Crosslinking density influences chondrocyte metabolism in dynamically loaded photocrosslinked poly(ethylene glycol) hydrogels. Ann Biomed Eng 2004;32:407–17.

[11] Nicodemus GD, Skaalure SC, Bryant SJ. Gel structure has an impact on pericellular and extracellular matrix deposition, which subsequently alters metabolic activities in chondrocyte-laden PEG hydrogels. Acta Biomater 2011;7:492–504.

[12] Bryant SJ, Bender RJ, Durand KL, Anseth KS. Encapsulating Chondrocytes in degrading PEG hydrogels with high modulus: Engineering gel structural changes to facilitate cartilaginous tissue production. Biotechnol Bioeng 2004;86:747–55.

[13] Anseth KS, Bryant SJ. Controlling the spatial distribution of ECM components in degradable PEG hydrogels for tissue engineering cartilage. J Biomed Mater Res Part A 2003;64A:70–9.

[14] Roberts JJ, Nicodemus GD, Greenwald EC, Bryant SJ. Degradation Improves Tissue Formation in (Un)Loaded Chondrocyte-laden Hydrogels. Clin Orthop Relat Res 2011.

[15] West JL, Hubbell JA. Polymeric Biomaterials with Degradation Sites for Proteases Involved in Cell Migration. Macromolecules 1999;32:241–4.

[16] Fairbanks BD, Schwartz MP, Halevi AE, Nuttelman CR, Bowman CN, Anseth KS. A Versatile Synthetic Extracellular Matrix Mimic via Thiol-Norbornene Photopolymerization. Adv Mater 2009;21:5005–10.

[17] Lutolf MP, Lauer-Fields JL, Schmoekel HG, Metters AT, Weber FE, Fields GB, et al. Synthetic matrix metalloproteinase-sensitive hydrogels for the conduction of tissue regeneration: engineering cell-invasion characteristics. Proc Natl Acad Sci U S A 2003;100:5413–8.

[18] Patterson J, Hubbell JA. Enhanced proteolytic degradation of molecularly engineered PEG hydrogels in response to MMP-1 and MMP-2. Biomaterials 2010;31:7836–45.

[19] West JL, Lee SH, Miller JS, Moon JJ. Proteolytically degradable hydrogels with a fluorogenic substrate for studies of cellular proteolytic activity and migration. Biotechnol Prog 2005;21:1736–41.

[20] Lévesque SG, Shoichet MS. Synthesis of enzyme-degradable, peptide-cross-linked dextran hydrogels. Bioconjug Chem 2007;18:874–85.

[21] Vernerey FJ, Greenwald EC, Bryant SJ. Triphasic mixture model of cell-mediated enzymatic degradation of hydrogels. Comput Methods Biomech Biomed Engin 2012;15:1197–210.

[22] Dhote V, Vernerey FJ. Mathematical model of the role of degradation on matrix development in hydrogel scaffold. Biomech Model Mechanobiol 2013.

[23] Bahney CS, Hsu C-W, Yoo JU, West JL, Johnstone B. A bioresponsive hydrogel tuned to chondrogenesis of human mesenchymal stem cells. FASEB J 2011;25:1486–96.

[24] Park Y, Lutolf MP, Hubbell JA, Hunziker EB, Wong M. Bovine primary chondrocyte culture in synthetic matrix metalloproteinase-sensitive poly(ethylene glycol)-based hydrogels as a scaffold for cartilage repair. Tissue Eng 2004;10:515–22.

[25] Roberts JJ, Bryant SJ. Comparison of photopolymerizable thiol-ene PEG and acrylate-based PEG hydrogels for cartilage development. Biomaterials 2013;34:9969–79.

[26] Manicourt DH, Devogelaer JP, Thonar EJMA. Products of Cartilage Metabolism. In: Seibel MJ, Robins SP, Bilezikian JP, editors. Dyn. Bone Cartil. Metab., vol. 1, Burlington: Elsevier; 2006, p. 421–49.

[27] Knudson CB, Knudson W. Cartilage proteoglycans. Semin Cell Dev Biol 2001;12:69–78.

[28] Buckwalter JA, Rosenberg LC. Electron-Microscopic Studies of Cartilage Proteoglycans - Direct Evidence for the Variable Length of the Chondroitin Sulfate-Rich Region of Proteoglycan Subunit Core Protein. J Biol Chem 1982;257:9830–9.

[29] Caterson B, Flannery CR, Hughes GE, Little CB. Mechanisms involved in cartilage proteoglycan catabolism. Matrix Biol 2000;19:333–44.

[30] Durigova M, Nagase H, Mort JS, Roughley PJ. MMPs are less efficient than ADAMTS5 in cleaving aggrecan core protein. Matrix Biol 2011;30:145–53.

[31] Lark MW, Gordy JT, Weidner JR, Ayala J, Kimura JH, Williams HR, et al. Cell-mediated Catabolism of Aggrecan. J Biol Chem 1995;270:2550–6.

[32] Ilic MZ, Handley CJ, Robinson HC, Mok MT. Mechanism of Catabolism of Aggrecan by Articular Cartilage. Arch Biochem Biophys 1992;294:115–22.

[33] Flannery CR, Little CB, Caterson B. Molecular cloning and sequence analysis of the aggrecan interglobular domain from porcine, equine, bovine and ovine cartilage: comparison of proteinase-susceptible regions and sites of keratan sulfate substitution. Matrix Biol 1998;16:507–11.

[34] Lutolf MP, Raeber GP, Zisch AH, Tirelli N, Hubbell JA. Cell-Responsive Synthetic Hydrogels. Adv Mater 2003;15:888–92.

[35] Shih H, Lin C-C. Visible Light-Mediated Thiol-Ene Hydrogelation Using Eosin-Y as the Only Photoinitiator. Macromol Rapid Commun 2013;34:269–73.

[36] Kim YJ, Sah RLY, Doong JYH, Grodzinsky AJ. Fluorometric Assay of DNA in Cartilage Explants Using Hoechst-33258. Anal Biochem 1988;174:168–76.

[37] Woessner JF. Determination of Hydroxyproline in Tissue and Protein Samples Containing Small Proportions of This Imino Acid. Arch Biochem Biophys 1961;93:440–7.

[38] Templeton DM. The Basis and Applicability of the Dimethylmethylene Blue Binding Assay for Sulfated Glycosaminoglycans. Connect Tissue Res 1988;17:23–32.

[39] Martin JA, Buckwalter JA. Aging, articular cartilage chondrocyte senescence and osteoarthritis. Biogerontology 2002;3:257–64.

[40] Mok SS, Masuda K, Hauselmann HJ, Aydelotte MB, Thonar EJMA. Aggrecan Synthesized by Mature Bovine Chondrocytes Suspended in Alginate - Identification of 2 Distinct Metabolic Matrix Pools. J Biol Chem 1994;269:33021–7.

[41] Homandberg GA, Davis G, Maniglia C, Shrikhande A. Cartilage chondrolysis by fibronectin fragments causes cleavage of aggrecan at the same site as found in osteoarthritic cartilage. Osteoarthr Cartil 1997;5:450–3.

[42] Struglics A, Larsson S, Hansson M, Lohmander LS. Western blot quantification of aggrecan fragments in human synovial fluid indicates differences in fragment patterns between joint diseases. Osteoarthr Cartil 2009;17:497–506.

[43] Nagase H, Kashiwagi M. Aggrecanases and cartilage matrix degradation. Arthritis Res Ther 2003;5:94–103.

[44] Martel-Pelletier J, Boileau C, Pelletier J-P, Roughley PJ. Cartilage in normal and osteoarthritis conditions. Best Pract Res Clin Rheumatol 2008;22:351–84.

[45] Middleton J, Manthey A, Tyler J. Insulin-like growth factor (IGF) receptor, IGF-I, interleukin-1 beta (IL-1 beta), and IL-6 mRNA expression in osteoarthritic and normal human cartilage. J Histochem Cytochem 1996;44:133–41.

[46] Flannery CR, Little CB, Hughes CE, Curtis CL, Caterson B, Jones SA. IL-6 and its soluble receptor augment aggrecanase-mediated proteoglycan catabolism in articular cartilage. Matrix Biol 2000;19:549–53.

[47] Edwards DR, Porter S, Clark IM, Kevorkian L. The ADAMTS metalloproteinases. Biochem J 2005;386:15–27.

[48] Tortorella MD, Liu R-Q, Burn T, Newton RC, Arner E. Characterization of human aggrecanase 2 (ADAM-TS5): substrate specificity studies and comparison with aggrecanase 1 (ADAM-TS4). Matrix Biol 2002;21:499–511.

[49] Lee MS, Ikenoue T, Trindade MCD, Wong N, Goodman SB, Schurman DJ, et al. Protective effects of intermittent hydrostatic pressure on osteoarthritic chondrocytes activated by bacterial endotoxin in vitro. J Orthop Res 2003;21:117–22.

[50] Patel L, Sun W, Glasson SS, Morris EA, Flannery CR, Chockalingam PS. Tenascin-C induces inflammatory mediators and matrix degradation in osteoarthritic cartilage. BMC Musculoskelet Disord 2011;12.

[51] Morales TI, Wahl LM, Hascall VC. The Effect of Bacterial Lipopolysaccharides on the Biosynthesis and Release of Proteoglycans from Calf Articular Cartilage Cultures. J Biol Chem 1984;259:6720–9.

[52] Roberts JJ, Nicodemus GD, Greenwald EC, Bryant SJ. Degradation Improves Tissue Formation in (Un)Loaded Chondrocyte-laden Hydrogels. Clin Orthop Relat Res 2011.

[53] Mok SS, Masuda K, Hauselmann HJ, Aydelotte MB, Thonar EJMA. Aggrecan Synthesized by Mature Bovine Chondrocytes Suspended in Alginate - Identification of 2 Distinct Metabolic Matrix Pools. J Biol Chem 1994;269:33021–7.

[54] Hauselmann HJ, Masuda K, Hunziker EB, Neidhart M, Mok SS, Michel BA, et al. Adult human chondrocytes cultured in alginate form a matrix similar to native human articular cartilage. Am J Physiol Physiol 1996;271:C742–C752.

[55] Buttner FH, Hughes CE, Margerie D, Lichte A, Tschesche H, Caterson B, et al. Membrane type 1 matrix metalloproteinase (MT1-MMP) cleaves the recombinant aggrecan substrate rAgg1mut at the “aggrecanase” and the MMP sites. Biochem J 1998;333:159–65.

[56] Roberts JJ, Nicodemus GD, Giunta S, Bryant SJ. Incorporation of biomimetic matrix molecules in PEG hydrogels enhances matrix deposition and reduces load-induced loss of chondrocyte-secreted matrix. J Biomed Mater Res Part A 2011;97A:281–91.

[57] Guilak F, Butler DL, Goldstein SA. Functional tissue engineering - The role of biomechanics in articular cartilage repair. Clin Orthop Relat Res 2001:S295–S305.

[58] Darling EM, Athanasiou KA. Biomechanical strategies for articular cartilage regeneration. Ann Biomed Eng 2003;31:1114–24.

[59] Nicodemus GD, Bryant SJ. Mechanical loading regimes affect the anabolic and catabolic activities by chondrocytes encapsulated in PEG hydrogels. Osteoarthr Cartil 2010;18:126–37.

[60] De Croos JNA, Dhaliwal SS, Grynpas MD, Pilliar RM, Kandel RA. Cyclic compressive mechanical stimulation induces sequential catabolic and anabolic gene changes in chondrocytes resulting in increased extracellular matrix accumulation. Matrix Biol 2006;25:323–31.

Chapter 7

[1] Nicodemus GD, Bryant SJ. Cell encapsulation in biodegradable hydrogels for tissue engineering applications. Tissue Eng Part B-Reviews 2008;14:149–65.

[2] Slaughter B V, Khurshid SS, Fisher OZ, Khademhosseini A, Peppas NA. Hydrogels in regenerative medicine. Adv Mater 2009;21:3307–29.

[3] Bryant SJ, Anseth KS. Photopolymerization of Hydrogel Scaffolds. In: Ma PX, Elisseeff JH, editors. Scaffolding Tissue Eng., Boca Raton, FL: CRC Press, Inc.; 2006, p. 71–90.

[4] Ifkovits JL, Burdick JA. Review: photopolymerizable and degradable biomaterials for tissue engineering applications. Tissue Eng 2007;13:2369–85.

[5] Anseth KS, Kloxin AM, Kloxin CJ, Bowman CN. Mechanical Properties of Cellularly Responsive Hydrogels and Their Experimental Determination. Adv Mater 2010;22:3484–94.

[6] Lynn AD, Blakney AK, Kyriakides TR, Bryant SJ. Temporal progression of the host response to implanted poly(ethylene glycol)-based hydrogels. J Biomed Mater Res Part A 2011;96A:621–31.

[7] Nicodemus GD, Skaalure SC, Bryant SJ. Gel structure has an impact on pericellular and extracellular matrix deposition, which subsequently alters metabolic activities in chondrocyte-laden PEG hydrogels. Acta Biomater 2011;7:492–504.

[8] Benoit DSW, Durney AR, Anseth KS. Manipulations in Hydrogel Degradation Behavior Enhance Osteoblast Function and Mineralized Tissue Formation. Tissue Eng 2006;12:1663–73.

[9] Mahoney MJ, Anseth KS. Three-dimensional growth and function of neural tissue in degradable polyethylene glycol hydrogels. Biomaterials 2006;27:2265–74.

[10] Roberts JJ, Nicodemus GD, Greenwald EC, Bryant SJ. Degradation Improves Tissue Formation in (Un)Loaded Chondrocyte-laden Hydrogels. Clin Orthop Relat Res 2011.

[11] Anseth KS, Bryant SJ. Controlling the spatial distribution of ECM components in degradable PEG hydrogels for tissue engineering cartilage. J Biomed Mater Res Part A 2003;64A:70–9.

[12] Anseth KS, Metters AT, Bryant SJ, Martens PJ, Elisseeff JH, Bowman CN. In situ forming degradable networks and their application in tissue engineering and drug delivery. J Control Release 2002;78:199–209.

[13] Bryant SJ, Davis-Arehart KA, Luo N, Shoemaker RK, Arthur JA, Anseth KS. Synthesis and Characterization of Photopolymerized Multifunctional Hydrogels: Water-Soluble Poly(Vinyl Alcohol) and Chondroitin Sulfate Macromers for Chondrocyte Encapsulation. Macromolecules 2004;37:6726–33.

[14] Li Q, Williams CG, Sun DDN, Wang J, Leong K, Elisseeff JH. Photocrosslinkable polysaccharides based on chondroitin sulfate. J Biomed Mater Res Part A 2004;68A:28–33.

[15] Burdick JA, Prestwich GD. Hyaluronic Acid Hydrogels for Biomedical Applications. Adv Mater 2011;23:H41–H56.

[16] Burdick JA, Chung C, Jia XQ, Randolph MA, Langer R. Controlled degradation and mechanical behavior of photopolymerized hyaluronic acid networks. Biomacromolecules 2005;6:386–91.

[17] Shu XZ, Liu Y, Luo Y, Roberts MC, Prestwich GD. Disulfide Cross-Linked Hyaluronan Hydrogels. Biomacromolecules 2002;3:1304–11.

[18] Prestwich GD, Marecak DM, Marecek JF, Vercruysse KP, Ziebell MR. Controlled chemical modification of hyaluronic acid: synthesis, applications, and biodegradation of hydrazide derivatives. J Control Release 1998;53:93–103.

[19] Zhu JM. Bioactive modification of poly(ethylene glycol) hydrogels for tissue engineering. Biomaterials 2010;31:4639–56.

[20] West JL, Hubbell JA. Polymeric Biomaterials with Degradation Sites for Proteases Involved in Cell Migration. Macromolecules 1999;32:241–4.

[21] Park Y, Ph D, Lutolf MP, Hubbell JA, Hunziker EB, Wong M, et al. Bovine Primary Chondrocyte Culture in Synthetic Matrix Hydrogels as a Scaffold for Cartilage Repair 2004;10.

[22] Lutolf MP, Lauer-Fields JL, Schmoekel HG, Metters AT, Weber FE, Fields GB, et al. Synthetic matrix metalloproteinase-sensitive hydrogels for the conduction of tissue regeneration: engineering cell-invasion characteristics. Proc Natl Acad Sci U S A 2003;100:5413–8.

[23] Lutolf MP, Raeber GP, Zisch AH, Tirelli N, Hubbell JA. Cell-Responsive Synthetic Hydrogels. Adv Mater 2003;15:888–92.

[24] West JL, Lee SH, Miller JS, Moon JJ. Proteolytically degradable hydrogels with a fluorogenic substrate for studies of cellular proteolytic activity and migration. Biotechnol Prog 2005;21:1736–41.

[25] Bahney CS, Hsu C-W, Yoo JU, West JL, Johnstone B. A bioresponsive hydrogel tuned to chondrogenesis of human mesenchymal stem cells. FASEB J 2011;25:1486–96.

[26] Patterson J, Hubbell JA. Enhanced proteolytic degradation of molecularly engineered PEG hydrogels in response to MMP-1 and MMP-2. Biomaterials 2010;31:7836–45.

[27] Dhote V, Vernerey FJ. Mathematical model of the role of degradation on matrix development in hydrogel scaffold. Biomech Model Mechanobiol 2013;13:167–83.

[28] Vernerey FJ, Greenwald EC, Bryant SJ. Triphasic mixture model of cell-mediated enzymatic degradation of hydrogels. Comput Methods Biomech Biomed Engin 2012;15:1197–210.

[29] French MF, Bhown A, Van Wart HE. Identification of Clostridium histolyticum Collagenase Hyperreactive Sites in Type I, II, and III Collagens: Lack of Correlation with Local Triple Helical Stability. J Protein Chem 1992;11:83–97.

[30] Sandor M, Enscore D, Weston P, Mathiowitz E. Effect of protein molecular weight on release from micron-sized PLGA microspheres. J Control Release 2001;76:297–311.

[31] Cohen S, Yoshioka T, Lucarelli M, Hwang LH, Langer R. Controlled Delivery Systems for Proteins Based on Poly(Lactic Glycolic Acid) Microspheres. Pharm Res 1991;8:713–20.

[32] Fairbanks BD, Schwartz MP, Halevi AE, Nuttelman CR, Bowman CN, Anseth KS. A Versatile Synthetic Extracellular Matrix Mimic via Thiol-Norbornene Photopolymerization. Adv Mater 2009;21:5005–10.

[33] Turk BE, Huang LL, Piro ET, Cantley LC. Determination of protease cleavage site motifs using mixture-based oriented peptide libraries. Nat Biotechnol 2001;19:661–7.

[34] Lineweaver H, Burk D. The Determination of Enzyme Dissociation Constants. J Am Chem Soc 1934;56:658–66.

[35] Ashton RS, Banerjee A, Punyani S, Schaffer DV, Kane RS. Scaffolds based on degradable alginate hydrogels and poly(lactide-co-glycolide) microspheres for stem cell culture. Biomaterials 2007;28:5518–25.

[36] Roberts JJ, Bryant SJ. Comparison of photopolymerizable thiol-ene PEG and acrylate-based PEG hydrogels for cartilage development. Biomaterials 2013;34:9969–79.

[37] Shih H, Lin C-C. Visible Light-Mediated Thiol-Ene Hydrogelation Using Eosin-Y as the Only Photoinitiator. Macromol Rapid Commun 2013;34:269–73.

[38] Gould ST, Darling NJ, Anseth KS. Small peptide functionalized thiol-ene hydrogels as culture substrates for understanding valvular interstitial cell activation and de novo tissue deposition. Acta Biomater 2012;8:3201–9.

[39] Peppas NA, Barr-Howell BD. Characterization of the cross-linked structure of hydrogels. In: Peppas NA, editor. Hydrogels Med. Pharmacy, Vol. I Fundam., Boca Raton, FL: CRC Press, Inc.; 1986, p. 27–56.

[40] Canal T, Peppas NA. Correlation between mesh size and equilibrium degree of swelling of polymeric networks. J Biomed Mater Res 1989;23:1183–93.

[41] Korson L, Drost-Hansen W, Millero FJ. Viscosity of Water at Various Temperatures. J Phys Chem 1969;73:34–9.

[42] Lustig SR, Peppas NA. Solute diffusion in swollen membranes. IX. Scaling laws for solute diffusion in gels. J Appl Polym Sci 1988;36:735–47.

[43] Amsden B. Solute Diffusion within Hydrogels. Mechanisms and Models. Macromolecules 1998;31:8382–95.

[44] Dhote V, Skaalure S, Akalp U, Roberts J, Bryant SJ, Vernerey FJ. On the role of hydrogel structure and degradation in controlling the transport of cell-secreted matrix molecules for engineered cartilage. J Mech Behav Biomed Mater 2013;19:61–74.

[45] Drury JL, Mooney DJ. Hydrogels for tissue engineering: scaffold design variables and applications. Biomaterials 2003;24:4337–51.

[46] Brandl F, Sommer F, Goepferich A. Rational design of hydrogels for tissue engineering: Impact of physical factors on cell behavior. Biomaterials 2007;28:134–46.

[47] Nicodemus GD, Skaalure SC, Bryant SJ. Gel structure has an impact on pericellular and extracellular matrix deposition, which subsequently alters metabolic activities in chondrocyte-laden PEG hydrogels. Acta Biomater 2011;7:492–504.

[48] Nagase H, Fields GB. Human matrix metalloproteinase specificity studies using collagen sequence-based synthetic peptides. Biopolymers 1996;40:399–416.

[49] Allison SD. Analysis of initial burst in PLGA microparticles. Expert Opin Drug Deliv 2008;5:615–28.

[50] Nagase H, Visse R, Murphy G. Structure and function of matrix metalloproteinases and TIMPs. Cardiovasc Res 2006;69:562–73.

[51] Woessner JF. Matrix Metalloproteinases and Their Inhibitors in Connective Tissue Remodeling. Faseb J 1991;5:2145–54.

[52] Murphy G, Baker AH, Edwards DR. Metalloproteinase inhibitors: biological actions and therapeutic opportunities. J Cell Sci 2002;115:3719–27.

[53] Gomez DE, Alonso DF, Yoshiji H, Thorgeirsson UP. Tissue inhibitors of metalloproteinases: structure, regulation and biological functions. Eur J Cell Biol 1997;74:111–22.

[54] Brew K, Kashiwagi M, Tortorella M, Nagase H. TIMP-3 is a potent inhibitor of aggrecanase 1 (ADAM-TS4) and aggrecanase 2 (ADAM-TS5). J Biol Chem 2001;276:12501–4.

[55] Edwards DR, Porter S, Clark IM, Kevorkian L. The ADAMTS metalloproteinases. Biochem J 2005;386:15–27.

Chapter 8

[1] Perera JR, Gikas PD, Bentley G. The present state of treatments for articular cartilage defects in the knee. Ann R Coll Surg Engl 2012;94:381–7.

[2] Gillogly SD, Myers TH. Treatment of full-thickness chondral defects with autologous chondrocyte implantation. Orthop Clin North Am 2005;36:433–46.

[3] Bartlett W, Skinner JA, Gooding CR, Carrington RWJ, Flanagan AM, Briggs TWR, et al. Autologous chondrocyte implantation versus matrix-induced autologous chondrocyte implantation for osteochondral defects of the knee: a prospective, randomised study. J Bone Joint Surg Br 2005;87:640–5.

[4] Bekkers JEJ, Inklaar M, Saris DBF. Treatment selection in articular cartilage lesions of the knee: a systematic review. Am J Sports Med 2009;37 Suppl 1:148S–55S.

[5] Hootman JM, Helmick CG. Projections of US prevalence of arthritis and associated activity limitations. Arthritis Rheum 2006;54:226–9.

[6] Zhu JM. Bioactive modification of poly(ethylene glycol) hydrogels for tissue engineering. Biomaterials 2010;31:4639–56.

[7] Kloxin AM, Kloxin CJ, Bowman CN, Anseth KS. Mechanical Properties of Cellularly Responsive Hydrogels and Their Experimental Determination. Adv Mater 2010;22:3484–94.

[8] Bryant SJ, Anseth KS. Hydrogel properties influence ECM production by chondrocytes photoencapsulated in poly(ethylene glycol) hydrogels. J Biomed Mater Res 2002;59:63–72.

[9] Anseth KS, Bryant SJ. Controlling the spatial distribution of ECM components in degradable PEG hydrogels for tissue engineering cartilage. J Biomed Mater Res Part A 2003;64A:70–9.

[10] Roberts JJ, Nicodemus GD, Greenwald EC, Bryant SJ. Degradation Improves Tissue Formation in (Un)Loaded Chondrocyte-laden Hydrogels. Clin Orthop Relat Res 2011.

[11] Bryant SJ, Durand KL, Anseth KS. Manipulations in hydrogel chemistry control photoencapsulated chondrocyte behavior and their extracellular matrix production. J Biomed Mater Res Part A 2003;67A:1430–6.

[12] Bryant SJ, Bender RJ, Durand KL, Anseth KS. Encapsulating Chondrocytes in degrading PEG hydrogels with high modulus: Engineering gel structural changes to facilitate cartilaginous tissue production. Biotechnol Bioeng 2004;86:747–55.

[13] Anseth KS, Metters AT, Bryant SJ, Martens PJ, Elisseeff JH, Bowman CN. In situ forming degradable networks and their application in tissue engineering and drug delivery. J Control Release 2002;78:199–209.

[14] Anseth KS, Metters AT, Bowman CN. Fundamental studies of a novel, biodegradable PEG-b-PLA hydrogel. Polymer (Guildf) 2000;41:3993–4004.

[15] Knudson CB, Knudson W. Cartilage proteoglycans. Semin Cell Dev Biol 2001;12:69–78.

[16] Roughley PJ. The structure and function of cartilage proteoglycans. Eur Cell Mater 2006;12:92–101.

[17] Kawasaki K, Ochi M, Uchio Y, Adachi N, Matsusaki M. Hyaluronic acid enhances proliferation and chondroitin sulfate synthesis in cultured chondrocytes embedded in collagen gels. J Cell Physiol 1999;179:142–8.

[18] Allison DD, Grande-Allen KJ. Review. Hyaluronan: A powerful tissue engineering tool. Tissue Eng 2006;12:2131–40.

[19] Stern R, Asari AA, Sugahara KN. Hyaluronan fragments: An information-rich system. Eur J Cell Biol 2006;85:699–715.

[20] Roberts JJ, Elder RM, Neumann AJ, Jayaraman A, Bryant SJ. Interaction of Hyaluronan Binding Peptides with Glycosaminoglycans in Poly(ethylene glycol) Hydrogels. Biomacromolecules 2014.

[21] Urban JPG, Hall AC, Gehl KA. Regulation of Matrix Synthesis Rates by the Ionic and Osmotic Environment of Articular Chondrocytes. J Cell Physiol 1993;154:262–70.

[22] Villanueva I, Bishop NL, Bryant SJ. Medium Osmolarity and Pericellular Matrix Development Improves Chondrocyte Survival When Photoencapsulated in Poly(Ethylene Glycol) Hydrogels at Low Densities. Tissue Eng Part A 2009;15:3037–48.

[23] Amin AK, Huntley JS, Bush PG, Simpson AHRW, Hall AC. Osmolarity influences chondrocyte death in wounded articular cartilage. J Bone Jt Surgery-American Vol 2008;90A:1531–42.

[24] Fairbanks BD, Schwartz MP, Halevi AE, Nuttelman CR, Bowman CN, Anseth KS. A Versatile Synthetic Extracellular Matrix Mimic via Thiol-Norbornene Photopolymerization. Adv Mater 2009;21:5005–10.

[25] Gould ST, Darling NJ, Anseth KS. Small peptide functionalized thiol-ene hydrogels as culture substrates for understanding valvular interstitial cell activation and de novo tissue deposition. Acta Biomater 2012;8:3201–9.

[26] Aimetti AA, Machen AJ, Anseth KS. Poly(ethylene glycol) hydrogels formed by thiol-ene photopolymerization for enzyme-responsive protein delivery. Biomaterials 2009;30:6048–54.

[27] Roberts JJ, Bryant SJ. Comparison of photopolymerizable thiol-ene PEG and acrylate-based PEG hydrogels for cartilage development. Biomaterials 2013.

[28] Vinatier C, Mrugala D, Jorgensen C, Guicheux J, Noel D. Cartilage engineering: a crucial combination of cells, biomaterials and biofactors. Trends Biotechnol 2009;27:307–14.

[29] Domm C, Schünke M, Christesen K, Kurz B. Redifferentiation of dedifferentiated bovine articular chondrocytes in alginate culture under low oxygen tension. Osteoarthritis Cartilage 2002;10:13–22.

[30] Nesic D, Whiteside R, Brittberg M, Wendt D, Martin I, Mainil-Varlet P. Cartilage tissue engineering for degenerative joint disease. Adv Drug Deliv Rev 2006;58:300–22.

[31] Mollon B, Kandel R, Chahal J, Theodoropoulos J. The clinical status of cartilage tissue regeneration in humans. Osteoarthritis Cartilage 2013;21:1824–33.

[32] McCall JD, Anseth KS. Thiol-ene photopolymerizations provide a facile method to encapsulate proteins and maintain their bioactivity. Biomacromolecules 2012;13:2410–7.

[33] McCall JD, Luoma JE, Anseth KS. Covalently tethered transforming growth factor beta in PEG hydrogels promotes chondrogenic differentiation of encapsulated human mesenchymal stem cells. Drug Deliv Transl Res 2012;2:305–12.

[34] Nagase H, Visse R, Murphy G. Structure and function of matrix metalloproteinases and TIMPs. Cardiovasc Res 2006;69:562–73.

[35] Woessner JF. Matrix Metalloproteinases and Their Inhibitors in Connective Tissue Remodeling. Faseb J 1991;5:2145–54.

[36] Murphy G, Baker AH, Edwards DR. Metalloproteinase inhibitors: biological actions and therapeutic opportunities. J Cell Sci 2002;115:3719–27.

[37] Gomez DE, Alonso DF, Yoshiji H, Thorgeirsson UP. Tissue inhibitors of metalloproteinases: structure, regulation and biological functions. Eur J Cell Biol 1997;74:111–22.

[38] Brew K, Kashiwagi M, Tortorella M, Nagase H. TIMP-3 is a potent inhibitor of aggrecanase 1 (ADAM-TS4) and aggrecanase 2 (ADAM-TS5). J Biol Chem 2001;276:12501–4.

[39] Edwards DR, Porter S, Clark IM, Kevorkian L. The ADAMTS metalloproteinases. Biochem J 2005;386:15–27.

[40] Shiozaki M, Maeda K, Miura T, Kotoku M, Yamasaki T, Matsuda I, et al. Discovery of (1S,2R,3R)-2,3-Dimethyl-2-phenyl-1-sulfamidocyclopropanecarboxylates: Novel and Highly Selective Aggrecanase Inhibitors. J Med Chem 2011;54:2839–63.

[41] Nagase H, Kashiwagi M. Aggrecanases and cartilage matrix degradation. Arthritis Res Ther 2003;5:94–103.

[42] Purcell BP, Lobb D, Charati MB, Dorsey SM, Wade RJ, Zellars KN, et al. Injectable and bioresponsive hydrogels for on-demand matrix metalloproteinase inhibition. Nat Mater 2014.

[43] Mok SS, Masuda K, Hauselmann HJ, Aydelotte MB, Thonar EJMA. Aggrecan Synthesized by Mature Bovine Chondrocytes Suspended in Alginate - Identification of 2 Distinct Metabolic Matrix Pools. J Biol Chem 1994;269:33021–7.

[44] Hauselmann HJ, Masuda K, Hunziker EB, Neidhart M, Mok SS, Michel BA, et al. Adult human chondrocytes cultured in alginate form a matrix similar to native human articular cartilage. Am J Physiol Physiol 1996;271:C742–C752.

[45] Durigova M, Nagase H, Mort JS, Roughley PJ. MMPs are less efficient than ADAMTS5 in cleaving aggrecan core protein. Matrix Biol 2011;30:145–53.

[46] Lark MW, Gordy JT, Weidner JR, Ayala J, Kimura JH, Williams HR, et al. Cell-mediated Catabolism of Aggrecan. J Biol Chem 1995;270:2550–6.

[47] Ilic MZ, Handley CJ, Robinson HC, Mok MT. Mechanism of Catabolism of Aggrecan by Articular Cartilage. Arch Biochem Biophys 1992;294:115–22.

[48] Fosang AJ, Last K, Stanton H, Weeks DB, Campbell IK, Hardingham TE, et al. Generation and novel distribution of matrix metalloproteinase-derived aggrecan fragments in porcine cartilage explants. J Biol Chem 2000;275:33027–37.

[49] Sandy JD. A contentious issue finds some clarity: on the independent and complementary roles of aggrecanase activity and MMP activity in human joint aggrecanolysis. Osteoarthritis Cartilage 2006;14:95–100.

[50] Tortorella MD, Pratta M, Liu R-Q, Austin J, Ross OH, Abbaszade I, et al. Sites of Aggrecan Cleavage by Recombinant Human Aggrecanase-1 (ADAMTS-4). J Biol Chem 2000;275:18566–73.

[51] Pratta MA, Tortorella MD, Arner EC. Age-related changes in aggrecan glycosylation affect cleavage by aggrecanase. J Biol Chem 2000;275:39096–102.

[52] Wong M, Park Y, Lutolf MP, Hubbell JA, Hunziker EB. Bovine primary chondrocyte culture in synthetic matrix metalloproteinase-sensitive poly(ethylene glycol)-based hydrogels as a scaffold for cartilage repair. Tissue Eng 2004;10:515–22.

[53] Nagase H, Fields GB. Human matrix metalloproteinase specificity studies using collagen sequence-based synthetic peptides. Biopolymers 1996;40:399–416.

[54] Nagase H, Fields CG, Fields GB. Design and Characterization of a Fluorogenic Substrate Selectively Hydrolyzed by Stromelysin-1 (Matrix Metalloproteinase-3). J Biol Chem 1994;269:20952–7.

[55] Waldman SD, Couto DC, Grynpas MD, Pilliar RM, Kandel RA. A single application of cyclic loading can accelerate matrix deposition and enhance the properties of tissue-engineered cartilage. Osteoarthr Cartil 2006;14:323–30.

[56] Mauck RL, Seyhan SL, Ateshian GA, Hung CT. Influence of seeding density and dynamic deformational loading on the developing structure/function relationships of chondrocyte-seeded agarose hydrogels. Ann Biomed Eng 2002;30:1046–56.

[57] Bian L, Zhai DY, Zhang EC, Mauck RL, Burdick JA. Dynamic Compressive Loading Enhances Cartilage Matrix Synthesis and Distribution and Suppresses Hypertrophy in hMSC-Laden Hyaluronic Acid Hydrogels. Tissue Eng Part A 2012;18:715–24.

[58] Blain EJ. Mechanical regulation of matrix metalloproteinases. Front Biosci 2007;12:507–27.

[59] Bryant SJ, Nicodemus GD. Mechanical loading regimes affect the anabolic and catabolic activities by chondrocytes encapsulated in PEG hydrogels. Osteoarthr Cartil 2010;18:126–37.

[60] De Croos JNA, Dhaliwal SS, Grynpas MD, Pilliar RM, Kandel RA. Cyclic compressive mechanical stimulation induces sequential catabolic and anabolic gene changes in chondrocytes resulting in increased extracellular matrix accumulation. Matrix Biol 2006;25:323–31.

[61] Kisiday JD, Lee JH, Siparsky PN, Frisbie DD, Flannery CR, Sandy JD, et al. Catabolic Responses of Chondrocyte-Seeded Peptide Hydrogel to Dynamic Compression. Ann Biomed Eng 2009;37:1368–75.

[62] Farnsworth NL, Antunez LR, Bryant SJ. Dynamic compressive loading differentially regulates chondrocyte anabolic and catabolic activity with age. Biotechnol Bioeng 2013;110:2046–57.

[63] Tuan RS. Stemming cartilage degeneration: adult mesenchymal stem cells as a cell source for articular cartilage tissue engineering. Arthritis Rheum 2006;54:3075–8.

[64] Ichinose S, Yamagata K, Sekiya I, Muneta T, Tagami M. Detailed examination of cartilage formation and endochondral ossification using human mesenchymal stem cells. Clin Exp Pharmacol Physiol 2005;32:561–70.

[65] Wei Y, Zeng W, Wan R, Wang J, Zhou Q, Qiu S, et al. Chondrogenic Differentiation of Induced Pluripotent Stem Cells from Osteoarthritc Chondrocytes in Alginate Matrix. Eur Cell Mater 2012;23:1–12.

[66] Vernerey FJ, Greenwald EC, Bryant SJ. Triphasic mixture model of cell-mediated enzymatic degradation of hydrogels. Comput Methods Biomech Biomed Engin 2012;15:1197–210.

[67] Dhote V, Skaalure S, Akalp U, Roberts J, Bryant SJ, Vernerey FJ. On the role of hydrogel structure and degradation in controlling the transport of cell-secreted matrix molecules for engineered cartilage. J Mech Behav Biomed Mater 2013;19:61–74.

[68] Dhote V, Vernerey FJ. Mathematical model of the role of degradation on matrix development in hydrogel scaffold. Biomech Model Mechanobiol 2013.

Appendix 1

[1] Lai WM, Hou JS, Mow VC. A Triphasic Theory for the Swelling and Deformation Behaviors of Articular Cartilage. J Biomech Eng 1991;113:245.

[2] Maroudas A. Balance between swelling pressure and collagen tension in normal and degenerate cartilage. Nature 1976;260:808–9.

[3] Hardingham TE. Proteoglycans and Glycosaminoglycans. In: Seibel MJ, Robins SP, Bilezikian JP, editors. Dyn. bone Cartil. Metab., Burlington: Elsevier Science; 2006, p. 85–98.

[4] Guilak F, Alexopoulos LG, Upton ML, Youn I, Choi JB, Cao L, et al. The pericellular matrix as a transducer of biomechanical and biochemical signals in articular cartilage. Ann New York Acad Sci Skelet Dev Remodel Heal Dis Aging 2006;1068:498–512.

[5] Poole CA. Articular cartilage chondrons: form, function and failure. J Anat 1997;191 (Pt 1:1–13.

[6] Engvall E, Hessle H, Klier G. Molecular assembly, secretion, and matrix deposition of type VI collagen. J Cell Biol 1986;102:703–10.

[7] Poole CA, Flint MH, Beaumont BW. Chondrons in cartilage: ultrastructural analysis of the pericellular microenvironment in adult human articular cartilages. J Orthop Res 1987;5:509–22.

[8] Bidanset DJ, Guidry C, Rosenberg LC, Choi HU, Timpl R, Hook M. Binding of the proteoglycan decorin to collagen type VI. J Biol Chem 1992;267:5250–6.

[9] Guidetti GF, Bartolini B, Bernardi B, Tira ME, Berndt MC, Balduini C, et al. Binding of von Willebrand factor to the small proteoglycan decorin. FEBS Lett 2004;574:95–100.

[10] Wiberg C, Klatt AR, Wagener R, Paulsson M, Bateman JF, Heinegård D, et al. Complexes of matrilin-1 and biglycan or decorin connect collagen VI microfibrils to both collagen II and aggrecan. J Biol Chem 2003;278:37698–704.

[11] Larson CM, Kelley SS, Blackwood AD, Banes AJ, Lee GM. Retention of the native chondrocyte pericellular matrix results in significantly improved matrix production. Matrix Biol 2002;21:349–59.

[12] Sandy JD, O'Neill JR, Ratzlaff LC. Acquisition of hyaluronate-binding affinity in vivo by newly synthesized cartilage proteoglycans. Biochem J 1989;258:875–80.

[13] Ruoslahti E, Yamaguchi Y. Proteoglycans as modulators of growth factor activities. Cell 1991;64:867–9.

[14] Brandl F, Sommer F, Goepferich A. Rational design of hydrogels for tissue engineering: Impact of physical factors on cell behavior. Biomaterials 2007;28:134–46.

[15] Elisseeff JH, Lee A, Kleinman HK, Yamada Y. Biological Response of Chondrocytes to Hydrogels. Ann N Y Acad Sci 2002;961:118–22.

[16] Nicodemus GD, Bryant SJ. Cell encapsulation in biodegradable hydrogels for tissue engineering applications. Tissue Eng Part B-Reviews 2008;14:149–65.

[17] Dimicco MA, Kisiday JD, Gong H, Grodzinsky AJ. Structure of pericellular matrix around agarose-embedded chondrocytes. Osteoarthritis Cartilage 2007;15:1207–16.

[18] Connelly JT, Wilson CG, Levenston ME. Characterization of proteoglycan production and processing by chondrocytes and BMSCs in tissue engineered constructs. Osteoarthr Cartil 2008;16:1092–100.

[19] Buschmann MD, Gluzband YA, Grodzinsky AJ, Hunziker EB. Mechanical compression modulates matrix biosynthesis in chondrocyte agarose culture. J Cell Sci 1995;108:1497–508.

[20] Davisson T, Kunig S, Chen A, Sah R, Ratcliffe A. Static and dynamic compression modulate matrix metabolism in tissue engineered cartilage. J Orthop Res 2002;20:842–8.

[21] Mauck RL, Nicoll SB, Seyhan SL, Ateshian GA, Hung CT. Synergistic action of growth factors and dynamic loading for articular cartilage tissue engineering. Tissue Eng 2003;9:597–611.

[22] Mauck RL, Wang CCB, Oswald ES, Ateshian GA, Hung CT. The role of cell seeding density and nutrient supply for articular cartilage tissue engineering with deformational loading. Osteoarthr Cartil 2003;11:879–90.

[23] Hung CT, Mauck RL, Wang CCB, Lima EG, Ateshian GA. A paradigm for functional tissue engineering of articular cartilage via applied physiologic deformational loading. Ann Biomed Eng 2004;32:35–49.

[24] Ng L, Hung H-H, Sprunt A, Chubinskaya S, Ortiz C, Grodzinsky A. Nanomechanical properties of individual chondrocytes and their developing growth factor-stimulated pericellular matrix. J Biomech 2007;40:1011–23.

[25] Kisiday J, Jin M, Kurz B, Hung H, Semino C, Zhang S, et al. Self-assembling peptide hydrogel fosters chondrocyte extracellular matrix production and cell division: Implications for cartilage tissue repair. Proc Natl Acad Sci U S A 2002;99:9996–10001.

[26] Kisiday JD, Jin MS, DiMicco MA, Kurz B, Grodzinsky AJ. Effects of dynamic compressive loading on chondrocyte biosynthesis in self-assembling peptide scaffolds. J Biomech 2004;37:595–604.

[27] Bryant SJ, Anseth KS. Hydrogel properties influence ECM production by chondrocytes photoencapsulated in poly(ethylene glycol) hydrogels. J Biomed Mater Res 2002;59:63–72.

[28] Bryant SJ, Chowdhury TT, Lee DA, Bader DL, Anseth KS. Crosslinking density influences chondrocyte metabolism in dynamically loaded photocrosslinked poly(ethylene glycol) hydrogels. Ann Biomed Eng 2004;32:407–17.

[29] Bryant SJ, Durand KL, Anseth KS. Manipulations in hydrogel chemistry control photoencapsulated chondrocyte behavior and their extracellular matrix production. J Biomed Mater Res Part A 2003;67A:1430–6.

[30] Villanueva I, Klement BJ, von Deutsch D, Bryant SJ. Cross-linking density alters early metabolic activities in chondrocytes encapsulated in poly(ethylene glycol) hydrogels and cultured in the rotating wall vessel. Biotechnol Bioeng 2009;102:1242–50.

[31] Appelman TP, Mizrahi J, Elisseeff JH, Seliktar D. The differential effect of scaffold composition and architecture on chondrocyte response to mechanical stimulation. Biomaterials 2009;30:518–25.

[32] Anseth KS, Bryant SJ. Controlling the spatial distribution of ECM components in degradable PEG hydrogels for tissue engineering cartilage. J Biomed Mater Res Part A 2003;64A:70–9.

[33] Bryant SJ, Bender RJ, Durand KL, Anseth KS. Encapsulating Chondrocytes in degrading PEG hydrogels with high modulus: Engineering gel structural changes to facilitate cartilaginous tissue production. Biotechnol Bioeng 2004;86:747–55.

[34] Rice MA, Anseth KS. Encapsulating chondrocytes in copolymer gels: bimodal degradation kinetics influence cell phenotype and extracellular matrix development. J Biomed Mater Res A 2004;70:560–8.

[35] Rice MA, Anseth KS. Controlling cartilaginous matrix evolution in hydrogels with degradation triggered by exogenous addition of an enzyme. Tissue Eng 2007;13:683–91.

[36] Yang F, Williams CG, Wang D-A, Lee H, Manson PN, Elisseeff J. The effect of incorporating RGD adhesive peptide in polyethylene glycol diacrylate hydrogel on osteogenesis of bone marrow stromal cells. Biomaterials 2005;26:5991–8.

[37] Bryant SJ, Arthur JA, Anseth KS. Incorporation of tissue-specific molecules alters chondrocyte metabolism and gene expression in photocrosslinked hydrogels. Acta Biomater 2005;1:243–52.

[38] Lee HJ, Lee J-S, Chansakul T, Yu C, Elisseeff JH, Yu SM. Collagen mimetic peptide-conjugated photopolymerizable PEG hydrogel. Biomaterials 2006;27:5268–76.

[39] Schmidt O, Mizrahi J, Elisseeff J, Seliktar D. Immobilized Fibrinogen in PEG Hydrogels Does not Improve Chondrocyte-Mediated Matrix Deposition in Response to Mechanical Stimulation. Biotechnol Bioeng 2006;95:1061–9.

[40] Villanueva I, Hauschulz DS, Mejic D, Bryant SJ. Static and dynamic compressive strains influence nitric oxide production and chondrocyte bioactivity when encapsulated in PEG hydrogels of different crosslinking densities. Osteoarthr Cartil 2008;doi:10.101.

[41] Watkins AW, Anseth KS. Investigation of Molecular Transport and Distributions in Poly(ethylene glycol) Hydrogels with Confocal Laser Scanning Microscopy. Macromolecules 2005;38:1326–34.

[42] Weber LM, Lopez CG, Anseth KS. Effects of PEG hydrogel crosslinking density on protein diffusion and encapsulated islet survival and function. J Biomed Mater Res A 2009;90:720–9.

[43] Bryant SJ, Anseth KS, Lee DA, Bader DL. Crosslinking density influences the morphology of chondrocytes photoencapsulated in PEG hydrogels during the application of compressive strain. J Orthop Res 2004;22:1143–9.

[44] Nicodemus GD, Bryant SJ. The role of hydrogel structure and dynamic loading on chondrocyte gene expression and matrix formation. J Biomech 2008;41:1528–36.

[45] Bryant SJ, Nicodemus GD, Villanueva I. Designing 3D photopolymer hydrogels to regulate biomechanical cues and tissue growth for cartilage tissue engineering. Pharm Res 2008;25:2379–86.

[46] Elisseeff J, McIntosh W, Anseth K, Riley S, Ragan P, Langer R. Photoencapsulation of chondrocytes in poly(ethylene oxide)-based semi-interpenetrating networks. J Biomed Mater Res 2000;51:164–71.

[47] Farndale RW, Buttle DJ, Barrett AJ. Improved Quantitation and Discrimination of Sulfated Glycosaminoglycans by Use of Dimethylmethylene Blue. Biochim Biophys Acta 1986;883:173–7.

[48] Bryant SJ, Nicodemus GD. Mechanical loading regimes affect the anabolic and catabolic activities by chondrocytes encapsulated in PEG hydrogels. Osteoarthr Cartil 2010;18:126–37.

[49] Von der Mark K. Structure, Biosynthesis and Gene Regulation of Collagens in Cartilage and Bone. Dyn. bone Cartil. Metab., Elsevier; 2006, p. 3–40.

[50] Hardingham TE, Fosang AJ. Proteoglycans - Many Forms and Many Functions. Faseb J 1992;6:861–70.

[51] Hardingham TE, Muir H. The specific interaction of hyaluronic acid with cartilage proteoglycans. Biochim Biophys Acta 1972;279:401–5.

[52] Hardingham TE. The role of link-protein in the structure of cartilage proteoglycan aggregates. Biochem J 1979;177:237–47.

[53] Spicer AP, McDonald JA. Characterization and Molecular Evolution of a Vertebrate Hyaluronan Synthase Gene Family. J Biol Chem 1998;273:1923–32.

[54] De Croos JNA, Dhaliwal SS, Grynpas MD, Pilliar RM, Kandel RA. Cyclic compressive mechanical stimulation induces sequential catabolic and anabolic gene changes in chondrocytes resulting in increased extracellular matrix accumulation. Matrix Biol 2006;25:323–31.

[55] Hardingham TE, Fosang AJ. The structure of aggrecan and its turnover in cartilage. J Rheumatol Suppl 1995;43:86–90.

[56] Murphy G, Hembry RM, Hughes CE, Fosang AJ, Hardingham TE. Role and regulation of metalloproteinases in connective tissue turnover. Biochem Soc Trans 1990;18:812–5.

[57] Sandy JD. A contentious issue finds some clarity: on the independent and complementary roles of aggrecanase activity and MMP activity in human joint aggrecanolysis. Osteoarthritis Cartilage 2006;14:95–100.

[58] Blain EJ. Mechanical regulation of matrix metalloproteinases. Front Biosci 2007;12:507–27.

[59] Blain EJ, Gilbert SJ, Wardale RJ, Capper SJ, Mason DJ, Duance VC. Up-regulation of matrix metalloproteinase expression and activation following cyclical compressive loading of articular cartilage in vitro. Arch Biochem Biophys 2001;396:49–55.

[60] Engler AJ, Sen S, Sweeney HL, Discher DE. Matrix elasticity directs stem cell lineage specification. Cell 2006;126:677–89.

[61] Peppas NA., Hilt JZ, Khademhosseini A, Langer R. Hydrogels in Biology and Medicine: From Molecular Principles to Bionanotechnology. Adv Mater 2006;18:1345–60.

[62] Rice MA, Sanchez-Adams J, Anseth KS. Exogenously triggered, enzymatic degradation of photopolymerized hydrogels with polycaprolactone subunits: experimental observation and modeling of mass loss behavior. Biomacromolecules 2006;7:1968–75.

Appendix 2

[1] Hootman JM, Helmick CG. Projections of US prevalence of arthritis and associated activity limitations. Arthritis Rheum 2006;54:226–9.

[2] Slaughter BV, Khurshid SS, Fisher OZ, Khademhosseini A, Peppas NA. Hydrogels in regenerative medicine. Adv Mater 2009;21:3307–29.

[3] Anseth KS, Bryant SJ. Controlling the spatial distribution of ECM components in degradable PEG hydrogels for tissue engineering cartilage. J Biomed Mater Res Part A 2003;64A:70–9.

[4] Elisseeff J, Anseth K, Sims D, McIntosh W, Randolph M, Yaremchuk M, et al. Transdermal photopolymerization of poly(ethylene oxide)-based injectable hydrogels for tissue-engineered cartilage. Plast Reconstr Surg 1999;104:1014–22.

[5] Sawhney AS. Bioerodible Hydrogels Based on Photopolymerized Poly(ethy1ene. Macromolecules 1993;26:581–7.

[6] West JL, Lee SH, Miller JS, Moon JJ. Proteolytically degradable hydrogels with a fluorogenic substrate for studies of cellular proteolytic activity and migration. Biotechnol Prog 2005;21:1736–41.

[7] Nicodemus GD, Skaalure SC, Bryant SJ. Gel structure has an impact on pericellular and extracellular matrix deposition, which subsequently alters metabolic activities in chondrocyte-laden PEG hydrogels. Acta Biomater 2011;7:492–504.

[8] Ateshian GA, Kim JJ, Grelsamer RP, Mow VC, Warden WH. Finite deformation of bovine material properties cartilage compression. J Biomech 1997;30:97.

[9] Holmes MH, Mow VC. The nonlinear characteristics of soft gels and hydrated connective tissues in ultrafiltration. J Biomech 1990;23:1145–56.

[10] Kwan MK, Lai WM, Mow VC. A finite deformation theory for cartilage and other soft hydrated connective tissues--I. Equilibrium results. J Biomech 1990;23:145–55.

[11] Sengers BG, Van Donkelaar CC, Oomens CWJ, Baaijens FPT. The local matrix distribution and the functional development of tissue engineered cartilage, a finite element study. Ann Biomed Eng 2004;32:1718–27.

[12] Dimicco MA, Sah RL. Dependence of Cartilage Matrix Composition on Biosynthesis, Diffusion, and Reaction. Transp Porous Media 2003;50:57–73.

[13] Trewenack AJ, Please CP, Landman KA. A continuum model for the development of tissue-engineered cartilage around a chondrocyte. Math Med Biol 2009;26:241–62.

[14] Vernerey FJ, Greenwald EC, Bryant SJ. Triphasic mixture model of cell-mediated enzymatic degradation of hydrogels. Comput Methods Biomech Biomed Engin 2012;15:1197–210.

[15] Haider MA, Olander JE, Arnold RF, Marous DR, McLamb AJ, Thompson KC, et al. A phenomenological mixture model for biosynthesis and linking of cartilage extracellular matrix in scaffolds seeded with chondrocytes. Biomech Model Mechanobiol 2011;10:915–24.

[16] Sawhney AS, Pathak CP, Hubbell JA. Bioerodible Hydrogels Based on Photopolymerized Poly(ethylene glycol)-co-poly(alpha-hydroxy acid) Diacrylate Macromers. Macromolecules 1993;26:581–7.

[17] Lin-Gibson S, Bencherif S, Cooper JA, Wetzel SJ, Antonucci JM, Vogel BM, et al. Synthesis and characterization of PEG dimethacrylates and their hydrogels. Biomacromolecules 2004;5:1280–7.

[18] Peppas NA. Hydrogels in Medicine and Pharmacy. Boca Raton, FL: CRC Press; 1986.

[19] Vernerey FJ, Foucard L, Farsad M. Bridging the Scales to Explore Cellular Adaptation and Remodeling. Bionanoscience 2011;1:110–5.

[20] Vernerey FJ, Farsad M. A constrained mixture approach to mechano-sensing and force generation in contractile cells. J Mech Behav Biomed Mater 2011;4:1683–99.

[21] Li C, Borja RI, Regueiro R a. Dynamics of porous media at finite strain. Comput Methods Appl Mech Eng 2004;193:3837–70.

[22] Flory PJ. Principles of Polymer Chemistry. Ithaca, New York: Cornell University Press; 1953.

[23] Treloar LRG. The physics of rubber elasticity. New York: Oxford University Press; 1975.

[24] Cowie JMG, Arrighi V. Polymers: Chemistry and Physics of Modern Materials. Boca Raton, FL: CRC Press; 2008.

[25] Bell CL, Peppas NA. Biomedical membranes from hydrogels and interpolymer complexes. Adv Polym Sci 1995;122:125–75.

[26] Metters AT, Bowman CN, Anseth KS. A statistical kinetic model for the bulk degradation of PLA-b-PEG-b-PLA hydrogel networks. J Phys Chem B 2000;104:7043–9.

[27] Bryant SJ, Bender RJ, Durand KL, Anseth KS. Encapsulating Chondrocytes in degrading PEG hydrogels with high modulus: Engineering gel structural changes to facilitate cartilaginous tissue production. Biotechnol Bioeng 2004;86:747–55.

[28] Skaalure SC, Milligan IL, Bryant SJ. Age impacts extracellular matrix metabolism in chondrocytes encapsulated in degradable hydrogels. Biomed Mater 2012;7.

[29] Mason MN, Metters AT, Bowman CN, Anseth KS. Predicting controlled-release behavior of degradable PLA-b-PEG-b-PLA hydrogels. Macromolecules 2001;34:4630–5.

[30] Bryant SJ, Nicodemus GD. Mechanical loading regimes affect the anabolic and catabolic activities by chondrocytes encapsulated in PEG hydrogels. Osteoarthr Cartil 2010;18:126–37.

[31] Hardingham TE. Proteoglycans and Glycosaminoglycans. In: Seibel MJ, Robins SP, Bilezikian JP, editors. Dyn. bone Cartil. Metab., Burlington: Elsevier Science; 2006, p. 85–98.

[32] Von der Mark K. Structure, Biosynthesis and Gene Regulation of Collagens in Cartilage and Bone. Dyn. bone Cartil. Metab., Elsevier; 2006, p. 3–40.

[33] Roberts JJ, Nicodemus GD, Greenwald EC, Bryant SJ. Degradation Improves Tissue Formation in (Un)Loaded Chondrocyte-laden Hydrogels. Clin Orthop Relat Res 2011.

[34] Rubinstein M, Colby RH. Polymer Physics. New York: Oxford University Press; 2003.

[35] Lustig SR, Peppas NA. Solute diffusion in swollen membranes. IX. Scaling laws for solute diffusion in gels. J Appl Polym Sci 1988;36:735–47.

[36] Farsad M, Vernerey FJ. An XFEM-based numerical strategy to model mechanical interactions between biological cells and a deformable substrate. Int J Numer Methods Eng 2012;92:238–67.

[37] Metters AT, Anseth KS, Bowman CN. A statistical kinetic model for the bulk degradation of PLA-b-PEG-b-PLA hydrogel networks: Incorporating network non-idealities. J Phys Chem B 2001;105:8069–76.

[38] Mok SS, Masuda K, Hauselmann HJ, Aydelotte MB, Thonar EJMA. Aggrecan Synthesized by Mature Bovine Chondrocytes Suspended in Alginate - Identification of 2 Distinct Metabolic Matrix Pools. J Biol Chem 1994;269:33021–7.

[39] Foucard L, Vernerey FJ. A thermodynamical model for stress-fiber organization in contractile cells. Appl Phys Lett 2012;100:13702–137024.

[40] Foucard L, Vernerey FJ. Dynamics of Stress Fibers Turnover in Contractile Cells. J Eng Mech 2012;138:1282–7.

[41] Vernerey FJ, Farsad M. An Eulerian/XFEM formulation for the large deformation of cortical cell membrane. Comput Methods Biomech Biomed Engin 2011;14:433–45.

[42] Vernerey FJ. The Effective Permeability of Cracks and Interfaces in Porous Media. Transp Porous Media 2012;93:815–29.

[43] Vernerey FJ. On the Application of Multiphasic Theories to the Problem of Cell-Substrate Mechanical Interactions. Adv. Cell Mech., Berlin: Springer; 2011, p. 189–224.

Appendix 3

[1] Roberts JJ, Bryant SJ. Comparison of photopolymerizable thiol-ene PEG and acrylate-based PEG hydrogels for cartilage development. Biomaterials 2013;34:9969–79.

[2] Shih H, Lin C-C. Visible Light-Mediated Thiol-Ene Hydrogelation Using Eosin-Y as the Only Photoinitiator. Macromol Rapid Commun 2013;34:269–73.

[3] Fairbanks BD, Schwartz MP, Halevi AE, Nuttelman CR, Bowman CN, Anseth KS. A Versatile Synthetic Extracellular Matrix Mimic via Thiol-Norbornene Photopolymerization. Adv Mater 2009;21:5005–10.

[4] Treloar LRG. The physics of rubber elasticity. New York: Oxford University Press; 1975.

[5] Gould ST, Darling NJ, Anseth KS. Small peptide functionalized thiol-ene hydrogels as culture substrates for understanding valvular interstitial cell activation and de novo tissue deposition. Acta Biomater 2012;8:3201–9.

[6] Rubinstein M, Colby RH. Polymer Physics. New York: Oxford University Press; 2003.

Appendix 1

Gel Structure has an Impact on Pericellular and Extracellular Matrix Deposition, which Subsequently Alters Metabolic Activities in Chondrocyte-laden PEG Hydrogels

As appearing in *Acta Biomaterialia* 2011

A1.1 Abstract

While designing poly(ethylene glycol) hydrogels with high moduli suitable for in situ placement is attractive for cartilage regeneration, the impact of a tighter crosslinked structure on the organization and deposition of matrix is not fully understood. The objectives for this study were to characterize the composition and spatial organization of neo-matrix as a function of gel crosslinking and study its impact on chondrocytes via anabolic and catabolic gene expressions, and catabolic activity. Bovine articular chondrocytes were encapsulated in hydrogels of three crosslinking densities (compressive moduli were 60, 320 and 590 kPa) and cultured for 25 days. Glycosaminoglycan production increased with culture time and was greatest in gels with lowest crosslinking. Collagens II and VI, aggrecan, link protein, and decorin were localized to pericellular regions in all gels, but their presence decreased with increases in gel crosslinking. Collagen II and aggrecan expressions were initially up-regulated in gels with higher crosslinking, but increased similarly up to day 15. Matrix metalloproteinases (MMP)-1 and -13 expressions were elevated (~25-fold) in gels with higher crosslinking throughout the study, while MMP-3 was not affected by gel crosslinking. The presence of aggecan and collagen degradation products confirmed MMP activity. These findings indicate that chondrocytes synthesize the major cartilage components within PEG hydrogels, however, gel structure strongly impacts the

composition and spatial organization of the neo-tissue and impacts how chondrocytes respond to their environment, particularly with respect to their catabolic expressions.

A1.2 Introduction

The complex structure and organization of cartilage gives the tissue its unique ability to withstand large forces. Articular cartilage is a complex fibrillar mesh of interacting collagens, proteoglycan aggregates, and other non-collagenous proteins, which all reside in a highly aqueous environment. Proteoglycans contain large amounts of negatively charged, sulfated glycosaminoglycans (sGAG), predominantly that of chondroitin sulfate, resulting in an osmotic environment with high swelling pressures that are counteracted by the collagen fiber network [1,2]. These aggregates, along with the collagen type II mesh, form the bulk of the extracellular matrix (ECM) [3].

The pericellular matrix (PCM), which has a distinctly different composition from the ECM, serves to protect the chondrocyte from mechanical stresses and is thought to regulate both biochemical and biophysical cues presented to the cells, thus influencing their biological function [4,5]. The PCM is characterized by the presence of a collagen VI mesh network, although aggrecan and collagen II are also present in the PCM. Collagen VI fibrils, found exclusively in the PCM [6,7], contain multiple globular units with binding motifs that can assemble with smaller proteoglycans, such as decorin and biglycan [8–10]. These assemblies, which are unique to the PCM, help to bridge the surrounding ECM with the cells, and may also participate in the assembly of aggregates prior to their release into the ECM [11,12]. The composition and structure of the PCM also serves to regulate the passage of soluble factors that can interact with the cell (i.e. cytokines, growth factors, matrix catabolites) [13]. Therefore, extracellular cues that affect the development and/or maintenance of the PCM may in turn directly impact the signals perceived by the cells and subsequently affect the long-term formation and/or maintenance of the ECM.

One of the major goals in designing scaffolds for cartilage tissue engineering is to provide cells with an environment in which they can synthesize and deposit a neotissue that recapitulates the native tissue's composition, structure, and mechanics towards restoring joint function. A variety of natural and synthetic hydrogels have been examined as chondrocyte carriers due to their ability to maintain the chondrocyte phenotype and the highly swollen network that supports nutrient and cell waste diffusion [14–16]. For example, isolated chondrocytes encapsulated in agarose have been shown to support the development of a distinct PCM region [17], rich in collagen VI, followed by the maturation of a cartilage-like ECM composed of collagen II and full-length aggrecan [18]. In some cases, these constructs have resulted in physiologic concentrations of glycosaminoglycans and have approached the compressive moduli of cartilage [19–22] even though collagen content and dynamic mechanical properties remained inferior to that of native articular cartilage [23]. Chondrocytes cultured in alginate gels developed a mechanically stiff PCM, composed of collagen and proteoglycans, as early as day 7 of culture [24]. Recent developments of peptides that self-assemble into hydrogels have also shown to support the deposition of neotissue by encapsulated chondrocytes, exhibiting an ECM rich in collagen type II and glycosaminoglycans [25,26]. However, one of the limitations with many of the aforementioned hydrogel systems is that their mechanical properties are often much lower than that of the native tissue limiting their ability to withstand the high stresses seen in the native environment, at least initially, until sufficient matrix has been deposited.

In an effort to design synthetic hydrogels capable of matching the high compressive moduli of articular cartilage, photopolymerizable poly(ethylene glycol) (PEG) based hydrogels have been studied [27–31]. The mild polymerization allows for in situ formation and the encapsulation of cells, while the synthetic chemistry may be modified to introduce degradable linkages [32–35] and/or biomimetic moieties [36–39]. The mechanical properties of the hydrogel may be finely tuned through manipulations in gel crosslinking density (ρ_x), which can

be controlled through simple changes in the gel formulation. High moduli PEG hydrogels (~900 kPa) have been used to successfully encapsulate chondrocytes, maintaining cell viability and matrix synthesis [27,40]. However, changes in ρ_x will impact other properties such as water content and diffusion of molecules [41], including newly deposited matrix molecules, throughout the network [27,42]. These properties will have a significant impact on how the encapsulated chondrocytes sense their environment, which can in turn affect their proliferation, metabolism, and the ECM synthesis and deposition [28,30,40,43–45].

Gross examination of neotissue development within PEG hydrogels has demonstrated that the ECM matrix is composed of sGAGs and collagen type II [27,46]. Short-term studies have indicated that a PCM develops, based on deposition of chondroitin sulfate, within a few days in the PEG hydrogel constructs [44], followed by the deposition of sGAGs into the ECM. The extent of PCM and ECM development has been shown to be dependent on the gel ρ_x, illustrating that a higher ρ_x resulted in a thinner, denser PCM with decreased sGAG deposition in the extracellular regions of the hydrogel. These previous studies illustrate that the crosslinked structure impacts the developing tissue, at least by gross examination of sGAGs and collagen. However, the structure and composition of cartilage, which gives rise to its unique functional properties, is much more complex. Therefore, in designing hydrogels with high moduli suitable for in situ placement, it is equally important to understand how the crosslinked structure impacts the structural organization of the developing tissue.

Therefore, the objectives for this study were two-fold. First, we assessed the role of gel crosslinked structure on the composition and distribution of newly deposited cartilage matrix molecules, particularly matrix molecules which give rise to the PCM (e.g., collagen VI), play an important role in the organization of the tissue (*e.g.*, link protein, and decorin), and contribute to the PCM, but also more importantly make up most of the native ECM (*i.e.*, chondroitin sulfate a building block of aggrecan, aggrecan and collagen type II). Because the PCM is thought to be a critical mechanism by which cells receive external cues, any differences in the PCM

composition and structure may impact the function of the chondrocyte. Therefore, in the second part of this study, we assessed the role of the crosslinked structure in mediating anabolic and catabolic functions of chondrocytes through gene expression analysis and by assaying for catabolic activity through the detection of degraded matrix. Overall, our findings illustrate that PEG hydrogels are supportive of cartilage-matrix molecule deposition, but that the crosslinked structure largely impacts the type of tissue deposited, the spatial deposition of the tissue, and the anabolic and catabolic activity by the chondrocytes. This information should aid in the design of high moduli hydrogels for cartilage tissue engineering applications.

A1.3 Materials and Methods

A1.3.1 Materials

Collagenase type II and papain were from Worthington Biochemical (Lakeshore, NJ). Fetal bovine serum (FBS), Dulbecco's Modified Eagle's Medium (DMEM), 100x penicillin-streptomycin (P/S), fungizone, HEPES-buffer, gentamicin, and MEM-nonessential amino acids (NEAA), goat anti-rabbit IgG Alexa Fluor 488, goat anti-mouse IgG Alexa Fluor 546, DAPI and all D-LUX PCR primers were from Invitrogen (Carlsbad, CA). L-proline, ascorbic acid, bovine serum albumin (BSA), 1,9-dimethylmethylene blue (DMMB), protease-free chondroitinase ABC, hyaluronidase, methylene chloride, methacryloyl chloride, ethyl ether, triethylamine, dithiothreiotol (DTT), and iodoacetamide were from Sigma-Aldrich (St. Louis, MO). Irgacure 2959 was from Ciba Specialty Chemicals (Newport, DE). E.Z.N.A.-Total RNA Mini-kit was from Omega-Biotek (Norcross, GA). High Capacity cDNA kit and Taqman® Fast Universal PCR Master Mix were from Applied Biosystems (Foster City, CA).

The aggrecan (A1059-53F) and collagen II (C5710-20F) antibodies were from US Biologicals (Swampscott, MA). Chondroitin-6-sulfate antibody (MAB2035) was from Chemicon (Billerica, MA). The anti-collagen VI antibody (ab6588) was from Abcam (Cambridge, UK). Decorin (7b1), and link protein (9/30/8-A-4) antibodies were from the University of Iowa Developmental Studies Hybridoma Bank (Iowa City, IA). The C1,2C ELISA kit was from IBEX

Pharmaceuticals (Quebec, Canada). BCA Protein Assay kit was from Thermo Scientific Pierce (Rockford, IL). For western blot analysis, primary antibodies for mouse monoclonal to aggrecan and N- terminal neoepitope FFG4 were acquired from MD Biosciences (St. Paul, MN). Western blot gels, membranes, buffers, Tween-20, and blot equipment were from Bio-Rad Labs (Hercules, CA).

A1.3.2 Chondrocyte isolation

Full depth articular cartilage was harvested from the patellar-femoral groove of 1-3 week old calves (*n* = 2, Research 87, Marlborough, MA) within 24 hours of slaughter and digested in 500 units/mL collagenase II in DMEM supplemented with 5% FBS for 16 h at 37 °C on an orbital shaker (40 rpm). The digest was passed through a 100 µm cell-strainer, pelleted and rinsed 3x with PBS containing 1% P/S, 0.5 µg/mL fungizone, and 20 µg/mL gentamicin (PBS-Antis). Isolated cells were counted using trypan blue exclusion assay and resuspended in chondrocyte medium (DMEM supplemented with 10% FBS (v/v), 0.04 mM L-proline, 50 mg/L L-ascorbic acid, 10 mM HEPES, 0.1 M MEM-NEAA, 1% P/S, 0.5 µg/mL fungizone, and 20 µg/mL gentamicin) prior to encapsulation.

A1.3.3 Hydrogel formation

Poly(ethylene glycol) dimethacrylate (PEGDM) was synthesized by reacting PEG (4.6 kDa) with methacryloyl chloride in the presence of triethylamine for 24 h at 4 °C. PEGDM was purified using a series of precipitations in chilled ethyl ether and analyzed by ^{1}H NMR (Varian YVR-500S), which indicated 90% methacrylation. PEGDM was dissolved in chondrocyte medium at 10, 15, or 20% (w/w) and mixed with 0.05, 0.022, or 0.0125 (w/w) photoinitiator Irgacure 2959, respectively. Sterile macromer solution was added to pelleted chondrocytes at 50 million cells/mL, mixed thoroughly, and immediately photopolymerized using 365 nm light (6 mW/cm^2) for 10 minutes. Hydrogel constructs (5 mm diameter x 5 mm height cylinders) were rinsed in PBS+Antis and individually placed into wells of a 24-well tissue culture plate. Gels

were cultured at 37 °C in 5% CO_2 and allowed to equilibrate for 24 hrs prior to the start of the experiment. Medium was changed every 2-3 days and saved at -20 °C for sGAG analysis.

A1.3.4 Hydrogel characterization

At day 0, equilibrated acellular hydrogels (n = 3) were weighed to obtain wet weight measurements. Hydrated hydrogels were subsequently compressed to 15% strain at 0.5 mm/min to obtain stress-strain curves (MTS Synergie 100, 10N). Hydrogels were then lyophilized for 48 h and their dry mass determined. Equilibrium volumetric swelling ratio (Q) was calculated from the mass swelling ratio (q). Crosslinking densities (ρ_x) and mesh sizes (ξ) were estimated from Q as described elsewhere [28].

A1.3.5 Biochemical analysis

At days 0, 5, 10, 15, and 20, hydrogels were removed from culture and cut in half. One half (n=3) was weighed to obtain wet weight, lyophilized for 48 h and subsequently homogenized and enzymatically digested by papain for 16 h at 60 °C. Gel samples and collected media samples were assessed for sGAG content by the DMMB dye method [47]. sGAG content within hydrogels were normalized to gel wet weights.

A1.3.6 Histological visualization

At 25 days of culture, constructs (n = 3) were fixed for 24 hours in 4% paraformaldehyde, dehydrated, paraffin-embedded, and sectioned (10 μm). Negatively charged glycosaminoglycans (sGAGs) were detected using Safranin-O/Fast Green while collagen deposition was analyzed by Masson's Trichrome. Cell nuclei were counterstained by hematoxylin. For immunohistochemistry, sections were analyzed for collagen type II and VI, aggrecan, link protein, chondroitin-6-sulfate, and decorin. Samples were treated with chondroitinase ABC (10 mU) and hyaluronidase (200 U) for 1 h at 37 °C. For antigen retrieval of the hyaluronan binding region and link protein, samples were also reduced and alkylated. All samples were blocked using 1% BSA for 30 minutes. Sections were then incubated overnight at 4 °C with primary antibodies for collagen II (1:100), collagen VI (1:100), aggrecan (1:10),

chondroitin-6-sulfate (1:100), hyaluronan (1:5), link protein (1:5), or decorin (1:5). Fluorescent detection of each protein was achieved using either secondary goat anti-rabbit IgG Alexa Fluor 488 or goat anti-mouse IgG Alexa Fluor 546 antibodies (1:200) and counterstained using DAPI (1:1000). Sections were mounted and preserved using VectaMount, and a laser scanning confocal microscope (Zeiss LSM 5 Pascal) was used to acquire images. All antibodies were validated to ensure their specificity. Negative controls were performed on sections from cell-laden hydrogels that did not receive primary antibody showing no positive staining. Positive controls were performed on hyaline cartilage and the data are shown in Figures 2-4.

A1.3.7 Gene Expression

Construct halves at 0, 5, 10, 15, and 20 days (n = 3) were immediately snap-frozen under liquid nitrogen and processed using E.Z.N.A-Total RNA Mini-Kit columns; total RNA was obtained with a A260/A280 ratio > 1.8 (Nanodrop, ND-1000, Thermo-Fisher). 100 ng of RNA was transcribed to cDNA using the High Capacity cDNA Kit. Real-time RT-PCR (ABI 7500 Fast) was performed for collagen type II (*COL2*), aggrecan (*AGC*) and matrix metalloproteinases (MMP) -1, -3, and -13 using the Taqman® Fast Universal PCR Master Mix [48]. Gene expression was measured relative to the expression of the mitochondrial ribosomal protein L30 (housekeeping gene) and normalized to 10% gels at each time point (calibrator) as described elsewhere [44].

A1.3.8 Western blot analysis

Whole constructs at 0 and 20 days (n = 2) were immediately snap-frozen in liquid nitrogen and stored at -80 °C. These constructs were later thawed and homogenized in assay buffer (0.05 M Tris HCl (pH 7.5), 0.2 M NaCl, 0.01 M $CaCl_2$, 0.02% NaN_3, and 0.05% Triton-X). Constructs and conditioned medium samples (n = 2) were assayed for aggrecan and its degradation products by Western blot analysis. Samples were measured for protein content using the BCA Protein kit, deglycosylated, mixed with reducing loading buffer, and loaded into wells of a 10% Criterion Tris-HCl gel (Bio-Rad). Each lane contained 10 µg of protein from the

construct samples or 30 μg of protein from the media samples. After separation by electrophoresis (40 min, 200V), proteins were transferred to Immun-Blot PVDF membranes for 1 h at 100V. The membranes were blocked with 5% BSA in phosphate buffered saline with 0.1% Tween-20 (PBS-T) for 2-4 h, and probed with 1 μg/mL primary antibodies for epitopes FFGV (BC-14) and the linear IGD domain of aggrecan (bovine-EPEEPFTFVPEV, 6B4) overnight at 4 °C. Secondary detection was performed using a goat anti-mouse Alexa Fluor 546 antibody (1:400) and imaged using a Bio-Rad Versadoc 4000 MP imaging system (3.5 AP/ Exp. 30 s).

A1.3.9 ELISA for collagen degradation products

Constructs and conditioned medium samples (n = 2) were assayed for the MMP-cleaved collagen degradation product. Equal volumes of media and of assay buffer from the homogenized constructs (described above for western blot analysis) were assayed for the carboxy terminus of the ¾ peptide (C1,2C or Col 2 ¾C Short) generated by cleavage of types I and II collagens by collagenases using the competitive immunoassay C1,2C ELISA per the manufacturer.

A1.3.10 Statistical analysis

Data are represented as a mean ± standard deviation. Accumulated sGAG release into the media is reported using the cumulative average (standard deviation) for each sampling (hydrogel and time point). Gene expression values as a function of culture time and gel crosslinking density were analyzed by two-way analysis of variance (ANOVA) and significant differences due to ρ_x at each time point were analyzed post-hoc using Tukey's HSD with a statistical significance of α = 0.05.

A1.4 Results

Hydrogels of three different crosslinking densities were fabricated from 10, 15 and 20% PEGDM macromer, referred to as 10, 15, and 20% PEG gels, respectively, which spanned a range of macroscopic properties, described in Table A1.1. All hydrogels imbibed high

equilibrium water contents, greater than 86%. The compressive moduli of the hydrogels ranged over an order of magnitude from 60 to 590 kPa with increasing crosslinking density. The mesh size or average distanced between crosslinks was estimated, decreasing from 195 to 65 Å with increasing crosslinking density.

Table A1.1. Properties of PEGDM hydrogels

PEGDM* (wt.%)	Equilibrium volumetric swelling ratio (Q)	Crosslinking density (mol l^{-1})	Water content (%)	Compressive modulus (kPa)	Mesh size (ξ) (Å)
10	11.6 ± 0.2	0.11 ± 0.01	91.6 ± 0.5	60 ± 10	148 ± 5
15	8.4 ± 0.1	0.22 ± 0.01	88.8 ± 0.2	320 ± 10	94 ± 2
20	6.5 ± 0.2	0.38 ± 0.02	85.9 ± 0.5	590 ± 10	65 ± 3

* PEGDM macromer concentration prior to photopolymerization

A1.4.1 Matrix deposition

Proteoglycan deposition and accumulation was measured by sGAG content (Fig. A1.1A, B). There was a significant increase in sGAG content with culture time for all three crosslinked hydrogels ($p < 0.0001$). Crosslinking density was a significant factor affecting sGAG content ($p < 0.0001$). After day 0, sGAG content was significantly higher in the 10% and 15% PEG gels compared to the 20% PEG gels. The mean sGAG content was generally higher in the 10% PEG gels when compared to the 15% PEG gels, which was significant at days 15 and 20, but by day 25 similar contents were reported. The presence of sGAGs in the culture medium (Fig. A1.1B) revealed significant loss from the construct and accumulation in the medium with culture time. The percentage of sGAG lost was 36%, 34% and 49% of the total sGAG deposited (*i.e.*, sGAGs in the construct + sGAG in medium) after 25 days for the 10%, 15%, and 20% PEG gels, respectively.

The relative size of the aggrecan molecules, after deglycosylation, present within the constructs was also probed at days 0 and 20 by western blot analysis (Fig. A1.1C). While the same amount of protein was loaded into each well for analysis, the total protein extracted from

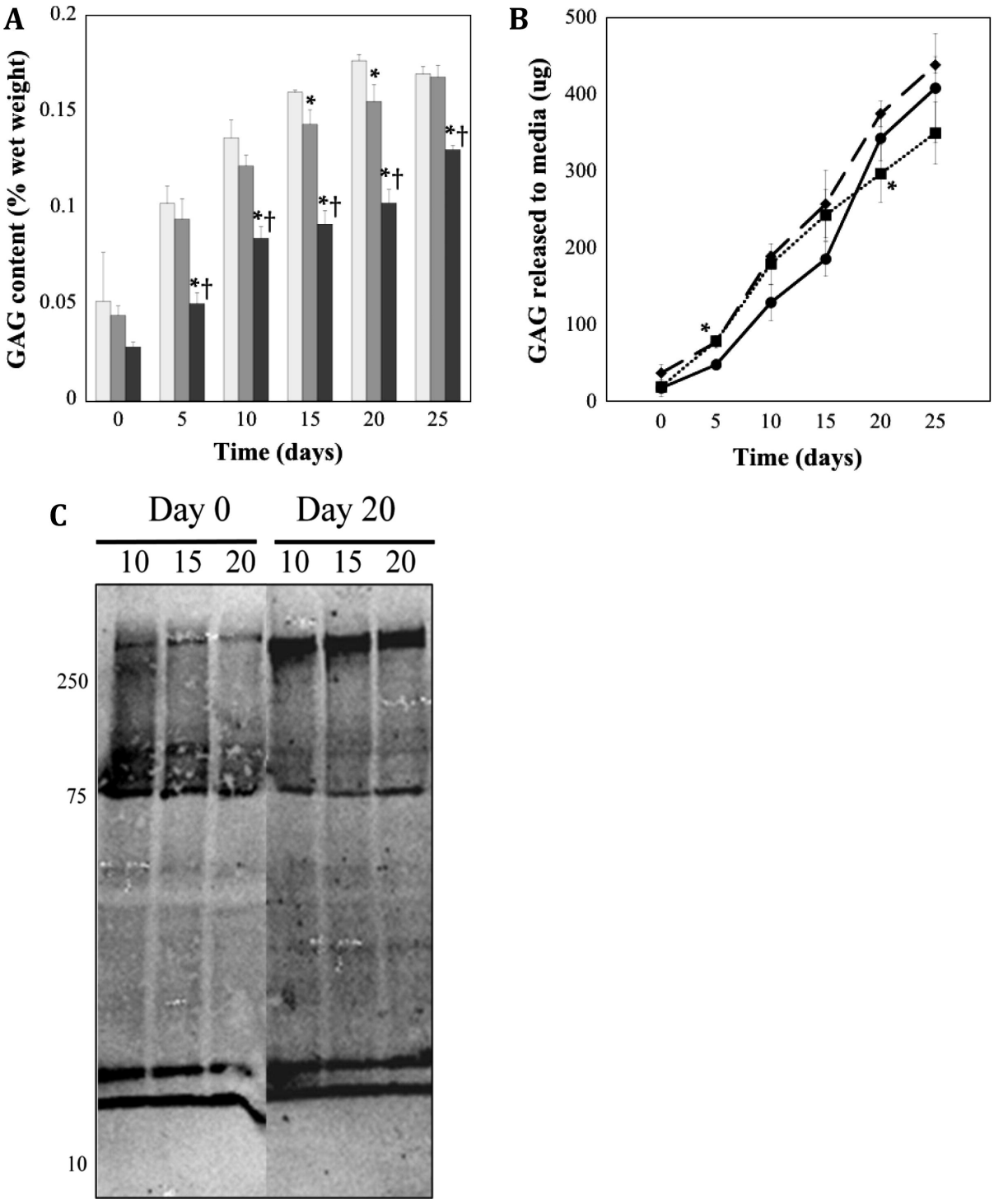

Figure A1.1 The total amount of sGAG (A) accumulated in the hydrogel construct per wet weight hydrogel as a function of crosslinking density and culture time for 10% (□), 15% (▒), and 20% (▓) (w/w) PEG gels. Accumulated sGAG released from construct (B) into surrounding media during FS culture time for 10% (solid ●), 15% (dashed ◆), and 20% (dotted ■) gels at each time point. * indicates significant difference from 10% gels ($p<0.05$), † indicates a significant difference from 15% gels ($p<0.05$). Aggrecan detection by western blot analysis (C) within 10, 15, and 20% PEG gels at days 0 and 20. Anti-IGD probes were used to detect the intact IGD region between G1 and G2 domains of aggrecan.

the hydrogels differed and was highest in the 10% PEG gels and lowest in the 20% PEG gels. The amounts were 265 ± 9, 229 ± 3, and 204 ± 3 μg at day 0 and 304 ± 20, 254 ± 14 and 219 ± 13 μg at day 20 for the 10%, 15% and 20% gels, respectively. Several sizes of aggrecan molecules were detected, which were consistent across crosslinking densities, but differed between days 0 and 20. At day 0, the majority of aggrecan was ~75 kDa and ~15-20 kDa. By day 20, aggrecan was much larger with sizes in the range of 275 kDa with few of the intermediate sizes, but a similar presence of the smaller molecules (~15-20 kDa).

To determine the influence of crosslinked structure on matrix formation, deposition, and distribution, sulfated glycosaminoglycans were initially evaluated by Safranin-O staining and immunofluorescence (Fig. A1.2). After 25 days of culture, sGAGs distribution in the 10% PEG gels was present throughout the extracellular regions, mimicking to a certain degree the spatial distribution of sGAGs in native cartilage. However, a sharp contrast in sGAG deposition was observed in gels with higher crosslinking. The higher gel crosslinking resulted in decreased sGAG diffusion throughout the hydrogel, to the extent that sGAGs were solely localized to the immediate pericellular region in the 20% PEG gels. Detection of the major sGAG, chondroitin-6-sulfate, and major proteoglycan, aggrecan, also showed significant differences with gel crosslinking. The decreased presence of chondroitin sulfate deposition in the extracellular regions as crosslinking increased mirrored that of the general sGAG stain. Chondroitin sulfate staining in the ECM regions was greatest in the 10% PEG gels, but in the PCM region, it was greater in the 15% PEG gels compared to the 10% PEG gels. Further increases in gel crosslinking from 15% to 20% PEG gels resulted in decreased chondroitin sulfate presence where not all cells showed the same level of deposition. Aggrecan was detected only in the PCM for all three crosslinked gels. Staining for aggrecan also decreased with increasing crosslinking density, but did not match the observed chondroitin sulfate or general sGAG distributions. It should be noted that the interpretation of the PCM encompasses matrix excreted and deposited adjacent to the cell and matrix that has been synthesized by the cell, but which

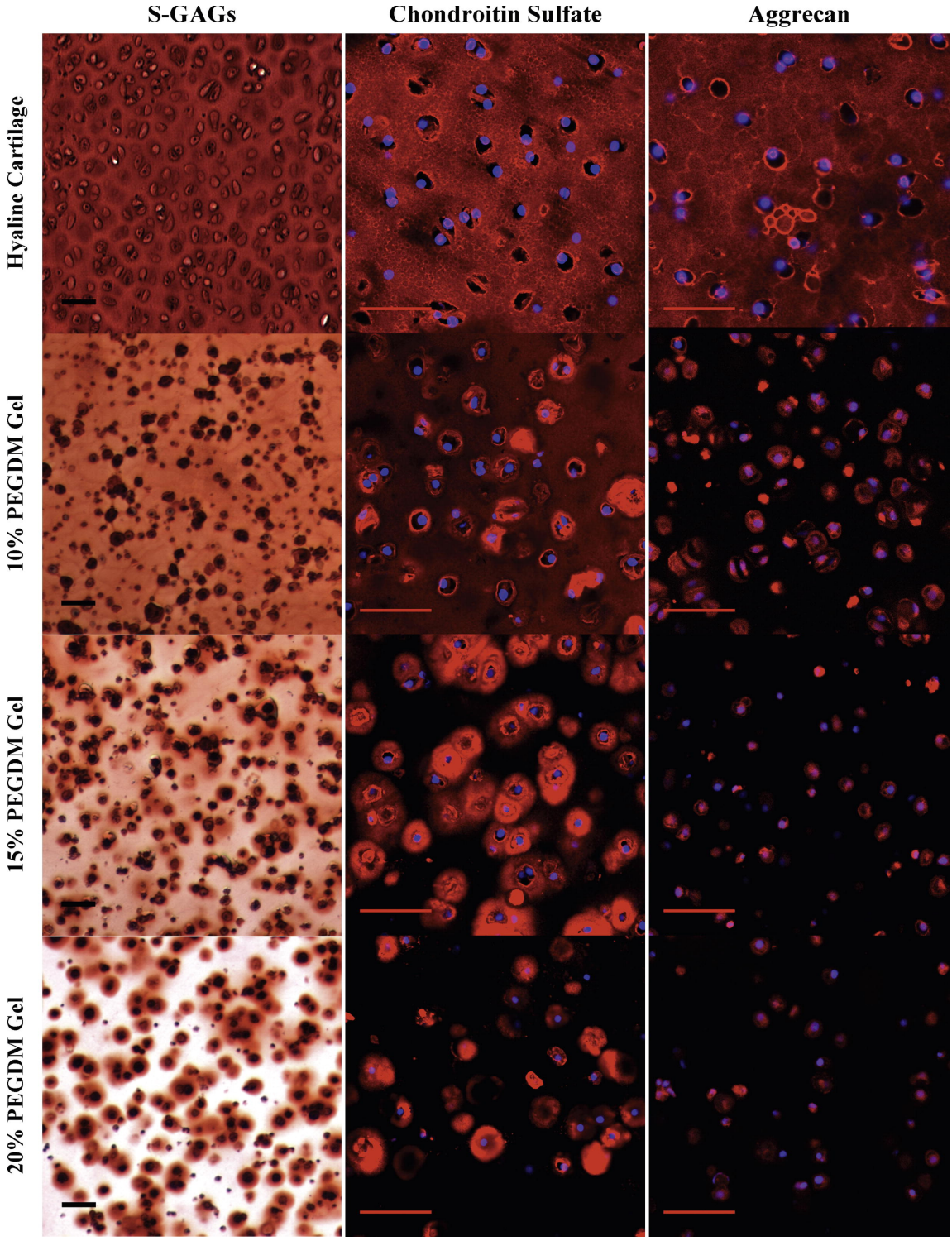

Figure A1.2 Gross examination of proteoglycan matrix deposition by histological and immunohistochemical (IHC) evaluation for chondrocytes encapsulated in 10, 15, or 20% PEG gels and cultured for 4 weeks. Sections were stained for negatively charged glycosaminoglycans (sGAGs) (red) using Safranin O/Fast green. Cell nuclei (dark purple) were counterstained using hematoxylin. For IHC, sections were using antibodies against chondroitin-6-sulfate (red), and aggrecan (red). Cell nuclei (blue) were counterstained using DAPI. Images were acquired by laser scanning confocal microscopy. Scale bars represent 50 μm.

has not yet been excreted. In cartilage and to a certain extent in the 10% PEG gels, the PCM deposited extracellularly is more evident, while in the higher crosslinked gels the distinction between extracellular and intracellular matrix is less clear.

A decrease in the presence of other matrix proteins was also observed with higher ρ_x gels. Collagen II deposition was restricted to the pericellular regions, which correlated with the collagen staining seen with Masson's Trichrome (Fig. A1.3). Pericellular staining for collagen VI revealed inhomogeneities in the staining where not all cells showed the same level of deposition regardless of crosslinking. Cells in the 10% PEG gels exhibiting collagen VI deposition showed thick, spherical staining, whereas higher crosslinked gels resulted in more diffuse, non-uniform collagen VI distribution. Similar trends were observed for link protein and decorin (Fig. A1.4). Link protein was densest in the pericellular region and showed little to no deposition in the 20% PEG gels. The pattern of decorin deposition followed closely with collagen type II distribution, showing uniform densities in the PCM and greatest accumulation in the 10% PEG gels.

A1.4.2 Chondrocyte matrix expression

The effects of hydrogel crosslinking on the gene regulation of structural proteins, collagen II (*COL2*) and aggrecan (AGG), as well as catabolic enzymes, matrix metalloproteinases-1, -3, and -13, were assessed. Analysis by two-way ANOVA revealed that *COL2* and *AGC* were significantly regulated by culture time ($p < 0.001$), whereas culture time, gel crosslinking, and their interactions, affected all MMP expressions ($p < 0.001$). Specifically, differences in gel crosslinking affected initial expression levels of *COL2* and *AGC* but these differences diminished by day 20 (Fig. A1.5). Regardless of crosslinking and culture time, *COL2* expression was approximately 10-fold higher than *AGC* expression, which is consistent with greater collagen II accumulation seen by immunohistochemistry. A strong positive correlation ($r = 0.86$) was observed between *COL2* and *AGC* expressions regardless of culture time and gel structure. Analysis of MMPs-1, -3, and -13 showed opposite expression profiles from the anabolic trends, exhibiting an overall decrease in expressions compared to day 0.

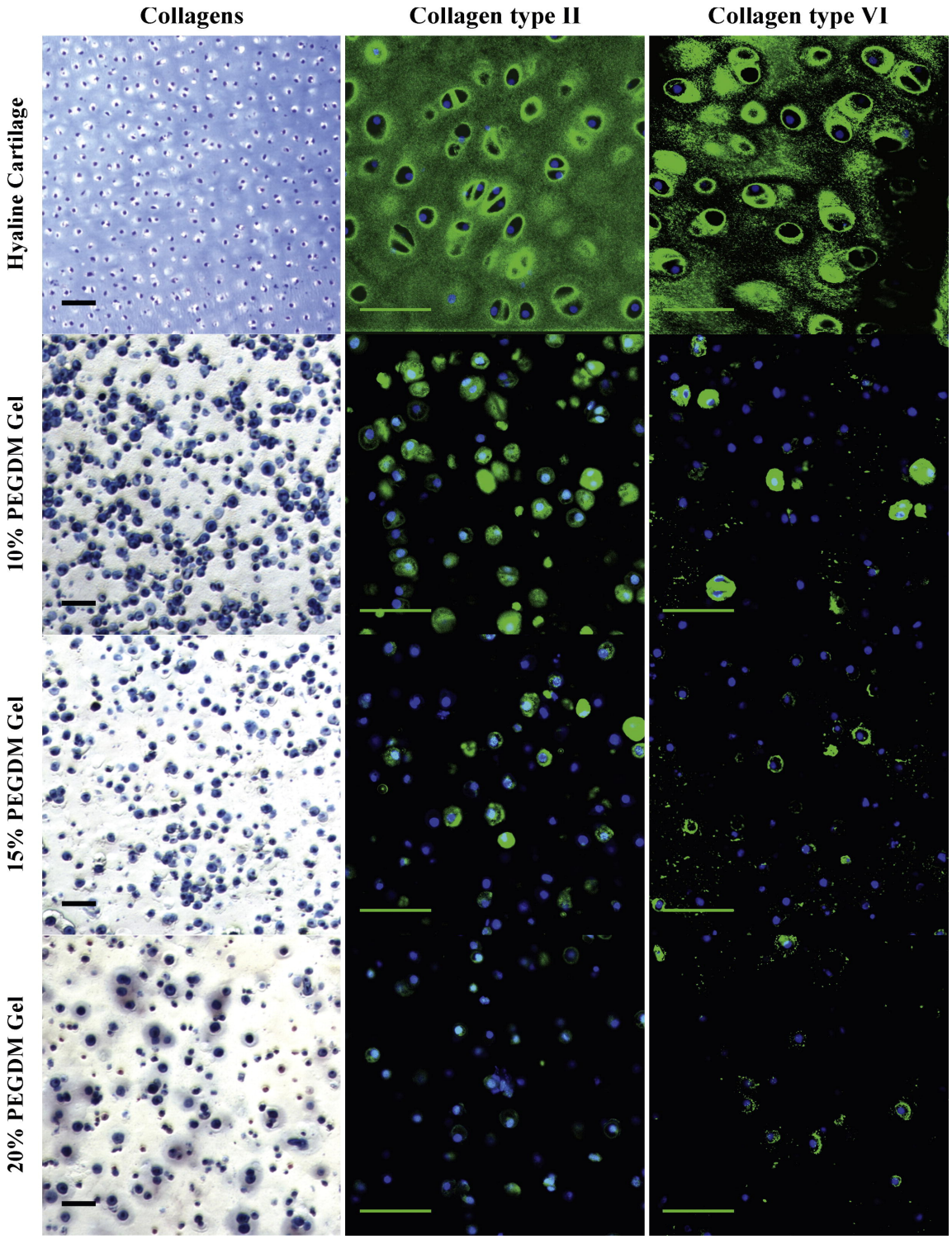

Figure A1.3 Gross examination of collagen matrix deposition by histological and immunohistochemical (IHC) evaluation for chondrocytes encapsulated in 10, 15, or 20% PEG gels and cultured for 4 weeks. Sections were stained for collagens (blue) using Masson's Trichrome. Cell nuclei (dark purple) were counterstained using hematoxylin. For IHC, sections were stained using antibodies against collagen type II (green) and collagen type VI (green). Cell nuclei (blue) were counterstained using DAPI. Images were acquired by laser scanning confocal microscopy. Scale bars represent 50 μm.

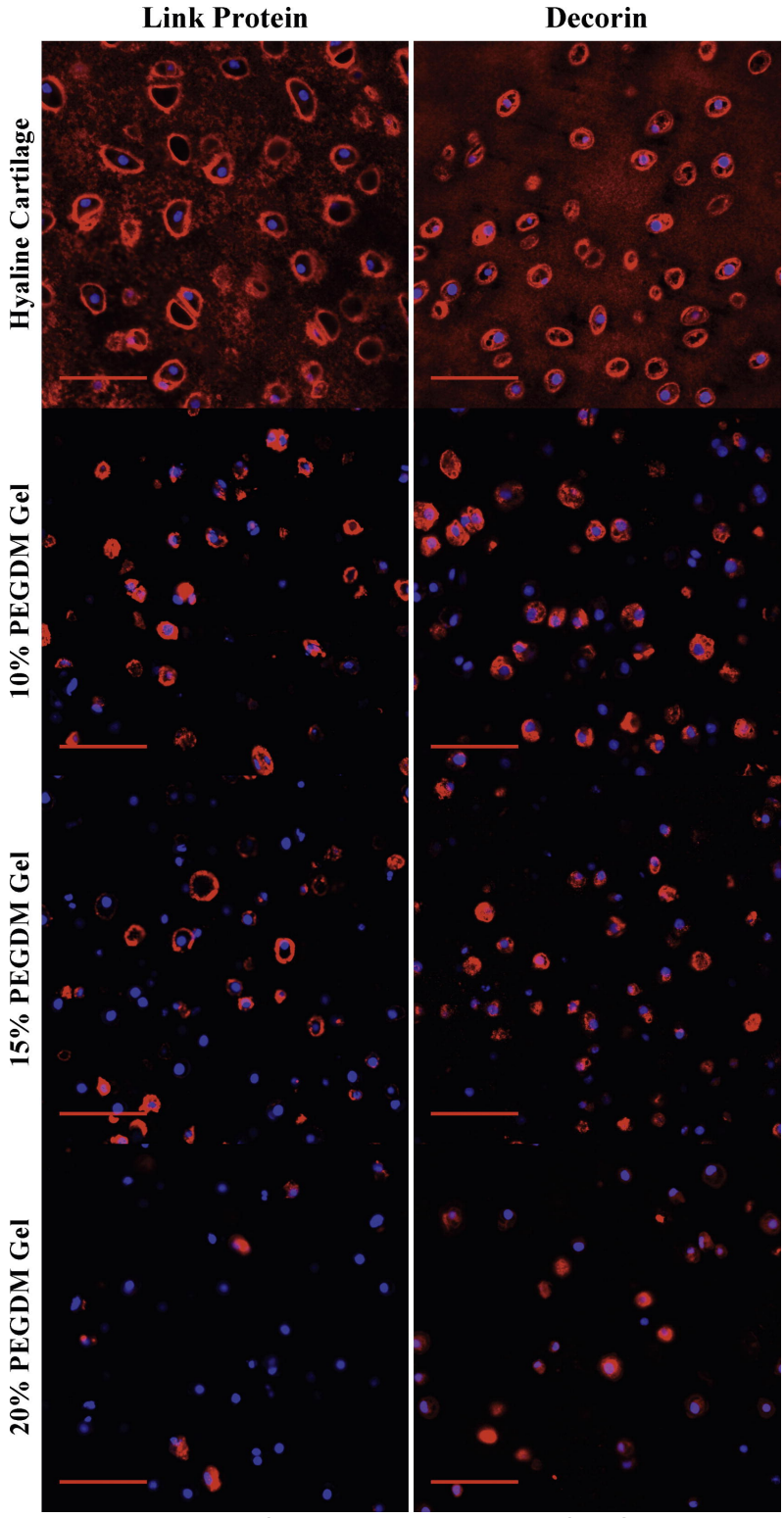

Figure A1.4 Gross examination of matrix deposition of ECM connective proteins by immunohistochemical (IHC) evaluation for chondrocytes encapsulated in 10, 15, or 20% PEG gels and cultured for 4 weeks. Sections were stained using antibodies against link protein (red), and decorin (red). Cell nuclei (blue) were counterstained using DAPI. Images were acquired by laser scanning confocal microscopy. Scale bars represent 50 μm.

MMP-3 was expressed at the highest levels of the three MMPs. Interestingly, 15% and 20% PEG gels exhibited sharp increases in MMP-1 and -13 expression between 5-15 days of culture, whereas 10% PEG gels exhibited a continual decrease in all MMP levels over the 20 day culture period. Following day 5 of culture, a positive correlation between MMP-3 and *AGC* expression was observed (r = 0.73) as well as between MMP-1 and -13 (r = 0.78).

To investigate differences in gene expression levels due to hydrogel crosslinking, relative expression levels were normalized to the 10% PEG gel values at their respective time points (Fig. A1.6). Initially, increasing crosslinking from the 10% to 15% PEG gels promoted both *COL2* and *AGC* expression (1.4x), which was further enhanced in the 20% PEG gels by 2x. However, by 20 days of culture, expression of these genes reached similar levels regardless of crosslinking. Analysis of MMP-1 revealed that 20% PEG gels expressed higher levels at all time points compared to 10% PEG gels (as high as 25x at day 15). MMP-13 expressions were highly dependent on ρ_x showing similar characteristics to MMP-1 for 20% PEG gels (as high as 35x at day 15 when compared to 10% PEG gels). Crosslinking density did not affect MMP-3 levels at any of the observed time points.

A1.4.3 Presence of matrix degradation products

The activity of catabolic enzymes MMP-1, MMP-13, and MMP-3 were assessed by assaying for their respective matrix degraded products using two different methods. First, the amount of C1,2C fragment, which results from MMP-1 and MMP-13 cleavage of collagen I or II, was measured by ELISA in the constructs (Fig. A1.7A) and in the media (Fig. A1.7B). There were no significant changes in content of C1,2C fragments in the gel as a function of culture time or as a function of gel crosslinking. Although, the mean levels dropped around days 10 and 15 for all crosslinked gels, but returned to levels that were similar to day 0. There were no significant changes in the amount of C1,2C fragment present in the culture medium as a function of culture time or as a function of gel crosslinking.

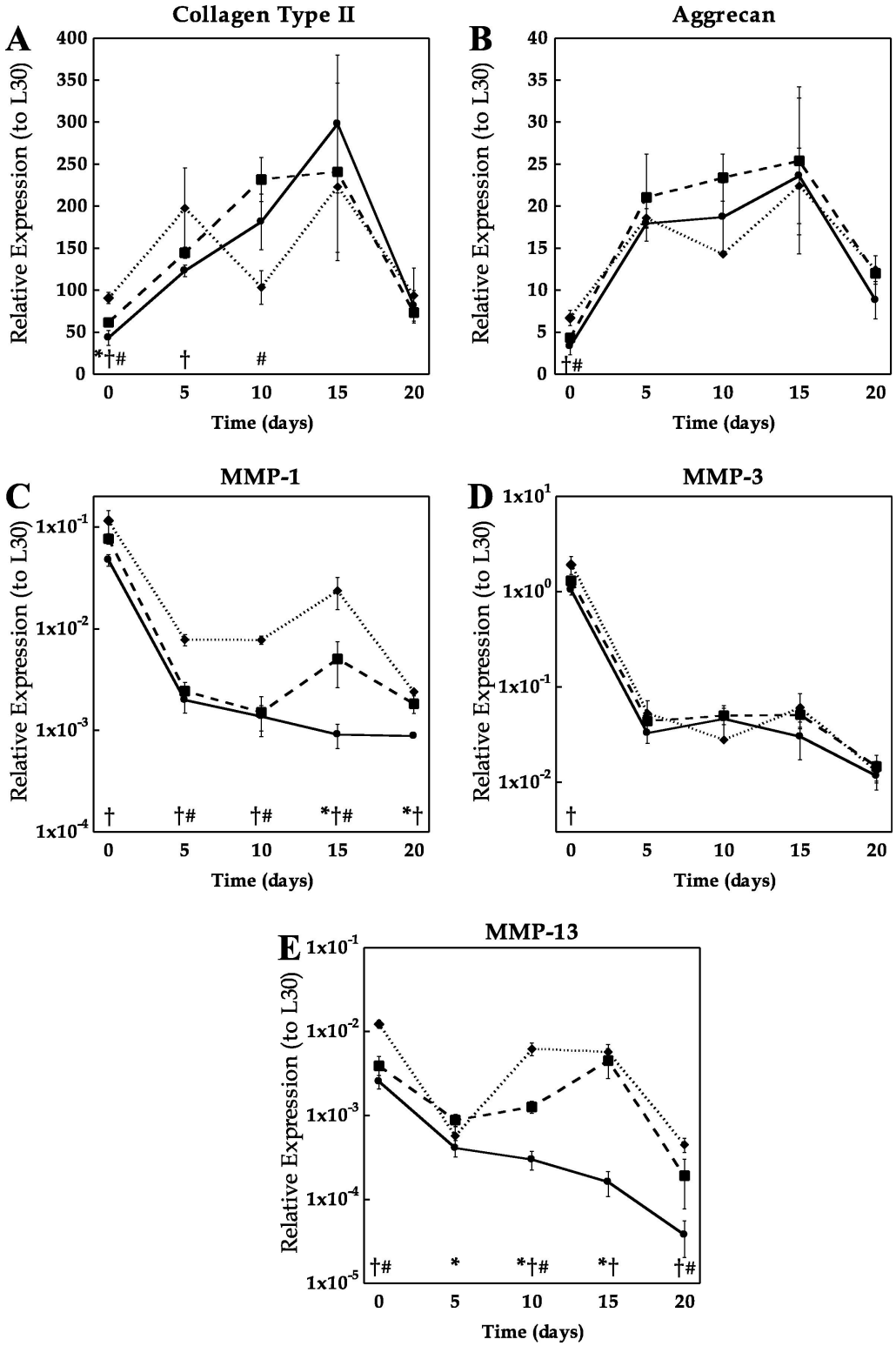

Figure A1.5 Relative gene expression for collagen II (A), aggrecan (B), matrix metalloproteinase (MMP) -1 (C), -3 (D), and -13 (E) compared to the housekeeping gene (HKG) L30 for 10% (solid ●), 15% (dashed ◆), and 20% (dotted ■) PEG gels conditioned up to 20 days in culture. Significant differences ($p<0.05$) between crosslinking densities at specific time points are represented as (*) for 10% vs. 15%, (†) 10% vs. 20%, and (#) 15% vs. 20%.

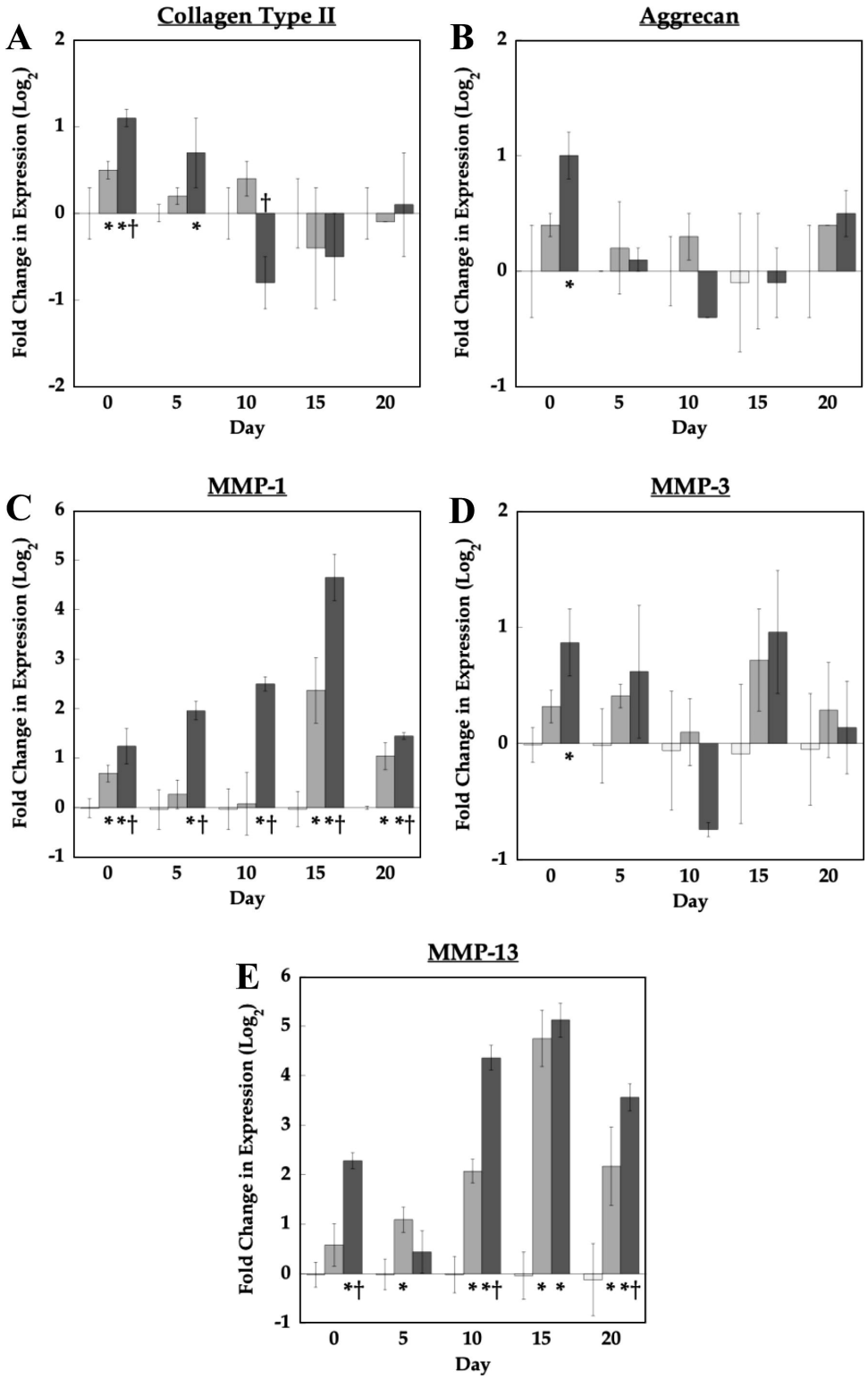

Figure A1.6 The effects of crosslinking density on gene expression at specific time points for collagen type II (A), aggrecan (B), matrix metalloproteinase (MMP) -1 (C), -3 (D), and -13 (E) 10% (□), 15% (▒), and 20% (■) PEG gels. Data are presented as normalized expression relative to 10% gels at each specified time point. * indicates a significant difference from 10% gels ($p < 0.05$).

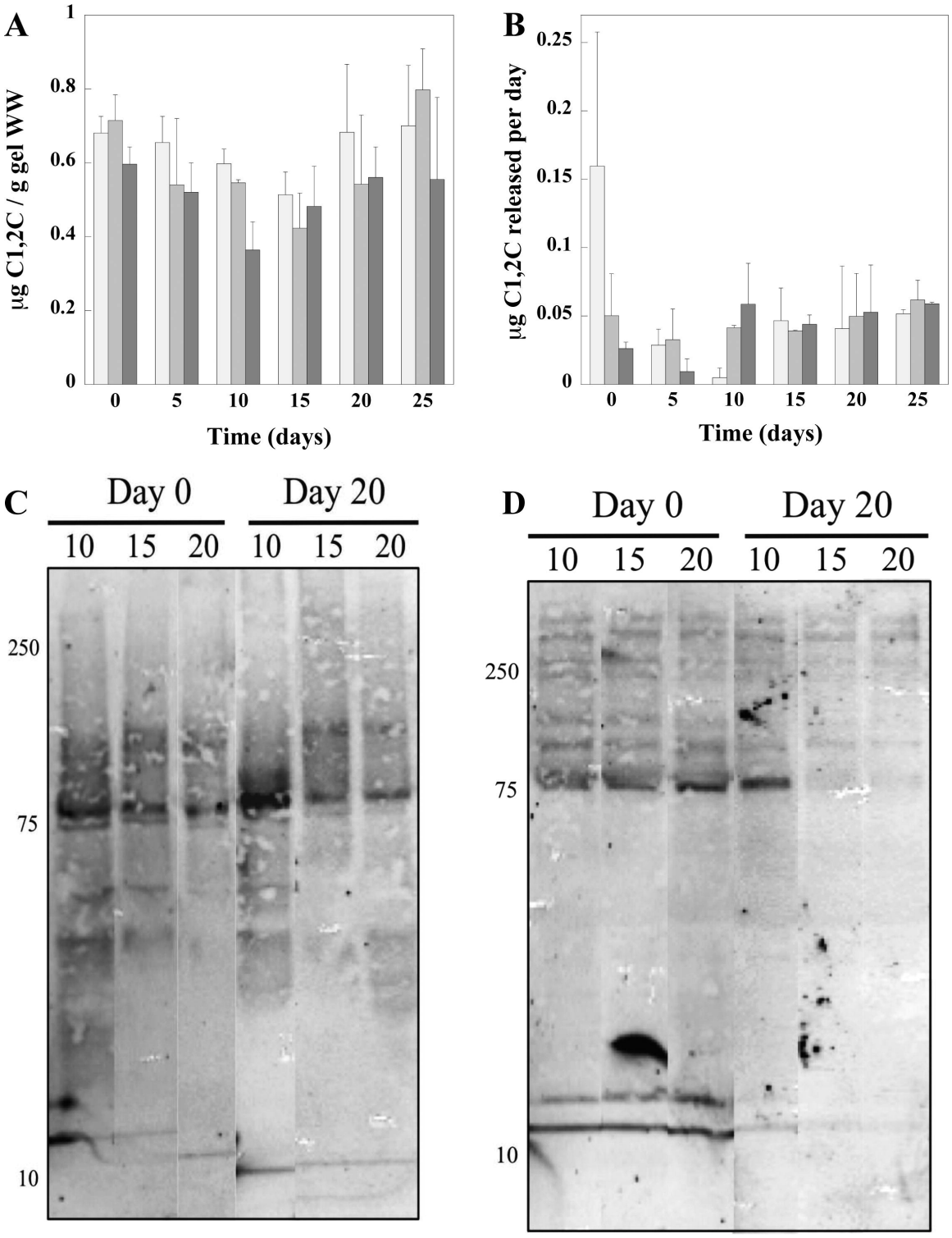

Figure A1.7 The total amount of C1,2C accumulated in the hydrogel constructs (A) and total amount of C1,2C released to the media per day (B) as a function of gel crosslinking density and culture time for 10% (□), 15% (▒), and 20% (■) PEG gels. Detection of MMP-3 cleaved aggecan degradation product, FFGV fragment, by western blot analysis for 10, 15, and 20% PEG hydrogels at days 0 and 20 within the construct (C) and in the culture medium (D).

Presence of the N-terminal FFGV fragment, which is generated by MMP-3 cleavage of aggrecan, was determined for the constructs (Fig. A1.7C) and for the media (Fig. A1.7D) using western blot analysis. In the constructs, FFGV fragments were detected at ~75 kDa, which appeared to be more abundant in the 10% gels at both days 0 and 20; although the total amount of protein extracted from the 10% gels was highest. Total protein amounts extracted from the culture medium were much higher due to the fact that the majority of the proteins were from the serum and generally similar for all crosslinked gels. There were several FFGV fragments present in the media at day 0 with two distinct bands between 15 and 20 kDa and a band ~75 kDa along with several faint bands visible at higher MWs. By day 20, all of these same bands were visible but much fainter, with the most intense band occurring ~75 kDa in the 10% gels.

A1.5 Discussion

The ability of the scaffold to promote deposition and organization of an engineered tissue is critical towards engineering functional cartilage. Initially, cells will 'see' cues provided by the scaffold, but as neotissue is deposited the biochemical cues perceived by the cells will change and be largely dictated by the matrix molecules comprising the neotissue. This interplay will likely impact the long-term growth and maturation of the engineered tissue. Overall, the PEG hydrogels supported the deposition of cartilage-specific matrix molecules comprised of the two main building blocks of cartilage ECM (aggrecan and collagen II), the primary matrix molecule found in the PCM of cartilage (collagen VI), and smaller matrix molecules which are thought to be important in matrix assembly (link protein and decorin). However, the newly deposited tissue was largely limited to the immediate pericellular regions within all of the three crosslinked gels. Increasing the gel crosslinking density resulted in decreased positive staining for collagens II and VI and aggrecan. Together, these findings illustrate the distinct differences in composition and organization of the neotissue as a function of the PEG crosslinked structure

and that after 25 days the neotissue deposited remains in an immature state when compared to native cartilage.

Examining both the building blocks of the ECM, such as sGAGs, the large ECM molecules including collagen type II and aggrecan, and one of the molecules associated with the aggregation of aggrecan (i.e. link protein) revealed large spatial discrepancies as a result of the crosslinked structure. For all crosslinked gels, there was limited diffusion observed for collagen II, which is not surprising as it has characteristic fibril dimensions ranging from 40-300 nm in length and 1-2 nm in diameter [49]. The average mesh size of the PEG hydrogels used in this study ranged between 5 and 20 nm. The major proteoglycan in cartilage, aggrecan, reaches molecular weights between 1-4 MDa depending on the amount of glycosylation [50]. The N-terminal G1 domain of aggrecan interacts solely with long chains of hyaluronan [51], which are stabilized by the 45-kDa link protein [52]. The synthesis of both aggrecan and link protein occurs through the same intracellular pathways whereas hyaluronan is synthesized on the plasma membrane and is translocated directly into the extracellular space [53]. Thus both aggrecan and link protein assemble with hyaluronan through extracellular mechanisms, and can result in aggregates reaching several hundred million Daltons on the order of 1-2 μm in length [3]. Although proteins upwards of 65 kDa have been observed to diffuse through similar gels [42], diffusion of aggrecan and the larger proteoglycan aggregates are hindered by the gels' smaller mesh sizes. Therefore, it is not surprising that aggrecan is localized to the PCM region in all crosslinked gels. The localization of link protein in the PCM region suggests that it is likely binding to aggrecan and beginning to form an organized matrix. Interestingly, there was a range of aggrecan sizes (which did not stain positive as a FFGV fragment or to the same degree) detected in the constructs suggesting that this molecule is in different stages of organization throughout the culture period. The smaller molecules that are present at both early and late cultures may indicate that the cells are continuing to produce new, smaller aggregates, which may be being assembled at the cell membrane. It should be noted that the deglycosylation step

will substantially reduce the size of the aggregan molecules detected by western blot analysis. In addition, there was positive staining for sGAG and chondroitin sulfate in the extracellular regions of the hydrogel but only for the 10% PEG gels, which may suggest the presence of smaller proteoglycans, such as the small leucine-rich proteoglycans associated with matrix binding or of degraded aggrecan fragments that are capable of diffusing through the hydrogel (discussed below). Overall, the restricted deposition of collagen II and aggrecan suggests that the mesh size of the PEG hydrogels is not sufficient to permit diffusion of these large macromolecules into the extracellular space of the hydrogel.

Cells receive insoluble biochemical signals by interacting with their surrounding matrix, and in the case of cartilage by interacting directly with the PCM [4]. Here, we demonstrate that the pericellular matrix produced by chondrocytes within PEG hydrogels was distinctly different from the native PCM environments and was drastically affected by changes in crosslinking density. Findings reported here indicate that the gel structure hinders the deposition of collagen VI in the PCM. In the native tissue, collagen type VI forms an organized, multimeric fibrillar network specific to the PCM, which interacts with collagen II present in the PCM [8,10]. Even though a majority of cells exhibited collagen II and decorin in their PCM region, a lower fraction (~40%) of chondrocytes stained positive with collagen VI deposition. Increases in crosslinking caused a decrease in the density and thickness of collagen VI in the PCM even though the fraction of cells staining positive for collagen VI remained the same. Chondrocytes cultured in agarose gels also exhibited collagen VI within their PCM, however, significant structural differences in the orientation and distribution of the fibrillar mesh were observed compared to native cartilage [17]. This study suggested that the agarose environment did not provide adequate spatial requirements for the unique structural organization of collagen VI, which may explain the decreased staining observed in our hydrogels with higher crosslinking. In addition, the heterogeneity observed in the collagen VI staining may be due to the fact that chondrocytes encapsulated in the PEG hydrogels were isolated from full-depth cartilage, where the degree of

staining for collagen VI was noted to vary with depth in our cartilage explants (data not shown). Similarly, the density and thickness of collagen type II and aggrecan in the PCM regions also decreased with increasing gel crosslinking. These overall differences in the PCM composition *and* structure as a result of gel crosslinking will likely affect how cells interact with their surrounding environment, respond to external stimuli, and ultimately form tissue.

In native cartilage, matrix molecules are secreted into the pericellular space, where they are able to interact and assemble to form large macromolecules. In the PEG hydrogel systems, we observe that the major cartilage-matrix components are in fact being produced by the cells and localized to the PCM region. It is thought that enzymatic activity within the PCM may be necessary to release these molecules from the PCM [18,54], permitting their diffusion into the surrounding extracellular spaces and forming the ECM. In addition, chondrocytes are known to maintain cartilage through a balance of anabolic and catabolic mechanisms, where, for example there is a normal turnover of aggrecan through cell-secreted proteolytic enzymes [55–57]. Therefore, anabolic *and* catabolic events may be important to initiate a remodeling phase for regenerating functional cartilage. For example, when MMP-inhibitors were delivered to chondrocyte-laden agarose constructs, GAG content and mechanical properties were negatively impacted, strongly suggesting an important role of MMPs in matrix formation [18]. Other studies have similarly suggested the importance of proteolytic activities in tissue remodeling phases [26,48,54,58,59].

Here, we observed a significant increase in anabolic gene expression for *AGC* and *COL2* during early culture times for all three PEG hydrogels, corresponding with synthesis and deposition of new matrix. Interestingly, the anabolic response was initially higher in gels with higher crosslinking. This observation may be partly attributed to differences in gel stiffness whereby the cells may ‘sense’ higher resistance during matrix deposition, and hence stress, which may have impacted their function. By day 20, however, *AGC* and *COL2* expression levels decreased significantly suggesting that after the development of a collagen and sGAG-rich

PCM, cells may reach homeostatic levels. Additional studies are necessary to confirm these hypotheses.

MMP-3 catabolic activity was confirmed by the presence of the N-terminal FFGV fragment in the constructs and in the culture medium. The predominate FFGV fragment appears to be ~75 kDa in the constructs and a second smaller fragment between 15-20 kDa which was mainly found in the culture medium (both are confirmed to be aggrecan, Fig A1.1). While MMP-3 expression decreased with culture time, there was evidence of the FFGV fragment in the constructs at early and late culture times. Since degradation products can be metabolized by cells, we cannot confirm whether the FFGV fragments were cleaved early during the culture period (when expression levels were high) and retained or whether downstream processes differentially regulated translation of MMP-3 and/or its activation. More interesting is the decreased presence of two FFGV fragments in the culture medium after longer culture periods, which more closely agrees with the MMP-3 expression data and is more representative of temporal changes in catabolic activity. However, some discrepancies are observed for the low crosslinked gel. While MMP-3 expression was similar among all gels, there was a greater presence of the FFGV fragment in the low crosslinked gel. Interestingly, in the low crosslinked gels there was evidence of chondroitin sulfate, but not aggrecan in the extracellular space of the hydrogels, which may be indicative of an aggrecan degradation product. In addition, the sGAGs released into the culture medium will include any degraded aggrecan. However, the amount of sGAG released was similar among the crosslinked hydrogels, yet there was little detected at least for the higher crosslinked gels. Since the FFGV fragment encompasses the G1 domain of the aggrecan molecule, and the other MMP-3 cleaved fragment (not tested) will encompass the glycosylated region of the aggrecan, it is possible that the other fragment more readily diffuses into the culture medium and was detected by the sGAG assay and not by western blot. Therefore, it is likely that some of the sGAGs released are degraded aggrecan, but we cannot confirm to what degree, all or some. In addition, other enzymes involved in matrix breakdown

may be responsible for sGAG release, specifically that of the aggrecanases (ADAMTS-4/-5). Nonetheless, the positive correlation between aggrecan and MMP-3 expression supports the involvements of MMPs in matrix synthesis and remodeling. Additional studies, however, are needed to confirm this hypothesis.

Interestingly, increases in crosslinking density resulted in higher expression levels of MMP-1 and -13, most notably after 5 days of culture, indicating that the structure of the hydrogel significantly impacted catabolic gene expression. This up-regulation may be in part due to the fact that gels with higher crosslinking tended to be more restrictive to PCM formation whereby the cells would need to breakdown this nearby matrix to create space for new matrix and/or to allow these matrix molecules to diffuse and deposit into the ECM. The presence of C1,2C fragments indicates that MMP's were indeed synthesized and activated within the PEG hydrogels. While there were no significant differences in the total amount of C1,2C fragments in the construct or the culture medium as a function of gel crosslinking, the lower collagen content observed in the histology images suggests that there may be a higher fraction of C1,2C fagment generated in the gels with higher crosslinking. This observation is supported by the increased expressions in MMP-1 and -13 observed in the higher crosslinked gels. However, it is important to note that C1,C2 fragments are also generated from MMP cleavage of type I collagen, which was not evaluated in this study.

While we have limited the scope of our discussion to the role that gel crosslinking has on the diffusion of matrix molecules and its subsequent effect on cells, changes in the crosslinking density will alter the mechanical properties of the hydrogel. Therefore, differences in how chondrocyte's response to changes in crosslinking density may be a result of not only the disparate PCM, but also due to mechanotransduction events as the cells 'sense' differences in the substrate stiffness [60]. Since the hydrogel structure and chemistry dictate the mesh size and the mechanical properties of the hydrogel [61], it is not possible to de-couple the physical from the mechanical effects that the hydrogel is having on chondrocyte response. However, by

manipulating the hydrogel chemistry, it is possible to de-couple these two effects and gain a better understand of their individual contributions to mediating chondrocyte response, but is beyond the scope of the current study.

While these findings indicate that encapsulated chondrocytes synthesize the major cartilage components (aggrecan, collagen II and VI) within PEG hydrogels, the restricted location of these molecules to the regions of the PCM strongly indicates the need for engineering degradation into the hydrogels. Previous studies have shown that hydrolytically degradable PEG hydrogels permit the evolution of a macroscopic cartilage-like tissue composed of sGAGs and collagen II, which was not possible in non-degrading PEG hydrogels [32,33]. We are currently incorporating degradable linkages, based on poly(lactic acid), into the PEG hydrogels and our initial unpublished findings confirm the ability for these large macromolecules of aggrecan and collagen II to diffuse into the extracellular space. One of the attractive features of designing synthetic biodegradable hydrogels is the ability to tailor the degradation to control changes in the gel properties with time [35,62] and to match degradation with tissue evolution.

A1.6 Conclusions

The ability to design *in situ* forming scaffolds with high moduli is attractive for creating a material suitable to withstand the large stresses *in vivo*. However, our findings illustrate that the relatively tight mesh network provided by the crosslinked PEG hydrogels dramatically impacts the type of tissue deposited and the spatial evolution of the tissue. While hydrogels with high moduli are supportive of cartilage-specific matrix deposition, the use of these high moduli gels must be coordinated with hydrogel degradation. Our long-term goal is to design synthetic degradable hydrogels by which the gel itself provides initial stiffness to support the loads *in situ* and as tissue is deposited and the hydrogel matrix erodes, the load is then transferred to the developing tissue.

A1.7 Acknowledgements

This research was supported by a grant from the National Institute of Health (grant number K22DE016608), a Department of Education's Graduate Assistantships in Areas of National Need (GAANN) fellowship to GN, and a Chancellor's Fellowship to SCS. The authors would also like to thank Eric Greenwald for his technical assistance in immunohistochemistry. The antibodies developed by B. Caterson (link protein) and G.A. Pringle (decorin) used here were obtained from the Developmental Studies Hybridoma Bank developed under the auspices of the NICHD and maintained by the University of Iowa, Department of Biology, Iowa City, IA 52242.

A1.8 References

[1] Lai WM, Hou JS, Mow VC. A Triphasic Theory for the Swelling and Deformation Behaviors of Articular Cartilage. J Biomech Eng 1991;113:245.

[2] Maroudas A. Balance between swelling pressure and collagen tension in normal and degenerate cartilage. Nature 1976;260:808–9.

[3] Hardingham TE. Proteoglycans and Glycosaminoglycans. In: Seibel MJ, Robins SP, Bilezikian JP, editors. Dyn. bone Cartil. Metab., Burlington: Elsevier Science; 2006, p. 85–98.

[4] Guilak F, Alexopoulos LG, Upton ML, Youn I, Choi JB, Cao L, et al. The pericellular matrix as a transducer of biomechanical and biochemical signals in articular cartilage. Ann New York Acad Sci Skelet Dev Remodel Heal Dis Aging 2006;1068:498–512.

[5] Poole CA. Articular cartilage chondrons: form, function and failure. J Anat 1997;191 (Pt 1:1–13.

[6] Engvall E, Hessle H, Klier G. Molecular assembly, secretion, and matrix deposition of type VI collagen. J Cell Biol 1986;102:703–10.

[7] Poole CA, Flint MH, Beaumont BW. Chondrons in cartilage: ultrastructural analysis of the pericellular microenvironment in adult human articular cartilages. J Orthop Res 1987;5:509–22.

[8] Bidanset DJ, Guidry C, Rosenberg LC, Choi HU, Timpl R, Hook M. Binding of the proteoglycan decorin to collagen type VI. J Biol Chem 1992;267:5250–6.

[9] Guidetti GF, Bartolini B, Bernardi B, Tira ME, Berndt MC, Balduini C, et al. Binding of von Willebrand factor to the small proteoglycan decorin. FEBS Lett 2004;574:95–100.

[10] Wiberg C, Klatt AR, Wagener R, Paulsson M, Bateman JF, Heinegård D, et al. Complexes of matrilin-1 and biglycan or decorin connect collagen VI microfibrils to both collagen II and aggrecan. J Biol Chem 2003;278:37698–704.

[11] Larson CM, Kelley SS, Blackwood AD, Banes AJ, Lee GM. Retention of the native chondrocyte pericellular matrix results in significantly improved matrix production. Matrix Biol 2002;21:349–59.

[12] Sandy JD, O'Neill JR, Ratzlaff LC. Acquisition of hyaluronate-binding affinity in vivo by newly synthesized cartilage proteoglycans. Biochem J 1989;258:875–80.

[13] Ruoslahti E, Yamaguchi Y. Proteoglycans as modulators of growth factor activities. Cell 1991;64:867–9.

[14] Brandl F, Sommer F, Goepferich A. Rational design of hydrogels for tissue engineering: Impact of physical factors on cell behavior. Biomaterials 2007;28:134–46.

[15] Elisseeff JH, Lee A, Kleinman HK, Yamada Y. Biological Response of Chondrocytes to Hydrogels. Ann N Y Acad Sci 2002;961:118–22.

[16] Nicodemus GD, Bryant SJ. Cell encapsulation in biodegradable hydrogels for tissue engineering applications. Tissue Eng Part B-Reviews 2008;14:149–65.

[17] Dimicco MA, Kisiday JD, Gong H, Grodzinsky AJ. Structure of pericellular matrix around agarose-embedded chondrocytes. Osteoarthritis Cartilage 2007;15:1207–16.

[18] Connelly JT, Wilson CG, Levenston ME. Characterization of proteoglycan production and processing by chondrocytes and BMSCs in tissue engineered constructs. Osteoarthr Cartil 2008;16:1092–100.

[19] Buschmann MD, Gluzband YA, Grodzinsky AJ, Hunziker EB. Mechanical compression modulates matrix biosynthesis in chondrocyte agarose culture. J Cell Sci 1995;108:1497–508.

[20] Davisson T, Kunig S, Chen A, Sah R, Ratcliffe A. Static and dynamic compression modulate matrix metabolism in tissue engineered cartilage. J Orthop Res 2002;20:842–8.

[21] Mauck RL, Nicoll SB, Seyhan SL, Ateshian GA, Hung CT. Synergistic action of growth factors and dynamic loading for articular cartilage tissue engineering. Tissue Eng 2003;9:597–611.

[22] Mauck RL, Wang CCB, Oswald ES, Ateshian GA, Hung CT. The role of cell seeding density and nutrient supply for articular cartilage tissue engineering with deformational loading. Osteoarthr Cartil 2003;11:879–90.

[23] Hung CT, Mauck RL, Wang CCB, Lima EG, Ateshian GA. A paradigm for functional tissue engineering of articular cartilage via applied physiologic deformational loading. Ann Biomed Eng 2004;32:35–49.

[24] Ng L, Hung H-H, Sprunt A, Chubinskaya S, Ortiz C, Grodzinsky A. Nanomechanical properties of individual chondrocytes and their developing growth factor-stimulated pericellular matrix. J Biomech 2007;40:1011–23.

[25] Kisiday J, Jin M, Kurz B, Hung H, Semino C, Zhang S, et al. Self-assembling peptide hydrogel fosters chondrocyte extracellular matrix production and cell division: Implications for cartilage tissue repair. Proc Natl Acad Sci U S A 2002;99:9996–10001.

[26] Kisiday JD, Jin MS, DiMicco MA, Kurz B, Grodzinsky AJ. Effects of dynamic compressive loading on chondrocyte biosynthesis in self-assembling peptide scaffolds. J Biomech 2004;37:595–604.

[27] Bryant SJ, Anseth KS. Hydrogel properties influence ECM production by chondrocytes photoencapsulated in poly(ethylene glycol) hydrogels. J Biomed Mater Res 2002;59:63–72.

[28] Bryant SJ, Chowdhury TT, Lee DA, Bader DL, Anseth KS. Crosslinking density influences chondrocyte metabolism in dynamically loaded photocrosslinked poly(ethylene glycol) hydrogels. Ann Biomed Eng 2004;32:407–17.

[29] Bryant SJ, Durand KL, Anseth KS. Manipulations in hydrogel chemistry control photoencapsulated chondrocyte behavior and their extracellular matrix production. J Biomed Mater Res Part A 2003;67A:1430–6.

[30] Villanueva I, Klement BJ, von Deutsch D, Bryant SJ. Cross-linking density alters early metabolic activities in chondrocytes encapsulated in poly(ethylene glycol) hydrogels and cultured in the rotating wall vessel. Biotechnol Bioeng 2009;102:1242–50.

[31] Appelman TP, Mizrahi J, Elisseeff JH, Seliktar D. The differential effect of scaffold composition and architecture on chondrocyte response to mechanical stimulation. Biomaterials 2009;30:518–25.

[32] Anseth KS, Bryant SJ. Controlling the spatial distribution of ECM components in degradable PEG hydrogels for tissue engineering cartilage. J Biomed Mater Res Part A 2003;64A:70–9.

[33] Bryant SJ, Bender RJ, Durand KL, Anseth KS. Encapsulating Chondrocytes in degrading PEG hydrogels with high modulus: Engineering gel structural changes to facilitate cartilaginous tissue production. Biotechnol Bioeng 2004;86:747–55.

[34] Rice MA, Anseth KS. Encapsulating chondrocytes in copolymer gels: bimodal degradation kinetics influence cell phenotype and extracellular matrix development. J Biomed Mater Res A 2004;70:560–8.

[35] Rice MA, Anseth KS. Controlling cartilaginous matrix evolution in hydrogels with degradation triggered by exogenous addition of an enzyme. Tissue Eng 2007;13:683–91.

[36] Yang F, Williams CG, Wang D-A, Lee H, Manson PN, Elisseeff J. The effect of incorporating RGD adhesive peptide in polyethylene glycol diacrylate hydrogel on osteogenesis of bone marrow stromal cells. Biomaterials 2005;26:5991–8.

[37] Bryant SJ, Arthur JA, Anseth KS. Incorporation of tissue-specific molecules alters chondrocyte metabolism and gene expression in photocrosslinked hydrogels. Acta Biomater 2005;1:243–52.

[38] Lee HJ, Lee J-S, Chansakul T, Yu C, Elisseeff JH, Yu SM. Collagen mimetic peptide-conjugated photopolymerizable PEG hydrogel. Biomaterials 2006;27:5268–76.

[39] Schmidt O, Mizrahi J, Elisseeff J, Seliktar D. Immobilized Fibrinogen in PEG Hydrogels Does not Improve Chondrocyte-Mediated Matrix Deposition in Response to Mechanical Stimulation. Biotechnol Bioeng 2006;95:1061–9.

[40] Villanueva I, Hauschulz DS, Mejic D, Bryant SJ. Static and dynamic compressive strains influence nitric oxide production and chondrocyte bioactivity when encapsulated in PEG hydrogels of different crosslinking densities. Osteoarthr Cartil 2008;doi:10.101.

[41] Watkins AW, Anseth KS. Investigation of Molecular Transport and Distributions in Poly(ethylene glycol) Hydrogels with Confocal Laser Scanning Microscopy. Macromolecules 2005;38:1326–34.

[42] Weber LM, Lopez CG, Anseth KS. Effects of PEG hydrogel crosslinking density on protein diffusion and encapsulated islet survival and function. J Biomed Mater Res A 2009;90:720–9.

[43] Bryant SJ, Anseth KS, Lee DA, Bader DL. Crosslinking density influences the morphology of chondrocytes photoencapsulated in PEG hydrogels during the application of compressive strain. J Orthop Res 2004;22:1143–9.

[44] Nicodemus GD, Bryant SJ. The role of hydrogel structure and dynamic loading on chondrocyte gene expression and matrix formation. J Biomech 2008;41:1528–36.

[45] Bryant SJ, Nicodemus GD, Villanueva I. Designing 3D photopolymer hydrogels to regulate biomechanical cues and tissue growth for cartilage tissue engineering. Pharm Res 2008;25:2379–86.

[46] Elisseeff J, McIntosh W, Anseth K, Riley S, Ragan P, Langer R. Photoencapsulation of chondrocytes in poly(ethylene oxide)-based semi-interpenetrating networks. J Biomed Mater Res 2000;51:164–71.

[47] Farndale RW, Buttle DJ, Barrett AJ. Improved Quantitation and Discrimination of Sulfated Glycosaminoglycans by Use of Dimethylmethylene Blue. Biochim Biophys Acta 1986;883:173–7.

[48] Bryant SJ, Nicodemus GD. Mechanical loading regimes affect the anabolic and catabolic activities by chondrocytes encapsulated in PEG hydrogels. Osteoarthr Cartil 2010;18:126–37.

[49] Von der Mark K. Structure, Biosynthesis and Gene Regulation of Collagens in Cartilage and Bone. Dyn. bone Cartil. Metab., Elsevier; 2006, p. 3–40.

[50] Hardingham TE, Fosang AJ. Proteoglycans - Many Forms and Many Functions. Faseb J 1992;6:861–70.

[51] Hardingham TE, Muir H. The specific interaction of hyaluronic acid with cartilage proteoglycans. Biochim Biophys Acta 1972;279:401–5.

[52] Hardingham TE. The role of link-protein in the structure of cartilage proteoglycan aggregates. Biochem J 1979;177:237–47.

[53] Spicer AP, McDonald JA. Characterization and Molecular Evolution of a Vertebrate Hyaluronan Synthase Gene Family. J Biol Chem 1998;273:1923–32.

[54] De Croos JNA, Dhaliwal SS, Grynpas MD, Pilliar RM, Kandel RA. Cyclic compressive mechanical stimulation induces sequential catabolic and anabolic gene changes in chondrocytes resulting in increased extracellular matrix accumulation. Matrix Biol 2006;25:323–31.

[55] Hardingham TE, Fosang AJ. The structure of aggrecan and its turnover in cartilage. J Rheumatol Suppl 1995;43:86–90.

[56] Murphy G, Hembry RM, Hughes CE, Fosang AJ, Hardingham TE. Role and regulation of metalloproteinases in connective tissue turnover. Biochem Soc Trans 1990;18:812–5.

[57] Sandy JD. A contentious issue finds some clarity: on the independent and complementary roles of aggrecanase activity and MMP activity in human joint aggrecanolysis. Osteoarthritis Cartilage 2006;14:95–100.

[58] Blain EJ. Mechanical regulation of matrix metalloproteinases. Front Biosci 2007;12:507–27.

[59] Blain EJ, Gilbert SJ, Wardale RJ, Capper SJ, Mason DJ, Duance VC. Up-regulation of matrix metalloproteinase expression and activation following cyclical compressive loading of articular cartilage in vitro. Arch Biochem Biophys 2001;396:49–55.

[60] Engler AJ, Sen S, Sweeney HL, Discher DE. Matrix elasticity directs stem cell lineage specification. Cell 2006;126:677–89.

[61] Peppas NA., Hilt JZ, Khademhosseini A, Langer R. Hydrogels in Biology and Medicine: From Molecular Principles to Bionanotechnology. Adv Mater 2006;18:1345–60.

[62] Rice MA, Sanchez-Adams J, Anseth KS. Exogenously triggered, enzymatic degradation of photopolymerized hydrogels with polycaprolactone subunits: experimental observation and modeling of mass loss behavior. Biomacromolecules 2006;7:1968–75.

Appendix 2

On the Role of Hydrogel Structure and Degradation in Controlling the Transport of Cell-secreted Matrix Molecules for Engineered Cartilage

As appearing in *Journal of the Mechanical Behavior of Biomedical Materials* 2013

A2.1 Abstract

Damage to cartilage caused by injury or disease can lead to pain and loss of mobility, diminishing one's quality of life. Because cartilage has a limited capacity for self-repair, tissue engineering strategies, such as cells encapsulated in synthetic hydrogels, are being investigated as a means to restore the damaged cartilage. However, strategies to date are suboptimal in part because designing degradable hydrogels is complicated by structural and temporal complexities of the gel and evolving tissue along multiple length scales. To address this problem, this study proposes a multi-scale mechanical model using a triphasic formulation (solid, fluid, unbound matrix molecules) based on a single chondrocyte releasing extracellular matrix molecules within a degrading hydrogel. This model describes the key players (cells, proteoglycans, collagen) of the biological system within the hydrogel encompassing different length scales. Two mechanisms are included: temporal changes of bulk properties due to hydrogel degradation, and matrix transport. Numerical results demonstrate that the temporal change of bulk properties is a decisive factor in the diffusion of unbound matrix molecules through the hydrogel. Transport of matrix molecules in the hydrogel contributes both to the development of the pericellular matrix and the extracellular matrix and is dependent on the relative size of matrix molecules and the hydrogel mesh. The numerical results also demonstrate that osmotic pressure, which leads to changes in mesh size, is a key parameter for

achieving greater diffusivity of matrix molecules. The numerical model is confirmed with experimental results of matrix synthesis by chondrocytes in biodegradable poly(ethylene glycol)-based hydrogels. This model may ultimately be used to predict key hydrogel design parameters towards achieving optimal cartilage growth.

A2.2 Introduction

It is well known that damage of articular cartilage due to injury, disease or genetic disorders can lead to joint pain and reduced mobility, drastically affecting one's quality of life. With the prevalence of cartilage-related joint problems on the rise [1] and current surgical procedures offering imperfect solutions, new treatments are clearly warranted. Tissue engineering is one promising treatment option having the potential to yield living functional cartilage. Within this context, scaffolds are being developed to deliver chondrocytes (cartilage cells) to the damaged site and support new tissue deposition [2]. However, engineering functionally competent and well-integrated cartilage remains a hurdle, limiting clinical translation of cartilage tissue engineering.

Encapsulation of cells in photopolymerizable and biodegradable hydrogels is one promising strategy being investigated for cartilage tissue engineering. This hydrogel platform can be injected and polymerized *in situ* for site-specific cell delivery and tailored to degrade over time, providing necessary space for new tissue growth. Poly(ethylene glycol) (PEG)-based hydrogels formed by photopolymerization hold promise because they recapitulate important aspects of the native tissue (*e.g.*, maintaining the rounded chondrocyte morphology which is key to preserving the phenotype) [3,4] and are easily functionalized with degradable linkers [5] and bioactive molecules [6]. For *in situ* cartilage tissue engineering, the scaffold must also withstand the *in vivo* physiological forces, a requirement that becomes even more important in large defects and joint resurfacing. In addition, hydrogel degradation must be incorporated to permit macroscopic tissue growth, but its rate should match tissue growth in order to maintain mechanical integrity and thus function throughout tissue development.

In optimizing the design of biodegradable hydrogels for cartilage tissue engineering, it is critical to understand how hydrogel structure, across multiple length scales and its temporal changes with degradation, supports the production, transport and deposition of extracellular matrix (ECM). Hydrogels are crosslinked polymer networks with an average crosslink density that influences the mechanical properties, degree of swelling, mesh size, and subsequently transport properties. Because ECM molecules typically have high molecular weights, a large mesh size is often desirable to promote transport of these molecules through the gel for homogeneous tissue development. But, this leads to a mechanically inferior hydrogel. In contrast, a high crosslink density, which can conserve mechanical integrity similar to that of cartilage, is usually prohibitory to ECM transport [3,7]. As a result, ECM transport is restricted to regions near chondrocytes (the pericellular region). This increased local matrix deposition may in turn further inhibit long-range ECM transport. While the introduction of degradation into the hydrogels can overcome many of these shortcomings, this strategy is only beneficial if degradation kinetics properly match matrix transport and deposition. The latter has not yet been achieved.

Designing the structure and degradation behavior of hydrogels for optimal tissue development is challenging due to the nonlinearity of the processes involved and the multiscale aspect of the problem. However, mathematical models can provide an important tool to guide hydrogel design as well as to provide a better understanding of the mechanisms controlling tissue production, transport and deposition. Theories of mixture and poro-elasticity have proven to be excellent frameworks onto which the deformation of tissues, such as cartilage, can be studied [8–10]. In cartilage, the problem of matrix diffusion, transport and deposition has been addressed at cellular [11] and tissue scales [12]. More recently, mathematical models have been expanded to cartilage tissue engineering strategies predicting matrix diffusion from cells within scaffolds [13]. The problem of cell mediated gel degradation was also assessed with a

triphasic mixture model [14] to better understand how degradation may affect both transport properties and gel mechanics. Finally, on a more global scale, a multiphasic model (made of linked ECM, scaffold and cells) was used to derive a steady-state solution for tissue growth as a function of scaffold properties [15]. While the above studies have enabled a more quantitative understanding of the processes of synthesis, diffusion and deposition, few have considered the coupled physics of scaffold deformation, degradation and ECM transport for cells encapsulated in a degrading crosslinked hydrogel for which the size scale of porosity is of similar magnitude to that of many ECM molecules. Experimentally these processes have proven to be keys in designing hydrogel scaffolds with encapsulated cells.

In the present work, we take an integrated experimental/modeling approach to further understand the role of hydrogel structure and degradation on the development of new tissue synthesized and deposited by chondrocytes (Fig. A2.1). The problem is described in terms of an ECM-producing chondrocyte surrounded by a triphasic mixture consisting of a degrading hydrogel, aqueous solvent and diffusing ECM molecules. The model shows, in agreement with experimental observations, how microstructural details such as crosslink density and degradation kinetics, lead to variations in matrix deposition and diffusion. In particular, we aim to illustrate that a quantitative understanding of the relationship between hydrogel structure and tissue development is essential to designing successful engineered tissues.

The paper is organized as follows. In section 2, the overall method to produce cell-encapsulated hydrogels is discussed with an introduction to the general modeling approach to describe hydrogel evolution. Section 3 describes the microscopic mechanisms of hydrogel deformation and degradation with a particular emphasis on the influence of processing parameters. The processes of ECM molecule production by cells and unbound ECM molecule diffusion in the hydrogel are discussed in section 4. Finally, this paper concludes by presenting numerical simulation and experimental observations which together illustrate the impact of

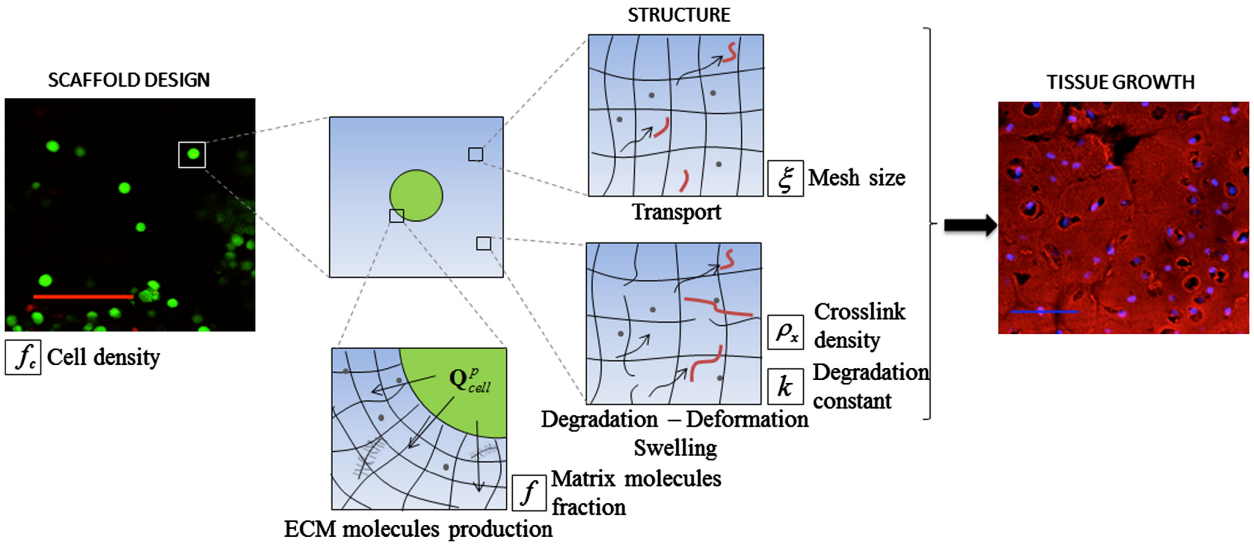

Figure A2.1 Mutiscale approach to modeling tissue production by cells encapsulated in hydrogels. Refer to the next sections for the parameters. Left: chondrocytes encapsulated within a PEG hydrogel, shown at day 3 after encapsulation. Cytosol of live cells fluoresce green showing the chondrocytic round morphology. Nuclei of dead cells fluoresce red. Scale bar indicates 100 microns. Right: chondroitin sulfate elaboration (red) by chondrocytes encapsulated within a degradable PEG hydrogel after 28 days in vitro. Cell nuclei are stained blue. Scale bar indicates 50 microns.

hydrogel structure on the nature of tissue growth. Results are discussed in detail and recommendations for future tissue engineering strategies are given.

A2.3 Hydrogel Structure: Processing and Mathematical Description

A2.3.1 Processing of cell-laden hydrogels and control of initial hydrogel structure

The methods used to form biodegradable PEG hydrogels and encapsulate cells are described. Poly(ethylene glycol) (PEG) can be functionalized in numerous ways to add moieties for degradation and polymerization. Hydrolytically degradable lactides were reacted with PEG, MW 4600, to produce oligo(lactic acid)-PEG-oligo(lactic acid) (LA-PEG-LA) with an average of 2-3 lactic acid repeat units per side [16]. PEG (MW 4600) and LA-PEG-LA were endcapped with polymerizable methacrylates by microwave methacrylation [17] to produce non-degradable PEG dimethacrylate (PEGDM) and degradable LA-PEG-LA dimethacrylate (PEG-LA-DM) macrmolecular monomers or macromers, respectively. Primary bovine chondrocytes isolated from the femoral-patellar groove of a 1-3 week old calf (Research 87, Marlborough, MA) [7][7]

were used as the model cell type. Hydrogels with different initial crosslink densities were formed through photopolymerization (365 nm, 10 min) of PEGDM and/or PEG-LA-DM macromers at varying macromer concentrations (10, 15, or 20% w/w) with a photoinitiator (Irgacure 2959, 0.05% w/w) in chondrocyte culture medium. For cell encapsulations, chondrocytes were suspended in macromer solution at 50 million cells per mL macromer and photopolymerized. Cylindrical hydrogels (5mm height and 5 mm diameter) were cultured up to 4 weeks in a humid environment at 37 °C in 5% CO_2. The LIVE/DEAD® membrane integrity assay was used to qualitatively assess cell viability within hydrogel constructs. Images were acquired using a confocal laser scanning microscope (CLSM, Zeiss LSM 510, Thornwood, NY).

A2.3.2 Overall modeling strategy of the macroscopic tissue evolution

Multiscale computational modeling was employed to understand key microscopic processes driving tissue growth in terms of hydrogel structure, degradation and cell density. At the tissue level, these processes may be entirely described by continuous field equations in terms of hydrogel displacement u, solvent pressure *p* and concentration c^p of ECM molecules (proteins), all functions of location **X** and time *t*. To reduce the complexity of the problem, a homogeneous cell distribution was considered such that the analysis of the entire tissue could be summarized by a model volume consisting of a single spherical chondrocyte of radius R_c embedded in a spherical hydrogel domain with radius R_g. Overall cell volume fraction, f_c, (Fig. A2.2) can then be described through the relation:

$$R_c / R_g = (f_c)^{1/3} \quad (1)$$

In spherical coordinates, the fields are functions of R, θ and φ. However, in this simplified system, under centro-symmetric assumption, the continuous fields only depend on the distance R from the center of the chondrocyte (in the initial, dry state). The macroscopic problem therefore consists of evaluating the evolution of the following three fields:

$$u(R,T), p(R,t), c^p(R,t) \tag{2}$$

These fields evolve as a result of the constant release of ECM molecules by chondrocytes from the cell membrane and changes in the osmotic swelling of the hydrogel resulting from bulk degradation. As we will see, the combination of degradation and ECM production that results in the growth and organization of the new tissue is highly dependent on the initial hydrogel structure and the design of its degradation through the number of degradable linkages.

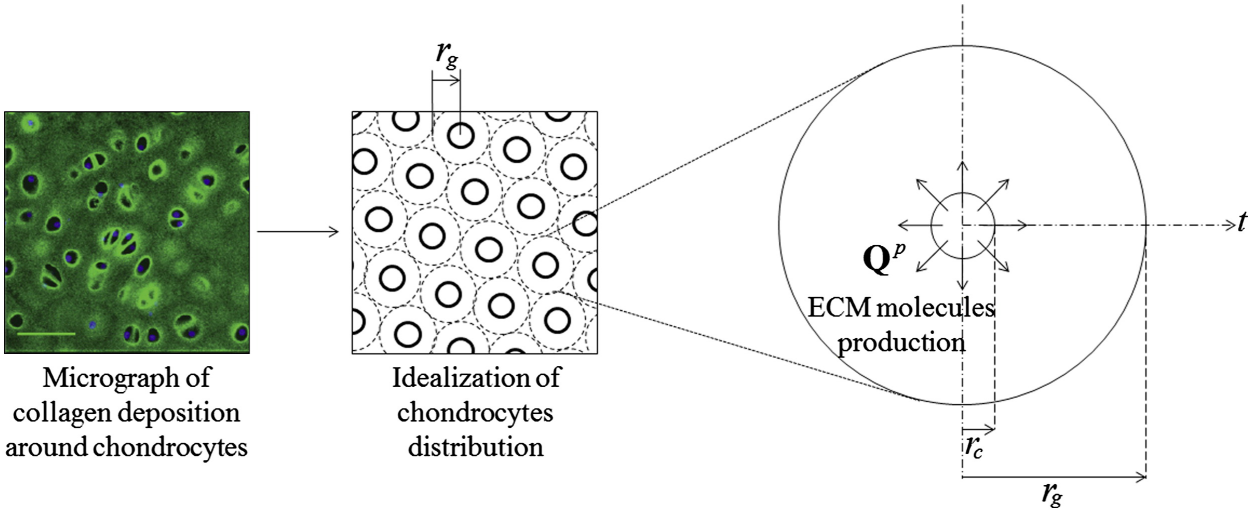

Figure A2.2 From real engineered tissues to an idealized mathematical model. Left picture shows cell nuclei (blue) and collagen (green). Scale bar represents 50 μm.

The crosslinked polymer network of the hydrogel can be considered as a hydrated elastic solid whose mechanics highly depend on the underlying molecular structure [18]. To represent hydrogel degradation and tissue growth, the hydrogel was considered as a mixture [14,19,20] of three different phases that consist of the solid (or polymer) phase, the fluid (or solvent) phase, and the unbound ECM molecules (proteoglycans, collagens) phase. Consistent with mixture theory, each phase (denoted by $\alpha = s, f, p$, respectively) is described with its volume fraction ϕ^α such that

$$\phi^s + \phi^f + \phi^p = 1 \qquad \text{and} \qquad \phi^p \ll 1 \tag{3}$$

This equation implies that each phase is saturated within the mixture. It is also reasonable to assume that each phase is incompresssible at the microscopic level due to the relatively low physiological pressure encountered *in vivo*. In other words, the true mass density $\rho^{\alpha R}$ of various phases remains constant during the growth process. Growth can however be measured by the change in effective mass density representing the mass of each phase per unit volume of mixture through the relation:

$$\rho^{\alpha}(R) = \phi^{\alpha}(R)\rho^{\alpha R}(R) \tag{4}$$

Deformation and swelling: A particular feature of hydrogels, and soft tissue in general, is that they commonly undergo very large deformations (changes in volume can reach more than 1000% during swelling). Such deformable materials are usually described within finite deformation elasticity. In this context, the location **x** of a material point on the crosslinked polymer is related to its original position **X** before deformation through the deformation gradient tensor $\mathbf{F}$:

$$\mathbf{F} = \frac{\mathbf{dx}}{\mathbf{dX}}, \text{ or in centro-symmetric } dr = F_{rr}dR, \text{ where } F_{rr} = \partial r / \partial R \tag{5}$$

where the current radius r is mapped to the initial radius R (before swelling). The determinant of **F** measures the change of volume between initial (dry polymer before swelling) and final configuration as follows:

$$dV = JdV_0 \text{ where } J = \det(\mathbf{F}) = \left(\partial r / \partial R\right)\left(r / R\right)^2 \tag{6}$$

The value of J at equilibrium is denoted as the volumetric equilibrium swelling ratio Q, which can be determined from experiments. The volume fraction ϕ^s_{eq} of the polymer at swelling equilibrium is related to Q:

$$\phi^s_{eq} = 1/Q \tag{7}$$

where the volume fraction for the dry polymer is one.

Mechanical equilibrium: The hydrogel is subjected to a variety of mechanical forces which through hydrogel deformation, have strong effects on gel permeability and degradation as well as transport and deposition of unbound ECM molecules. These forces are accounted for through the balance of momentum of the hydrogel in the form [21][21]:

$$\nabla_{\mathbf{X}} \cdot (\mathbf{P}^{eff} - J\pi\mathbf{F}^{-T}) = 0 \tag{8}$$

where $\mathbf{P}^{eff}$ is the nominal effective stress tensor i.e. the stress acting on the crosslinked polymer only, and π is the interstitial fluid pressure. The notation $\nabla_{\mathbf{X}}$ refers to the spatial differential operator with respect to the initial coordinates $\mathbf{X}$. This equation clearly shows the effect of fluid pressure on the stress experienced by the polymer network.

A2.4 The Evolving Structure and Properties of Degrading Hydrogels

The solid phase of the gel (described as a crosslinked polymer) is mechanically represented as a rubber-like material, where polymethacrylate chains are linked together by PEG or PEG-LA crosslinks and swollen in an aqueous solvent (Fig. A2.3). The mathematical model to describe its deformation and swelling is introduced below.

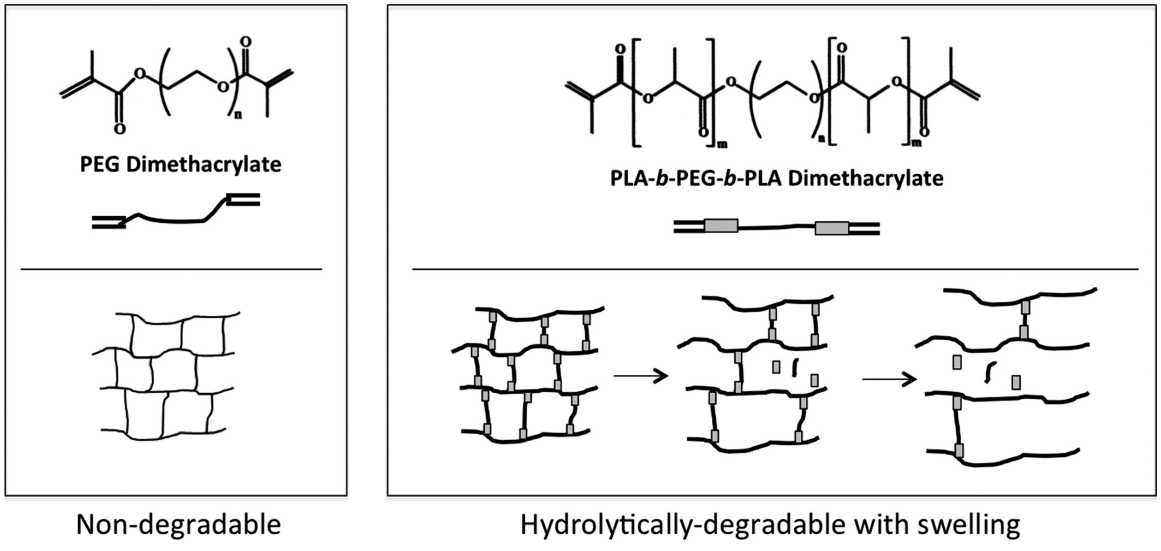

Figure A2.3 Schematics representing an idealized network structure formed from PEGDM or PEG-LA-DM macromers by radical chain polymerization. Left, non-degrading (based on experimental timescale) PEGDM hydrogels form a stable network structure. Right, hydrolytically degradable hydrogels made of PEG-LA-DM exhibit degradation and swelling with time.

A2.4.1 Physical model of the hydrogel

Free energy: The physical properties of a crosslinked polymer swollen with solvent (neglecting contributions from ECM molecules) are described by Flory-Rehner and rubber elasticity theories [22,23]. These theories are based on the description of the free energy of a swollen gel [24] as the sum of contributions from elasticity/distortion ΔG^{el} and solvent mixing ΔG^{mix}.

$$\Delta G = \Delta G^{el} + \Delta G^{mix} \tag{9}$$

where ΔG^{mix} is described by Flory-Huggins theory [24] for two phases:

$$\Delta G^{mix} = kT\left[N_f \ln \phi^f + N_s \ln \phi^s + N_f \ln \phi^s \chi\right] \tag{10}$$

where N is the number of molecules and χ is the Flory-Huggins parameter (polymer-solvent interaction). The latter is the change in energy when a solvent molecule is replaced by a polymer molecule. A high positive χ denotes a repulsive interaction between the solvent and polymer molecules. Because the polymer network is one molecule, we assume a negligible contribution from term 2 ($N_s \ln \phi^s$) in Eq. (11). The elastic contribution to the free energy ΔG is derived from Treloar [23], neglecting the phantom network theory [25] for simplicity. Denoting the quantities λ_1, λ_2 and λ_3 as the principal stretches in the principal directions of the right stretch tensor, the elastic free energy reads:

$$\Delta G^{el} = \frac{1}{2}\left(\lambda_1^2 + \lambda_2^2 + \lambda_3^2 - 3 - 2\ln(\lambda_1\lambda_2\lambda_3)\right) \quad \text{where} \quad G = \rho \bar{v} \rho_X RT(\phi^s)^{1/3} \tag{11}$$

where G is denoted as the shear modulus [23,25] and is a function of the specific volume $\bar{v}$ (inverse of density) of the solvent, the crosslink density ρ_X and is an increasing function of the polymer volume fraction ϕ^s. We also note that that for isochoric deformation $\lambda_1\lambda_2\lambda_3 = 1$ and

ΔG^{el} becomes the strain density energy of a Neo-Hookean material. When the polymer interacts with water, however, significant volume change can be generated by osmotic pressure and the product $\lambda_1\lambda_2\lambda_3$ may become large enough to dominate the gel response.

Effective stress and osmotic pressure: The effective stress $\mathbf{P}^{eff}$ is thermodynamically defined as the energy conjugate of the deformation gradient $\mathbf{F}$. It can therefore be defined in terms of the elastic free energy as:

$$\mathbf{P}^{eff} = \partial \Delta G^{el} / \partial \mathbf{F} \tag{12}$$

The osmotic pressure, based on the same idea as a Cauchy and Piola-Kirchhoff stress can be defined as

$$\boldsymbol{\Pi} = \partial \Delta G^{mix} / \partial \mathbf{F} \quad \text{where} \quad \boldsymbol{\Pi} = J\pi \mathbf{F}^{-T} \tag{13}$$

Where π is defined as a "Cauchy osmotic pressure" and Π is its associated "Piola-Kirchhoff osmotic pressure". This equation, together with the mechanic equilibrium is defined as

$$\mathbf{P}^{eff} - J\pi \mathbf{F}^{-T} = \partial \Delta G^{el} / \partial \mathbf{F} - \partial \Delta G^{mix} / \partial \mathbf{F} = 0 \tag{14}$$

The only unknown the mechanic equilibrium contains is the Flory-Huggins parameter χ, which can be solved for by taking the derivatives of the elastic and mixing free energies with respect to the deformation gradient. Thus, Eq. (11), (12) and (15) gives a Flory-Huggins parameter $\chi = 0.670$. This relation enables the determination of osmotic pressure from free swelling experiments (described next). In particular, Eq. (15) can be used to relate the swelling ratio $Q = 1/\phi_{eq}^{s}$ to crosslink density ρ_x at constant osmotic pressure as depicted in Fig. A2.4.

A2.4.2 Hydrolytic degradation

During degradation, the macroscopic properties of the hydrogel evolve dynamically. As a first approach, hydrolytic degradation is described by pseudo first-order kinetics [26], where crosslink density decreases with degradation time:

$$\frac{d\rho_x}{dt} = -k\rho_x \tag{15}$$

where k is the pseudo first order rate constant for hydrolytic degradation. Thus as time evolves, crosslinks degrade randomly within the gel, which leads to decreases in the shear elastic modulus G (Eq. (13)) but increases in swelling (Eq. (15)) and mesh size, where the latter improves transport of ECM molecules through the gel. Solving Eq. (16) yields the evolution of crosslink density in time as:

$$\rho_x(t) = \rho_{x0}\exp(-kt) \tag{16}$$

where ρ_{x0} is the initial crosslink density of the swollen hydrogel. It is important to note that this model represents a simplified model for degradation kinetics. As such, it does not capture more subtle elements of degradation such as the phenomenon of reverse gelation. Reverse gelation refers to the point when there are fewer than two crosslinks per kinetic chain resulting in highly branched soluble polymer chains [22]. The crosslink density at which reverse gelation occurs will depend largely on the length of the kinetic chain [26]. Consequently, very short kinetic chains can lead to reverse gelation at relatively high crosslink densities. While not explicitly incorporated into this equation, the importance of this physical point should not be underestimated as it has the potential to dramatically influence how well macroscopic tissue can form prior to reverse gelation. It was shown that reverse gelation typically occurs when there is a 60%-80% mass loss for similar PEG-LA hydrogels [26].

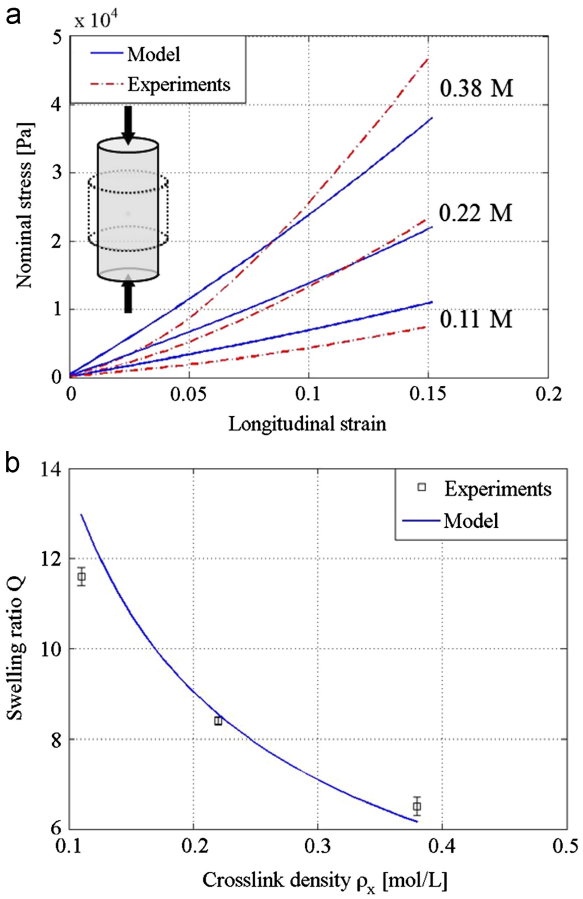

Figure A2.4 (a) shows the nonlinear compressive/elastic modulus through the stress-strain curves for different crosslink densities. Experimental results and the model are compared. (b) shows the equilibrium swelling ratio as a function of crosslinking density for stable PEG hydrogels formed from PEGDM macromers obtained both experimentally and determined by the model. Error bars indicate standard deviation (n = 3).

A2.4.3 Hydrogel processing and measurement of overall properties

In the above model, it can be seen that gel behavior is mainly described in terms of the structural quantity crosslink density ρ_x, which dictates shear modulus G, and the degradation behavior. Initial crosslinking density can be controlled experimentally by varying macromer length or the weight percent of PEG macromer in solution. While the rate of hydrolysis of the ester bond will not depend on hydrogel structure, the overall effective degradation rate can be altered by initial crosslink density and the number of ester bonds within the crosslink. Two macroscopic experiments were performed to indirectly measure these quantities. For stable hydrogels formed from PEGDM macromers with no degradable esters in the crosslink, the

equilibrium mass swelling ratio was measured and converted to volumetric swelling ratio Q, and direct unconfined compressive tests were performed. In addition bimodal degrading hydrogels were formed such that a fraction of the crosslinks would degrade (PEG-LA crosslinks), while the remaining crosslinks remain stable (PEG crosslinks) preventing the gel from undergoing rapid degradation and dissolution and loss of mechanical integrity [27,28]. For the bimodal degrading hydrogels, equilibrium volumetric swelling ratio Q was determined as a function of time. For the first experiment, hydrogels with varying crosslink density were made with 10, 15, and 20% PEGDM by weight, yielding 0.11, 0.22, and 0.38 M crosslinking densities, respectively, from Eq. (20). Swelling ratio and modulus were determined as a function of crosslink density and compared to theoretical prediction as shown in Fig. A2.4.

Crosslinking density: The swelling ratio Q can be determined experimentally by measuring the equilibrium swollen mass M_s of hydrogels, and then lyophilizing to obtain the dry polymer mass, M_d [18].

$$Q = J_{eq} = \frac{V}{V_0} = 1 + \frac{\rho_{pegdm}}{\rho_{solv}}\left(\frac{M_s}{M_d} - 1\right) \tag{17}$$

In this relationship, ρ_{pegdm} and ρ_{solv} are the density of the PEGDM macromer and the solvent, and J_{eq} is the equilibrium jacobian, equivalent to Q. Therefore $\phi_{eq}^{\ s}$ is equal to the inverse of the swelling ratio Q.

At swelling equilibrium, considering the chemical equilibrium, we can assume that the change in chemical potential is zero, and we apply the definition that the partial derivative of ΔG (Eq. (11)) with respect to N_s is equal to the change in chemical potential. Applying this definition, simplifying and rearranging leads to the following definition for crosslinking density ρ_x (number of crosslinks per volume) of a polymer scaffold (see [22], chapter XIII 3 for more

details). Neglecting the phantom network theory (no distinction between chain and chain-ends), one can show:

$$\rho_x = \frac{-1}{V_1}\left(\frac{\ln(1-\phi_{eq}{}^s) + \phi_{eq}{}^s + \chi(\phi_{eq}{}^s)^2}{(\phi_{eq}{}^s)^{1/3} - \frac{\phi_{eq}{}^s}{2}} \right) \tag{18}$$

where V_1 is the molar volume of the solvent. From this equation, experimental measurements of the swelling ratio Q are used to estimate hydrogel crosslinking density.

Gel elastic modulus: To ensure consistency between model and experiments regarding the change of gel stiffness with crosslink density, the stress-strain response of the hydrogel in uniaxial, unconfined compression was assessed through two different routes. On the experimental side, unconfined cylindrical hydrogels were compressed to 15% strain at a constant rate of 0.5 mm per minute (MTS Synergie 100, 10 N) and the resulting stress was assessed by dividing the compressive force by the initial specimen cross-sectional area (nominal stress). On the theoretical side, these conditions were reproduced by evaluating the longitudinal stress and strains (subjected to zero transversal stress) of a hydrogel cylinder with varying crosslink densities using Eq. (13), (8) and (9). Comparing numerical and experimental results provided in Fig. A2.4 (a) shows that the present model captures the key trends in gel behavior with a minimal number of material parameters. A more sophisticated model of the hydrogel mechanics may be able to provide a closer estimation of the results.

Rate of degradation: The measurement of degradation rate can be inferred by measuring the evolution of swelling ratio exhibited by a gel over time. As crosslinks degrade, the equilibrium volume fraction ϕ_{eq}^s of polymer decreases in a fashion dictated by Eq. (15). This informs us about the evolution of the equilibrium volumetric swelling ratio $Q = 1/\phi_{eq}^s$ over time. Using this method, it was possible to obtain a good match between the theoretical model and

experimental measurements for a degradation pseudo first-order rate constant k equal to 0.11 /day (Fig. A2.5). Swelling shows a general trend of an exponential increase with time [29], which was verified in a bimodally degradable system where 15 weight % macromer was used, where 95% of the macromer consisted of degradable PEG-LA-DM and 5% was non-degradable PEGDM.

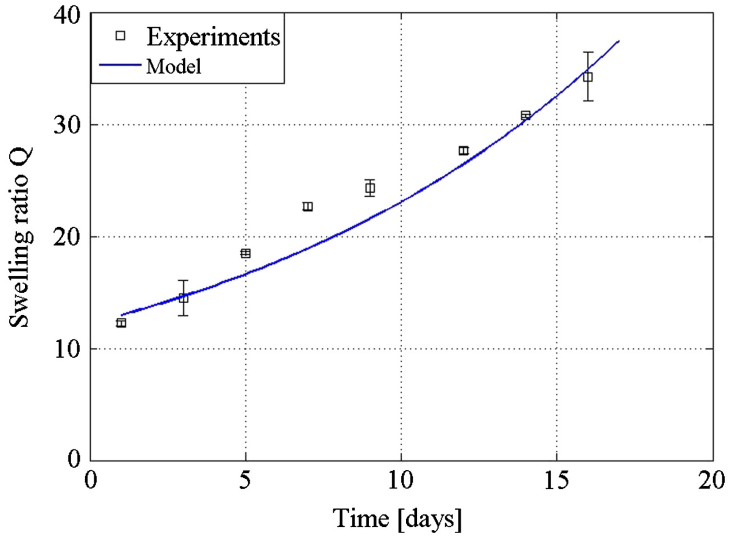

Figure A2.5 Swelling ratio Q over time in a bimodally degradable hydrogel consisting of a 95:5 weight ratio of PEG-LA-DM and PEGDM.

A2.5 Production and Transport of ECM Molecules Within an Evolving Hydrogel Structure

In vivo, chondrocytes produce all of the components of cartilage, which include the collagens and proteoglycans described in Table A2.1. Tissue deposition is typified initially by the formation of a protective pericellular matrix found immediately surrounding the cell, characterized by a meshwork of collagen VI as well as collagen II and aggrecan [30]. Macroscopic tissue deposition can only occur when matrix is secreted and retained throughout the surrounding extracellular matrix. When encapsulated in a hydrogel network, chondrocytes similarly secrete extracellular matrix molecules, which, in time, begin to recapitulate the structure and organization of native cartilage. However, in this case, the evolving nature of the scaffold structure strongly influences the way matrix molecules are transported and deposited to form a new tissue.

A2.5.1 Classification of ECM molecules and experimental observation

At the molecular scale, the hydrogel is composed of a crosslinked network structure with a characteristic mesh size (varying with crosslinking density and degradation) that can permit or restrict diffusion of soluble molecules, which have a characteristic radius of gyration in solvent, depending on their size relative to the average mesh size. The proposed model treats matrix molecules as either 'large' or 'small' to demonstrate restricted vs. free diffusion through the hydrogel mesh. Future versions of the model will attempt to account for the wide variety of matrix molecules secreted by chondrocytes. For reference, a summary of the main ECM molecules that make up articular cartilage is presented in Table A2.1. Relative composition of components is expressed as a percentage of wet weight [31], and the size scale and structure of collagens [32] and proteoglycans [31] are presented.

Table A2.1. Composition of native cartilage. The symbol ξ represents the gel mesh size.

	% by wet weight	Component	Size scale	Structure	Category
Collagens	20	Collagen II	400 nm	Linear fibers	**Large molecules**
		Collagen VI	100 nm	Fibrillar	
Aggrecan, proteoglycans, and their building blocks	5-7	Aggrecan aggregates	100 MDa	Highly branched	**Large molecules**
		Aggrecan	1-4 MDa	Branched	
		Hyaluronan	MDa	Linear	
		Link protein	45 kDa	Globular	
		Glycosaminoglycans	5-30 kDa	Linear	
		Decorin	40 kDa	Globular	
		Biglycan	40 kDa	Globular	
Other	70-75	Water	<< ξ	-	**Small molecules**
		Salts	<< ξ	-	

For cell-laden photopolymerized hydrogels cultured for several weeks, deposition of matrix molecules can be characterized experimentally in a variety of ways. For this study, we present qualitative methods which demonstrate spatial deposition of specific matrix molecules via immunohistochemical techniques. Immunohistochemical staining for chondroitin sulfate was applied to dehydrated, paraffin-embedded 10 micron-thick sections of hydrogels as previously

described [7,33]. Briefly, sections were mounted onto slides and rehydrated, treated with chondroitinase ABC, and probed with a primary antibody against chondroitin-6-sulfate (Chemicon, Billerica, MA) followed by an AlexaFluor 546-conjugated secondary antibody and counterstained with DAPI. Images were acquired with a confocal laser scanning microscope at 40x magnification (Fig. A2.8 and A2.9).

A2.5.2 Modeling molecular transport and deposition in deforming hydrogels

The transport of cell-secreted extracellular matrix molecules is a critical component of tissue growth, and tissue engineering strategies should aim to facilitate such processes. In the case of cells encapsulated in gels, controlled degradation of the gel crosslinks is required to achieve homogeneous distribution of cell-secreted matrix. Particularly, the rate and timing of this degradation are important factors. If the degradation occurs too quickly, then major defects may develop that can have negative consequences on the macroscopic geometry and mechanical properties. If the degradation occurs too slowly, the gel will prevent timely distribution of ECM molecules and tissue regeneration, entrapping the matrix molecules between cells and the gel, yielding only pericellular matrix tissue deposition. Better understanding of these processes requires a mathematical model that is able to capture the coupled physics between molecular transport, gel deformation and degradation. The theory of mixture provides an excellent framework in this context.

Mass transport: From a modeling point of view, transport of water (*f*) and unbound extracellular matrix molecules (*p*) can be described by their volumetric flux, taken with respect to polymer motion:

$$\mathbf{q}^{\alpha} = \phi^{\alpha}(\mathbf{v}^{\alpha} - \mathbf{v}^{s}) \tag{19}$$

where $\alpha = f, p$. Note that this definition of flux is consistent with an Eulerian approach, *i.e.*, the flux is defined as the volume of constituent α per unit of time, passing through a unit surface S

in the deformed configuration. When large deformations are considered, however, it is convenient to define the Lagrangian flux

$$\mathbf{Q}^{\alpha} = J\mathbf{F}^{-1}\mathbf{q}^{a} \tag{20}$$

as the amount of constituent α passing through a unit area in the reference gel configuration (defined in the dry state, i.e. initial configuration). Eq. (22) therefore shows the mapping of the flux from the current configuration to the dry polymer configuration. Using the assumption of incompressibility for all constituents, it is possible to derive the equation of mass balance in the form:

$$J\frac{D\phi^{\alpha}}{Dt} + \nabla_{\mathbf{X}} \cdot \mathbf{Q}^{\alpha} = -\phi^{\alpha}\frac{DJ}{Dt} \quad \text{where} \quad \alpha = f, p \tag{21}$$

Here, the first equation quantifies the balance of mass of the fluid phase, while the second equation describes the balance of mass of the ECM molecules. Eq. (23) implies that the volumetric flux of the fluid phase (mapped back to the dry configuration) is directly linked to the swelling (or deswelling) J of the tissue.

Constitutive equation: An important aspect of the present study is the introduction of realistic constitutive relations governing the transport of ECM molecules and water through the gel and their relation to gel deformation and degradation. Assuming the effect of ECM molecules to be negligible on water flux, fluid flow can be expressed in terms of the pressure gradient $\nabla_x p$ as stated by Darcy's law:

$$\mathbf{Q}^{f} = -\kappa J\mathbf{F}^{-1}\left(\nabla_{X} p\right) \text{ , where } \quad \kappa = \frac{\xi^{2}(1-\phi^{s})}{8\bar{\mu}_{f}\delta} \tag{22}$$

where κ is the isotropic gel permeability, δ is the tortuosity of the gel structure and $\bar{\mu}_f$ is the fluid viscosity (see Table A2.2). We note that the gel permeability to water is a function of polymer mesh size ξ [9], which is itself a function of gel crosslinking and can be related to swelling. This dependency was introduced by Bell and Peppas [25] as follows:

$$\xi = \xi_0(\phi^s)^{-1/3}, \text{ where } \xi_0 = C_n^{1/2} n^{1/2} l \tag{23}$$

where ξ_0 is the mesh size of the dry polymer, l is the average bond length, C_n is the polymer characteristic ratio, and *n* is the number of bonds between crosslinks, which is determined from the molecular weight between crosslinks and molecular weight of the polymer repeat unit (see Table A2.2). It is clear from Eq. (20) and (24) that gel swelling (through hydrolytic degradation for instance), by decreasing the value of ϕ^s, ultimately increases gel permeability and facilitates transport of water through the hydrogel. But also, the number of bonds between crosslinks n changes with changes in crosslink density [22], which means that the mesh size evolves with degradation.

Because of their relatively small volume fraction, driving forces affecting the motion of unbound ECM molecules are of three types: an advection term (molecules tend to follow the solvent in its flow), a diffusion term within the solvent and thirdly, a term that describes resisting frictional forces from the hydrogel. To separate each contribution, we take the following approach. First, it is convenient to eliminate the friction force from the gel by considering the motion of ECM molecules in a pure solvent. In this case, the flux $\mathbf{q}_\infty^p$ can be readily decomposed into a component that follows the solvent flux given by Eq. (23) and a component representing the relative diffusion of the molecules in the solvent using Fick's law. This leads to [19][14]:

$$\mathbf{q}_\infty^p = \left(D_\infty \nabla_x c^p - \frac{M^p}{\rho^{pR}} \kappa \nabla_x p \right) \qquad \text{where } D_\infty = \frac{k_B T}{6\pi \bar{\mu}_f r_s} \tag{24}$$

Here, M^p is the average molar mass of ECM molecules and D_∞ is the free solution diffusivity defined by the Stokes-Einstein relation [34], r_s is the radius of gyration of small matrix molecules and k_B is the Boltzmann constant. The effect of the gel resistance on molecule

transport can then be captured by realizing that when the ratio of radius of gyration r_s of ECM molecules is significantly smaller that the polymer mesh size ($r_s / \xi \ll 1$), gel resistance is negligible and the ECM molecule flux $\mathbf{q}^p$ becomes $\mathbf{q}_\infty^p$. However, as r_s increases, we assume that gel resistance results in a decrease of $\mathbf{q}^p$ that is expressed in the form:

$$\mathbf{q}^p = \mathbf{q}_\infty^p g(\xi) \quad \text{where} \quad g(\xi) = \frac{1}{2}\left[1+\text{erf}\left(\frac{2}{\Delta}\left(\xi - \delta - \text{r}_s\right)\right)\right] \tag{25}$$

where Δ is a parameter of the Gauss error function erf.

The function g used in this study attempts to capture the nonlinear relationship between ECM transport processes and the relative sizes of ECM molecules and hydrogel mesh. As shown in Fig. A2.6, this function clearly implies that (1) as ECM molecules become larger than the hydrogel mesh size, ECM transport is fully hindered ($g \to 0$) and (2) as the hydrogel mesh size becomes significantly larger than ECM molecules size, gel resistance becomes negligible ($g \to 1$). This expression was originally motivated by the work of Lustig and Peppas in [35] in their method to describe the change in diffusivity with the ratio r / ξ.

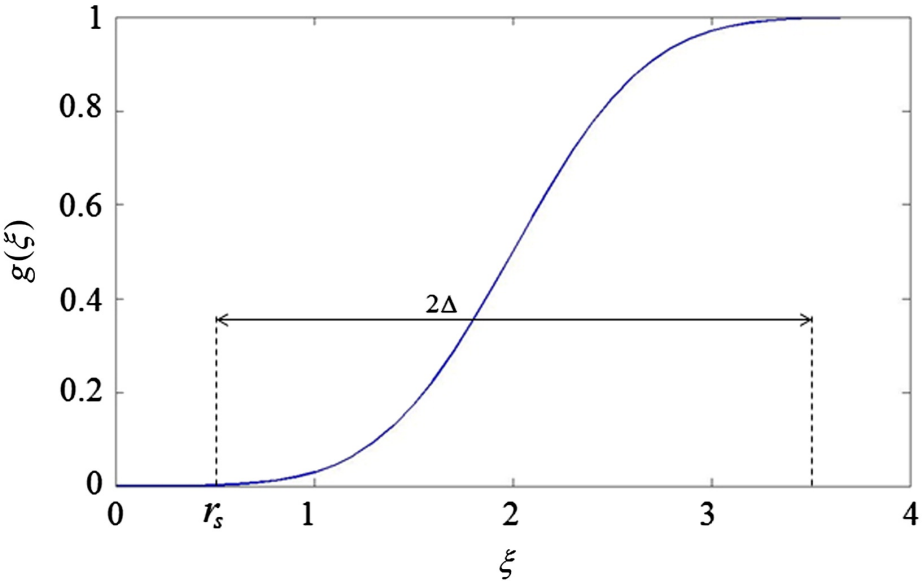

Figure A2.6 Gauss error function used in the model to describe the constitutive relations. Δ is taken as $4r_s$ in the above figure.

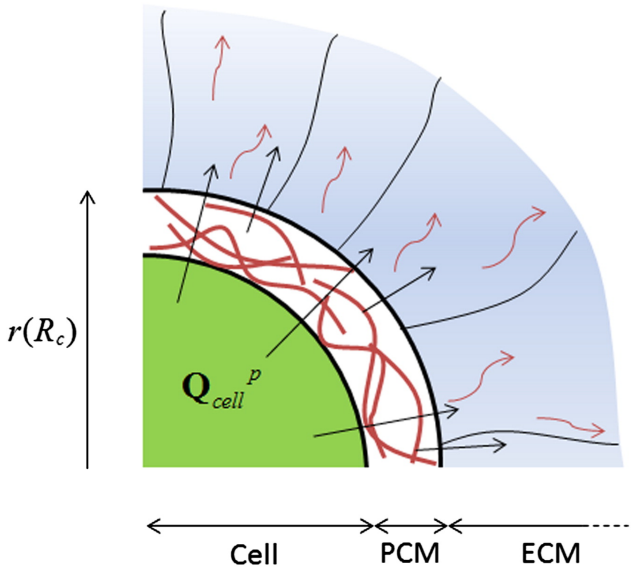

Figure A2.7 Diffusivity of proteins through the hydrogel. How the size of a protein impacts the boundary conditions.

Release of ECM molecules: As mentioned earlier (Table A2.1), chondrocytes produce different types of ECM molecules, which for our purposes may be distinguished by their size. "Small" molecules have a radius of gyration smaller than the initial hydrogel mesh size ξ and are therefore able to freely diffuse throughout the gel according to Eq. (28). "Large" molecules are distinguished by a radius that is larger than ξ and because they are unable to diffuse in the gel, they tend to accumulate between the cell and the scaffold, causing the gel to be pushed away from the cell. As depicted in Fig. A2.7, this behavior is modeled by prescribing appropriate "flux" boundary conditions at the cell membrane in the following fashion. We first introduce the normal ECM molecule flux release from the cell as Q_{cell}^{p} such that the release of large and small molecules can be split with the ratio f as:

$$\mathbf{Q}_{small}^{p} = f\mathbf{Q}^{p} \quad \text{and} \quad \mathbf{Q}_{large}^{p} = (1-f)\mathbf{Q}^{p} \tag{26}$$

We note here that the value of f is entirely dependent on the cell metabolism and is not considered here as a tunable parameter. Considering the mass balance of the volume between the cell and the hydrogel, denoted by the pericellular matrix in Fig. A2.7, it can be shown that

the above considerations translate into a two-fold boundary condition at the gel boundary R = R_c:

$$\dot{r}(R_c) = (1-f)\boldsymbol{Q}^p_{cell}$$

$$c^p_{gel} = f c^p_{cell} \tag{27}$$

where a superimposed dot refers to a time derivative. Matrix molecule release is regulated by the cell itself, which is able to detect the ECM concentration. Then, the small matrix molecule release is represented by a Dirichlet boundary condition. From these expressions, it is clear that if $f = 1$ all molecules released from chondrocytes get transported into the gel ($c^p(R_c) = c^p_{cell}$). If $f = 0$, however, ECM molecule release translates into a deformation of the gel at the cell/gel boundary ($\dot{r}(R_c) = \boldsymbol{Q}^p_{cell}$) and no diffusion of unbound ECM molecules into the hydrogel is observed ($c^p(R_c) = 0$). A more realistic situation is actually in an intermediate range with $f \sim 0.8$, which is a reasonable estimate, such that both gel deformation and unbound ECM molecule diffusion occur simultaneously.

A2.6 Results and Discussion

This section presents a combined modeling and experimental approach to investigate the dynamics of tissue transport and deposition in various hydrogel environments. Briefly, the computational model consists of numerically solving the balance of mass and momentum equations presented in Eq. (23), (24) and (8), respectively, together with the constitutive equation describing the hydrogel. These nonlinear equations were discretized on a one-dimensional finite-element mesh using centro-symmetric assumptions and the resulting transient analysis was solved for three interacting fields (consisting of solid displacement u, fluid pressure p and ECM molecule concentration c^p) with an implicit Newton-Raphson scheme as described in [36]. In the experimental component of our study, tissue production is measured by the deposition of chondroitin sulfate, an abundant linear glycosaminoglycan with an average

molecular weight of 20 kDa [31] and is most closely associated with proteoglycans, specifically aggrecan. This molecule is advantageous from a modeling perspective because it can exist as part of a smaller proteoglycan (1-4 MDa, Table A2.1), or as a part of a larger aggrecan aggregate (100 MDa, Table A2.1), which will exhibit more restricted diffusion. Chondroitin sulfate thus provides a good model molecule to demonstrate the deposition of an extracellular matrix composed of molecules of different size scales.

Model parameters were chosen in agreement with experimental observation, i.e., the initial volume fraction of cells was taken as $f_{cell} = 0.01$ and the cell radius was set to $R_c = 10\mu m$. The true density of the polymer was fixed at $\rho_{pegdm} = 1.07 g/cm^3$ and the true density of the matrix molecules was assumed to have the density of water i.e. $\rho^{pR} = 1 g/cm^3$. Other model inputs are described in Table A2.2.

Table A2.2. Inputs used in the model

Inputs	Value	Unit	Reference
V_1	0.018	L/mol	Commonly known
$\bar{u}$	1	mL/g	Commonly known
ρ_{pegdm}	1.07	g/mL	Estimate
ρ_{solv}	1	g/mL	Commonly known
C_n	4.0	-	(Merrill *et al*., 1993)
l	1.47	Å	Commonly known
T	310	K	Physiological temp
δ	2	-	(Kestin *et al*., 1981)
μ_f	0.65 x 10^{-3}	N.s/m^2	(Thorne *et al*., 1995)
M_p	20	kDa	(Hardingham, 2006)

A2.6.1 Role of initial hydrogel mesh size on ECM distribution

We first aim to assess the effect of crosslink density on the diffusion of unbound ECM molecules throughout the gel in the absence of degradation. For this, gels were made with

poly(ethylene glycol) dimethacrylate (PEGDM) with 10, 15, and 20% by weight compositions, yielding 0.11, 0.22, and 0.38 M crosslinking densities based on Eq (20).

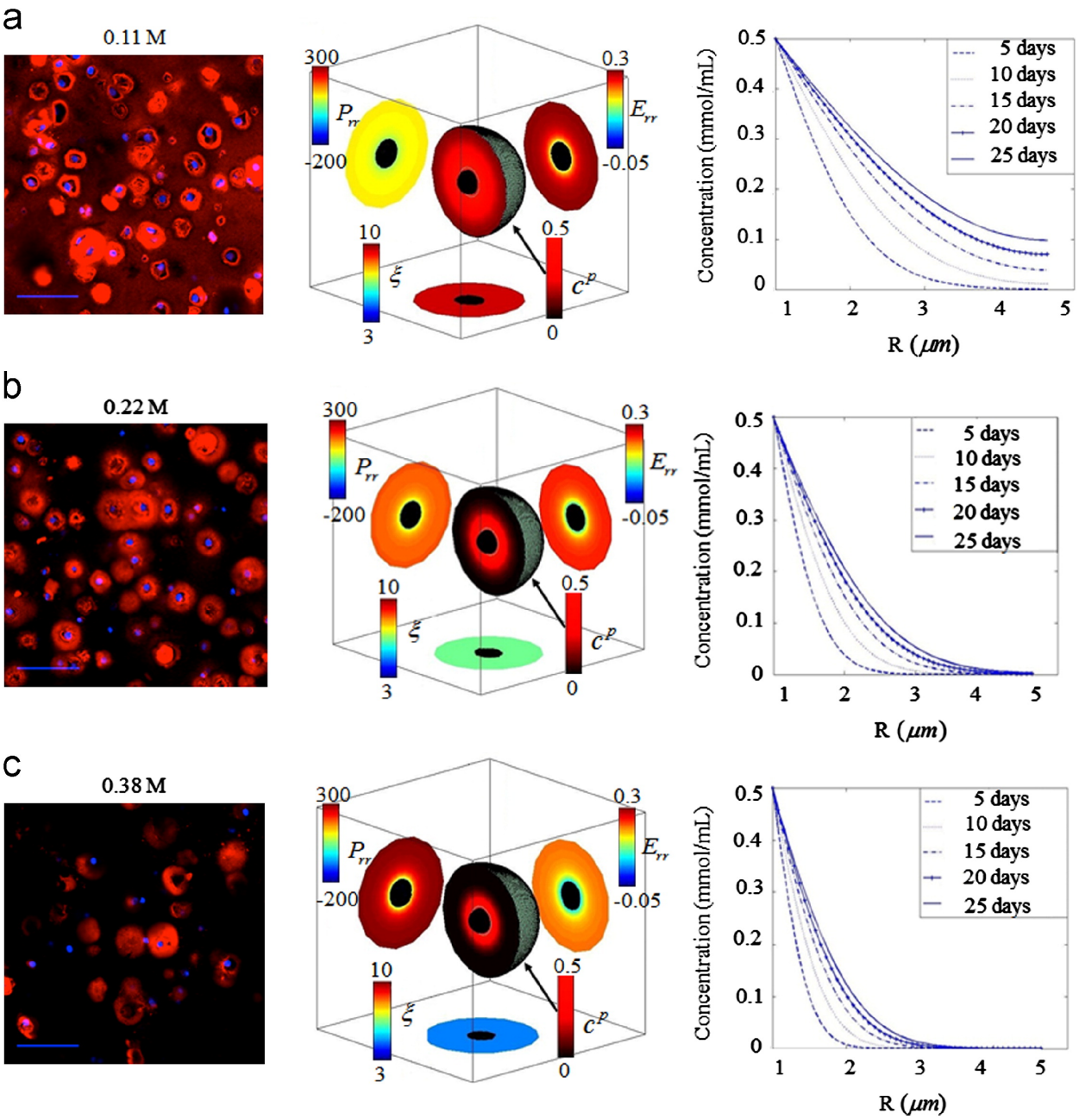

Figure A2.8 Figures (a), (b) and (c) show an experimental result and the model results for different crosslink densities of a stable hydrogel. Regarding the experimental pictures, chondroitin sulfate elaboration (red) by chondrocytes encapsulated within PEGDM hydrogels and cultured for 25 days in vitro with varied crosslinking density. Cell nuclei are stained blue. Scale bars indicate 50 microns. In the three-dimensional plots, the stress P_{rr} (kPa), strain E_{rr}, mesh size ξ (nm) and concentration c^p (mmol/mL) can be observed.

The concentration of chondroitin sulfate throughout the gel was evaluated by immunohistochemical staining 25 days after encapsulation. As shown in Fig. A2.8, results show that higher crosslink densities (i.e., 0.22 and 0.38 M) reduce unbound ECM molecule diffusion and consequently lead to localized elaboration of ECM surrounding the chondrocytes within the hydrogel. To better understand these processes, the presented mixture model was used to assess the variation of various quantities (hydrogel stress, strain, unbound ECM molecule concentration and hydrogel mesh size) for the three crosslink densities considered in experiments. Model results are generally in agreement with experimental observations with respect to the spatial deposition of chondroitin sulfate (Fig. A2.8). Most notably, the numerical results capture the presence of matrix molecules that have diffused far from the cell into the extracellular space of the hydrogel for the low crosslink gel (0.11 M), where there is a distinct lack of these matrix molecules in the extracellular space of the higher crosslink gels (0.22 and 0.38 M). They also illustrate a few important mechanisms of ECM deposition in hydrogels.

First, the change in chondroitin sulfate deposition for different crosslink densities can be explained by the fact that ECM diffusivity is an increasing function of hydrogel mesh size (Eq. (28)), which is dependent on crosslink density. Indeed, lower crosslink densities are associated with a higher swelling ratio (Fig. A2.4), a lower polymer volume fraction and thus, a larger mesh size according to Eq. (26). This can be easily seen in the contour plots depicting mesh size distributions for the three considered crosslink densities in Fig. A2.8. This higher diffusivity enables ECM molecules to diffuse more homogeneously throughout the gel as seen in the concentration as a function of radial position plots in Fig. A2.8.

Second, the model clearly indicates the appearance of a pericellular matrix around the cell, consisting of large matrix molecules (MDa size scale, see Table A2.1) that accumulate between the chondrocyte and the surrounding gel due to their restricted diffusion. The growing pericellular matrix around the cell may result in compressive deformation of the gel near the cells, which is captured in the simulation results of Fig. A2.8. We note that this mechanism

tends to decrease the mesh size immediately surrounding chondrocytes and may potentially hinder ECM diffusion in a local region around the cell.

A2.6.2 Role of hydrolytic degradation on ECM transport

As observed in the previous section, homogeneous tissue deposition is difficult to achieve with non-degradable hydrogel systems. A solution to this problem therefore consists of introducing gels with crosslinks that can be cleaved over time and thus increase ECM molecule diffusivity over time. While this greatly improves ECM molecule transport, hydrogel degradation ultimately results in a weakening of the gel properties and if reverse gelation occurs before substantial tissue can be elaborated, complete loss of cells will occur. To investigate the effects of degradation, we compared the extent of ECM deposition after 28 days in (a) a non-degradable and (b) a degradable hydrogel that both initially possess a crosslink density of 0.11 M (Fig. A2.9). The degradable gel was characterized by the degradation kinetics discussed in section 3. Results presented in Fig. A2.9 show a dramatic increase of ECM molecule deposition and more homogeneous matrix deposition for the degradable system. Model predictions exhibit a similar trend and emphasize the underlying mechanisms of such behavior (Fig. A2.10a). As the hydrogel degrades, the radial stress decreases and swelling (or radial strain) increases under the effect of the osmotic pressure. These changes results in a significant increase in mesh size and, consequently, the enhancement of the diffusivity of ECM molecules (Fig. A2.11). In comparison, non-degradable hydrogels do not see any changes in swelling and diffusivity of ECM molecules. ECM molecule deposition in this system is therefore highly restricted.

As can be seen in Fig. A2.10b, the rate of degradation also has a large influence on the diffusion of matrix molecules within the hydrogel. In the process of designing a degradable hydrogel, the hydrolytic pseudo first order rate constant (Eq. (16) and (17)) may be optimized to enable maximum ECM molecule deposition before the hydrogel scaffold reaches the reverse

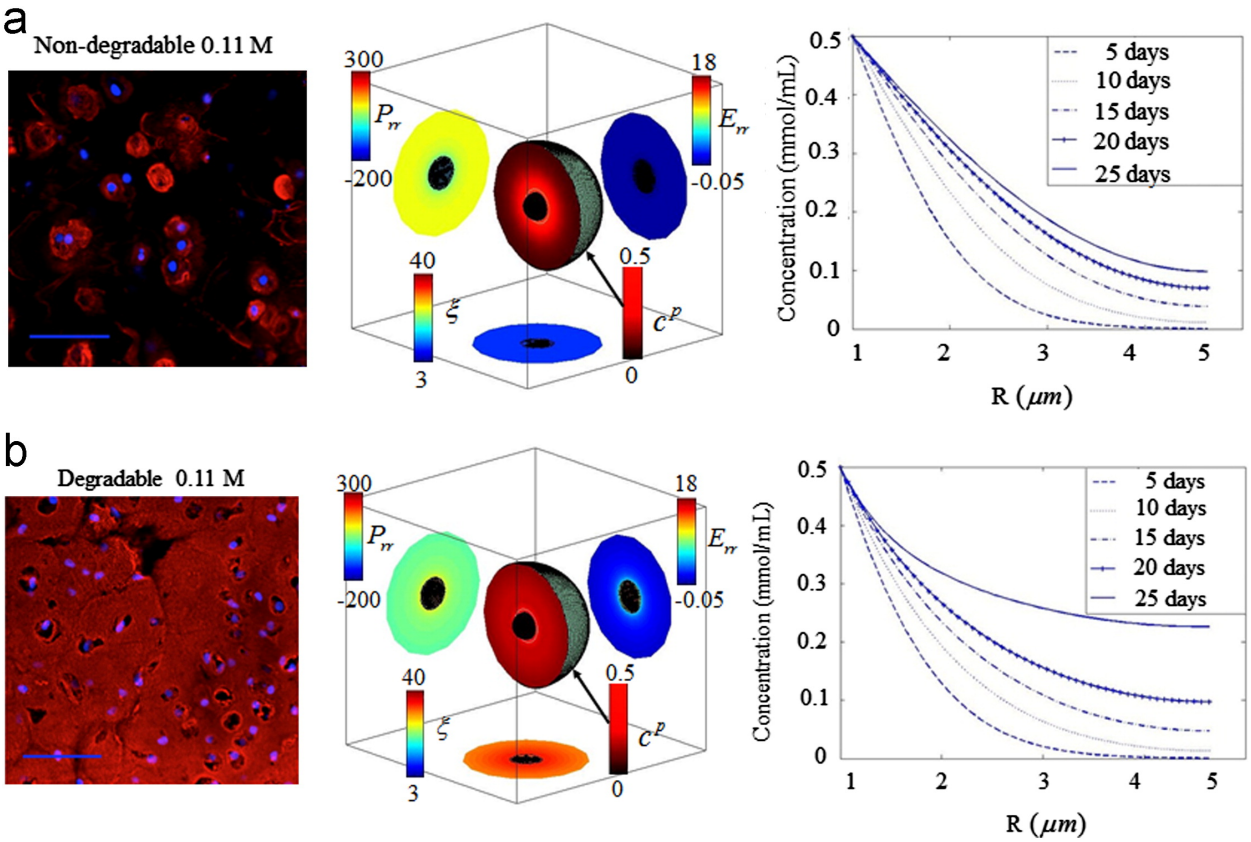

Figure A2.9 (a) shows the results for a non-degradable stable hydrogel, while (b) shows it for a degradable hydrogel. First image is the experiment showing chondroitin sulfate elaboration (red) by chondrocytes at day 28 encapsulated within 10% w/w non-degradable PEGDM and degradable PEG-LA-DM hydrogels. Cell nuclei are stained blue. Scale bars indicate 50 microns. In the three-dimensional plots, the stress P_{rr} (kPa), strain E_{rr}, mesh size ξ (nm) and concentration c^p (mmol/mL) can be observed. Note that due to differences in image processing between experiments, chondroitin sulfate staining is of lower intensity than shown in Fig. (8).

gelation point. From Eq. (20), it has been shown that for highly swollen gels ($Q > 10$) an estimate of the swelling can be found as Q; $\rho_x^{-3/5}$ [37]. Then, we can estimate accurately the reverse gelation point when $\rho_x / \rho_{x0} < (Q/Q_0)^{-5/3}$. Using the values of Fig. A2.5, this happens when ρ_x / ρ_{x0} becomes smaller than 20% (Fig. A2.10a and A2.11). In Fig. A2.9, macroscopic tissue deposition was observed at day 28, indicating that the evolution of ECM was able to maintain some level of three dimensional integrity after the hydrogel scaffold was fully degraded. However, a previous assessment of the overall mechanics of similar cell-laden

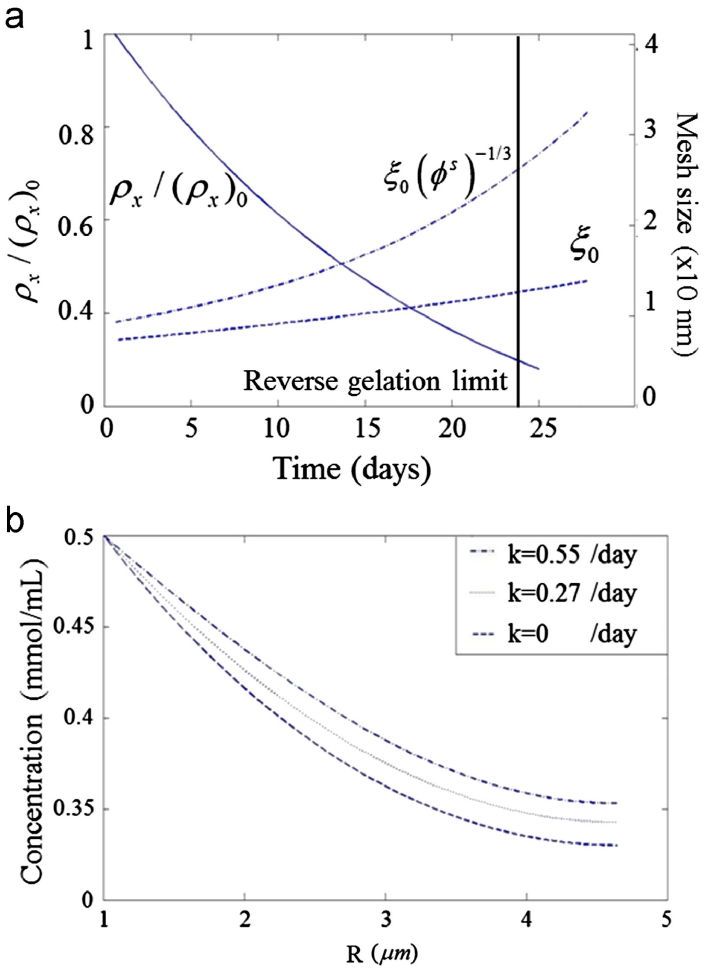

Figure A2.10 (a) shows the effect of swelling on the mesh size. And (b) shows the effect of the degradation rate k on the distribution of matrix molecules in the scaffold at day 25.

hydrogels showed a significant drop in compressive modulus from the initial cell-laden hydrogel to the engineered tissue as a result of hydrogel degradation [33]. These findings indicate that additional optimizations are needed to better match hydrogel degradation with tissue elaboration. With this mathematical model, we will now be able to better predict optimal degradation parameters that support macroscopic tissue evolution in degradable hydrogels without losing mechanical integrity.

A2.6.3 Role of osmotic pressure in diffusion of molecules and creation of tissue

Osmotic pressure is an important player in tissue transport as it is responsible for gel swelling and consequently controls hydrogel mesh size (and thus ECM molecule diffusivity). To

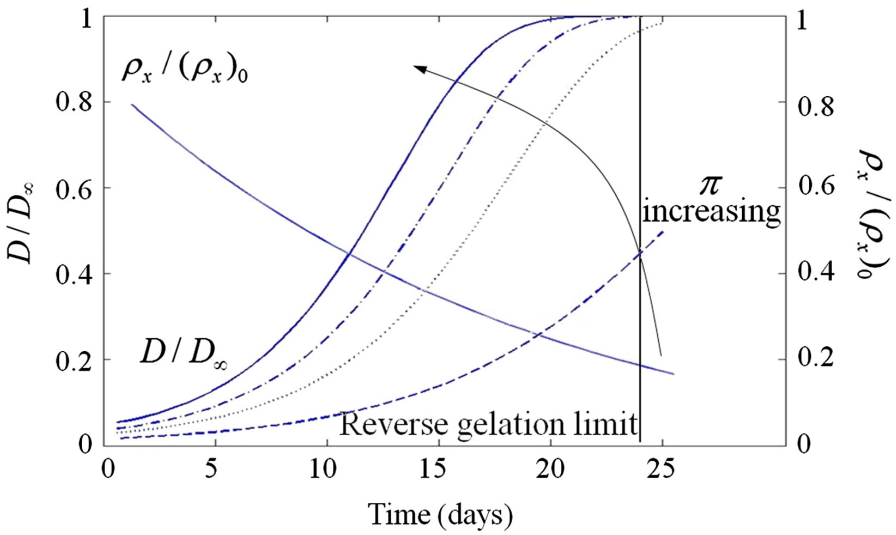

Figure A2.11 shows the different osmotic pressures (respectively 20, 200, 300, and 400 kPa) applied on the model to see the evolution of the diffusivity.

investigate this aspect, we used the theoretical model to predict the effect of changing osmotic pressure on the evolution of ECM diffusivity through a degradable gel. Fig. A2.11 shows the obtained trends for four different osmotic pressures ($\pi = 20$, 200, 300 and 400 kPa, see Eq. (18)). As expected, we observe that an increase in osmotic pressure precipitates a change in ECM molecule diffusivity through the gel. This observation is explained as follows: as a gel degrades, its bulk modulus decreases and its mechanical resistance to osmotic pressure becomes weaker; this results in significant gel swelling during degradation. Increasing the osmotic pressure tends to reinforce this swelling effect and thus enhance ECM molecule diffusivity due to the associated rise in mesh size. This mechanism is important as it could potentially enable a more homogeneous tissue distribution before a scaffold reaches the reverse gelation point.

A2.6.4 Concluding remarks

The presented model provides a platform for better understanding the role of hydrogel scaffold structure on cartilage tissue engineering. It evaluates both degradable and non-degradable PEG-based hydrogels, which have shown promise in creating successful engineered cartilage. The developed model demonstrates the limitations associated with tissue

deposition in non-degradable PEGDM hydrogels and confirms the necessity of adding degradable units to hydrogels in order to enable the diffusion of ECM molecules throughout the scaffold. Despite providing a good basis for better understanding the effects of hydrolytic degradation, this model demonstrates that large ECM molecules (see Table A2.1) will not diffuse throughout the hydrogel until after the reverse gelation point. As an attempt to account for the existence of various ECM molecule sizes, the model splits these molecules in two categories, thus including the diffusion mechanism and the deposition of larger molecules forming the PCM. Moreover, the model is able to simulate the concentration distribution of molecules in the scaffold, and to clearly show how crosslink density impacts ECM molecule diffusion. The model also emphasizes that osmotic pressure plays an important role in promoting diffusion through the gel. These results provide valuable insight into potentially effective tissue engineering strategies.

However, there are many limitations to the current modeling approach and their acknowledgment is critical for improving mathematical models in the future. With regards to modeling the solvent, hydrogels are typically swollen in cell culture medium, consisting of proteins, growth factors, and salts. As opposed to water (as considered in our model), these components may interact with secreted ECM molecules, and can potentially affect both osmotic pressure and cell response. The model, while focusing on a single cell encapsulated in a spherical gel domain, accounts for the density of cells in the hydrogel through the cell volume fraction. Future work could consist of developing a three-dimensional model, which may show adhesion and inhomogeneous cell-cell interactions. Indeed, in order to create a macroscopic tissue, there must be overlap between the tissue being produced from separate cells in order to create a homogeneous tissue structure. Finally, another component, which is ultimately difficult to model, is the dynamic nature of cells and the tissues they produce. Once matrix is deposited, it is not permanent, but is subject to reorganization or degradation by secreted enzymes. This process is necessary *in vivo* to transport newly synthesized ECM molecules from the pericellular

region to the extracellular space [38]. Similarly, modeling the secretion of matrix molecules from cells may be improved in further studies; cells can up-or down-regulate matrix synthesis in response to external cues, yet this process is not yet fully understood, meriting future investigation. Previous modeling studies [39,40] have considered such mechano-transduction mechanisms and can potentially be used to describe the regulation of ECM synthesis. In particular, accurate models of the membrane deformation and permeability [41–43] will be critical in assessing the sensitivity of cells to mechanical loading and fluid flows.

Despite these limitations, this model provides excellent insight into the deposition of matrix molecules in non-degradable and degradable hydrogels and matches well with experimental results. In addition, these results are presented for a static culture environment, while cartilage is subjected to loading *in vivo*. Future directions that merit investigation include mechanical loading to mimic the physiological mechanical environment, and some form of localized cell-mediated degradation [19] that may prove an improvement over bulk hydrolytic degradation.

Overall, we have demonstrated that a computational triphasic model for tissue production by cells in hydrogels with varying structures and chemistries can generate simulations consistent with experimental observation. Despite the many assumptions and simplifications utilized, a powerful model has been developed that captures essential tissue dynamics in synthetic structures. The limitations serve to motivate future experimental work as well as eventually adding layers of complexity to the model. By validating the model in simple non-degradable and hydrolytically degradable systems, more complex chemistries and additives can feasibly be incorporated into the model in the future. This increasing level of sophistication could aid in the design and characterization of novel tissue engineering environments. These models can be employed to both predict and understand successful tissue engineering structures, which could lead to more rapid development of clinically applied therapies.

A2.7 References

[1] Hootman JM, Helmick CG. Projections of US prevalence of arthritis and associated activity limitations. Arthritis Rheum 2006;54:226–9.

[2] Slaughter BV, Khurshid SS, Fisher OZ, Khademhosseini A, Peppas NA. Hydrogels in regenerative medicine. Adv Mater 2009;21:3307–29.

[3] Anseth KS, Bryant SJ. Controlling the spatial distribution of ECM components in degradable PEG hydrogels for tissue engineering cartilage. J Biomed Mater Res Part A 2003;64A:70–9.

[4] Elisseeff J, Anseth K, Sims D, McIntosh W, Randolph M, Yaremchuk M, et al. Transdermal photopolymerization of poly(ethylene oxide)-based injectable hydrogels for tissue-engineered cartilage. Plast Reconstr Surg 1999;104:1014–22.

[5] Sawhney AS. Bioerodible Hydrogels Based on Photopolymerized Poly(ethy1ene. Macromolecules 1993;26:581–7.

[6] West JL, Lee SH, Miller JS, Moon JJ. Proteolytically degradable hydrogels with a fluorogenic substrate for studies of cellular proteolytic activity and migration. Biotechnol Prog 2005;21:1736–41.

[7] Nicodemus GD, Skaalure SC, Bryant SJ. Gel structure has an impact on pericellular and extracellular matrix deposition, which subsequently alters metabolic activities in chondrocyte-laden PEG hydrogels. Acta Biomater 2011;7:492–504.

[8] Ateshian GA, Kim JJ, Grelsamer RP, Mow VC, Warden WH. Finite deformation of bovine material properties cartilage compression. J Biomech 1997;30:97.

[9] Holmes MH, Mow VC. The nonlinear characteristics of soft gels and hydrated connective tissues in ultrafiltration. J Biomech 1990;23:1145–56.

[10] Kwan MK, Lai WM, Mow VC. A finite deformation theory for cartilage and other soft hydrated connective tissues--I. Equilibrium results. J Biomech 1990;23:145–55.

[11] Sengers BG, Van Donkelaar CC, Oomens CWJ, Baaijens FPT. The local matrix distribution and the functional development of tissue engineered cartilage, a finite element study. Ann Biomed Eng 2004;32:1718–27.

[12] Dimicco MA, Sah RL. Dependence of Cartilage Matrix Composition on Biosynthesis, Diffusion, and Reaction. Transp Porous Media 2003;50:57–73.

[13] Trewenack AJ, Please CP, Landman KA. A continuum model for the development of tissue-engineered cartilage around a chondrocyte. Math Med Biol 2009;26:241–62.

[14] Vernerey FJ, Greenwald EC, Bryant SJ. Triphasic mixture model of cell-mediated enzymatic degradation of hydrogels. Comput Methods Biomech Biomed Engin 2012;15:1197–210.

[15] Haider MA, Olander JE, Arnold RF, Marous DR, McLamb AJ, Thompson KC, et al. A phenomenological mixture model for biosynthesis and linking of cartilage extracellular matrix in scaffolds seeded with chondrocytes. Biomech Model Mechanobiol 2011;10:915–24.

[16] Sawhney AS, Pathak CP, Hubbell JA. Bioerodible Hydrogels Based on Photopolymerized Poly(ethylene glycol)-co-poly(alpha-hydroxy acid) Diacrylate Macromers. Macromolecules 1993;26:581–7.

[17] Lin-Gibson S, Bencherif S, Cooper JA, Wetzel SJ, Antonucci JM, Vogel BM, et al. Synthesis and characterization of PEG dimethacrylates and their hydrogels. Biomacromolecules 2004;5:1280–7.

[18] Peppas NA. Hydrogels in Medicine and Pharmacy. Boca Raton, FL: CRC Press; 1986.

[19] Vernerey FJ, Foucard L, Farsad M. Bridging the Scales to Explore Cellular Adaptation and Remodeling. Bionanoscience 2011;1:110–5.

[20] Vernerey FJ, Farsad M. A constrained mixture approach to mechano-sensing and force generation in contractile cells. J Mech Behav Biomed Mater 2011;4:1683–99.

[21] Li C, Borja RI, Regueiro R a. Dynamics of porous media at finite strain. Comput Methods Appl Mech Eng 2004;193:3837–70.

[22] Flory PJ. Principles of Polymer Chemistry. Ithaca, New York: Cornell University Press; 1953.

[23] Treloar LRG. The physics of rubber elasticity. New York: Oxford University Press; 1975.

[24] Cowie JMG, Arrighi V. Polymers: Chemistry and Physics of Modern Materials. Boca Raton, FL: CRC Press; 2008.

[25] Bell CL, Peppas NA. Biomedical membranes from hydrogels and interpolymer complexes. Adv Polym Sci 1995;122:125–75.

[26] Metters AT, Bowman CN, Anseth KS. A statistical kinetic model for the bulk degradation of PLA-b-PEG-b-PLA hydrogel networks. J Phys Chem B 2000;104:7043–9.

[27] Bryant SJ, Bender RJ, Durand KL, Anseth KS. Encapsulating Chondrocytes in degrading PEG hydrogels with high modulus: Engineering gel structural changes to facilitate cartilaginous tissue production. Biotechnol Bioeng 2004;86:747–55.

[28] Skaalure SC, Milligan IL, Bryant SJ. Age impacts extracellular matrix metabolism in chondrocytes encapsulated in degradable hydrogels. Biomed Mater 2012;7.

[29] Mason MN, Metters AT, Bowman CN, Anseth KS. Predicting controlled-release behavior of degradable PLA-b-PEG-b-PLA hydrogels. Macromolecules 2001;34:4630–5.

[30] Bryant SJ, Nicodemus GD. Mechanical loading regimes affect the anabolic and catabolic activities by chondrocytes encapsulated in PEG hydrogels. Osteoarthr Cartil 2010;18:126–37.

[31] Hardingham TE. Proteoglycans and Glycosaminoglycans. In: Seibel MJ, Robins SP, Bilezikian JP, editors. Dyn. bone Cartil. Metab., Burlington: Elsevier Science; 2006, p. 85–98.

[32] Von der Mark K. Structure, Biosynthesis and Gene Regulation of Collagens in Cartilage and Bone. Dyn. bone Cartil. Metab., Elsevier; 2006, p. 3–40.

[33] Roberts JJ, Nicodemus GD, Greenwald EC, Bryant SJ. Degradation Improves Tissue Formation in (Un)Loaded Chondrocyte-laden Hydrogels. Clin Orthop Relat Res 2011.

[34] Rubinstein M, Colby RH. Polymer Physics. New York: Oxford University Press; 2003.

[35] Lustig SR, Peppas NA. Solute diffusion in swollen membranes. IX. Scaling laws for solute diffusion in gels. J Appl Polym Sci 1988;36:735–47.

[36] Farsad M, Vernerey FJ. An XFEM-based numerical strategy to model mechanical interactions between biological cells and a deformable substrate. Int J Numer Methods Eng 2012;92:238–67.

[37] Metters AT, Anseth KS, Bowman CN. A statistical kinetic model for the bulk degradation of PLA-b-PEG-b-PLA hydrogel networks: Incorporating network non-idealities. J Phys Chem B 2001;105:8069–76.

[38] Mok SS, Masuda K, Hauselmann HJ, Aydelotte MB, Thonar EJMA. Aggrecan Synthesized by Mature Bovine Chondrocytes Suspended in Alginate - Identification of 2 Distinct Metabolic Matrix Pools. J Biol Chem 1994;269:33021–7.

[39] Foucard L, Vernerey FJ. A thermodynamical model for stress-fiber organization in contractile cells. Appl Phys Lett 2012;100:13702–137024.

[40] Foucard L, Vernerey FJ. Dynamics of Stress Fibers Turnover in Contractile Cells. J Eng Mech 2012;138:1282–7.

[41] Vernerey FJ, Farsad M. An Eulerian/XFEM formulation for the large deformation of cortical cell membrane. Comput Methods Biomech Biomed Engin 2011;14:433–45.

[42] Vernerey FJ. The Effective Permeability of Cracks and Interfaces in Porous Media. Transp Porous Media 2012;93:815–29.

[43] Vernerey FJ. On the Application of Multiphasic Theories to the Problem of Cell-Substrate Mechanical Interactions. Adv. Cell Mech., Berlin: Springer; 2011, p. 189–224.

Appendix 3

Characterizing and Predicting the Properties of Multi-arm Thiol-norbornene PEG Hydrogels

---

A3.1 Abstract

The purpose of the presented work is to characterize multi-arm thiol-norbornene PEG hydrogels in an attempt to elucidate how experimentally controlled parameters for hydrogel design affect the resulting mechanical and swelling properties, which are bulk properties that depend on the hydrogel crosslinking density. PEG hydrogels formed from multi-armed macromers, where each arm is capped with a thiol-reactive norbornene group, can span a wide range of properties, depending on experimentally controlled variables. This elicits a high degree of tailorability, which is important when designing hydrogels for a variety of tissue engineering applications. The main parameters subject to experimental control include the number of PEG arms, the molecular weight of the multi-arm PEG macromer, the weight percent (concentration) of PEG macromer in pre-polymer solution, and the molar ratio of thiol groups to norbornenes, where the latter parameter determines the degree of crosslinking. The effect of varying these parameters was investigated, and resulting bulk properties (namely the compressive modulus and the volumetric swelling ratio) were determined and compared to theoretical predictions. The ultimate goal is to aid experimentalists in choosing hydrogel formulations for specific purposes requiring particular mechanical properties and swelling characteristics.

A3.2 Hydrogel Fabrication and Characterization

A3.2.1 Materials

8-arm PEG amine (MW 10,000 and 20,000) was from JenKem Technology USA (Allen, TX). 0-(7-azabenzotriazol-1-yl)-N,N,N’,N’-tetramethyluronium hexafluorophosphate (HATU) and

N,N'-diisopropylethylamine (DIEA) were from Chem-Impex International, Inc. (Wood Dale, IL). Ethyl ether and N,N-dimethylformamide (DMF) were from Fisher Scientific (Fair Lawn, NJ). Regenerated Cellulose 1000 MWCO dialysis tubing was from Spectrum Labs (Rancho Dominguez, CA). Irgacure 2959 was from Ciba Specialty Chemicals (Tarrytown, NY). Phosphate-buffered saline (PBS) was from Invitrogen (Carlsbad, CA). 5-norbornene-2-carboxylic acid and PEG-dithiol were from Sigma-Aldrich (St. Louis, MO).

A3.2.2 PEG macromer synthesis

8-arm PEG amine (MW 10,000 and 20,000) were reacted with norbornene acid to synthesize 8-arm PEG-amide-norbornene (8armPEG10K-NB and 8armPEG20K-NB) [1–3]. Briefly, norbornene acid (8x molar excess compared to amine-terminated PEG arms) in DMF was pre-reacted for 5 minutes under argon with HATU (4x excess) and DIEA (4x excess) at room temperature. The pre-reacted mixture was combined with 8-arm PEG amine in DMF, and the reaction proceeded overnight under argon at room temperature. 8armPEG-NB was recovered by precipitation in ethyl ether, and purified by dialyzing against DI H_20 for 2-3 days. Dialyzed 8armPEG-NB was filtered (0.2 μm) and lyophilized. ^{1}H-NMR spectroscopy determined norbornene conjugation (δ = 5.9 - 6.3 ppm) per 8-arm PEG molecule (δ = 3.4 – 3.9 ppm). On average, 100% of amine-terminated PEG arms were conjugated with norbornene (for both 8armPEG10K-NB and 8armPEG20K-NB).

A3.2.3 Hydrogel formation and characterization

Macromer solutions were formed with varying weight % (wt%) of 8armPEG10K-NB and 8armPEG20K-NB in PBS, and thiol:norbornene molar ratios were varied to create hydrogels with a range of crosslink densities. PEG-dithiol (1000 or 1500 MW to crosslink 8armPEG10K-NB or 8armPEG20K-NB, respectively) was used as a non-degradable crosslinker. Cylindrical hydrogels were formed (4 mm diameter x 3 mm height) by photopolymerizing with 0.05 wt% Irgacure 2959 for 8 min with 365 nm light (6 mW cm^{-2}). Hydrogels free swelled to equilibrium overnight in PBS at 37 °C before characterizing the compressive modulus and swelling ratio.

Q is the hydrogel volumetric swelling ratio, which is the swollen hydrogel volume divided by dry hydrogel volume. This was calculated from the swollen and lyophilized hydrogel masses, M_s and M_d, respectively, using the polymer density ρ_p (1.07 g ml^{-1}) and solvent density ρ_s (1 g ml^{-1}):

$$Q = 1 + \frac{\rho_p}{\rho_s}\left(\frac{M_s}{M_d} - 1\right) \quad (1)$$

To measure the compressive modulus, hydrogels were compressed to 15% strain at a strain rate of 0.5 mm min^{-1} to obtain stress-strain curves (MTS Synergie 100, 10N). The compressive modulus was estimated as the slope of the linear region of stress-strain curves. The shear modulus G was estimated from measurements of the compressive modulus, where the compressive modulus is assumed to serve as a reasonably good estimate for the Young's modulus, E (although imprecise because the compressive modulus is not determined from an equilibrium mechanical measurement, where the material is allowed to relax as it is deformed). Rubber elasticity theory relates E to G according to the following relationship [4]:

$$E = 2G(1 + \upsilon) \quad (2)$$

Here, υ is the Poisson ratio, which is assumed to equal 0.5. The hydrogel crosslinking density ρ_x is a property related to all bulk and microscopic hydrogel properties, including the modulus, swelling ratio, and mesh size. The crosslinking density cannot be measured directly but instead can be estimated indirectly from experimental bulk property measurements, yielding an experimentally determined value for ρ_x, which we will call $\rho_{x,exp}$ [4,5].

$$\rho_{x,exp} = \frac{GQ^{1/3}}{RT} \quad (3)$$

Here, R is the gas constant (8.314 J K^{-1} mol^{-1}) and T is temperature (310 K).

A3.3 Theoretical Crosslinking Density and Swelling Ratio

Because thiol-norbornene PEG hydrogels are formed by a step-growth method, the crosslinked hydrogel structure is well defined, therefore a theoretical crosslinking density ($\rho_{x,theo}$) can be estimated from the molar amounts of starting materials used and Q for the resulting

hydrogel after reaching swelling equilibrium (which will be referred to as Q_f). Each norbornene can only react with one thiol, and it takes two thiol-norbornene reactions (reacting one dithiol crosslinker) to create a crosslink. Macroscopic properties such as the compressive modulus and the swelling ratio of a hydrogel are dependent on the crosslinking density, which is the molar amount of crosslinks (where one crosslink arises from two thiol-norbornene reactions connecting two multi-arm PEG molecules) per unit volume. In order to tune hydrogel properties for a variety of applications, it is necessary to understand and predict how the hydrogel formulation ultimately affects the crosslinking density.

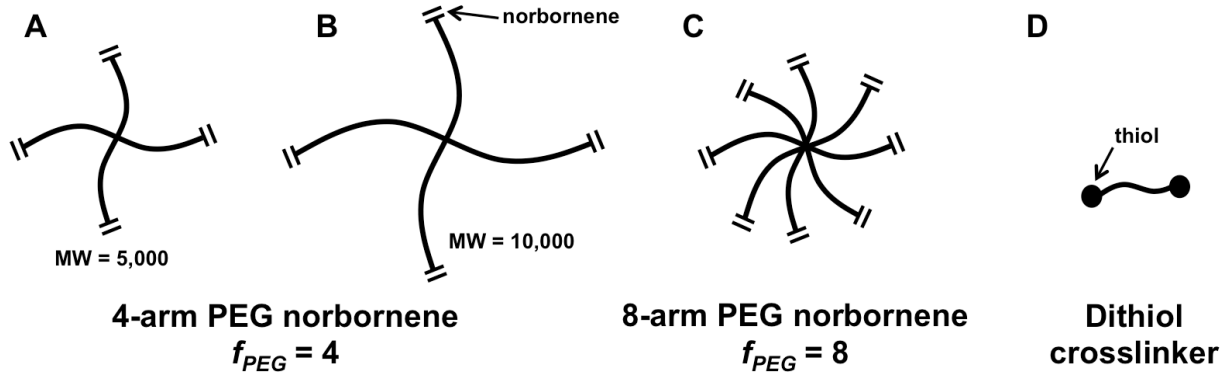

Figure A3.1 Schematic representing the components required to make multi-arm thiol-norbornene PEG hydrogels. (A) Low and (B) high MW PEG macromers, shown here for 4-arm PEG specifically, or (C) 8-arm PEG macromer, can be crosslinked with a dithiol molecule (D) into a 3D network.

The commonly used multi-arm PEG macromers include 4- and 8-arm PEG, where the molecular weight (MW) typically ranges from 5,000 to 40,000 Da (Fig. A3.1). The number of PEG arms per molecule is referred to as the functionality, or f_{PEG}, where f_{PEG} = 4 or 8 in these two cases (Fig. A3.1A-C). The norbornene-terminated arms of the PEG macromers can be reacted with dithiol molecules (Fig. A3.1D) to form crosslinks, but not every norbornene must necessarily be reacted. However, one must be aware of the gelation point, which describes the degree of conversion of norbornenes beyond which a gel can be formed, because if too few crosslinks are formed, a hydrogel network will not result (Fig. A3.2). The general rule is that the

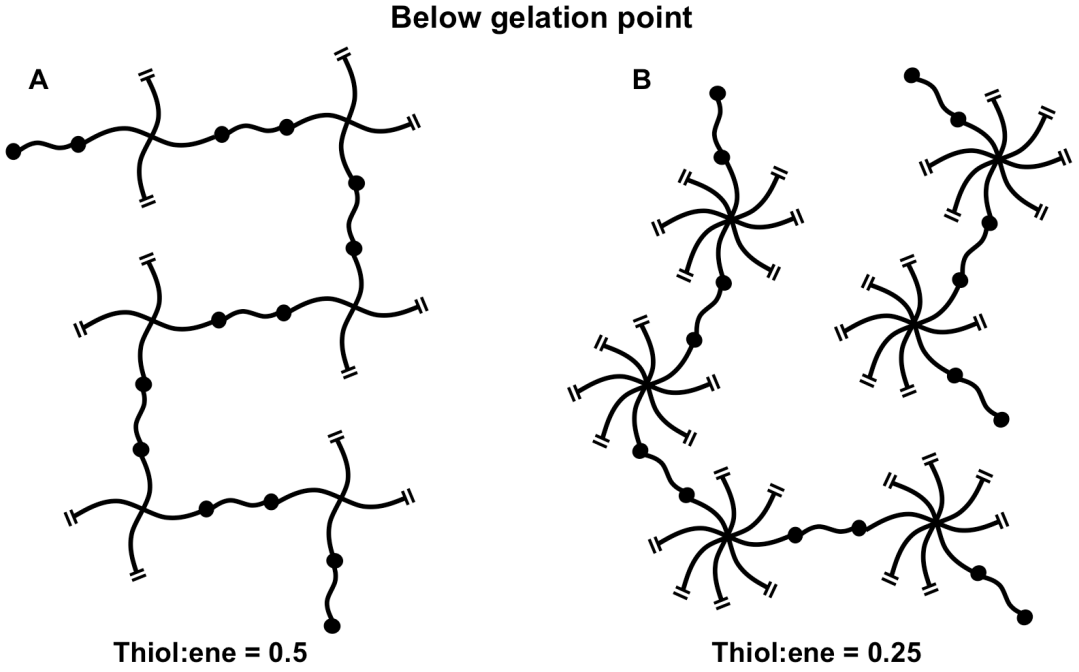

Figure A3.2 (A) 4-arm or (B) 8-arm PEG norbornene macromers with insufficient amount of dithiol crosslinker (indicated by the thiol:ene molar ratio) to lead to hydrogel formation.

gelation point occurs when each PEG molecule has an average of greater than 2 crosslinks, because at the 2 crosslinks per PEG limit, there would only be formation of long, soluble chains, but not an insoluble network. This means that for 4-arm PEG, the gel point occurs when >50% of norbornenes are reacted (Fig. A3.2A), and for 8-arm PEG, the gel point occurs when >25% of norbornenes are reacted (Fig. A3.2B), meaning that the 8-arm PEG can be used to achieve a wider range of properties because hydrogels can be formed between 25-100% norbornene reaction (Fig. A3.3). Here we term the percentage of norbornenes reacted with thiols the 'thiol:ene ratio', which is the molar ratio of crosslinking thiols (2 moles thiol per mole of dithiol crosslinker) to norbornenes. For example, when 25% of norbornenes are reacted, the thiol:ene ratio is 0.25. When 100% of norbornenes are reacted, the thiol:ene ratio is 1.0.

Because one norbornene can only react with one thiol, if the starting amounts of PEG macromer and dithiol crosslinker are known, assuming a complete and ideal reaction (all thiols react with a norbornene, and neglecting any non-idealities such as cyclization), the molar

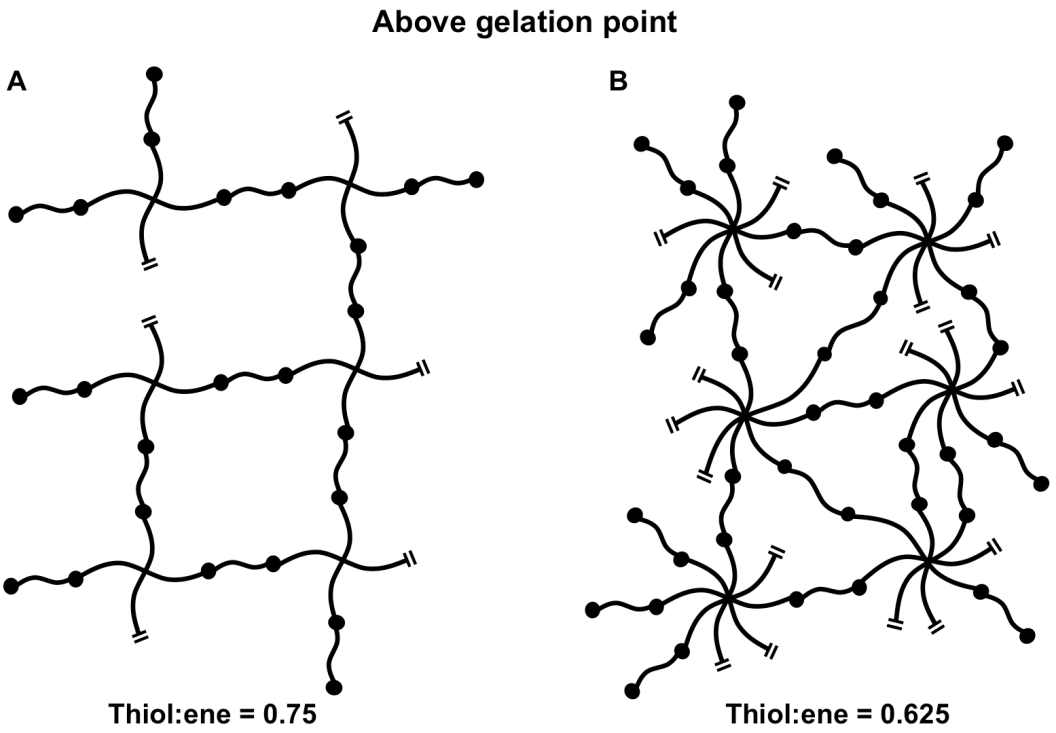

Figure A3.3 (A) 4-arm or (B) 8-arm PEG norbornene macromers with sufficient amount of dithiol crosslinker (indicated by the thiol:ene molar ratio) to lead to hydrogel formation.

amount of formed crosslinks can be estimated. The volume and concentration of the initial pre-polymer solution are known by the experimentalist, but the hydrogels will swell to an equilibrium swollen volume when allowed to equilibrate in aqueous solution for at least 12 hours. Assuming that none of the initially formed crosslinks are broken during the swelling phase, the total amount of crosslinks present before and after swelling are equivalent, and all that changes is the volume, which can be accounted for by measuring the equilibrium Q_f.

In order to calculate the theoretical crosslinking density, the approach is to calculate the crosslinking density of the hydrogel immediately after formation based on the starting formulation, and then to adjust for the change in volume. When forming PEG hydrogels, the concentration of the multi-arm PEG in pre-polymer solution is typically controlled by varying its weight % (wt%), which is equivalent to:

$$\frac{mass_{polymer}}{mass_{polymer} + mass_{solvent}} \quad (4)$$

In order to express this into a concentration (mass per volume), the denominator must be converted into volume, using the densities of both polymer and solvent, which were provided with equation (1). If we transform to a 100-gram scale for simplicity (where 1 wt% = 1 g), then the mass of multi-arm PEG per volume, shown in g ml^{-1}, can be expressed as follows:

$$\frac{mass_{polymer}}{\frac{mass_{polymer}}{\rho_p}+\frac{mass_{solvent}}{\rho_s}} = \frac{wt\%}{\frac{wt\%}{\rho_p}+\frac{100-wt\%}{\rho_s}} \quad (5)$$

Now we have the concentration expressed as mass of multi-arm PEG per volume, which is converted into moles per volume using the PEG MW. Using stoichiometry and the other formulation-specific parameters, moles of multi-arm PEG can be converted into moles of crosslinks, where two reacted thiols are required to form one crosslink (hence the ½ term):

$$\frac{wt\%}{\frac{wt\%}{\rho_p}+\frac{100-wt\%}{\rho_s}} \times \frac{1000\ ml}{L} \times \frac{1}{MW} \times f_{PEG} \times thiol{:}ene \times \frac{1}{2} = \frac{moles\ of\ crosslink}{initial\ volume\ (L)} \quad (6)$$

This calculation results in the theoretical crosslink density of the *initially* formed hydrogel (before any swelling or volume changes occur). In order to adjust the crosslink density to the equilibrium swollen volume, a simple volume conversion factor is needed:

$$\frac{moles\ of\ crosslink}{initial\ volume} \times \frac{initial\ volume}{equilibrium\ volume} = equilibrium\ crosslink\ density\ (\rho_{x,theo}) \quad (7)$$

To find a substitute for the volume conversion factor (second term), we will use the swelling ratio *Q*, which was described in equation (1) but is generically defined as:

$$Q = \frac{V_{swollen}}{V_{dry}} \quad (8)$$

In this equation, $V_{swollen}$ is the swollen hydrogel volume, and V_{dry} is the volume of polymer only (no solvent). In order to adjust using *Q*, we must define Q_i as the initial hydrogel swelling ratio (immediately after polymerization, and *not* at equilibrium), and Q_f as the final hydrogel swelling ratio after reaching swelling equilibrium. Q_i can be calculated similarly to equation (5):

$$Q_i = \frac{V_{initial}}{V_{dry}} = \frac{\frac{wt\%}{\rho_p}+\frac{100-wt\%}{\rho_s}}{\frac{wt\%}{\rho_p}} \quad (9)$$

Note that for Q_i and Q_f, V_{dry} has the same value, meaning that the ratio of Q_i/Q_f is equivalent to $V_{initial}/V_{swollen}$, which is the second term needed in equation (7). After combining equations (6), (7), and (9), several terms drop out, including wt% and ρ_s, resulting in the final expression for equilibrium theoretical crosslink density $\rho_{x,theo}$:

$$\rho_{x,theo}\ (\mathrm{mM}) = \frac{10^6 \rho_p f_{PEG}(thiol{:}ene)}{2(MW)Q_f} \tag{10}$$

This equation however requires that Q_f be experimentally determined from measurements of the wet and dry hydrogel masses. In order to create a purely predictive model (without requiring hydrogel fabrication or measurement), we can employ correlative relationships to predict Q_{theo}, which is the equilibrium swelling ratio for a particular formulation, that have been previously developed [6]:

$$Q_{theo} = (thiol{:}\,ene)^{-1/3}\left(\frac{\nu}{b^3}\right)^{0.53} N^{0.57} Q_i^{\,0.38} \tag{11}$$

where: b = Kuhn length of one PEG repeat in aqueous solution, b = 3.65 Å

$v = (1\text{-}2\chi)b^3$ and χ is the polymer-solvent interaction parameter, v = 0.426

N = the number of PEG repeats between crosslinks

N must be calculated based on the multi-arm PEG MW (MW_{PEG}), the functionality f_{PEG}, the MW of the dithiol crosslinker (MW_x), and the MW of one PEG repeat unit (MW_{ru} = 44):

$$N = \frac{\frac{2MW_{PEG}}{f_{PEG}} + MW_x}{MW_{ru}} \tag{12}$$

Therefore, the purely theoretically predicted crosslinking density (and the equation used to predict theoretical crosslinking density in the following sections) is calculated as follows, with Q_{theo} substituted for Q_f:

$$\rho_{x,theo}\ (\mathrm{mM}) = \frac{10^6 \rho_p f_{PEG}(thiol{:}ene)}{2(MW)Q_{theo}} \tag{13}$$

A3.4 Experimental Results and Discussion

Multi-arm thiol-norbornene PEG hydrogels were formed using an 8-arm PEG (20,000 MW), where either the weight % or thiol:ene ratio were held constant while the other parameter

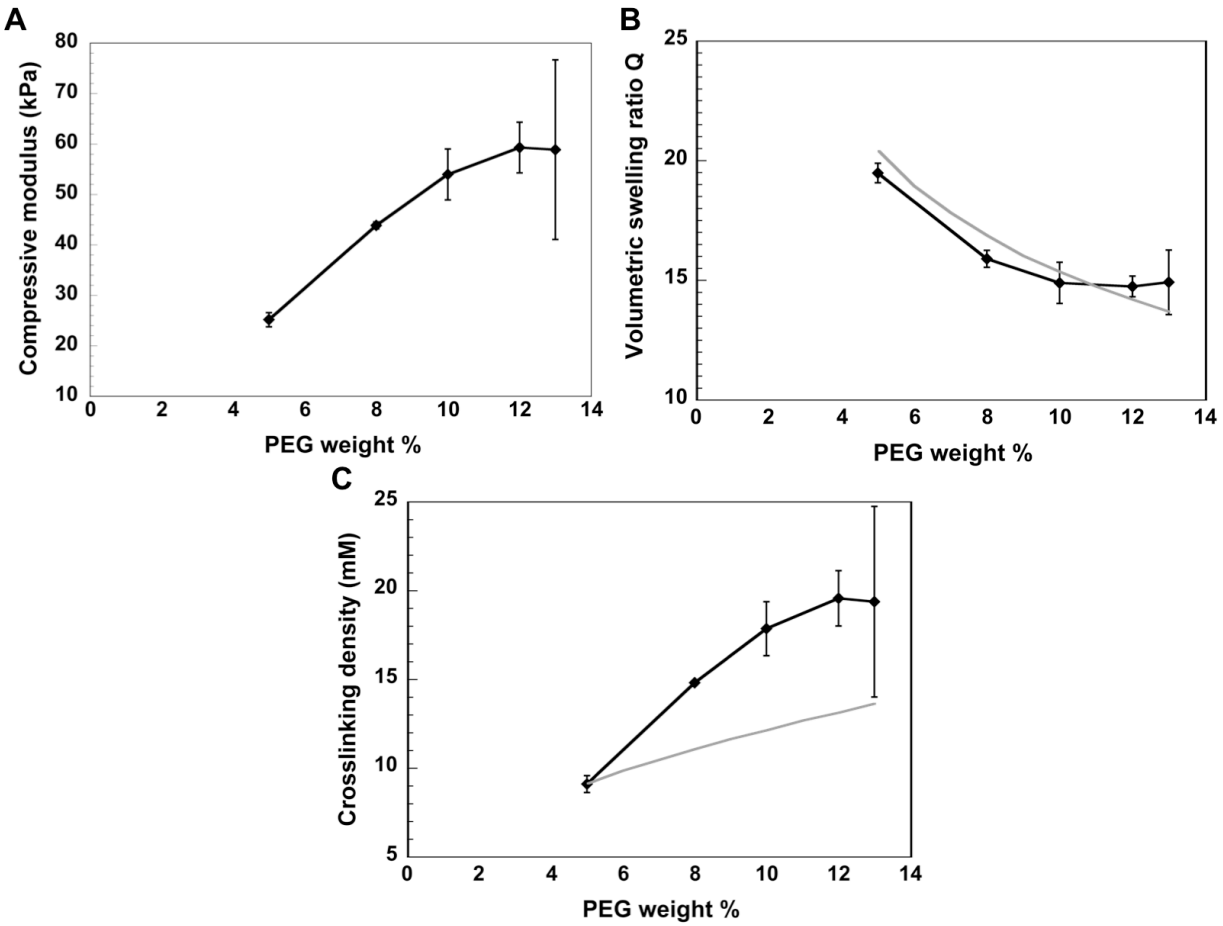

Figure A3.4 Characterization of hydrogels formed with 8-arm PEG norbornene, 20,000 MW, with varied weight % and a constant thiol:ene ratio of 0.95. (A) Experimentally determined compressive modulus, (B) volumetric swelling ratio, and (C) crosslinking density. For swelling ratio and crosslinking density, experimental observations were compared to theoretical predictions (shown by the gray solid line). Error bars represent standard deviation (*n* = 3-4).

was varied, in order to investigate how changing just one of those formulation variables affected the bulk properties. For one set of experiments, the weight % was varied between 5 and 13% while the thiol:ene ratio was held at 0.95 (Fig. A3.4). The compressive modulus increased with increasing weight %, but the effect leveled off after 12 wt% (Fig. A3.4A). This effect is attributed to a unique property of multi-arm hydrogels, because the concentration of PEG in macromer solution can always be increased (increasing the probability of crosslink formation and decreasing the probability of non-reaction or cyclization), but after swelling to equilibrium, there is always a well-defined distance between crosslinks due to the homogeneous network

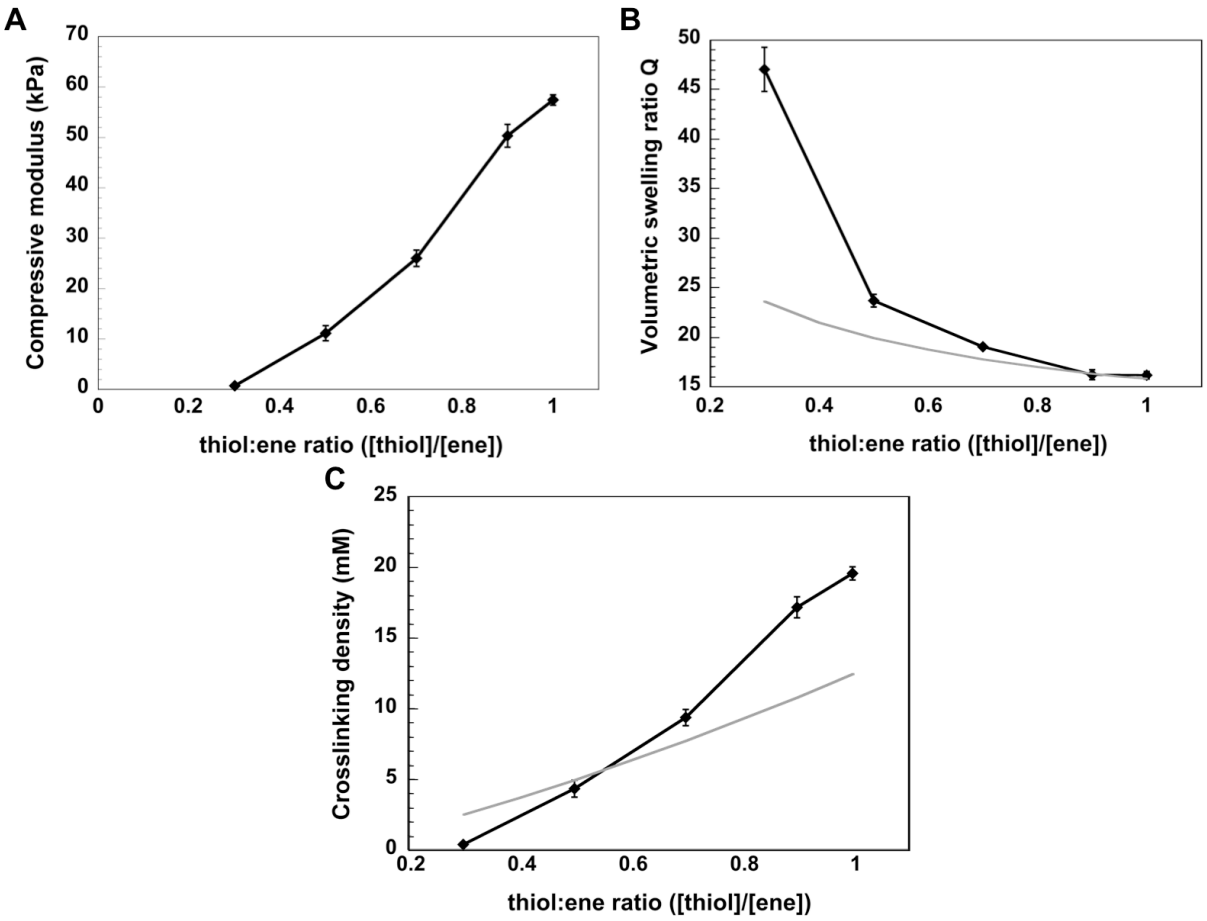

Figure A3.5 Characterization of hydrogels formed with 8-arm PEG norbornene, 20,000 MW, with varied thiol:ene ratio and a constant weight % of 9%. (A) Experimentally determined compressive modulus, (B) volumetric swelling ratio, and (C) crosslinking density. For swelling ratio and crosslinking density, experimental observations were compared to theoretical predictions (shown by the gray solid line). Error bars represent standard deviation (n = 3-4).

structure. Swelling ratio similarly decreased to a certain extent with increasing weight %, which was well predicted by Q_{theo}, calculated with equation (11) (Fig. A3.4B). Comparing the experimentally calculated crosslinking density $\rho_{x,exp}$ to the theoretical crosslinking density $\rho_{x,theo}$ (equation (13)) however revealed some discrepancies (Fig. A3.4C), as $\rho_{x,exp}$ tended to be higher than $\rho_{x,theo}$ at all except for the lower wt% hydrogels. Because $\rho_{x,theo}$ assumes a completely efficient crosslinking reaction, this means that in the real system there could be physical entanglements that increase the crosslinking density, which would increase in prevalence with

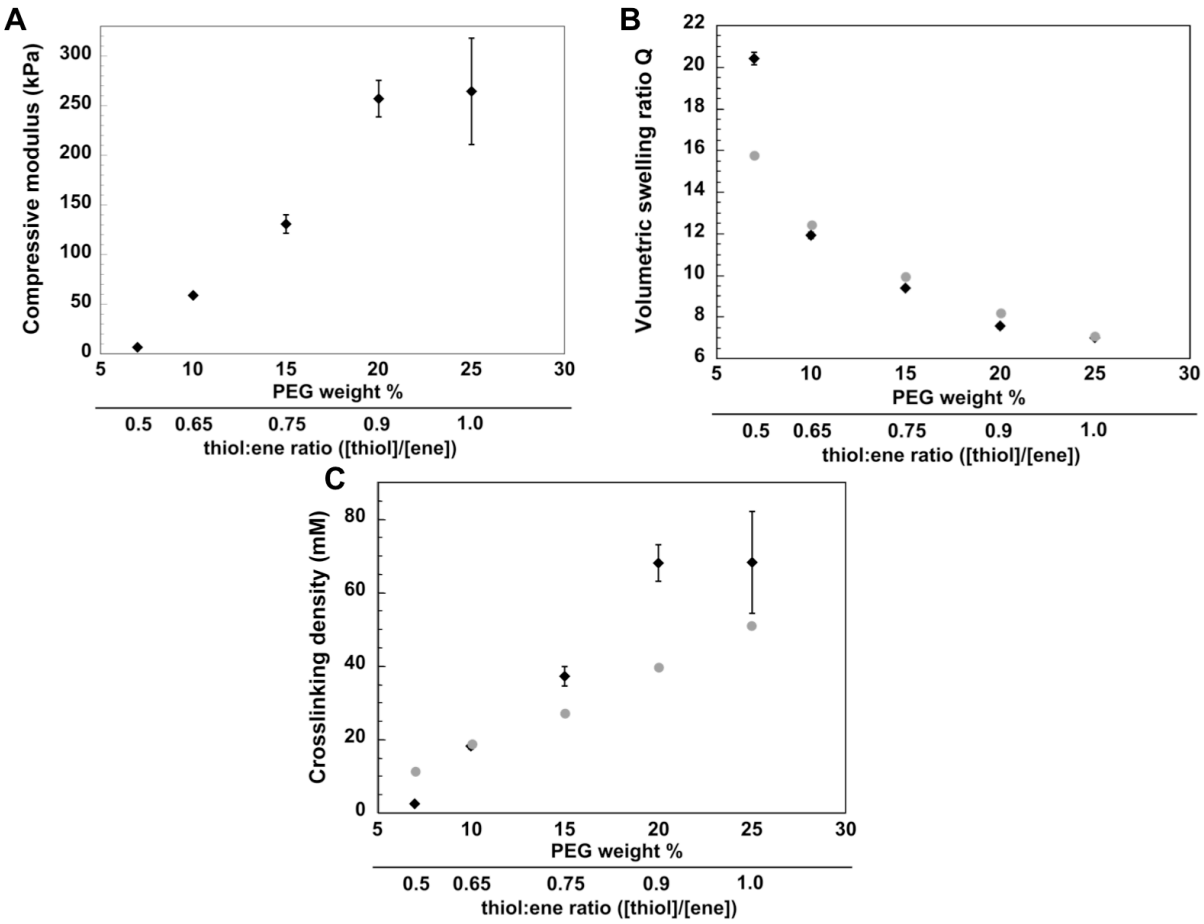

Figure A3.6 Characterization of hydrogels formed with 8-arm PEG norbornene, 10,000 MW, with simultaneously varied weight % and thiol:ene ratio. (A) Experimentally determined compressive modulus, (B) volumetric swelling ratio, and (C) crosslinking density. For swelling ratio and crosslinking density, experimental observations were compared to theoretical predictions (shown by gray circles). Error bars represent standard deviation (n = 3-4).

increased wt%, or that our measurement for compressive modulus might be overestimating the Young's modulus E, falsely elevating $\rho_{x,exp}$.

For another set of experiments with the 8-arm PEG (20,000 MW), the thiol:ene ratio was varied between 0.3 and 1.0 while the wt% was held at 9% (Fig. A3.5). The compressive modulus increased nearly linearly with increasing thiol:ene (Fig. A3.5A), which intuitively makes sense as the amount of crosslinker is increased. The theoretical prediction for Q_{theo} did not perfectly match experimental observations, especially when the thiol:ene ratio was low (Fig. A3.5B). This may be attributed to non-idealities that occur when the thiol:ene ratio is close to the

gel point, because the probability of forming a crosslink, as opposed to cyclization or non-reaction, decreases as the amount of crosslinker present decreases. The theoretical crosslinking density was a reasonably good match for the experimental crosslinking density, and increased linearly with increasing thiol:ene (Fig. A3.5C). Overall for the 8-arm PEG with 20,000 MW, the theoretical predictions were closest to experimental measurements when the wt% was lower (below the saturation), and the thiol:ene ratio was higher.

Similar experiments were conducted with 8-arm PEG, MW 10,000, whereas both thiol:ene ratio and wt% were varied simultaneously in order to characterize a wide range of possible properties (Fig. A3.6). Similar to before, increasing the wt% led to a saturation where further increasing wt% did not increase modulus, which occurred around 20% (Fig. A3.6A). Compared to the 10,000 MW PEG, this was much higher, suggesting that wt% can span a wider range when the MW is lower. Q_{theo} (Fig. A3.6B) and $\rho_{x,theo}$ (Fig. A3.6C) were similarly reasonably matched to experimental data, and were most accurate at higher thiol:ene ratios and lower wt%.

A3.5 Conclusions

Overall, the experimental data present a wide range of bulk hydrogel properties that are possible to achieve using two molecular weights of 8-arm PEG, which will aid experimentalists in choosing hydrogel formulations for specific applications. Additionally, theoretical predictions for Q_{theo} and $\rho_{x,theo}$ were validated with experimental data, meaning that bulk hydrogel properties can be reasonably predicted based solely on a chosen hydrogel formulation, without having to physically fabricate or characterize any actual hydrogels. Together this information summarizes some useful tools that can be applied to multi-arm thiol-norbornene PEG hydrogels.

A3.6 References

[1] Roberts JJ, Bryant SJ. Comparison of photopolymerizable thiol-ene PEG and acrylate-based PEG hydrogels for cartilage development. Biomaterials 2013;34:9969–79.

[2] Shih H, Lin C-C. Visible Light-Mediated Thiol-Ene Hydrogelation Using Eosin-Y as the Only Photoinitiator. Macromol Rapid Commun 2013;34:269–73.

[3] Fairbanks BD, Schwartz MP, Halevi AE, Nuttelman CR, Bowman CN, Anseth KS. A Versatile Synthetic Extracellular Matrix Mimic via Thiol-Norbornene Photopolymerization. Adv Mater 2009;21:5005–10.

[4] Treloar LRG. The physics of rubber elasticity. New York: Oxford University Press; 1975.

[5] Gould ST, Darling NJ, Anseth KS. Small peptide functionalized thiol-ene hydrogels as culture substrates for understanding valvular interstitial cell activation and de novo tissue deposition. Acta Biomater 2012;8:3201–9.

[6] Rubinstein M, Colby RH. Polymer Physics. New York: Oxford University Press; 2003.